

THEORY OF THE LAMELLAR EUTECTOID TRANSFORMATION  
IN  
BINARY AND TERNARY SYSTEMS

THEORY OF THE EUTECTOID TRANSFORMATION  
IN  
BINARY AND TERNARY SYSTEMS

By  
GEORGES-MARIE ANTOINE BOLZE

A Thesis  
Submitted to the School of Graduate Studies  
in Partial Fulfilment of the Requirements  
for the Degree  
Doctor of Philosophy

McMaster University

May 1970

DOCTOR OF PHILOSOPHY (1970)  
(Metallurgy and Materials Science)

McMASTER UNIVERSITY  
Hamilton, Ontario.

TITLE: Theory of the Eutectoid Transformation in Binary  
and Ternary Systems

AUTHOR: Georges-Marie Antoine Bolze, Ingenieur (Ecole Centrale des  
Arts et Manufactures de Paris)

SUPERVISOR: Professor J.S. Kirkaldy

NUMBER OF PAGES: (xii); 236

SCOPE AND CONTENTS:

The theory of the lamellar eutectoid reaction by volume diffusion has been extended to account for solute segregation within the product phases and the effect of dilute third element additions. It has been demonstrated for symmetric binary systems that the segregation can account for 10% or more of the free energy stored in the product phases and can lead correspondingly to a predicted lamellar spacings appreciably greater than those obtained when segregation is neglected. This segregation is relatively high in the systems Cu-In, Cu-Be and Ag-Cd and may account for the fact that a secondary coarse-grained pearlitic reaction follows the initial fine grained one in these systems. The binary theory has been used to analyse the available data for the eutectoid reaction in the Cu-Al and Fe-C systems and satisfactory agreement is obtained.

The theory for ternary systems, while complete in principle, proves to be intractable in all but the simplest version of the solution thermodynamics. It is concluded that the effect of the third element on the binary eutectoid reaction is mainly through its effect on the phase diagram, the ternary cross effects in the diffusion matrix tending to cancel out. Any additional element which lowers the eutectoid temperature will retard the reaction.

Idealism and metaphysics are the easiest things in the world, because people can talk as much nonsense as they like without basing it on objective reality or having it tested against reality. Materialism and dialectics, on the other hand, need effort. They must be based on and tested by objective reality. Unless one makes the effort, one is liable to slip into idealism and metaphysics.

Mao

A tous ceux qui me sont chers.

## ACKNOWLEDGMENTS

On many occasions during the preparation of this thesis I have relied upon my supervisor, Professor J.S. Kirkaldy, for encouragement and help. To him I wish to express my deepest gratitude.

I am also particularly grateful to Dr. A. Salvadori for his assistance with the correction of the draft, to all the graduate students and the staff of the Department of Metallurgy and Materials Science for technical and theoretical advice, and to McMaster University and Falconbridge Nickel Mines, Ltd., which have materially contributed to the realization of this work.

## TABLE OF CONTENTS

		Page
	INTRODUCTION	1
I	REVIEW OF THE LITERATURE	4
II	THEORY OF ISOTHERMAL BINARY EUTECTOID TRANSFORMATION	15
II-A	Classical Structure of the Eutectoid Growth Problem	16
	1/ Solution of the binary diffusion equation	16
	2/ Effect of pressure on the interface concentrations	18
	a - First version of the Gibbs-Thomson equation	19
	b - Second version of the Gibbs-Thomson equation	20
	3/ The mass balance	22
	4/ The second boundary condition	25
II-B	Hillert's Complete Solution of the Eutectoid Problem	27
II-C	Revised Solution - First Thermodynamic Version	33
	1/ General treatment	33
	2/ Symmetric lamellar configuration	40
II-D	Revised Solution - Second Thermodynamic Version	43
	1/ General treatment	43
	2/ Symmetric lamellar configuration	48
	3/ Physical Significance of $\phi$ and $S_c$	54

	<u>Page</u>
III THEORY OF TERNARY EUTECTOIDS	59
III-A Structure of the Problem	59
1/ Solution of the ternary diffusion problem	59
2/ Influence on the concentration of the pressure due to curvature	69
First thermodynamic version	71
Second thermodynamic version	74
3/ The mass balance	77
4/ Second boundary condition	81
III-B Theory of Ternary Systems with the First Thermodynamic Version and for a Symmetrical Configuration	82
III-C Theory of Ternary Systems with the Second Thermodynamic Version	95
IV COMPARISON OF THEORY AND EXPERIMENTS	112
IV-A Details of the Calculation of the $v(S)$ relationship	113
IV-B Aluminum Bronze Binary System	114
IV-C Iron Carbon Binary System	127
IV-D Effect of the Stored Free Energy	136
SUMMARY AND CONCLUSIONS	141
APPENDICES	143
LIST OF REFERENCES	234

## TABLE OF APPENDICES

		<u>Page</u>
I	Integration of the Gibbs-Duhem equations for a binary dilute solution: First thermodynamic version	143
II	Integration of the Gibbs-Duhem equation for a binary dilute solution: Second thermodynamic version	152
III	Calculation of the Fourier series coefficients of a step function	159
IV	Calculation of the Fourier series coefficients by application of the first thermodynamic version of the Gibbs-Thomson relation for binary systems	162
V	Complete solution of the problem in the symmetrical configuration with the first thermodynamic version	168
VI	General calculation of the Fourier series coefficients by application of the second version of the Gibbs-Thomson relation for binary systems	180
VII	Complete solution of the problem in the symmetric configuration with the second thermodynamic version	185
VIII	Comparison between our $v(S)$ relation and Hillert's relation for a symmetric configuration	198
IX	Integration of the Gibbs-Duhem equations for a ternary dilute solution with the first thermodynamic version	203
X	Integration of the Gibbs-Duhem equations for a ternary dilute solution with the second thermodynamic version	208



		<u>Page</u>
XI	Calculation of the Fourier series coefficients for ternary solutions under the second thermodynamic version	212
XII	Approximate calculation of the Fourier series coefficients for ternary solutions with the second thermodynamic version in the symmetrical configuration	224

## LIST OF FIGURES

<u>Figure</u>		<u>Page</u>
1	Micrograph showing interface shape for the carbon tetrabromide-hexachloroethane eutectic	2
2	Schematic sketch showing the interface shape and theoretical frame of reference	5
3	Hillert's predictions for the interface shape as a function of lamellar spacing	10
4	Schematic variation of $v$ as a function of $S$ (after Hillert)	32
5	Schematic variation of $v$ as a function of $S$ and $S^\alpha/S$ from our own general standpoint	39
6	Schematic symmetric binary eutectoid phase diagram	42
7	Free energy composition diagram for a symmetric binary eutectoid system: significance of $\phi$	56
8	Ternary phase diagram corresponding to the first thermodynamic version	72
9	Ternary phase diagram corresponding to the second thermodynamic version	76
10	Symmetric ternary phase diagram corresponding to the first thermodynamic version	83
11	Symmetric ternary phase diagram corresponding to the second thermodynamic version	102

		<u>Page</u>
12	Domain of variation of $C_{1\infty}$ deduced for the second thermodynamic version	108
13	Diffusion coefficient as a function of temperature for the Cu-Al system	115
14	Symmetricized phase diagram for the Cu-Al system	117
15	Theoretical curve $v(S)$ at $550^{\circ}\text{C}$ for the Cu-Al system	121
16	Theoretical curve $v(S)$ at $530^{\circ}\text{C}$ for the Cu-Al system	122
17	Theoretical curve $v(S)$ at $510^{\circ}\text{C}$ for the Cu-Al system	123
18	Plot of $v$ versus temperature for the Cu-Al system	125
19	Plot of $1/S$ versus temperature for the Cu-Al system	126
20	Phase diagram for the Fe-C system	128
21	Symmetricized phase diagram for the Fe-C system	130
22	Theoretical curve $v(S)$ at $698^{\circ}\text{C}$ for the Fe-C system	133
23	Theoretical curve $v(S)$ at $668^{\circ}\text{C}$ for the Fe-C system	134
24	Theoretical curve $v(S)$ at $638^{\circ}\text{C}$ for the Fe-C system	135
25	Plot of velocity versus temperature for the Fe-C system	137
26	Plot of the inverse of lamellar spacing versus temperature for the Fe-C system	138
27	Effect of pressure on the concentrations corresponding to first thermodynamic version of the Gibbs-Thomson equations	149

		<u>Page</u>
28	Free energy-composition diagram corresponding to the first thermodynamic version	150
29	Effect of pressure on the concentrations corresponding to second thermodynamic version of the Gibbs-Thomson equations	156
30	Free energy-composition diagram corresponding to the second thermodynamic version	158
31	Representation of a step function	160
32	Representation of the two parabolas $y_1$ and $y_2$ as a function of $X$	171

## LIST OF TABLES

<u>Table</u>		<u>Page</u>
I	Tabulation of the function $f(Z)$	51
II	Adjustment of composition values in symmetrization of the Cu-Al phase diagram	116
III	Parameters for calculating the $v(S)$ relationship for the Cu-Al system	119
IV	Variation of the diffusion coefficient with temperature for the Cu-Al system	120
V	Predicted optimum velocity and lamellar spacing for the Cu-Al system	124
VI	Tabulated phase diagram for the Fe-C system	129
VII	Adjusted and tabulated phase diagram for the Fe-C system	131
VIII	Parameters used for calculation of the $v(S)$ relation for the Fe-C system	131
IX	Variation of the diffusion coefficient with temperature for the Fe-C system	132
X	Predicted optimum values for the velocity and lamellar spacing for the Fe-C system	136
XI	Predicted values of the parameter $\phi/S_c$ for the Cu-Be, Cu-In and Cd-Ag systems as a function of temperature	140

## INTRODUCTION

Metallurgists have long been intrigued by eutectic or eutectoid reactions, for from a homogeneous solution a highly ordered two phase structure spontaneously evolves, even when the boundary conditions for the reaction are rather imprecise (see Fig. 1). The reaction products usually appear in the lamellar or rod-like form, although more complex ordered structures are sometimes observed (notably in the Al-Si system<sup>1</sup>), and for high supersaturations the cooperative character of the reaction breaks down and more random morphologies appear.

The ordered morphologies can be produced both in an isothermal reaction (usually the solid to solid eutectoid reaction) or in a controlled steady state reaction (usually the liquid to solid eutectic reaction).

It is strongly apparent that the exceptional stability of these structures is closely related to the forces of surface tension which exist at curved two phase interfaces and at three phase triple points (see Fig. 1) and any viable theory must explicitly take account of the influence of these forces on the transport processes (diffusion and heat conduction) near the reaction front.

It is clearly not feasible at this time to develop a mathematical theory for the evolution of the reaction up to the stable steady state from the time when nuclei of the product phases first appear in the system. This evolution is a complex dendritic branching process which is not amenable to

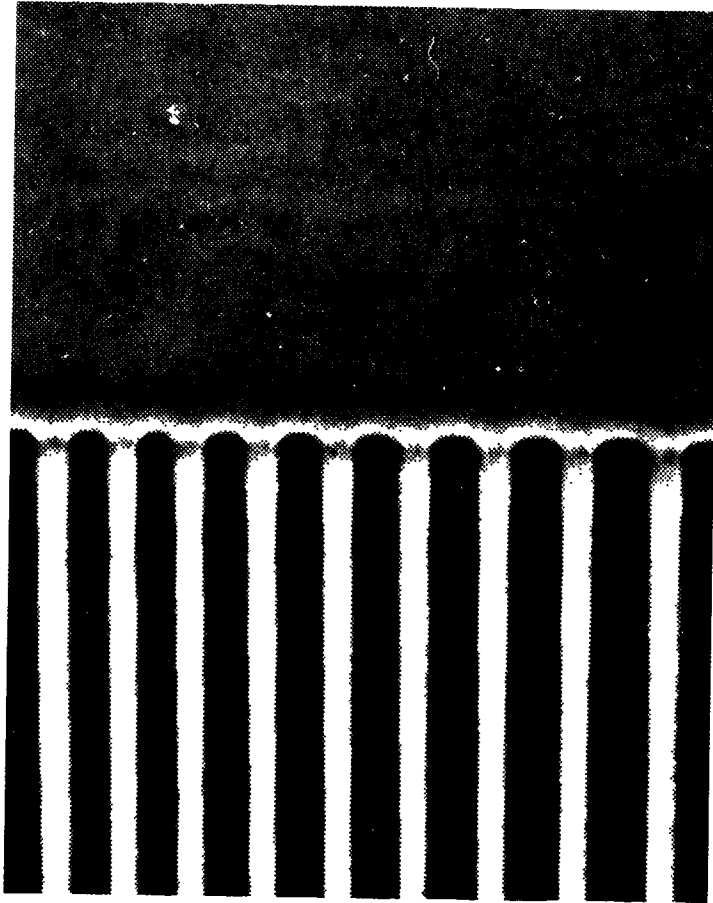


Fig. 1: Micrograph showing interface shape for the carbon tetrabromide-hexachloroethane eutectic (Jackson and Hunt<sup>2</sup>).

continuum mathematical analysis. We thus, with the multitude, concentrate on the discussion of the steady state when and if it is empirically observed. The associated theoretical gaps in the argument (omission of a prediction of the existence of the steady state) leaves an open degree of freedom in the system of equations which appears as an undetermined steady state parameter (e.g., front velocity or lamellar spacing). There remains considerable controversy in the literature as to how this degree of freedom should be removed so as to define a unique steady state. We will not concern ourselves with this important theoretical problem in this work, but will instead concentrate on the solutions of the diffusion problem subject to pressure dependent boundary conditions in binary and ternary systems.



## I. REVIEW OF THE LITERATURE

There have been many attempts to give a theoretical interpretation of edgewise lamellar eutectoid (or eutectic)\* precipitation on the basis of volume diffusion<sup>3-11</sup>. None to date have been able to accurately predict experimental observations. This failure has encouraged workers to investigate models other than volume diffusion in the parent phase<sup>2,8-18</sup>. Unfortunately all such endeavours to date introduce experimentally inaccessible internal parameters (reaction rate constants and phase boundary diffusion coefficients) so tests based on these theories still leave much to be desired.

Brandt<sup>3</sup> and Scheil<sup>4</sup> were the first to construct comprehensive mathematical models of the pearlitic transformation based on volume diffusion. Brandt made the assumption that steady state precipitation is always achieved after a certain time following a transient non-steady state stage and so attempted only to describe the steady state. This tactic has been adopted by all subsequent workers. A schematic representation of the reaction configuration is given in Fig. 2.

The diffusion equation for a binary system has been solved by Brandt subject to the condition of stationary uniform lamellar precipitation. His volume diffusion calculations have been reproduced with only minor alterations

---

\* In all of the following we use the term eutectoid (solid to solid) as inclusive of eutectic (liquid to solid) reactions.

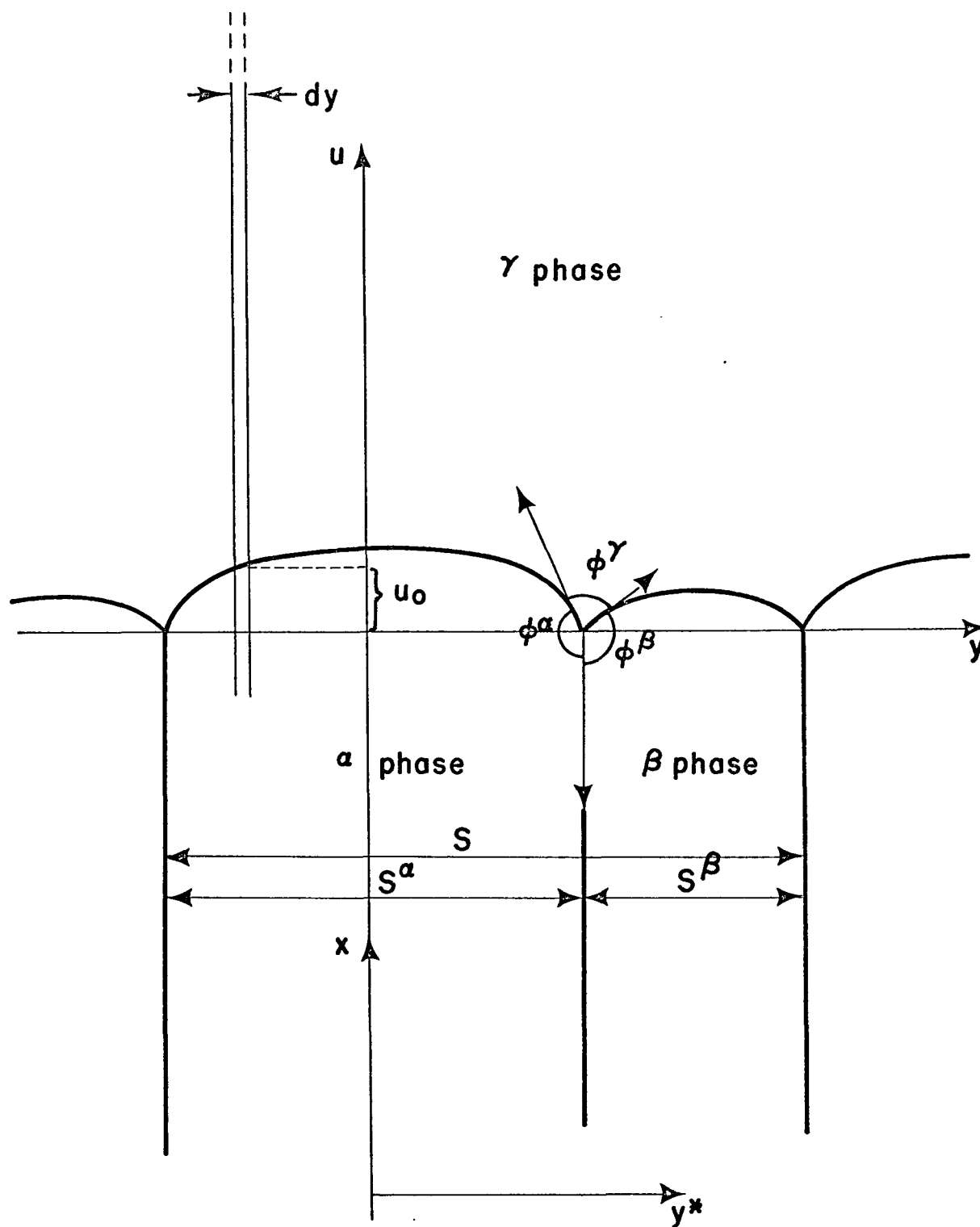


Fig. 2: Schematic sketch showing the interface shape and theoretical frame of reference.

by many workers and indeed, by ourselves in our presentation of a new theory for binary systems.

The solution takes the form of a Fourier series for which the coefficients are to be determined by the boundary conditions. In this class of physical problems these boundary conditions must be formulated as a well defined function which itself is to be developed in a Fourier series. The identity of terms between series provides the expressions for evaluation of the Fourier coefficients of the solution.

In specifying the boundary condition Brandt chose to impose precise values of the periodic concentrations at only two points of the interface, namely, the centers of two adjacent lamellae. Such concentration values were obtained from the extrapolated binary phase diagram at zero pressure. This procedure of course contains the assumptions either that at these points of the interface the pressure vanishes, or that the adoption of such values does not lead to a significant error. Unfortunately Brandt never recognized the significance of pressure due to surface tension and was therefore equivocal about the thermodynamic problem raised by the junction of the two lamellae where locally three phases must coexist. In contrast to having a concentration function known at all points of the interface, the two given values of the concentration at the tip of adjacent lamellae allows the determination of only two coefficients of the Fourier series. This explains why Brandt's solution is given only to the first harmonic in the expansion. Nonetheless, within this limitation, the calculations are absolutely correct and yield important results.

Because of the neglect of surface tension it is not possible to obtain the correct relation between the growth velocity and lamellar spacing

nor a prediction of the interface shape. However, Brandt was able to demonstrate that the velocity increases when either the temperature or the lamellar spacing decreases.

Cellular or lamellar precipitation occurs for a range of compositions and temperatures below the eutectoid temperature of a binary system. At such phase points the constant pressure equilibrium diagram allows only two phases in equilibrium and these are the product phases  $\alpha$  and  $\beta$  precipitated from the parent phase  $\gamma$ . However, in the case of cooperative precipitation such as edgewise lamellar growth (see Fig. 2) there is a situation at the junction of two lamellae where, if local equilibrium is to be sustained, three phases must coexist at temperatures below the eutectoid temperature. This can only be achieved through deformation of the phase diagram due to capillarity. In this way the concentration of the parent phase can vary smoothly across the junction of the two lamellae and mechanical equilibrium of the surface tensions can simultaneously be accommodated. A completely flat interface could conceivably occur but this could only be consistent with the mechanical requirement if the surface tension between the product phases were zero. It is therefore essential to admit a curvature of the interface between the mother and product phases. The local radius of curvature generates a pressure which acts mainly upon the product phases. This pressure, when properly balanced mechanically, provides the deformation of the diagram as discussed above.

It is important to note that for a given temperature the deformation of the phase diagram is not unique. Indeed we can conceive, for a given experimental temperature, that different pressures in the phases will deform the phases boundaries differently. This will give different triple point

compositions. Through such considerations we can anticipate the ability of the interface to accommodate to different ratios of lamellar thickness at the same temperature.

We see that for a correct analysis it is absolutely essential to take account of variations of composition due to the pressure. It is usually assumed that this pressure acts only on the precipitate phases. Notwithstanding this fact, the pressure leads to concentration changes in both parent and product phases.

These considerations were articulated for the first time by Zener<sup>5</sup>. By dimensional arguments he obtained a relation between the undercooling, the velocity and the spacing. Zener assumed a driving force proportional to the undercooling, i.e., to  $C_0^{\gamma\alpha} - C_0^{\gamma\beta}$ , where  $C_0^{\gamma\alpha}$  and  $C_0^{\gamma\beta}$  are the parent  $\gamma$  phase compositions in contact with  $\alpha$  and  $\beta$  phases in the absence of pressure, and corrected this for surface tension by a Gibbs-Thomson term,  $1 - S_c/S$ , where  $S$  is the lamellar spacing and  $S_c$  is that spacing for which the free energy per unit volume of parent and product phases are the same. Indeed,  $S_c$  is the analogue of the critical radius for nucleation in a two-phase reaction. Zener multiplies this driving force by a mobility proportional to  $D/S$ , where  $D$  is the volume diffusion coefficient, to obtain the expression for the velocity

$$v \propto D \frac{S^2}{S^\alpha S^\beta} \frac{C_0^{\gamma\alpha} - C_0^{\gamma\beta}}{C^\gamma - C^\alpha} \frac{1}{S} \left(1 - \frac{S_c}{S}\right) \quad (1.1)$$

where  $S^\alpha$  and  $S^\beta$  are the respective lamellar thicknesses of the precipitate

phases.

Zener's crude calculation reveals an important generic characteristic of such steady state calculations, viz., that the exact solution of the diffusion problem does not uniquely specify the stable configuration of the system. Zener suggested that one should remove the degree of freedom apparent in eq. 1.1 by assuming that nature chooses that spacing which maximizes the growth velocity with respect to spacing. Although this has considerable intuitive compulsion, it is now known to be an incorrect criterion<sup>2,8-10,12,19-21</sup>. Nonetheless Zener's predictions for the Fe-C isothermal eutectoid transformation are in fair order of magnitude agreement with observations.

A more complete calculation based on Brandt's series solution, leading to the same functional relation between the velocity and the spacing, has been performed by Hillert<sup>6,7</sup>. In order to simplify the calculations, Hillert made the rather strong assumption that the concentrations in the precipitate phases are uniform and equal to those at equilibrium when there is no pressure. Hillert's calculations in total will be presented later in the text as the basis of our own detailed calculations for a volume diffusion controlled reaction.

Hillert's major contribution consists in the fact that his formulation allows the detailed calculation of the interface shape. Fig. 3 shows his prediction of the interface shape of the isothermal Fe-C eutectoid as a function of the free parameter  $S/S_c$ . If Zener's criterion for stability (maximum velocity giving  $S = 2S_c$ ) is accepted then the observed interface should be as given in frame  $v/v_{\max} = 0.99$ . Metallographic observations tend to favor shapes which correspond to spacings somewhat greater than

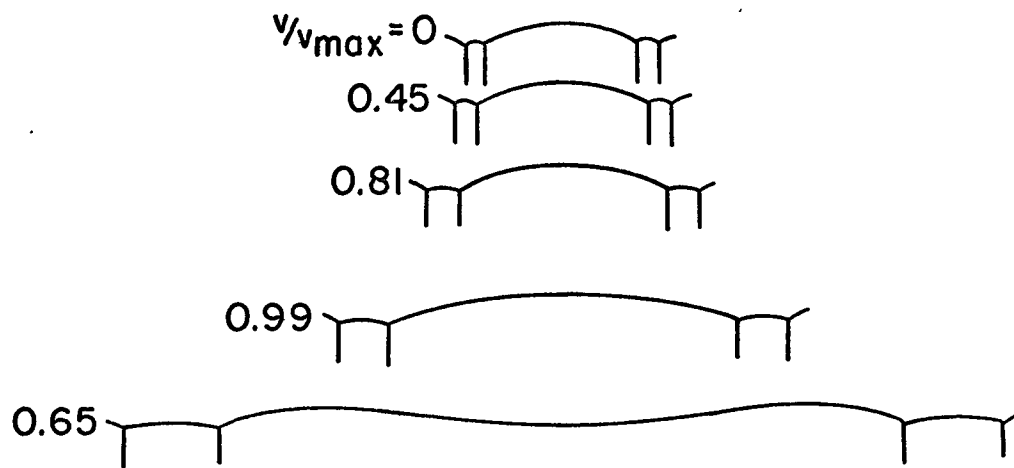


Fig. 3: Hillert's predictions for the interface shape as a function of lamellar spacing.

$2S_c$  2,13.

It is to be noted that the aforementioned calculations can be applied to isothermal eutectoid transformations (usually in quenched solids) or to controlled transformations at fixed velocity in a temperature gradient. In the latter case, with  $v$  fixed, eq. 1.1 represents a relation between the spacing and the undercooling. Tiller<sup>8</sup> postulated that in this configuration, nature chooses that spacing which minimizes the undercooling and found fair agreement between predictions and experiment.

A number of attempts have been made to give operational significance to the postulated optimal principles since if such principles are to be valid they must correspond to a Le Chatelier operational statement, or equivalently to an articulated perturbation test procedure. Chalmers<sup>9</sup> and Jackson and Hunt<sup>2</sup> have articulated perturbation models which are claimed to correspond very closely to the minimum undercooling criterion.

Kirkaldy<sup>10,21</sup> has espoused the proposition that to a fair approximation, both isothermal and controlled-growth eutectoid spacings are determined by a principle of maximum entropy production rate, a possibility first suggested by Cahn<sup>12</sup>. In the case of controlled growth, minimum undercooling and maximum entropy production are equivalent. Kirkaldy maintains that the stable state of a eutectoid may be defined more completely as a saddle point in the entropy production rate, a minimum with respect to local fluctuations of the spacing and a maximum with respect to fluctuations or variations in the mean spacing<sup>23</sup>. Since for theoretical purposes we always assume "a priori" that the spacing is uniform (Brandt's proposition), the minimal part of the statement is not required. Kirkaldy<sup>21</sup> has given a rather crude operational justification of the maximal part of the principle using an



argument rather closely related to Sundqvist's<sup>19,20</sup> proposition that nature chooses a spacing corresponding to incipient nucleation of a new lamella at the center of existing stable lamellae.

We will not consider this important but difficult problem further in this thesis. Since we will be focussing upon isothermal eutectoids we will accept the maximum entropy production criterion. For certain models this gives a stable spacing about 50% greater than that given by the maximum velocity criterion<sup>21</sup>, i.e.,

$$S_s \approx 1.5 S(v_{\max}) \quad (1.2)$$

where  $S(v_{\max})$  is easily calculated from a derived  $v(S)$  relation.

Generally speaking, calculations based on the volume diffusion model have not enjoyed great quantitative success, predicting spacings too small by factors of 2 to 16. This can be attributed to three factors: (a) the stability criterion is wrong; (b) the model is too crude, usually ignoring segregation in the product phases; and (c) diffusion is being short-circuited along the reaction interface. Turnbull<sup>24,25</sup> was the first to recognize factor (c) in relation to cellular, discontinuous precipitation which often occurs at very low temperatures and where phase boundary diffusion might be expected to dominate. A relation like Turnbull's can be obtained from Zener's relation simply by substituting  $D_s \delta/S$  for the volume diffusion coefficient  $D$ , where  $D_s$  is a surface diffusion coefficient and  $\delta$  is the effective boundary width. Thus

$$v \propto D_s \delta \frac{1}{S^2} \left(1 - \frac{S_c}{S}\right) \quad (1.3)$$

Cahn<sup>11,12</sup> attempted a calculation for eutectoids taking account of both (b) and (c) and indeed found that larger spacings should be expected. Unfortunately, his treatment ignores surface tension, gives up the principle of local equilibrium and introduces an inaccessible internal reaction rate parameter, so it is difficult if not impossible, to assess this contribution numerically. Shapiro and Kirkaldy<sup>13</sup> and independently, Hillert<sup>7</sup>, have carried out a similar calculation which eschews reaction rate control and retains the principle of local equilibrium as well as the necessity for segregation in the product phases.

In general the theory is intractable but in a simple symmetrical case yields a  $v(S)$  relation similar to eq. 1.2. More recently, Tu and Turnbull<sup>14-16</sup>, Aaronson et al.<sup>17,18</sup> and Sundqvist<sup>19,20</sup> have contributed variations upon the above themes.

It is clear that surface diffusion is an important factor in many eutectoid reactions, particularly at temperatures well below the liquidus line. These systems are excluded from the present discussion since we restrict attention to systems where volume diffusion is predominant. The latter includes all eutectics (liquid to solid) reactions and eutectoid (solid to solid) reactions which occur near the liquidus or at marginally lower temperatures where the diffusion mechanism is interstitial.

Our concern here is both with binary and ternary reactions. Indeed, when the program was begun we were interested primarily in ternaries lying

near the binary limits of the diagram. We discovered, however, that it was impossible to solve the ternary problem using the approximations that had been used to date for binaries. We therefore undertook first the revision and improvement of the binary calculations and this now represents a major contribution of this thesis.

There has been little theoretical discussion in the literature of the kinetics of ternary eutectoid reactions to date. Cahn and Hagel<sup>2</sup> and Hillert<sup>7</sup> have discussed some thermodynamic aspects of such reactions and Sundqvist<sup>17,18</sup> has supplied some experimental observations and has examined the kinetics of ternaries transforming by phase boundary diffusion. Kerr et al<sup>26,27</sup> have reported some observations of true ternary eutectic reactions (liquid to three solids). This complex ternary reaction will not be considered here. Rather we restrict attention to eutectoid reactions near the binary limits which react in the pseudo-binary form ( $\gamma$  to  $\alpha + \beta$ ).

Kirkaldy<sup>28</sup> has discussed the ternary pearlitic reaction from the point of view of parallel independent reactions  $\gamma$  to  $\alpha$  and  $\gamma$  to  $\beta$  and showed how the third element affects the reaction rate through the phase diagram and the ternary diffusion interactions. Purdy et al.<sup>24</sup> have further advanced our understanding of the ternary two-phase reactions ( $\gamma$  to  $\alpha$ ). A correct treatment of the ternary pearlitic reaction must be such as to link logically with the two-phase results.

## II. THEORY OF ISOTHERMAL BINARY EUTECTOID TRANSFORMATION

We suppose that the starting  $\gamma$  phase has been kept for a certain length of time at a temperature well above the eutectoid temperature so that it is perfectly homogenized. The composition, in moles per unit volume, of the solute component is taken as  $C_{\infty}$ . After this homogenization period, the system is quenched to a temperature below the eutectoid temperature and we suppose that the pearlitic transformation occurs at this uniform temperature. Our calculations can, however, accommodate a small temperature gradient perpendicular to the interface since the diffusion zone is sufficiently small in extent that to a good approximation the precipitation is isothermal. We have neglected the dissipation of latent heat of transformation which might be expected to perturb the uniformity of the temperature particularly in the solidification of a eutectoid. The interface has to be sufficiently flat that this gradient of temperature does not introduce variation of temperature along its span. These are the assumptions made also by numerous authors and only Jackson and Hunt<sup>2</sup> have taken temperature changes into consideration.

## II.A CLASSICAL STRUCTURE OF THE EUTECTOID GROWTH PROBLEM

### 1/ SOLUTION OF THE BINARY DIFFUSION EQUATION

With Brandt<sup>3</sup> and Hillert<sup>6,7</sup>, we assume that the precipitation proceeds in the steady state with a velocity  $v$  and that the problem is two-dimensional as shown in Fig. 2. The  $x$ -axis is directed perpendicular to the precipitation interface and towards the parent  $\gamma$  phase. The  $y^*$  axis is directed parallel to the average interface. It is also assumed that there is a symmetry both in the geometrical and concentration configurations around any center of lamella. This suggests that the symmetry axis of an  $\alpha$  lamella be taken as the  $x$ -axis.

Since we desire a steady state solution of the problem, we make a translation of the frame of reference via the relations

$$u = x - v t \quad (2.1a)$$

and

$$y = y^* \quad (2.1b)$$

In this frame, the diffusion of the solute component 1 satisfies the differential equation\*

---

\* We adopt consistently the following convention:  
 $C$  are moles per unit volume  
 $x$  are mole fractions.

$$-v \frac{\partial C}{\partial t} = D \left( \frac{\partial^2 C}{\partial u^2} + \frac{\partial^2 C}{\partial y^2} \right) \quad (2.2)$$

We seek a solution periodic in  $y$  with the period  $S$  (the lamellar spacing) which is also exponentially decreasing in  $u$  in order to obtain a composition  $C_\infty$  for any  $y$  at  $u = \infty$ . The well-known solution<sup>3-11</sup> is then

$$C = C_\infty + \sum_{n=0}^{\infty} A_n e^{\lambda_n u} \cos b_n y \quad (2.3)$$

where

$$b_n = \frac{2\pi n}{S} \quad (2.4)$$

and

$$\lambda_n = -\frac{v}{2D} \left( 1 + \sqrt{1 + 4 \frac{b_n^2 D^2}{v^2}} \right) \quad (2.5)$$

We will find with Hillert<sup>6-7</sup> that for all interesting experimental situations  $2\pi n D / Sv \gg 1$  so that to a very good approximation

$$\lambda_n \approx -b_n \quad (2.6)$$

In the expression for  $C$  above we have taken account of the boundary condition at  $u = \infty$  but we still have to satisfy the boundary

condition at the interface in general and the junction of two lamellae.

## 2/ EFFECT OF PRESSURE ON THE INTERFACE CONCENTRATIONS

Because the interface is curved, there are pressure changes along the y-axis. In the following we shall assume that the pressure remains constant in the parent  $\gamma$  phase but changes in the precipitate phases as in Hillert's contributions<sup>7,8</sup>. For solidification of a liquid eutectoid this is strictly true but for a eutectoid reaction this is an approximation which may be very bad if the  $\gamma$  phase is relatively hard.

Pressure changes in the precipitate phases necessarily lead to composition changes. In the interest of simplicity Hillert chose to ignore these changes. That is, he assumed constant concentrations in the precipitate phases for any variations of the pressure acting upon them. We have chosen to relax this very strong and thermodynamically unrealistic condition. This does not lead to complications in the Gibbs-Thomson equations which can still be easily linearized, but it does complicate the application of the interface boundary conditions.

Two binary  $\alpha$  (or  $\beta$ ) and  $\gamma$  phases in equilibrium, having respectively the compositions  $(x_1^\alpha, x_2^\alpha)$ ,  $(x_1^\gamma, x_2^\gamma)$  and the activities  $a_1$  and  $a_2$ , satisfy the Gibbs-Duhem relations

$$x_1^\gamma d \ln a_1 + x_2^\gamma d \ln a_2 = \frac{V^\gamma}{RT} dP^\gamma \quad (2.7a)$$

$$x_1^\alpha \, d \ln a_1 + x_2^\alpha \, d \ln a_2 = \frac{V^\alpha}{RT} \, dP^\alpha \quad (2.7b)$$

with

$$dP^\gamma = 0 \quad (2.7c)$$

In Appendices I and II we have developed two linear versions of the Gibbs-Thomson equations corresponding to two different thermodynamic assumptions and to dilute solutions of the product phases.

a - FIRST VERSION OF THE GIBBS-THOMSON EQUATION

As in Appendix I the compositions of element 1 in the two product phases and the  $\gamma$ -phase are in a ratio  $K^{\alpha,\beta}$  independent of the pressure, viz.,

$$K^\alpha = \frac{x_1^{\alpha\gamma}}{x_1^{\gamma\alpha}} \quad ; \quad K^\beta = \frac{x_1^{\beta\gamma}}{x_1^{\gamma\beta}} \quad (2.8a;b)$$

This approximation leads to the Gibbs-Thomson equations for the equilibrium between the  $\gamma$ - $\alpha$  and  $\gamma$ - $\beta$  phases

$$P^\alpha = RT \, h^\alpha \, (C_{10}^{\alpha\gamma} - C_1^{\alpha\gamma}) \quad (2.9)$$

$$P^\beta = RT \, h^\beta \, (C_1^{\beta\gamma} - C_1^{\beta\gamma}) \quad (2.10)$$



where

$$h^{\alpha} = \frac{1 - K^{\alpha}}{K^{\alpha} - x_{10}^{\alpha\gamma}} \quad (2.11)$$

$$h^{\beta} = \frac{K^{\beta} - 1}{1 - x_{10}^{\beta\gamma}} \quad (2.12)$$

and the subscript 0 indicates compositions at zero pressure.

It has also been shown in Appendix I that  $h^{\alpha}$  and  $h^{\beta}$  are equal in magnitude and opposite in sign for a symmetrical phase diagram. Equivalently, the pressure effect on the concentrations in the precipitate phases are symmetric for the  $\alpha$  and  $\beta$  phases. This symmetry breaks down for the effect of pressure on the concentrations in the parent phase. This is due to the rather special character of our approximation. For greater generality we, therefore, also consider a more complicated concentration partition relation.

## b - SECOND VERSION OF THE GIBBS-THOMSON EQUATION

As develops in Appendix II we no longer accept a simple proportionality between the concentrations in the parent and precipitate phases but interject a more complicated expression which we call the complex ratio\* such that

---

\* The ratios  $K$  and  $\chi$  can be expressed in terms either of concentrations or mole fractions.

$$\frac{x_1^{\gamma\alpha}}{x_1^{\alpha\gamma}} = \frac{x_2^{\alpha\gamma}}{x_2^{\gamma\alpha}} = x^\alpha \quad (2.13)$$

The physical meaning of the complex ratio is not immediately apparent but as is demonstrated in Appendix II it allows a much greater generality of thermodynamic behaviour than in the first version. Assumption 2.13 leads to the Gibbs-Thomson equations

$$p^\alpha = RT k^\alpha (C_{10}^{\alpha\gamma} - C_1^{\alpha\gamma}) \quad (2.14)$$

$$p^\beta = RT k^\beta (C_{10}^{\beta\gamma} - C_1^{\beta\gamma}) \quad (2.15)$$

where

$$k^\alpha = x^\alpha - 1 \quad (2.16)$$

$$k^\beta = x^\beta - 1 \quad (2.17)$$

The coefficients  $k^\alpha$  and  $k^\beta$  are here also equal in magnitude and opposite in sign for a symmetric diagram. As shown in Appendix II, eqs. 2.14 and 2.15 imply that the effect of pressure on the concentrations of the parent phase are nonlinear. Nonetheless for a symmetric phase diagram the effect of pressure on the composition in the parent phase remains

symmetric. For small pressure excursions the pressure dependency of the concentration in the parent phase can be linearized.

We wish to emphasize that both of the above approximations yield a linear dependence of the concentrations in the precipitate phases upon the pressure. This is contrary to Hillert's assumption that the compositions in the product phases are independent of the curvature and therefore the pressure. This is the essential point of departure of our treatment of the problem from that of Hillert.

### 3/ THE MASS BALANCE

In all the calculations presented herein we suppose that the concentration distribution in the precipitate phases is frozen. Under Hillert's assumption that the  $\alpha$  and  $\beta$  phases are homogeneous this is certainly legitimate. In our case, however, the assumption implies that the diffusion rates in the product phases are substantially zero. It is important to point out that a non-zero diffusion rate behind the interface could have a significant effect on the velocity of reaction at the steady state.

Consider with Hillert a differential volume element as shown on Fig. 2 lying parallel to the  $u$  plane. The net mass which is diffusing through its walls is compensated for by the excess of inflow at  $u = \infty$  in relation to outflow behind the interface. This can be expressed as

$$v (C_{\infty} - C_p) = - D \int_{u_0}^{\infty} \frac{\partial^2 C}{\partial y^2} du \quad (2.18)$$

In this expression  $C_p$  is to be interpreted as either the concentration in the  $\alpha$  or  $\beta$  phase,  $y$  is allowed to vary over a single period and  $u_0$  is the value of  $u$  at the interface at the  $y$  location of the differential element. From the solution for  $C$  (eq. 2.3) we have

$$\frac{\partial^2 C}{\partial y^2} = - \sum_{n=1}^{\infty} A_n b_n^2 e^{\lambda_n u} \cos b_n y \quad (2.19)$$

which we substitute in the mass balance to yield

$$v (C_{\infty} - C_p) = D \int_{u_0}^{\infty} \left( \sum_{n=1}^{\infty} A_n b_n^2 e^{\lambda_n u} \cos b_n y \right) du \quad (2.20)$$

The right hand side is a function of  $y$  because  $u_0$  is itself a function of  $y$ . Integration, therefore, yields

$$v (C_{\infty} - C_p) = - D \sum_{n=1}^{\infty} \frac{A_n b_n^2}{\lambda_n} e^{\lambda_n u_0(y)} \cos b_n y \quad (2.21)$$

This equation, in complete generality, gives us the expression for  $C_p$  as a function of  $y$ . For its evaluation we need to know the equation of the interface

$$u_0 = f(y) \quad (2.22)$$

or parametrically

$$u_0 = u_0(s) \quad (2.23a)$$

and

$$y = y(s) \quad (2.23b)$$

where  $s$  is the distance along the interface arc. We could proceed as Shapiro and Kirkaldy<sup>13</sup> have suggested and solve the differential equations:

$$\frac{d^2 u_0}{ds^2} = - \frac{P^{\alpha,\beta}}{\sigma^{\alpha,\beta}} \frac{dy}{ds} \quad \text{for the } (\alpha,\beta) \text{ lamella} \quad (2.24)$$

where  $P$  is expressed in terms of concentrations and therefore of  $y$ , and  $\sigma^{\alpha,\beta}$  is the surface tension between the  $(\alpha,\beta)$  and  $\gamma$  phases (see Fig. 2). This procedure has not been attempted here because of its obvious complexity. We have, therefore, assumed with Hillert that the interface is sufficiently flat for  $\exp(\lambda_n u_0)$  to be approximated by unity for all  $n$  and  $y$ . From eq. 2.21 we can then write

$$v(C_\infty - C_p) = -D \sum_{n=1}^{\infty} \frac{A_n b_n^2}{\lambda_n} \cos b_n y \quad (2.25)$$

which is equivalent to writing

$$v (C_{\infty} - C_p) = D \int_0^{\infty} \left( \sum_{n=1}^{\infty} A_n b_n^2 \right) e^{\lambda_n u} \cos b_n y \, du \quad (2.26)$$

Comparing eq. 2.26 with eq. 2.20 we then see that in our approximation we have set

$$D \int_{u_0}^0 \left( \sum_{n=1}^{\infty} A_n b_n^2 \right) e^{\lambda_n u} \cos b_n y \, du = 0 \quad (2.27)$$

In the case where the lateral diffusion occurs close against the interface, this approximation is not legitimate and the integral in eq. 2.27 is the most important term of eq. 2.20. This happens when the  $\lambda_n$  are large so that even with an approximately flat interface,  $\exp(\lambda_n u_0)$  cannot be approximated by unity. From equation 2.5 we can see that the magnitude of  $\lambda_n$  depends mainly upon the value of  $\frac{v}{D}$ . We conclude, therefore, that when  $v$  is large or  $D$  very small, e.g., at large undercooling our assumption (eq. 2.27) is defective. Such conditions for low temperatures are precisely those where surface diffusion becomes predominant<sup>12</sup> so the volume diffusion model breaks down.

#### 4/ THE SECOND BOUNDARY CONDITION

For given values of the surface tensions between the three phases

$\alpha$ ,  $\beta$  and  $\gamma$  the angles at the junction of the interfaces must satisfy the relations

$$\frac{\sigma^\alpha}{\sin\phi^\alpha} = \frac{\sigma^\beta}{\sin\phi^\beta} = \frac{\sigma^\gamma}{\sin\phi^\gamma} \quad (2.28)$$

where the angles  $\phi^\alpha$ ,  $\phi^\beta$  and  $\phi^\gamma$  are defined in Fig. 2. If we assume that the interface between the phases  $\alpha$  and  $\beta$  is planar and parallel to the  $u$  plane then we can use the geometric relations (Shapiro and Kirkaldy<sup>13</sup>)

$$-\cos\phi^\alpha = \int_0^{\frac{S^\alpha}{2}} \frac{1}{r} dy \quad \text{and} \quad -\cos\phi^\beta = \int_{\frac{S^\alpha}{2}}^{\frac{S}{2}} \frac{1}{r} dy \quad (2.29a;b)$$

along with the relation for the radius of curvature,

$$r = \frac{\sigma}{P} \quad (2.30)$$

and the previously calculated expressions for  $P$  as a function of the concentrations in the parent  $\gamma$  phase or the precipitate  $\alpha$  and  $\beta$  phases. We thus define the two equations which constrain the triple point boundary values.

In summary, we have written down the Fourier series for the concentration in the parent  $\gamma$  phase as a function of  $v$  and  $S$ . From this, and by application of the mass balance, we were able to deduce expressions for the concentrations in the precipitate  $\alpha$  and  $\beta$  phases. Upon these results we have imposed a geometric requirement which must be simultaneously

satisfied. The coefficients of the Fourier series remain to be calculated. They will be evaluated in all cases from thermodynamic relations, i.e., from information given by the pressure dependent binary phase diagram.

In completing the calculations we introduce three different ways of interpreting the phase diagram corresponding to different expressions for the pressure dependence.

## II.B HILLERT'S COMPLETE SOLUTION OF THE EUTECTOID PROBLEM

In his interpretation of the binary diagram, Hillert<sup>6,7</sup> insisted that the composition of the precipitate phases  $\alpha$  and  $\beta$  do not change with the pressure. Therefore, in the mass balance (eq. 2.25) the left hand side is a step function determined by the precipitate composition  $C_p$ . Furthermore, since the precipitate phases are homogeneous, the conservation of mass implies the validity of the lever rule

$$\begin{aligned} s^\alpha (C_\infty^\gamma - C_{10}^{\alpha\gamma}) &= s^\beta (C_{10}^{\beta\gamma} - C_\infty^\gamma) \\ &= \frac{s^\alpha s^\beta}{s} (C_{10}^{\beta\gamma} - C_{10}^{\alpha\gamma}) \end{aligned} \quad (2.31)$$

Thus equation 2.25 can be written as



$$\sum_{n=1}^{\infty} \frac{A_n b_n^2}{-\lambda_n} \cos b_n y = \begin{cases} S^\beta \frac{v}{DS} (C_{10}^{\beta\gamma} - C_{10}^{\alpha\gamma}) & \text{when } -\frac{S^\alpha}{2} < y < \frac{S^\alpha}{2} \\ -S^\alpha \frac{v}{DS} (C_{10}^{\beta\gamma} - C_{10}^{\alpha\gamma}) & \text{when } \frac{S^\alpha}{2} < y < \frac{S^\alpha}{2} + S^\beta \end{cases} \quad (2.32)$$

The right hand side is clearly a step function in  $y$ . In Appendix III, we have carried out the appropriate Fourier analysis to give

$$\sum_{n=1}^{\infty} \frac{A_n b_n^2}{-\lambda_n} \cos b_n y = \frac{v}{DS} (C_{10}^{\beta\gamma} - C_{10}^{\alpha\gamma}) \left[ \frac{S^\beta - S^\alpha}{2} + \frac{2S}{\pi} \sum_{n=1}^{\infty} \left( \frac{1}{n} \sin \pi n \frac{S^\alpha}{S} \right) \cos b_n y \right] \quad (2.33)$$

The identity of terms, for  $n > 0$ , gives

$$\frac{A_n b_n^2}{-\lambda_n} = \frac{4v}{DS b_n} (C_{10}^{\beta\gamma} - C_{10}^{\alpha\gamma}) \sin \pi n \frac{S^\alpha}{S} \quad (2.34)$$

Note, however, that the term in the right hand side for  $n = 0$  has a counterpart in the left hand side ( $b_0 = 0$ ) only if it is equated to zero, i.e., if and only if  $S^\alpha = S^\beta$ . This implies that Hillert's calculation is strictly applicable only to a completely symmetric phase diagram.

We have not been able to ascertain whether for non-symmetrical cases the failure of the equation of the zero order coefficients is a serious error or not. Hillert has proceeded as though this error is not important so for the moment we will also proceed without recognizing this potential limitation. Under the assumption of a constant value for the

concentration in the product phases, Hillert deduced linear Gibbs-Thomson relations for the concentrations in the parent phase

$$p^\alpha = RT H^\alpha (C_{10}^{\gamma\alpha} - C_1^{\gamma\alpha}) \quad (2.35)$$

and

$$p^\beta = RT H^\beta (C_{10}^{\gamma\beta} - C_1^{\gamma\beta}) \quad (2.36)$$

where  $H^\alpha$  and  $H^\beta$  are coefficients evaluated specifically for the unsymmetric Fe - C system. In a later section of this presentation where we will compare Hillert's result with our own symmetric result, we will evaluate  $H^\alpha$  and  $H^\beta$  on the basis of thermodynamic premises somewhat different than his. For the moment, however, we continue to follow his detailed analysis.

The complete Fourier series for the concentration in the parent phase is known, except for the coefficient  $A_0$ . We can make use of the eqs. 2.29, 2.35 and 2.36 to obtain two equations in  $A_0$ ,  $S$  and  $v$  as follows:

$$-\cos \phi^\alpha = \int_0^{\frac{S^\alpha}{2}} \frac{P}{\sigma^\alpha} dy = \frac{RT H^\alpha}{\sigma^\alpha} \int_0^{\frac{S^\alpha}{2}} (C_0^{\gamma\alpha} - C^{\gamma\alpha}) dy \quad (2.37)$$

$$= \frac{RT H^\alpha}{\sigma^\alpha} \int_0^{\frac{S^\alpha}{2}} (C_0^{\gamma\alpha} - C_\infty - \sum_{n=0}^{\infty} A_n \cos b_n y) dy \quad (2.38)$$

which, after integration, yields

$$-\frac{2 \sigma^\alpha \cos \phi^\alpha}{S^\alpha RT H^\alpha} = C_0^{\gamma\alpha} - C_\infty - A_0 - \frac{2}{S^{\alpha n=1}} \sum \frac{A_n}{b_n} \sin \pi n \frac{S^\alpha}{S} \quad (2.39)$$

A similar expression can be obtained for the  $\beta$  phase from

$$-\cos \phi^\beta = \int_{\frac{S^\alpha}{2}}^{\frac{S}{2}} \frac{P}{\sigma^\beta} dy \quad (2.40)$$

yielding

$$-\frac{2 \sigma^\beta \cos \phi^\beta}{S^\beta RT H^\beta} = C_0^{\gamma\beta} - C_\infty - A_0 - \frac{2}{S^\beta} \sum_{n=1}^{\infty} \frac{A_n}{b_n} \sin \pi n \frac{S^\alpha}{S} \quad (2.41)$$

To complete the calculations Hillert assumed that  $\lambda_n = -b_n$ . From eq. 2.5 this implies that  $2n\pi D/Sv$  is much larger than unity. This assumption has been verified in the final solution.

We can now eliminate  $C_0^{\gamma\alpha} - C_\infty - A_0$  between eqs. 2.39 and 2.41, and replace  $A_n$  from 2.34 to obtain the relation between  $v$  and  $S$  which is sought:

$$\frac{v}{D} = \pi^3 \frac{S^\alpha S^\beta}{S^2 \sum_{n=1}^{\infty} \frac{1}{n^3} \sin^2 \pi n \frac{S^\alpha}{S}} \frac{C_0^{\gamma\alpha} - C_0^{\gamma\beta}}{C_0^{\beta\gamma} - C_0^{\alpha\gamma}} \frac{1}{S} \left(1 - \frac{S_c}{S}\right) \quad (2.42)$$

where

$$S_c = \frac{-2}{RT (C_0^{\gamma\alpha} - C_0^{\gamma\beta})} \left( \frac{S \sigma^\alpha \cos \phi^\alpha}{S^\alpha H^\alpha} - \frac{S \sigma^\beta \cos \phi^\beta}{S^\beta H^\beta} \right) \quad (2.43)$$

Remembering that in Hillert's calculations  $S^\alpha$  and  $S^\beta$  are proportional to  $S$  (eq. 2.31) the relation between  $v$  and  $S$  can be summarized in the Zener expression

$$v = \Omega \frac{1}{S} \left( 1 - \frac{S_c}{S} \right) \quad (2.44)$$

which is represented schematically in Fig. 4.

The driving free energy for this reaction is

$$\Delta F = \Delta F^0 \left( 1 - \frac{S_c}{S} \right) \quad (2.45)$$

where  $\Delta F^0$  is a function of temperature only. Hence at constant temperature the rate of entropy production is<sup>12</sup>

$$\frac{dS}{dt} \propto v \Delta F \propto \frac{1}{S} \left( 1 - \frac{S_c}{S} \right)^2 \quad (2.46)$$

which maximizes at  $S = 3 S_c$ . Note that this is consistent with our general proposition (eq. 1.2) since  $S(v_{\max}) = 2 S_c$ .

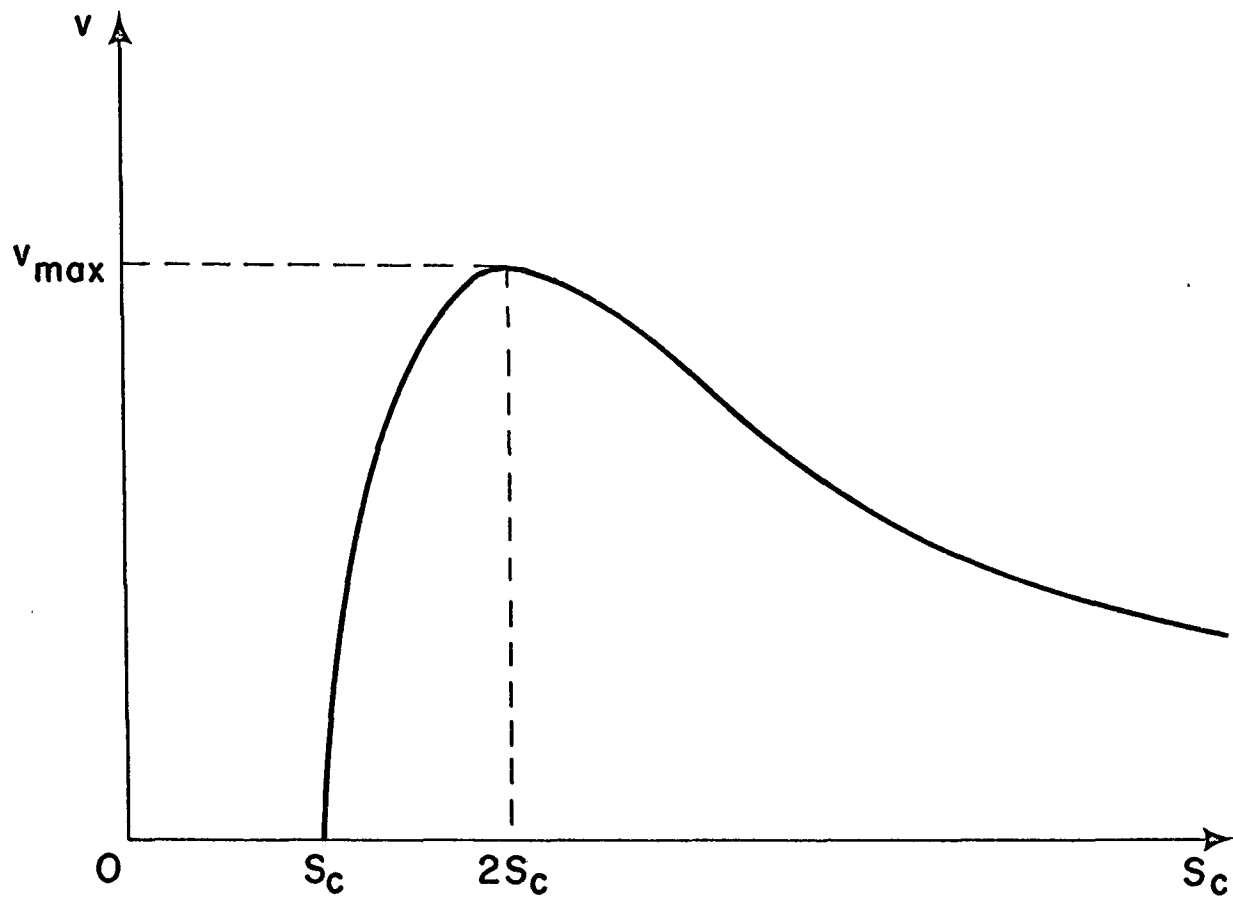


Fig. 4: Schematic variation of  $v$  as a function of  $S$  (after Hillert).

## II.C REVISED SOLUTION - FIRST THERMODYNAMIC VERSION

## 1/ GENERAL TREATMENT

We now remove the assumption that the concentrations in the precipitate phases  $\alpha$  and  $\beta$  are constant with changes in the pressure so that we are no longer allowed to use the lever rule as formulated in eq. 2.31. Eq. 2.21 gives us as a Fourier series in  $y$  the concentrations in either precipitate phase. We designate these as  $C_p$ . We have now to satisfy the thermodynamic requirement of equal activities on both sides of the interface for a given  $y$ . In this section we use the thermodynamic proposition 2.8 with the Gibbs-Thomson equations 2.9 and 2.10. That is to say we are assuming that the members of a certain pair of partition ratios are independent of pressure. The two ratios 2.8

$$K^\alpha = \frac{C_1^{\alpha\gamma}}{C_1^{\gamma\alpha}} \quad \text{and} \quad K^\beta = \frac{C_1^{\beta\gamma}}{C_1^{\gamma\beta}} \quad (2.47a;b)$$

give us

$$\frac{C_p}{C} \equiv K(y) = \begin{cases} K^\alpha & \text{when } -\frac{S^\alpha}{2} < y < \frac{S^\alpha}{2} \\ K^\beta & \text{when } \frac{S^\alpha}{2} < y < \frac{S^\alpha}{2} + S^\beta \end{cases} \quad (2.48)$$

It is to be particularly noted that this choice of pressure independent partition ratios implies a free energy curve for the  $\gamma$ -phase which is highly unsymmetric so the results of this calculation lack generality. We use it here mainly to demonstrate methodology.

The ratio eq. 2.48 is a step function in  $y$  which from Appendix III can be written as

$$\frac{C_p}{C} = \frac{K^\alpha + K^\beta}{2} + \frac{2(K^\alpha - K^\beta)}{\pi} \sum_{n=1}^{\infty} \left( \frac{1}{n} \sin \pi n \frac{S^\alpha}{S} \right) \cos b_n y \quad (2.49)$$

$$= \sum_{n=0}^{\infty} a_n \cos b_n y \quad (2.50)$$

From eq. 2.3 and eq. 2.25 we then deduce that

$$C = C_\infty + \sum_{n=0}^{\infty} A_n \cos b_n y \quad (2.51)$$

$$C_p = C_\infty + \frac{D}{V} \sum_{n=1}^{\infty} \frac{A_n b_n^2}{\lambda_n} \cos b_n y \quad (2.52)$$

which we can substitute into eq. 2.50 to yield

$$\sum_{n=0}^{\infty} a_n \cos b_n y = \frac{C_\infty + \frac{D}{V} \sum_{n=1}^{\infty} \frac{A_n b_n^2}{\lambda_n} \cos b_n y}{C_\infty + \sum_{n=0}^{\infty} A_n \cos b_n y} \quad (2.53)$$

where the  $a_n$  are given by eq. 2.49.

This expression allows us to calculate all the coefficients  $A_n$  by multiplication and identification of the coefficients of  $\cos b_n y$ . In principle, we can perform the calculations for any  $n$ .

Expression 2.52 has been evaluated to the second order in  $n$  in Appendix IV, and we write here the resulting expressions for  $A_0$ ,  $A_1$  and  $A_2$  (IV. 13)

$$A_0 = C_\infty \left[ \frac{(2a_0 + \frac{8\pi D}{Sv}) (2a_0 + a_2 + \frac{4\pi D}{Sv}) - (a_1 + a_3)^2}{\mathcal{D}} - 1 \right] \quad (2.54a)$$

$$A_1 = 2C_\infty \frac{(a_1 + a_3) a_2 - (2a_0 + \frac{8\pi D}{Sv}) a_1}{\mathcal{D}} \quad (2.54b)$$

$$A_2 = 2C_\infty \frac{(a_1 + a_3) a_1 - (2a_0 + a_2 + \frac{4\pi D}{Sv}) a_2}{\mathcal{D}}$$

where

$$\begin{aligned} \mathcal{D} = a_0 (2a_0 + \frac{8\pi D}{Sv}) (2a_0 + a_2 + \frac{4\pi D}{Sv}) - a_0 (a_1 + a_3) + 2a_1 a_2 (a_1 + a_3) \\ - a_1^2 (2a_0 + \frac{8\pi D}{Sv}) - a_2^2 (2a_0 + a_2 + \frac{4\pi D}{Sv}) \end{aligned} \quad (2.55)$$

In our expression for the coefficients we have three unknowns:  $v$ ,  $S$  and  $\frac{S^\alpha}{S}$ . We can obtain two relations between these variables by use of the second boundary condition as implied in eqs. 2.29. From this point, we shall always express  $P$  as a function of the concentrations in the precipitate phases. This has the advantage that  $P$  is always a linear



function of the concentrations and that the term in  $A_0$  is automatically excluded from the  $v$ ,  $S$  and  $S^\alpha/S$  relationship.

Thus, from eq. 2.9 and 2.29a we deduce

$$-\cos \phi^\alpha = \int_0^{\frac{S^\alpha}{2}} \frac{P}{\sigma^\alpha} dy = -\frac{h^\alpha RT}{\sigma^\alpha} \int_0^{\frac{S^\alpha}{2}} (C_p - C_{10}^{\alpha\gamma}) dy \quad (2.56)$$

and from the expression 2.52

$$\cos \phi^\alpha = \frac{h^\alpha RT}{\sigma^\alpha} \int_0^{\frac{S^\alpha}{2}} (C_\infty - C_{10}^{\alpha\gamma} + \frac{D}{v} \sum_{n=1}^{\infty} \frac{A_n b_n}{\lambda_n} \cos b_n y) dy \quad (2.57)$$

Finally

$$-\frac{\sigma^\alpha \cos \phi^\alpha}{h^\alpha RT} + (C_\infty - C_{10}^{\alpha\gamma}) \frac{S^\alpha}{2} = -\frac{D}{v} \sum_{n=1}^{\infty} \frac{A_n b_n}{\lambda_n} \sin \pi n \frac{S^\alpha}{S} \quad (2.58)$$

We can achieve similar results for the  $\beta$  lamella where

$$-\cos \phi^\beta = \int_{\frac{S^\alpha}{2}}^{\frac{S}{2}} \frac{P}{\sigma^\beta} dy = -\frac{h^\beta RT}{\sigma^\beta} \int_{\frac{S^\alpha}{2}}^{\frac{S}{2}} (C_p - C_{10}^{\beta\gamma}) dy \quad (2.59)$$

and

$$-\frac{\sigma^\beta \cos \phi^\beta}{h^\beta RT} + (C_\infty - C_{10}^{\beta\gamma}) \frac{S^\beta}{2} = \frac{D}{v} \sum_{n=1}^{\infty} \frac{A_n b_n}{\lambda_n} \sin \pi n \frac{S^\alpha}{S} \quad (2.60)$$

With the eqs. 2.58 and 2.60 we have a second relation between  $v$ ,  $S$  and  $\frac{S^\alpha}{S}$ . We can express these in a simpler form, if we add eqs. 2.58 and 2.60 to give

$$-\frac{\sigma^\alpha \cos \phi^\alpha}{h^\alpha RT} - \frac{\sigma^\beta \cos \phi^\beta}{h^\beta RT} + (C_\infty - C_0^\alpha) \frac{S^\alpha}{2} + (C_\infty - C_0^\beta) \frac{S^\beta}{2} = 0 \quad (2.61)$$

and, if we divide eqs. 2.58 and 2.60, respectively, by  $(C_\infty - C_{10}^{\alpha\gamma})/2$  and  $(C_\infty - C_{10}^{\beta\gamma})/2$  and add the two resulting equations, to give

$$-\frac{2}{RT} \left[ \frac{\sigma^\alpha \cos \phi^\alpha}{h^\alpha (C_\infty - C_{10}^{\alpha\gamma})} + \frac{\sigma^\beta \cos \phi^\beta}{h^\beta (C_\infty - C_{10}^{\beta\gamma})} \right] + S = \frac{2D}{v} \left( \frac{1}{C_\infty - C_{10}^{\beta\gamma}} - \frac{1}{C_\infty - C_{10}^{\alpha\gamma}} \right) . \quad (2.62)$$

$$\sum_{n=1}^{\infty} \frac{A_n b_n}{\lambda_n} \sin \pi n \frac{S^\alpha}{S}$$

In eq. 2.61 we recognize the equivalent of the lever rule to which it reduces in the particular case where

$$\frac{\sigma^\alpha \cos \phi^\alpha}{h^\alpha} + \frac{\sigma^\beta \cos \phi^\beta}{h^\beta} = 0 \quad (2.63)$$

This condition is fulfilled, in particular, when we have a symmetrical condition regarding the mechanical and thermodynamic properties of the two phases  $\alpha$  and  $\beta$ . This is a very exceptional case.

We can also write equation 2.61 in an equivalent form, where

$S^\beta$  is not explicit. By substitution of  $S^\beta = S - S^\alpha$  we get:

$$-\frac{2}{RT} \left( \frac{\sigma^\alpha \cos \phi^\alpha}{h^\alpha} + \frac{\sigma^\beta \cos \phi^\beta}{h^\beta} \right) = (C_{10}^{\beta\gamma} - C_\infty) S + (C_{10}^{\alpha\gamma} - C_{10}^{\beta\gamma}) S^\alpha \quad (2.64)$$

and, after division by  $S$ , we obtain:

$$S = -\frac{2}{RT} \frac{\frac{\sigma^\alpha \cos \phi^\alpha}{h^\alpha} + \frac{\sigma^\beta \cos \phi^\beta}{h^\beta}}{(C_{10}^{\beta\gamma} - C_\infty) + (C_{10}^{\alpha\gamma} - C_{10}^{\beta\gamma}) \frac{S^\alpha}{S}} \quad (2.65)$$

provided that

$$(C_{10}^{\beta\gamma} - C_\infty) + (C_{10}^{\alpha\gamma} - C_{10}^{\beta\gamma}) \frac{S^\alpha}{S} \neq 0 \quad (2.66)$$

The equality in eq. 2.66 occurs in the case where we have a symmetric diagram and properties and  $x_\infty = 0.5$ . We then obtain directly from 2.61,  $S^\alpha = S^\beta$ .

We can see in eq. 2.65 that the velocity  $v$  does not appear explicitly since the coefficients  $A_n$  have disappeared. It constitutes, therefore, a relationship of the hyperbolic form between  $S$  and  $S^\alpha/S$  only. Eq. 2.62 evaluated by the substitution of the  $A_n$  given by the expressions 2.54 yields the dependence of  $v$  on  $S$  and  $S^\alpha/S$ .

In summary, if we plot  $v$  along a vertical axis and  $S$  and  $S^\alpha/S$  along the axis of a horizontal plane, eq. 2.62 represents a surface (designated as surface I) as shown in Fig. 5. The construction of this

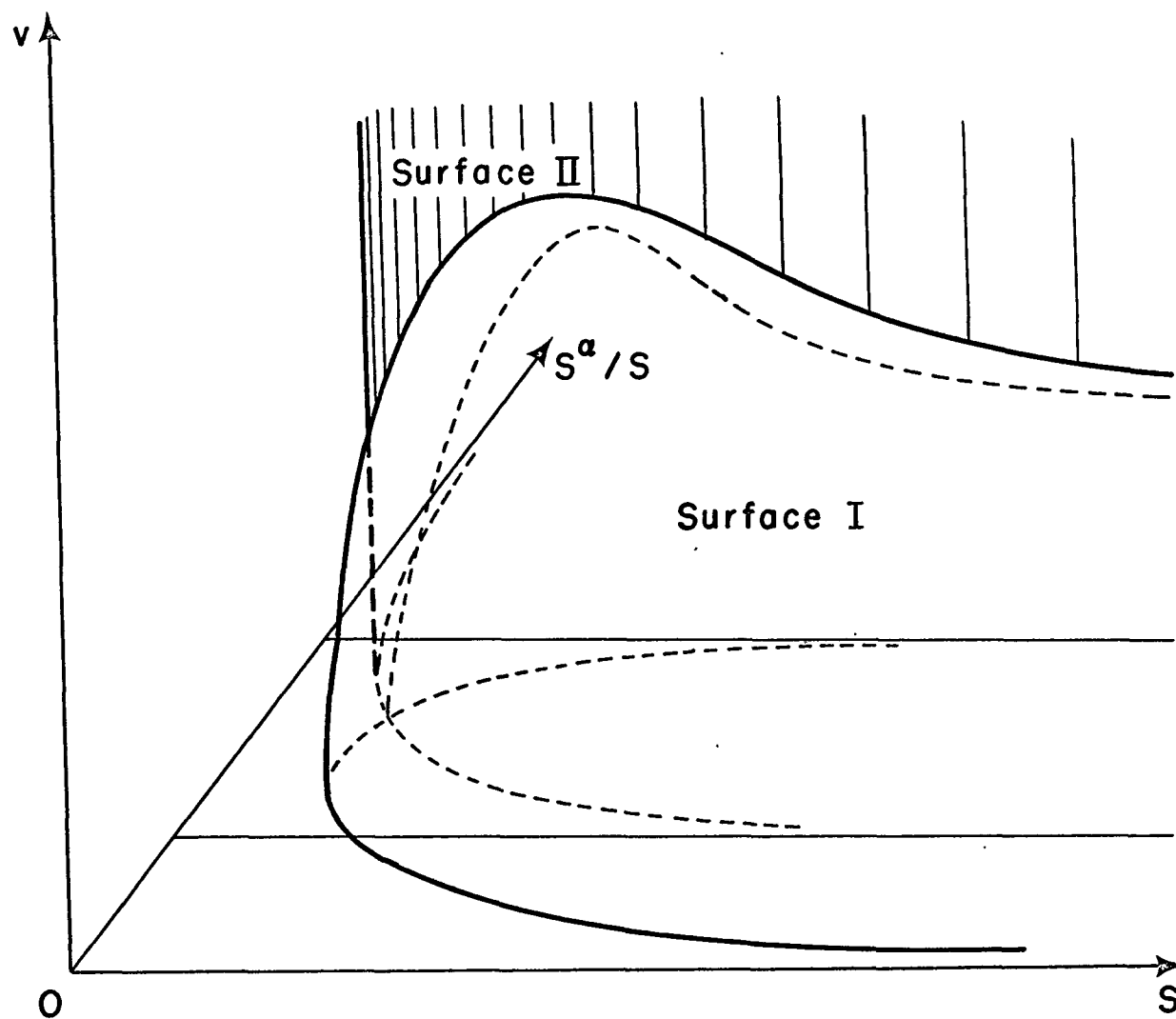


Fig. 5: Schematic variation of  $v$  as a function of  $S$  and  $S^\alpha/S$  from our own general standpoint.

surface is deduced from our calculations in Appendix IV where the coefficients have been evaluated to the second harmonic. It is a periodic surface in  $S^\alpha/S$  so we need only be concerned with the part of the surface for  $0 < S^\alpha/S < 1$ . For the sake of clarity we have only included that part of the surface which gives positive values of  $v$  and  $S$ . All intersections of the surface I with planes  $S^\alpha/S = \text{constant}$  are curves similar in shape to the one sketched in Fig. 5.

We note now that eq. 2.65 represents in the same space a cylinder (designated as surface II) parallel to the vertical axis. The surfaces I and II intersect along a curve of the space. Since by proposition eq. 2.2, we are seeking the point of maximum velocity we must find the highest point of this curve of intersection. This will give us simultaneously the lamellar spacings and the ratios  $S^\alpha/S$ .

From the shape of surface II we can readily see that very small variations of  $S^\alpha/S$  can induce considerable changes in the values of  $S$  and  $v$ . The value of  $S$  which corresponds to the maximum of the curve of intersection may be markedly larger than values suggested by a Hillert type calculation, particularly in the general unsymmetric case.

## 2/ SYMMETRIC LAMELLAR CONFIGURATION

In Appendix V we have examined the symmetrical configuration in some detail. This situation, although very restrictive with respect to its physical application, allowed us to perform the calculations completely and obtain some transparent and informative results. We recall here the

most significant conclusions.

The calculations up to the second harmonic revealed that the phase diagram must fulfill certain conditions to sustain steady state lamellar precipitation. In the notation

$$x = x_{10}^{\alpha\gamma} \quad ; \quad y = x_{10}^{\gamma\alpha} \quad : \quad x_{\infty} = \frac{1}{2} \quad (2.67a;b;c)$$

and for the symmetric phase diagram as shown on Fig. 6 the conditions are expressed by

$$y > \frac{1}{2} \quad (2.68)$$

$$x_{\min} < x < \frac{1}{2} \quad (2.69)$$

where

$$x_{\min} = \frac{1}{4} \left\{ (2 + K^{\alpha}) - \sqrt{(2 + K^{\alpha})^2 - 4 \left[ 1 + K^{\alpha} - (1 - K^{\alpha}) \frac{8}{\pi} \right]} \right\} \quad (2.70)$$

Condition 2.68 states the obvious: that we must have an undercooling. Condition 2.69 states that the solubility  $x$  in the  $\alpha$  phase must be between a minimum value ( $\sim 0.1$ ) and  $\frac{1}{2}$ . This condition could be in contradiction to our thermodynamic requirement that the solubility be small. We have not been able to decide if this latter condition is general because it was derived from calculations performed to a limited harmonic. As we shall see in the following sections for more general thermodynamic assumptions the restriction for a symmetric diagram does not appear.

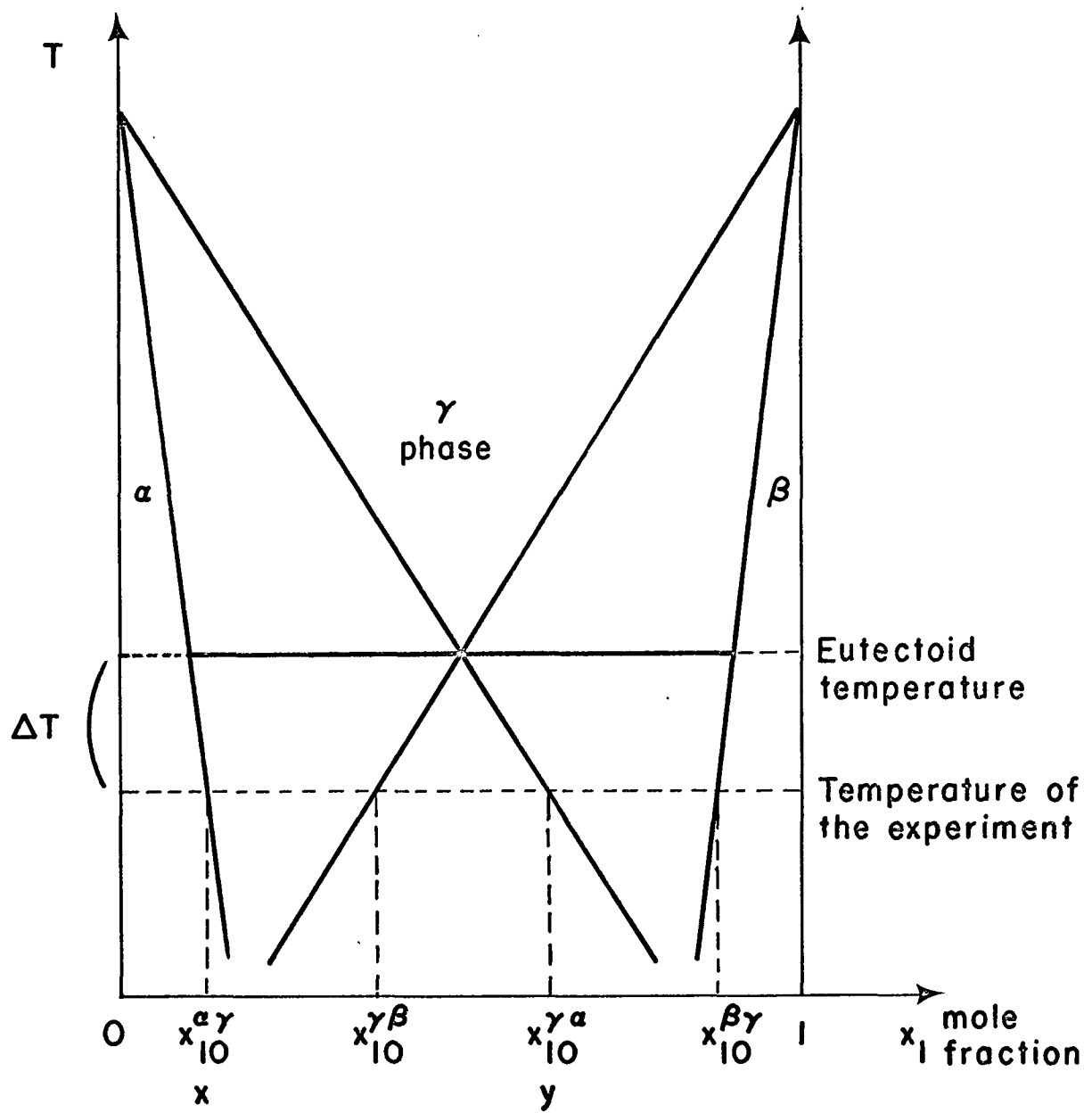


Fig. 6: Schematic symmetric binary eutectoid phase diagram.

## II.D REVISED SOLUTION - SECOND THERMODYNAMIC VERSION

## 1/ GENERAL TREATMENT

As demonstrated in Appendix II, the relation between the compositions of the two phases in equilibrium can be advantageously and rather generally represented by

$$\frac{x_1^{\gamma\alpha}}{x_1^{\alpha\gamma}} \frac{x_2^{\alpha\gamma}}{x_2^{\gamma\alpha}} = x^\alpha \quad (2.71)$$

This "complex ratio", when assumed to be independent of the pressure, allows us to accommodate thermodynamic symmetry in both the composition and pressure coordinates. This "complex ratio" can be expressed by Fourier series expansion as

$$\frac{C(1-C_p)}{C_p(1-C)} = x(y) \quad (2.72)$$

where  $x(y)$  is a step function in  $y$  having the values:

$$x(y) = \begin{cases} x^\alpha & \text{when } -\frac{S^\alpha}{2} < y < \frac{S^\alpha}{2} \\ x^\beta & \text{when } \frac{S^\alpha}{2} < y < \frac{S^\alpha}{2} + S^\beta \end{cases} \quad (2.73)$$



As in section II.C, where we had a simpler ratio, we are able in principle to determine all the coefficients of the Fourier series. However, even limiting ourselves to low orders of expansion, the resolution of the equations for the A's becomes intractable. Nonetheless, we shall show below that the ratio (eq. 2.71) can still be used with the help of a simplification. Indeed if we replace  $x_1^{\alpha\gamma}$ ,  $x_1^{\gamma\alpha}$ ,  $x_2^{\alpha\gamma}$  and  $x_2^{\gamma\alpha}$  in relation 2.71 by

$$x_1^{\alpha\gamma} = x_{10}^{\alpha\gamma} + \Delta x_1^{\alpha\gamma} \quad x_2^{\alpha\gamma} = x_{20}^{\alpha\gamma} - \Delta x_1^{\alpha\gamma} \quad (2.74a;b)$$

$$x_1^{\gamma\alpha} = x_{10}^{\gamma\alpha} + \Delta x_1^{\gamma\alpha} \quad x_2^{\gamma\alpha} = x_{20}^{\gamma\alpha} - \Delta x_1^{\gamma\alpha} \quad (2.74c;d)$$

equation 2.71 becomes

$$\frac{x_{10}^{\gamma\alpha} + \Delta x_1^{\gamma\alpha}}{x_{10}^{\alpha\gamma} + \Delta x_1^{\alpha\gamma}} \frac{x_{20}^{\alpha\gamma} - \Delta x_1^{\alpha\gamma}}{x_{20}^{\gamma\alpha} - \Delta x_1^{\gamma\alpha}} = x^\alpha \quad (2.75)$$

By multiplication and retention of increments up to the first power we get

$$\frac{x_{10}^{\gamma\alpha} x_{20}^{\alpha\gamma} - x_{10}^{\gamma\alpha} \Delta x_1^{\alpha\gamma} + x_{20}^{\alpha\gamma} \Delta x_1^{\gamma\alpha}}{x_{10}^{\alpha\gamma} x_{20}^{\gamma\alpha} + x_{20}^{\gamma\alpha} \Delta x_1^{\alpha\gamma} - x_{10}^{\alpha\gamma} \Delta x_1^{\gamma\alpha}} = x^\alpha \quad (2.76)$$

and

$$x_{10}^{\gamma\alpha} x_{20}^{\alpha\gamma} - x^\alpha x_{10}^{\gamma\alpha} x_{20}^{\alpha\gamma} = 0 = \Delta x_1^{\alpha\gamma} (x_{10}^{\gamma\alpha} + x^\alpha x_{20}^{\alpha\gamma}) - \Delta x_1^{\gamma\alpha} (x_{20}^{\alpha\gamma} + x^\alpha x_{10}^{\alpha\gamma}) \quad (2.77)$$

and finally we obtain

$$\frac{\Delta x_1^{\alpha\gamma}}{\Delta x_1^{\gamma\alpha}} = \frac{x_1^{\alpha\gamma} - x_{10}^{\alpha\gamma}}{x_1^{\gamma\alpha} - x_{10}^{\gamma\alpha}} = \frac{x_{20}^{\alpha\gamma} + x^\alpha x_{10}^{\alpha\gamma}}{x_{10}^{\gamma\alpha} + x^\alpha x_{20}^{\gamma\alpha}} = K_\alpha \quad (2.78)$$

Similarly for the  $\gamma$  and  $\beta$  phases we have in the notation of (II, 12)

$$\frac{x_1^{\beta\gamma} - x_{10}^{\beta\gamma}}{x_1^{\gamma\beta} - x_{10}^{\gamma\beta}} = \frac{x_{20}^{\beta\gamma} + \frac{1}{x^\beta} x_{10}^{\beta\gamma}}{x_{10}^{\gamma\beta} + \frac{1}{x^\beta} x_{20}^{\gamma\beta}} = K_\beta \quad (2.79)$$

It follows from eqs. 2.78 and 2.79 that eq. 2.72 can be replaced by

$$\frac{C_p - C_{p0}}{C - C_0} = K \quad (2.80)$$

where  $C$  and  $C_p$  are Fourier series expressed in eqs. 2.51 and 2.52 while  $C_0$ ,  $C_{p0}$  and  $K$  are step functions having the values

$$C_0 = \begin{bmatrix} C_0^{\gamma\beta} \\ C_0^{\beta\gamma} \end{bmatrix} \quad C_{p0} = \begin{bmatrix} C_{p0}^{\alpha\gamma} \\ C_{p0}^{\beta\gamma} \end{bmatrix} \quad K = \begin{bmatrix} K_\alpha & \text{when } -\frac{S^\alpha}{2} < y < \frac{S^\alpha}{2} \\ K_\beta & \text{when } \frac{S^\alpha}{2} < y < \frac{S^\alpha}{2} + S^\beta \end{bmatrix} \quad (2.81a;b;c)$$

In the case of a symmetric diagram  $x^\alpha = x^\beta$  (Appendix II) and from Fig. 6 and eqs. 2.78 and 2.79 we immediately see that  $K_\alpha = K_\beta$ .

Referring to Appendix III the Fourier coefficients of the step function are defined by

$$C_0 = \sum_{n=0}^{\infty} \alpha_n \cos b_n y \quad C_{p0} = \sum_{n=0}^{\infty} \alpha'_n \cos b_n y' \quad (2.82)$$

and expressed as

$$\alpha_0 = \frac{C_0^{\gamma\alpha} + C_0^{\gamma\beta}}{2} \quad \text{and} \quad \alpha_n = \frac{2(C_0^{\gamma\beta} - C_0^{\gamma\alpha})}{n\pi} \sin \pi n \frac{S^\alpha}{S} \quad (2.83a;b)$$

$$\alpha'_0 = \frac{C_0^{\alpha\gamma} + C_0^{\beta\gamma}}{2} \quad \text{and} \quad \alpha'_n = \frac{2(C_0^{\beta\gamma} - C_0^{\alpha\gamma})}{n\pi} \sin \pi n \frac{S^\alpha}{S} \quad (2.84a;b)$$

while K is developed with the same expression as found in eqs. 2.49 and 2.50. Substituting these expressions in eq. 2.80 we can calculate the coefficients  $A_n$  (see Appendix VI) as

$$A_0 = \alpha_0 - C_\infty + \frac{1}{2D} \left\{ \left[ (2a_0 + a_2 + \frac{4\pi D}{Sv}) (2a_0 + \frac{8\pi D}{Sv}) - (a_1 + a_3)^2 \right] X_1 - a_1 (2a_0 + \frac{8\pi D}{Sv}) - (a_1 + a_3) a_2 X_2 \right. \quad (2.85a)$$

$$\left. + a_1 (a_1 + a_3) - a_2 (2a_0 + a_2 + \frac{4\pi D}{Sv}) \right] X_3 \}$$

$$A_1 = \alpha_1 + \frac{1}{2D} \left\{ [a_2 (a_1 + a_3) - a_1 (2a_0 + \frac{8\pi D}{Sv})] X_1 + [a_0 (2a_0 + \frac{8\pi D}{Sv}) - a_2^2] X_2 - [a_0 (a_1 + a_3) - a_1 a_2] X_3 \right\} \quad (2.85b)$$

$$A_2 = \alpha_2 + \frac{1}{2D} \left\{ [a_1 (a_1 + a_3) - a_2 (2a_0 + a_2 + \frac{4\pi D}{Sv})] X_1 - [a_0 (a_1 + a_3) - a_1 a_2] X_2 \right. \quad (2.85c)$$

$$\left. + [a_0 (2a_0 + a_2 + \frac{4\pi D}{Sv}) - a_1^2] X_3 \right\}$$

where:

$$\mathcal{D} = a_0 \left(2a_0 + \frac{8\pi D}{Sv}\right) \left(2a_0 + a_2 + \frac{4\pi D}{Sv}\right) - a_0 (a_1 + a_3)^2 + 2a_1 a_2 (a_1 + a_3) - a_1^2 \left(2a_0 + \frac{8\pi D}{Sv}\right) - a_2^2 \left(2a_0 + a_2 + \frac{4\pi D}{Sv}\right) \quad (2.86)$$

the  $a_1$  are given by eqs. 2.49 and 2.50 and

$$x_1 = 2(C_\infty - \alpha'_0) \quad (2.87a)$$

$$x_2 = -2 \left(\frac{2\pi D}{Sv} \alpha_1 + \alpha'_1\right) \quad (2.87b)$$

$$x_3 = -2 \left(\frac{4\pi D}{Sv} \alpha_2 + \alpha'_2\right) \quad (2.87c)$$

The boundary condition eq. 2.29 at the junction of the two precipitate lamellae provides us with two relations between the parameters  $v$ ,  $S$  and  $\frac{S^\alpha}{S}$  upon substitution of the expressions 2.85 for the coefficients  $A_0$ ,  $A_1$  and  $A_2$ . As in the previous section, eqs. 2.29 and 2.30 yield in combination with eqs. 2.14 and 2.15 the relations

$$-\frac{\sigma^\alpha \cos \phi^\alpha}{k^\alpha RT} - \frac{\sigma^\beta \cos \phi^\beta}{k^\beta RT} + (C_\infty - C_{10}^{\alpha\gamma}) \frac{S^\alpha}{2} + (C_\infty - C_{10}^{\beta\gamma}) \frac{S^\beta}{2} = 0 \quad (2.88)$$

and

$$-\frac{2}{RT} \left[ \frac{\sigma^\alpha \cos \phi^\alpha}{k^\alpha (C_\infty - C_{10}^{\alpha\gamma})} + \frac{\sigma^\beta \cos \phi^\beta}{k^\beta (C_\infty - C_{10}^{\beta\gamma})} \right] + S = \quad (2.89)$$

(over)

$$\frac{2D}{v} \left( \frac{1}{C_{\infty} - C_{10}^{\beta\gamma}} - \frac{1}{C_{\infty} - C_{10}^{\alpha\gamma}} \right) \sum_{n=1}^{\infty} \frac{A_n b_n}{\lambda^n} \sin \pi n \frac{S^{\alpha}}{S}$$

If we substitute  $A_1$  and  $A_2$  according to their general expressions we obtain as before two equations for the surfaces I and II (Fig. 5). To determine the maximum lamellar growth rate we must find the highest point of intersection of these two surfaces.

## 2/ SYMMETRIC LAMELLAR CONFIGURATION

As an illustration we have again chosen a symmetrical configuration wherein the surface tensions  $\sigma^{\alpha}$  and  $\sigma^{\beta}$  are equal, the phase diagram is symmetric and  $x_{\infty} = \frac{1}{2}$  as specified on Fig. 6.

In this case eq. 2.88 becomes trivial and we have

$$S^{\alpha} = S^{\beta} \tag{2.90}$$

and, in eq. 2.89 the coefficients for even  $n$  vanish. In fact, the calculations of the coefficients  $A_n$  can now be easily performed to any order as demonstrated in Appendix VII. In particular,

$$A_{2i-1} = \frac{2}{\pi} \left[ K(C_{10}^{\gamma\alpha} - C_{10}^{\gamma\beta}) - (C_{10}^{\alpha\gamma} - C_{10}^{\beta\gamma}) \right] \frac{1}{2^{i-1}} \frac{\sin (2i-1)\frac{\pi}{2}}{K + \frac{2\pi D}{Sv} (2i-1)} \tag{2.91a}$$

and

$$A_{2i} = 0 \quad (2.91b)$$

where

$$K = \frac{x_{20}^{\alpha\gamma} + x^{\alpha} x_{10}^{\alpha\gamma}}{x_{10}^{\gamma\alpha} + x^{\alpha} x_{20}^{\gamma\alpha}} = \frac{x_{20}^{\beta\gamma} + \frac{1}{x^{\beta}} x_{10}^{\beta\gamma}}{x_{10}^{\gamma\beta} + \frac{1}{x^{\beta}} x_{20}^{\gamma\beta}} \quad (2.92)$$

Eq. 2.89 becomes

$$\frac{\phi}{S} + 1 = C' Z \sum_{n=1}^{\infty} \frac{1}{(2i-1) [1 + Z(2i-1)]} \quad (2.93)$$

where

$$Z = X/K, \quad (2.94)$$

the quantity

$$X = \frac{2\pi D}{Sv} \quad (2.95a)$$

being a standard dimensionless quantity in calculations of this kind,

$$\phi = - \frac{4}{RT} \frac{\sigma^{\alpha} \cos \phi^{\alpha}}{K_{\alpha} (C_{\infty} - C_{10}^{\alpha\gamma})} \quad (2.95b)$$

and

$$C' = - \frac{4}{\pi^2} \frac{K(C_{10}^{\gamma\alpha} - C_{10}^{\gamma\beta}) - (C_{10}^{\alpha\gamma} - C_{10}^{\beta\gamma})}{C_{\infty} - C_{10}^{\beta\gamma}} \quad (2.95c)$$

If we divide both members of eq. 2.93 by  $C'$  we obtain

$$\frac{1}{C'} \left( \frac{\phi}{S} + 1 \right) = \sum_{i=1}^{\infty} \frac{Z}{(2i - 1) [1 + Z(2i - 1)]} \quad (2.96)$$

The right hand side of eq. 2.96 is a universal function of  $Z$  which we designate as

$$f(Z) = \sum_{i=1}^{\infty} \frac{Z}{(2i - 1) [1 + Z(2i - 1)]} \quad (2.97)$$

This function has been computed and is recorded in Table 1 for different values of  $Z$ . The series is very slowly convergent, particularly for large values of  $Z$  so it was necessary for large  $Z$  to perform the calculation to very large values of  $i$  ( $i = 5,000$ ) to be sure of the fourth significant figure.

Subject to the assumption that  $1/Z$  is much smaller than unity we have shown in Appendix VII that eq. 2.96 leads to the very simple  $v(S)$  relation,

$$v = \Omega' \frac{1}{S} \frac{1 - \frac{S}{C}}{1 + \frac{\phi'}{S}} \quad (2.98)$$

where

Table 1

Z	f(Z)	Z	f(Z)	Z	f(Z)
1	0.6931	20	1.1835	300	1.2302
2	0.8776	30	1.1997	400	1.2311
3	0.9679	40	1.2080	500	1.2316
4	1.0216	50	1.2130	600	1.2319
5	1.0572	60	1.2164	700	1.2322
6	1.0826	70	1.2189	800	1.2324
7	1.1016	80	1.2207	900	1.2325
8	1.1163	90	1.2221	1000	1.2326
9	1.1281	100	1.2233	2000	1.2331
10	1.1377	200	1.2284	3000	1.2333

Tabulation of the function  $f(Z)$



$$\Omega' = \frac{2\pi D}{K} \frac{C' \frac{\pi^2}{8} - 1}{1 - 0.1819 C'} \quad (2.99a)$$

$$S_c = \frac{\phi}{C' \frac{\pi^2}{8} - 1} \quad (2.99b)$$

$$\phi' = \frac{\phi}{1 - 0.1819 C'} \quad (2.99c)$$

and  $C'$  is still given by eq. 2.94c.

This relation should be compared with eq. 2.44 due to Hillert. The two relations are identical if we set  $\phi = 0$ . An extensive interpretation of this result is to be found in the discussion given below.

The precise relation between  $v$  and  $S$  cannot be obtained analytically when we retain the complete series of eq. 2.93. Nonetheless, we have demonstrated in Appendix VII that we can exactly evaluate the critical lamellar spacing which reduces the velocity to zero. Interestingly, this is given by the same expression as in the approximation, eq. 2.99b.

In Appendix VIII, we briefly demonstrate that this critical lamellar spacing is identical to the one given by Hillert provided that we choose the same influence of the pressure on the concentrations in the parent phase. This demonstrates that the consideration of segregation in the precipitate phases introduces a significant variation of the expression for the velocity through the terms  $\phi'$  or  $\phi$  as shown in eq. 2.98. The segregation, however, does not alter the value of the spacing which reduces  $v$  to zero. This will be further commented upon in our general discussion.

We take again the convention expressed by eq. 2.67 and as illustrated in Fig. 6. We have demonstrated in Appendix VII that when  $i$  goes to infinity, there exists a condition imposed on the diagram eqs. VII.49 and VII.50, i.e.,

$$\frac{x(1-x)(1-2y)}{y(1-y)(1-2x)} < 0 \quad (2.100)$$

or equivalently, since  $x$ ,  $y$ ,  $1-x$  and  $1-y$  are positive quantities, we have:

$$(1-2x)(1-2y) < 0 \quad (2.101)$$

We can see that this condition does not introduce any physical restrictions. It simply states that there is an undercooling since  $y$  is larger than  $\frac{1}{2}$  and that the solubility in the  $\alpha$  phase is below  $\frac{1}{2}$ . We can anticipate that for non-symmetrical configurations inequality (eq. 2.101) will impose conditions on the original composition. This important result has never been suggested by any previous theory.

$S_c$  can also be expressed in terms of the parameters  $x$  and  $y$  by transforming eq. VII.55 to

$$S_c = \frac{8}{RT} \sigma^\alpha \cos \phi^\alpha \frac{y(1-y)^2}{(1-x)(y-x)(1-2y)} \quad (2.102)$$

We clearly see that  $S_c$  goes to infinity when  $y$  approaches the value  $\frac{1}{2}$  (no undercooling). This expression also requires that  $S_c$  go to zero

as  $y$  approaches unity, a possibility which is denied both by thermodynamics and by our low supersaturation requirement. That is to say, this extreme overextends the valid limits of our thermodynamic approximation.

### 3/ PHYSICAL SIGNIFICANCE OF $\phi$ AND $S_c$

The great similarity of our result (eq. 2.98) to Hillert's relation

$$v = \Omega \frac{1}{S} \left(1 - \frac{S_c}{S}\right) \quad (2.103)$$

makes it clear that the new factor  $\phi$  is uniquely related to the precipitate segregation accounted for in our calculation. We note that for the symmetric case that the effect of  $\phi$  is negligible if the terminal solubilities are small ( $x \rightarrow 0$ ), a fact of which Hillert was well aware<sup>30</sup>. When the undercooling is large, the velocity is large and the stable spacing correspondingly small, and  $\phi$  is large as we might expect intuitively for the segregation.

Most remarkably, we note for the symmetric case that the critical spacing  $S_c$  is independent of the presence or size of the  $\phi$  term (see Appendix VII). As we shall see below, this is simply because all segregation vanishes in the critical state ( $S = S_c$ ).

Pursuing this further in the symmetrical configuration and from eq. 2.94b we obtain the expression for  $\phi$

$$\phi = - \frac{4}{RT} \frac{\sigma^\alpha \cos \phi^\alpha}{k^\alpha (C_\infty^\alpha - C_{10}^{\alpha\gamma})} \quad (2.104)$$

Furthermore from eq. 2.29 combined with eq. 2.14 we have

$$\frac{\sigma^\alpha \cos \phi^\alpha}{RT k^\alpha} = - \int_0^{\frac{S^\alpha}{2}} (C_{10}^{\alpha\gamma} - C_1^{\alpha\gamma}) dy \quad (2.105)$$

so we can write  $\phi$  in the equivalent form

$$\phi = 4 \frac{\int_0^{\frac{S^\alpha}{2}} (C_{10}^{\alpha\gamma} - C_1^{\alpha\gamma}) dy}{C_\infty - C_{10}^{\alpha\gamma}} \quad (2.106)$$

From this expression we can see directly that  $\phi$  is intimately connected with the variations of composition along the interface in the precipitate phase. We see also from eqs. 2.104 and 2.105 that  $\phi$  is an important invariant of the system for the limit of the integral and  $C_1^{\alpha\gamma}$  are variables depending on the spacing  $S$ .

Referring to the free energy composition diagram of Fig. 7 and the locus of the contact points 6-1, which is close to a straight line, we see that the integral in eq. 2.107 is proportional to the free energy decrement associated with the reduced curvature as point  $y$  moves away from the triple point  $x_{1t}^{\alpha\gamma}$ .  $\phi$  must, therefore, be associated with the equal and opposite increment of free energy of solute enrichment which nature provides to compensate for the loss of curvature while attempting to maintain the free energy per unit volume as a constant in  $y$ .

Now when the spacing  $S$  equals  $S_c$  the curvature in both phases is constant at the triple point value and no segregation exists in either



phase. Since the velocity is zero the free energy per unit volume of the product phase must equal that of the parent phase and this free energy must be exactly equal to the surface energy per unit volume stored within the product phases,  $2\sigma^{\alpha\beta}/S_c$ .  $S_c/S$  is therefore a direct measure of the stored free energy associated with surface tension as a function of spacing for all  $S$  larger than  $S_c$  and appears clearly in this role in eqs. 2.98. The quantity  $\phi/S$  on the other hand is only realized as a full contribution to the stored free energy when  $S$  is appreciably greater than  $S_c$ . Indeed since  $\phi/S_c$  is usually less than 0.1, if  $S \gg 2 S_c$ , by the binomial theorem we can write eq. 2.98 as\*

$$v \propto \frac{D}{S} \left[ 1 - \frac{S_c + \phi}{S} \right] \quad (2.107)$$

which has the standard form of a mobility ( $D/S$ ) times a driving force

$$\Delta F \propto \left( 1 - \frac{S_c + \phi}{S} \right) \quad (2.108)$$

In this form  $\phi/S$  clearly represents an addition to the stored free energy over that provided by the surface term  $S_c/S$ . Thus according to the maximum entropy production criterion for stability

$$S_{opt} = 3 (S_c + \phi)** \quad (2.109)$$

---

\* The higher order term neglected in equating  $\phi$  to  $\phi'$  has tended to cancel out the second order term neglected in the binomial expansion and combination of  $\phi$  with  $S_c$ .

\*\* Actually, the binomial expansion is still too crude for calculating an optimum  $S$  which lies in the range about  $3S_c$ . A more precise calculation shows that the correction term in eq. 3.136 is closer to  $\phi/2$  than to  $\phi$ .

and this as expected has been increased by inclusion of the segregation term (see also Cahn<sup>11,12</sup>).

Since  $\phi$  is an invariant it can be evaluated from eq. 2.106 for  $S^\alpha/2 = S_c/4$ ,  $C_l^{\alpha\gamma} = C_{lt}^{\alpha\gamma}$  to give

$$\frac{\phi}{S_c} = \frac{C_{l0}^{\alpha\gamma} - C_{lt}^{\alpha\gamma}}{C_\infty - C_{l0}^{\alpha\gamma}} = \frac{x_{l0}^{\alpha\gamma} - x_{lt}^{\alpha\gamma}}{x_\infty - x_{l0}^{\alpha\gamma}} \quad (2.110)$$

this is the ratio of distances 1-4/1-2 on Fig. 7. If we associate the stored free energy connected to  $S_c$  with the length 6-4 = 3-2 then the free energy associated with  $\phi$  is given by 4-5. We see, therefore, that  $\phi/S_c$  will generally be appreciably less than unity. Nonetheless, the stored free energy associated with  $\phi$  will always be of the order of twice that associated with the condition that the base lines for the reaction are the metastable  $\alpha$ - $\gamma$  and  $\beta$ - $\gamma$  equilibria, these latter increments of stored free energy being equal to the distance 4-7.

### III. THEORY OF TERNARY EUTECTOIDS

#### III.A STRUCTURE OF THE PROBLEM

##### 1/ SOLUTION OF THE TERNARY DIFFUSION PROBLEM

The assumptions to be made in this part of the presentation are the same as the ones introduced for the binary problem. The precipitation is assumed to proceed at the steady state with velocity  $v$  and periodicity  $S$  as previously defined. In the parent phase we have two dimensional diffusion occurring, now between three elements, one of which is dilute in all phases. Component 1 will be designated as this dilute component. The phase  $\alpha$  will be assumed dilute in component 2 so component 3 will be the solvent for that phase. The role of components 2 and 3 are interchanged in the  $\beta$  phase.

We proceed now to solve the diffusion problem for components 1 and 2 in the  $\gamma$  phase. Assuming constant diffusion coefficients, the concentrations must satisfy the two simultaneous differential equations

$$\frac{\partial C_1}{\partial t} = \Delta (D_{11} C_1 + D_{12} C_2) \quad (3.1a)$$



$$\frac{\partial C_2}{\partial t} = \Delta (D_{21} C_1 + D_{22} C_2) \quad (3.1b)$$

where  $\Delta$  is the Laplacian. Let us invoke the matrix symbolism

$$C = \begin{pmatrix} C_1 \\ C_2 \end{pmatrix} \quad \text{and} \quad D = \begin{pmatrix} D_{11} & D_{12} \\ D_{21} & D_{22} \end{pmatrix} \quad (3.2a;b)$$

which allows us to write the system 3.1 in the form

$$\frac{\partial}{\partial t} C = \Delta D C \quad (3.3)$$

We now undertake the diagonalization of the diffusion matrix  $D$  and refer to Eves<sup>3</sup> for the basic matrix operations. This allows us to obtain ternary solutions as linear combinations of binary solutions in which the eigen-values of the  $D$  matrix take the place of the binary diffusion coefficients.

The eigen-values of the  $D$  matrix are the roots of the quadratic equation

$$\delta^2 + T \delta + \Delta = 0 \quad (3.4)$$

where  $T$  and  $\Delta$  are, respectively, the trace and the determinant of the

matrix D. Hence

$$\delta_1 = \frac{1}{2} (T - \sqrt{T^2 - 4 \Delta}) \quad (3.5a)$$

$$\delta_2 = \frac{1}{2} (T + \sqrt{T^2 - 4 \Delta}) \quad (3.5b)$$

We will restrict attention to solutions in the  $\gamma$  phase which lie sufficiently far from a critical point ( $\Delta = 0$ ) that<sup>32</sup>

$$D_{11} D_{22} \gg D_{12} D_{21} \quad (3.6)$$

Since in general<sup>33</sup>

$$D_{12} < D_{11} \quad \text{and} \quad D_{21} < D_{22} \quad (3.7)$$

We can to a good approximation always set one or more of the off-diagonal coefficients equal to zero. If  $D_{22} \gg D_{11}$  then  $D_{21}$  could be important but  $D_{12}$  would have a negligible effect on the solution. On the other hand, if  $D_{11} = D_{22}$  then both off-diagonal effects can be neglected<sup>33</sup>.

Therefore we can keep sufficient generality in our treatment if we set  $D_{12} = 0$  and choose  $D_{22} \geq D_{11}$ . In the case of the equality in the latter expression we can set  $D_{21} = 0$  as well.

In this approximation we have

$$T = D_{11} + D_{22} \quad \text{and} \quad \Delta = D_{11} D_{22} \quad (3.8a;b)$$

and we get immediately

$$\delta_1 = D_{11} \quad \delta_2 = D_{22} \quad (3.9a;b)$$

Referring again to Eves<sup>31</sup>, we have, for the eigen vectors

$$V_1 = \begin{pmatrix} 1 \\ \frac{D_{21}}{D_{11} - D_{22}} \end{pmatrix} \quad \text{and} \quad V_2 = \begin{pmatrix} 0 \\ 1 \end{pmatrix} \quad (3.10a;b)$$

We shall for brevity adopt the notation

$$\tau = \frac{D_{21}}{D_{11} - D_{22}} \quad (3.11)$$

When  $D_{21}$  can be set equal to zero the matrix becomes diagonal and all our subsequent calculations are trivial. The solutions for this case are simply achieved by equating  $\tau$  to zero.

The change of basis matrix  $\Lambda$  is composed of the eigen-vectors,  
viz.,

$$\Lambda = \begin{pmatrix} 1 & 0 \\ \tau & 1 \end{pmatrix} \quad (3.12)$$

and the matrix inverse of  $\Lambda$  is

$$\Lambda^{-1} = \begin{pmatrix} 1 & 0 \\ -\tau & 1 \end{pmatrix} \quad (3.13)$$

The matrix  $\Lambda$  diagonalizes the matrix  $D$  such that

$$\Lambda^{-1} D \Lambda = D^* = \begin{pmatrix} \delta_1 & 0 \\ 0 & \delta_2 \end{pmatrix} = \begin{pmatrix} D_{11} & 0 \\ 0 & D_{22} \end{pmatrix} \quad (3.14)$$

The following is a short verification of this transformation

$$D\Lambda = \begin{pmatrix} D_{11} & 0 \\ D_{21} & D_{22} \end{pmatrix} \begin{pmatrix} 1 & 0 \\ \frac{D_{21}}{D_{11} - D_{22}} & 1 \end{pmatrix} = \begin{pmatrix} D_{11} & 0 \\ \frac{D_{21} D_{11}}{D_{11} - D_{22}} & D_{22} \end{pmatrix} \quad (3.15)$$

$$\Lambda^{-1} D \Lambda = \begin{pmatrix} 1 & 0 \\ \frac{-D_{21}}{D_{11} - D_{22}} & 1 \end{pmatrix} \begin{pmatrix} D_{11} & 0 \\ \frac{D_{21} D_{11}}{D_{11} - D_{22}} & D_{22} \end{pmatrix} = \begin{pmatrix} D_{11} & 0 \\ 0 & D_{22} \end{pmatrix} \quad (3.16)$$

Now multiplying both members of eq. 3.3 from the left by  $\Lambda^{-1}$  and the right hand member from the right by  $\Lambda \Lambda^{-1} = I$  and noting that  $C I = I C$  we obtain

$$\frac{\partial}{\partial t} (\Lambda^{-1} C) = \Delta (\Lambda^{-1} D \Lambda) (\Lambda^{-1} C) \quad (3.17)$$

or

$$\frac{\partial}{\partial t} (\Lambda^{-1} C) = \Delta D^* (\Lambda^{-1} C) \quad (3.18)$$

Since  $D^*$  is diagonal it is clear that the two elements of  $\Lambda^{-1} C$

$$\begin{pmatrix} C^I \\ C^{II} \end{pmatrix} = \Lambda^{-1} \begin{pmatrix} C_1 \\ C_2 \end{pmatrix} \quad (3.19)$$

where

$$C^I = C_1 \quad (3.20a)$$

$$C^{II} = -\tau C_1 + C_2 \quad (3.20b)$$

are the binary functions which can be combined to give the ternary solutions.

We now introduce the assumption that the precipitation is in its steady state stage and make the change of variable

$$u = x - v t \quad y = y^* \quad (3.21a;b)$$

to obtain the two equations

$$\frac{v}{\delta_i} \frac{\partial C^i}{\partial u} + \frac{\partial^2 C^i}{\partial u^2} = - \frac{\partial^2 C^i}{\partial y^2} ; \quad i = I, II \quad (3.22a;b)$$

In such equations the variable can be easily separated by adoption of the new functions

$$C^i = U_n^i(u) \gamma_n^i(y) \quad ; \quad i = I, II \quad (3.23a;b)$$

which give for each  $i$  the simultaneous ordinary differential equations

$$\frac{d^2 U^i}{d u^2} + \frac{v}{\delta_i} \frac{d U_n^i}{d u} - b_n^2 U_n^i = 0 \quad (3.24a;b)$$

$$\frac{d^2 Y_n^i}{d y^2} + b_n^2 Y_n = 0 \quad (3.24c;d)$$

where

$$b_n = \frac{2\pi n}{S v} \quad (3.25)$$

The separation constant  $b_n$  must be such as to satisfy the periodicity of the geometrical configuration in  $y$  over a distance  $S$ , the lamellar spacing (Fig. 2).

The first differential equation of the system eq. 3.24a;b has the characteristic equation

$$\lambda^2 + \frac{v}{\delta_i} \lambda - b_n = 0 \quad (3.26a;b)$$

Since the product of the two roots must always be negative and equal to  $-b_n^2$  we can always find a negative root. This root is the one required for our physical solution since only a decaying exponential is acceptable.

This root is

$$\lambda_n^i = -\frac{1}{2} \left[ \frac{v}{\delta_i} + \sqrt{\left(\frac{v}{\delta_i}\right)^2 + 4 b_n^2} \right] \quad (3.27a;b)$$

In the binary treatment we have seen that eq. 2.5 can generally be replaced by eq. 2.6 and this approximation was checked by experimental values.

Similarly to the binary case and since  $D_{22}$  should be comparable in magnitude to  $D$  of the binary treatment we can assume that

$$\lambda_n^{II} \approx -b_n \quad (3.28)$$

We have seen above that  $D_{22} \geq D_{11}$  and it will be justified to take also the approximation

$$\lambda_n^I \approx -b_n \quad (3.29)$$

The solution of the first differential equation is therefore

$$U_n^i(u) = e^{\lambda_n^i u} \quad (3.30a;b)$$

From the second differential equations we have the well-known periodic solution

$$Y_n^i(y) = \cos b_n y \quad (3.31a;b)$$

where we retain only cosine terms since we chose the origin of our reference frame at the center of symmetry of an  $\alpha$  lamella (Fig. 2).



The general solution of the system 3.22 can now be written as

$$C^I = C_\infty^I + \sum_{n=0}^{\infty} A_n e^{\lambda_n^I u} \cos b_n y \quad (3.32a)$$

$$C^{II} = C_\infty^{II} + \sum_{n=0}^{\infty} B_n e^{\lambda_n^{II} u} \cos b_n y \quad (3.32b)$$

We can now transform these concentrations into physical space via the transformation of eq. 3.12 or

$$C_i = \Lambda C^i \quad (3.33a;b)$$

to yield

$$C_1 = C_{1\infty} + \sum_{n=0}^{\infty} A_n e^{\lambda_n^I u} \cos b_n y \quad (3.34a)$$

$$C_2 = C_{2\infty} + \sum_{n=0}^{\infty} (\tau A_n e^{\lambda_n^I u} + B_n e^{\lambda_n^{II} u}) \cos b_n y \quad (3.34b)$$

In eq. 3.22 we have a system of two differential equations of the second order and the general solution therefore depends on four integration constants. In the above solution (eqs. 3.34) we have already satisfied the two boundary conditions for  $u = \infty$ . To obtain the particular solution to our problem we will have to fulfill other conditions. This will be dealt with later.

Since the summation starts from  $n = 0$  we have

$$C_1 - C_{1\infty} = A_0 e^{-\frac{v}{D_{11}} u} + \sum_{n=1}^{\infty} A_n e^{\lambda_n^I u} \cos b_n y \quad (3.35a)$$

$$C_2 - C_{2\infty} = \tau A_0 e^{-\frac{v}{D_{11}} u} + B_0 e^{-\frac{v}{D_{22}} u} \quad (3.35b)$$

$$+ \sum_{n=1}^{\infty} (\tau A_n e^{\lambda_n^I u} + B_n e^{\lambda_n^{II} u}) \cos b_n y$$

i.e., there are in general pure exponential as well as periodic terms in the solution.

## 2/ INFLUENCE ON THE CONCENTRATIONS OF THE PRESSURE DUE TO CURVATURE

We have fully discussed for the binary case the influence of the

pressure on the composition due to the curvature of the interface. We will retain the same assumption that the pressure acts only on the precipitate phases. It has been found that Hillert's assumption of constant compositions in the precipitate phases is completely untenable in the ternary case since it represents such a strong condition that a solution consistent with the phase diagram is in general impossible.

The Gibbs-Duhem relations for the ternary  $\alpha$  and  $\gamma$  phases are

$$x_1^\gamma d\ln a_1 + x_2^\gamma d\ln a_2 + x_3^\gamma d\ln a_3 = 0 \quad (3.36a)$$

$$x_1^\alpha d\ln a_1 + x_2^\alpha d\ln a_2 + x_3^\alpha d\ln a_2 = \frac{V^\alpha}{RT} dP \quad (3.36b)$$

In these equations  $x_1^\gamma, x_2^\gamma, x_3^\gamma$  and  $x_1^\alpha, x_2^\alpha, x_3^\alpha$  are the compositions of the  $\gamma$  and  $\alpha$  phases, respectively. The activities for the three components which are equal in the two phases are  $a_1, a_2$  and  $a_3$ . There are analogous expressions for the  $\beta$  and  $\gamma$  phases.

In a ternary system, the extra degree of freedom leads to an infinite number of reference states for the above pair of differential equations, all of which lie on the equilibrium phase boundaries ( $P = 0$ ). We have found it in general convenient (and as we shall later see for our most complete treatment, essential) to choose this reference state with one coordinate at  $C_{10}^{\alpha\gamma} = C_{1\infty}$  and  $C_{10}^{\beta\gamma} = C_{1\infty}$ .

## FIRST THERMODYNAMIC VERSION

As an extension of the binary case we must assume three different ratios between the compositions of each element in the two phases in equilibrium, viz.,

$$\frac{x_1^{\alpha\gamma}}{x_1^{\gamma\alpha}} = K_1^\alpha \quad \frac{x_2^{\alpha\gamma}}{x_2^{\gamma\alpha}} = K_2^\alpha \quad \frac{x_3^{\alpha\gamma}}{x_3^{\gamma\alpha}} = K_3^\alpha \quad (3.37a;b;c)$$

and

$$\frac{x_1^{\beta\gamma}}{x_1^{\gamma\beta}} = K^\beta \quad \frac{x_2^{\beta\gamma}}{x_2^{\gamma\beta}} = K^\beta \quad \frac{x_3^{\beta\gamma}}{x_3^{\gamma\beta}} = K^\beta \quad (3.38a;b;c)$$

As in the binary case, this set of thermodynamic relations is not sufficiently general for most purposes. However, the working out of the problem is useful for explaining and demonstrating the methodology.

It is immediately apparent that these ratios cannot generally be simultaneously satisfied. However, if the phase boundaries are parallel to one side of the ternary diagram they can all be satisfied. Therefore, we assume that the phase boundaries of the equilibrium between the  $\gamma$  and  $\alpha$  phases are parallel to the side 1-2 of the triangle as illustrated on Fig. 8. We demonstrate in Appendix IX that this configuration can be somewhat relaxed since to a good approximation two ratios can be kept constant, the third varying inappreciably.

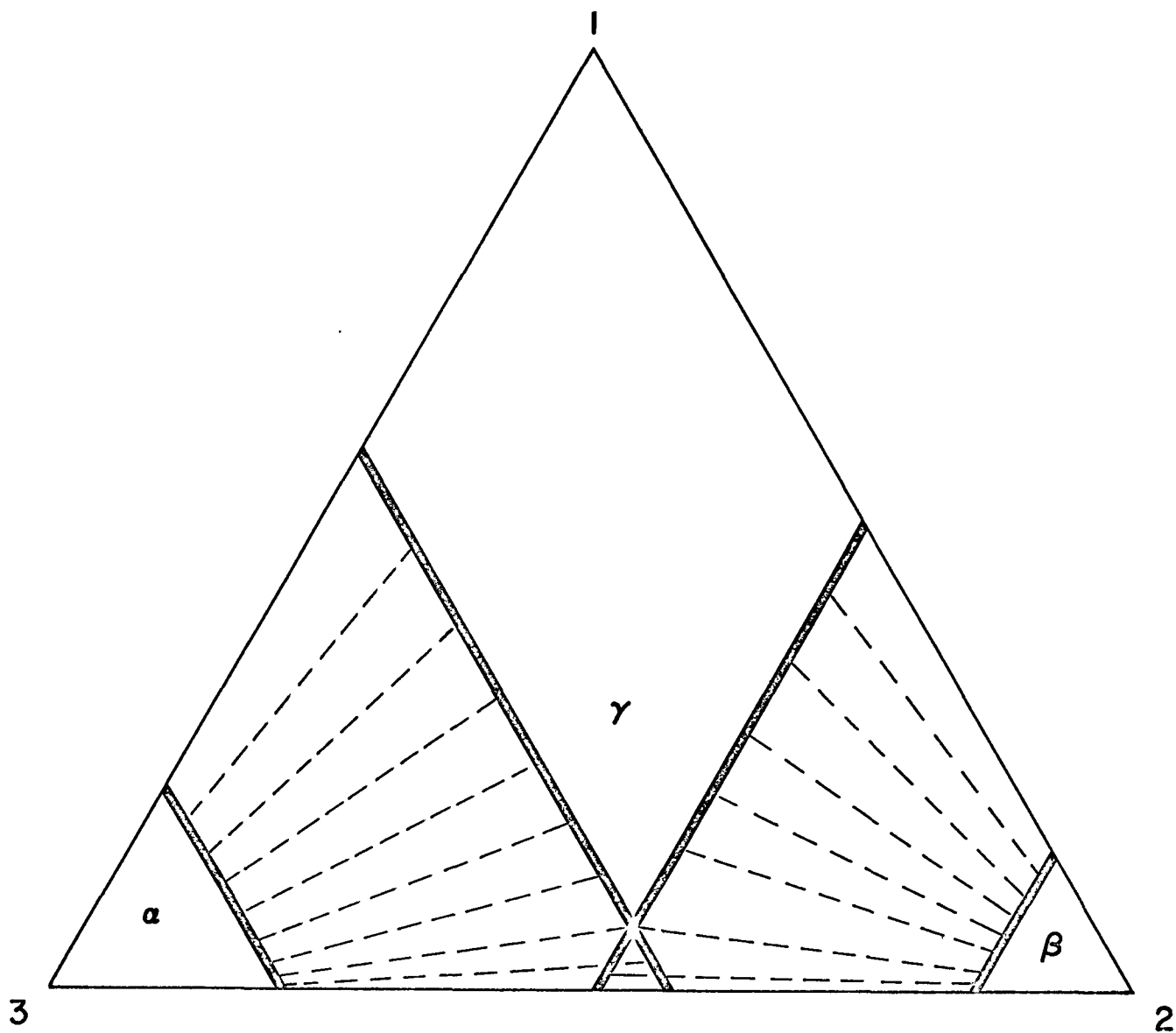


Fig. 8: Ternary phase diagram corresponding to the first thermodynamic version (the phase boundaries are straight lines).

The condition of strict parallelism is expressed by

$$K_1^\alpha = K_2^\alpha \quad \text{and} \quad K_1^\beta = K_3^\beta \quad (3.39a;b)$$

The calculations as carried out in Appendix IX lead to the linearized Gibbs-Thomson relations

$$P = RT h^\alpha (C_1^{\alpha\gamma} + C_2^{\alpha\gamma} - C_{10}^{\alpha\gamma} - C_{20}^{\alpha\gamma}) \quad (3.40a)$$

$$P = RT h^\beta (C_2^{\beta\gamma} - C_{20}^{\beta\gamma}) \quad (3.40b)$$

The subscript 0 corresponds to reference states for the  $\alpha$  and  $\beta$  phases when the pressure is equal to zero. The coefficients  $h^\alpha$  and  $h^\beta$  are defined by

$$h^\alpha = 1 - \frac{K_3^\alpha}{K_1^\alpha} = 1 - \frac{K_3^\alpha}{K_2^\alpha} \quad (3.41)$$

and

$$h^\beta = - \left( 1 - \frac{K_2^\beta}{K_3^\beta} \right) \quad (3.42)$$

These two coefficients are equal in magnitude and opposite in sign in the symmetric configuration where we impose the further relation

$$K_1^\alpha = K_1^\beta \quad (3.43)$$

In this situation the pressure displaces the  $\alpha\gamma$  and  $\beta\gamma$  phase boundaries symmetrically although this is not true for the  $\gamma\alpha$  and  $\gamma\beta$  phase boundaries\*.

## SECOND THERMODYNAMIC VERSION

As demonstrated in Appendix X a simple integral of the Gibbs-Duhem equation can be obtained by assuming that the two sets of complex ratios

$$\frac{x_1^{\gamma\alpha} x_3^{\alpha\gamma}}{x_1^{\alpha\gamma} x_3^{\gamma\alpha}} = x_1^\alpha \quad \frac{x_2^{\gamma\alpha} x_3^{\alpha\gamma}}{x_1^{\alpha\gamma} x_3^{\gamma\alpha}} = x_2^\alpha \quad (3.44a;b)$$

$$\frac{x_1^{\gamma\beta} x_2^{\beta\gamma}}{x_1^{\beta\gamma} x_2^{\gamma\beta}} = x_1^\beta \quad \frac{x_2^{\beta\gamma} x_3^{\gamma\beta}}{x_2^{\gamma\beta} x_3^{\beta\gamma}} = x_3^\beta \quad (3.44c;d)$$

can adequately represent the thermodynamics of the system. These ratios

---

\* In the notation " $\beta\gamma$  phase boundary" we designate the boundary such that the compositions in the  $\beta$  phase are in equilibrium with the  $\gamma$  phase.

are assumed to be independent of the pressure and are capable of representing any diagram of the form indicated in Fig. 9. Although not essential, the phase boundaries are always straight lines in the dilute solution thermodynamics which we have used for terminal phases.

The assumptions in eqs. 3.44 lead to the linearized Gibbs-Thomson equations

$$P = RT [k_1^\alpha (C_1^{\alpha Y} - C_{10}^{\alpha Y}) + k_2^\alpha (C_2^{\alpha Y} - C_{20}^{\alpha Y})] \quad (3.45a)$$

$$P = RT [(k_1^\beta - k_3^\beta)(C_1^{\beta Y} - C_{10}^{\beta Y}) - k_3^\beta (C_2^{\beta Y} - C_{20}^{\beta Y})] \quad (3.45b)$$

The subscript 0 designates the same reference state as before and the coefficients  $k$  are given by

$$k_1^\alpha = 1 - x_1^\alpha \quad k_2^\alpha = 1 - x_2^\alpha \quad (3.46a;b)$$

$$k_1^\beta = 1 - x_1^\beta \quad k_3^\beta = 1 - x_3^\beta \quad (3.46c;d)$$

In Appendix X we demonstrate that for a symmetrical diagram a symmetrical variation of composition with pressure can be achieved via eqs. 3.45.

If as with the binary case we express the Gibbs-Thomson relations in terms of the concentrations in the precipitate phases we find that they are again linear. The expression for the pressure dependency of the



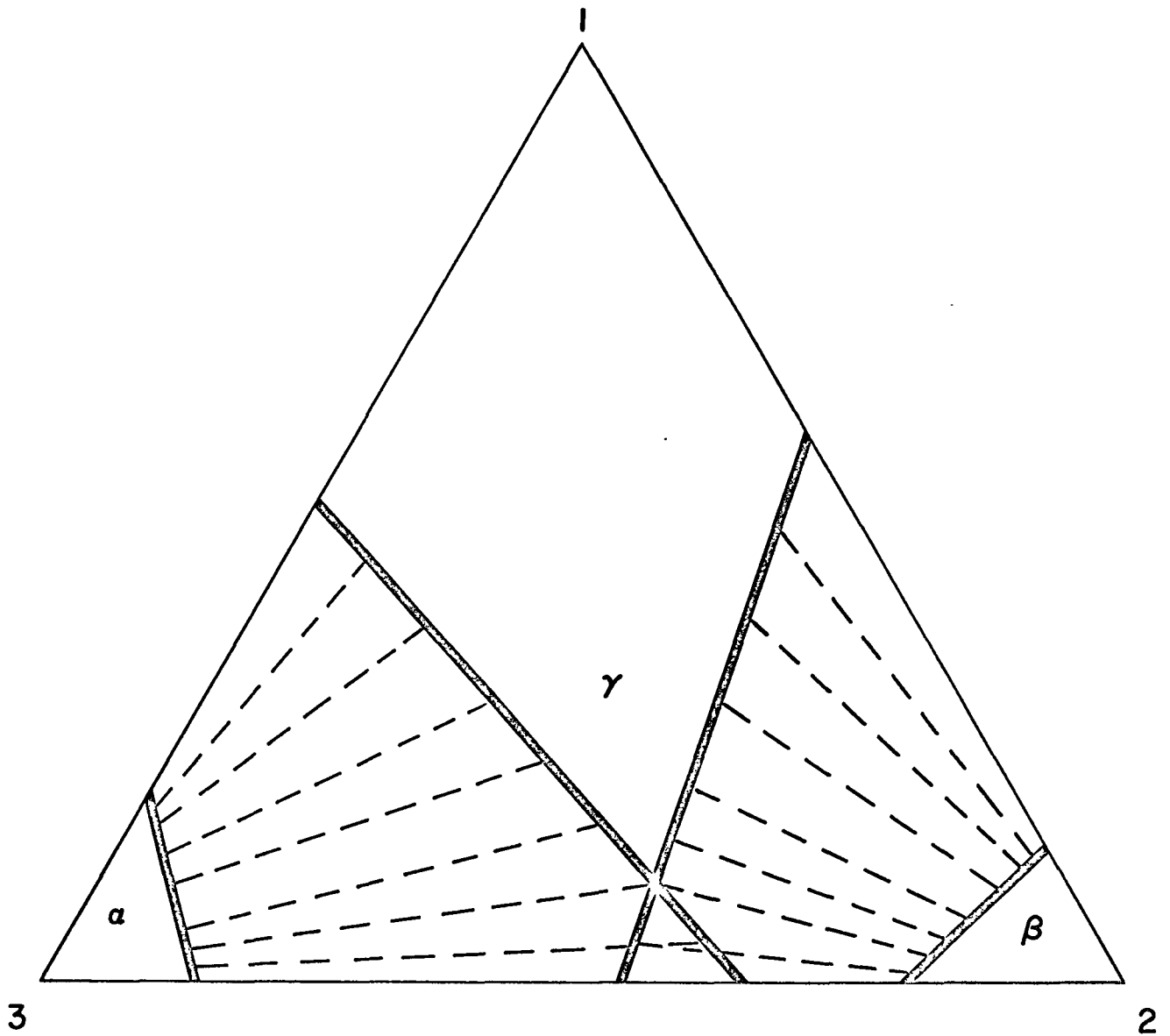


Fig. 9: Ternary phase diagram corresponding to the second thermodynamic version ( the phase boundaries are straight lines).

concentrations in the parent phase are given in Appendices IX and X. They will not be used in the subsequent calculations.

### 3/ THE MASS BALANCE

The Fourier series for the concentrations in the precipitate phases will be obtained from the mass balance. If we consider a volume element parallel to the  $u$  plane as shown in Fig. 2, we can write the mass balance as in the binary case, viz.,

$$v (C_{1\infty} - C_{1p}) = \int_{u_0}^{\infty} (D_{11} \frac{\partial^2 C_1}{\partial y^2}) du \quad (3.47a)$$

$$v (C_{2\infty} - C_{2p}) = \int_{u_0}^{\infty} (D_{21} \frac{\partial^2 C_1}{\partial y^2} + D_{22} \frac{\partial^2 C_2}{\partial y^2}) du \quad (3.47b)$$

The second derivatives of the concentrations with respect to  $y$  are expressed by

$$\frac{\partial^2 C_1}{\partial y^2} = - \sum_{n=1}^{\infty} A_n b_n^2 e^{-\lambda_n^I u} \cos b_n y \quad (3.48a)$$

$$\frac{\partial^2 C_2}{\partial y^2} = - \sum_{n=1}^{\infty} (\tau A_n e^{\lambda_n^I u} + B_n e^{\lambda_n^{II} u}) b_n^2 \cos b_n y \quad (3.48b)$$

We substitute these expressions into the mass balance eqs. 3.47 and obtain

$$v(C_{1\infty} - C_{1p}) = - \int_{u_0}^{\infty} \left[ \sum_{n=1}^{\infty} D_{11} A_n b_n^2 e^{\lambda_n^I u} \cos b_n y \right] du \quad (3.49a)$$

$$v(C_{2\infty} - C_{2p}) = - \int_{u_0}^{\infty} \sum_{n=1}^{\infty} [(D_{21} + D_{22}\tau) A_n e^{\lambda_n^I u} + D_{22} B_n e^{\lambda_n^{II} u}] b_n^2 \cos b_n y \, du \quad (3.49b)$$

Integration gives us

$$v(C_{1\infty} - C_{1p}) = \sum_{n=1}^{\infty} D_{11} \frac{A_n b_n^2}{\lambda_n^I} e^{\lambda_n^I u_0} \cos b_n y \quad (3.50a)$$

$$v(C_{2\infty} - C_{2p}) = \sum_{n=1}^{\infty} [(D_{21} + D_{22}\tau) \frac{A_n}{\lambda_n^I} e^{\lambda_n^I u_0} + D_{22} \frac{B_n}{\lambda_n^{II}} e^{\lambda_n^{II} u_0}] b_n^2 \cos b_n y \quad (3.50b)$$

where  $u_0$  is the abscissa of the interface and is a function of  $y$ . The right hand side of both equations is therefore a function of  $y$  through  $\cos b_n y$

and  $u_0$ . However, to a good approximation we will assume that  $u_0$  is so small or the interface so flat that all the exponentials in eqs. 3.50 can be equated to unity. Taking into account expression 3.11 for  $\tau$  we obtain

$$v(C_{1\infty} - C_{1p}) = D_{11} \sum_{n=1}^{\infty} \frac{A_n b_n^2}{\lambda_n^I} \cos b_n y \quad (3.51a)$$

$$v(C_{2\infty} - C_{2p}) = \sum_{n=1}^{\infty} \left( \frac{D_{21} D_{11}}{D_{11} - D_{22}} \frac{A_n}{\lambda_n^I} + D_{22} \frac{B_n}{\lambda_n^{II}} \right) b_n^2 \cos b_n y \quad (3.51b)$$

Finally for brevity we can write

$$C_{1p} - C_{1\infty} = \sum_{n=1}^{\infty} G_n \cos b_n y \quad (3.52a)$$

$$C_{2p} - C_{2\infty} = \sum_{n=1}^{\infty} G'_n \cos b_n y \quad (3.52b)$$

with

$$G_n = - \frac{D_{11}}{v} \frac{A_n b_n^2}{\lambda_n^I} \quad (3.53a)$$

$$G'_n = - \frac{b_n^2}{v} \left( \frac{D_{21} D_{11}}{D_{11} - D_{22}} \frac{A_n}{\lambda_n^I} + D_{22} \frac{B_n}{\lambda_n^{II}} \right) \quad (3.53b)$$

and we can express eqs. 3.53 in the matrix form

$$\begin{pmatrix} G_n \\ G'_n \end{pmatrix} = -\frac{b_n^2}{v} \Lambda \begin{pmatrix} \frac{D_{11} A_n}{\lambda_n} \\ \frac{D_{22} B_n}{\lambda_n} \end{pmatrix} \quad (3.54)$$

Analogously to the binary case eqs. 3.52 give us the concentrations in the precipitate phases immediately behind the interface. It has of course been implicitly assumed that the diffusion rates in the product phases are small enough that processes in these phases do not affect the kinetics of the reaction.

The fact that concentrations in the precipitate phases are Fourier series periodic in the spacing  $S$  assures that the average concentrations in these phases will be equal to  $C_{1\infty}$  and  $C_{2\infty}$  respectively.

The concentrations in the parent phase just ahead of the interface, eqs. 3.34, can be written as

$$C_1 = C_{1\infty} + A_0 + \sum_{n=1}^{\infty} A_n \cos b_n y \quad (3.55a)$$

$$C_2 = C_{2\infty} + \tau A_0 + B_0 + \sum_{n=1}^{\infty} (\tau A_n + B_n) \cos b_n y \quad (3.55b)$$

which clearly identifies the constant terms in the respective series.

## 4/ SECOND BOUNDARY CONDITION

In the above we have shown how to obtain the Fourier series representing the concentrations in the precipitate phases. We will obtain the numerical values of the coefficients as a function of  $v$ ,  $S$  and  $S^\alpha/S$  when we satisfy the thermodynamic requirement imposed by equal activities for the phases in equilibrium. The second boundary condition, as in the binary treatment, gives us two relations between the three parameters  $v$ ,  $S$  and  $S^\alpha/S$ , thus in principle enabling us to deduce a relation between the velocity and the spacing. This second boundary condition as in the binary case can be expressed as a condition on the phase angle at the junction of two lamellae and we have

$$-\cos \phi^\alpha = \int_0^{\frac{S^\alpha}{2}} \frac{1}{r} dy = \int_0^{\frac{S^\alpha}{2}} \frac{p}{\sigma^\alpha} dy \quad (3.56a)$$

$$-\cos \phi^\beta = \int_{\frac{S^\alpha}{2}}^{\frac{S}{2}} \frac{1}{r} dy = \int_{\frac{S^\alpha}{2}}^{\frac{S}{2}} \frac{p}{\sigma^\beta} dy \quad (3.56b)$$

The pressure as a function of the concentrations is given by the Gibbs-Thomson equations 3.40 or 3.45. By substitution the two expressions 3.56 yield the required relations.

In the following paragraphs we will demonstrate how to calculate the Fourier expansion coefficients according to two different thermodynamic

assumptions. In both cases we restrict our treatment to the symmetrical cases since otherwise the calculations become intractable.

### III.B THEORY OF TERNARY SYSTEMS WITH THE FIRST THERMODYNAMIC VERSION AND FOR A SYMMETRICAL CONFIGURATION

In this section we assume in the integration of the Gibbs-Duhem equations that the ratios of the concentrations between the precipitate phases and the parent phases are constants independent of the pressure. Our full calculation is given in Appendix IX. To preserve the symmetry of the diagram (Fig. 10) the partition ratio for element 1 is a constant, independent of the phase precipitated. Therefore the expansions of the concentrations  $C_{1p}$  in the precipitate phase and  $C_1$  in the parent phase must satisfy a proportionality relation

$$\frac{C_{1p}}{C_1} = K_1 \quad (3.57)$$

Since we have

$$C_1 = C_{1\infty} + A_0 + \sum_{n=1}^{\infty} A_n \cos b_n y \quad (3.58)$$

$$C_{1p} = C_{1\infty} - \frac{D_{11}}{v} \sum_{n=1}^{\infty} \frac{A_n b_n^2}{\lambda_n} \cos b_n y \quad (3.59)$$

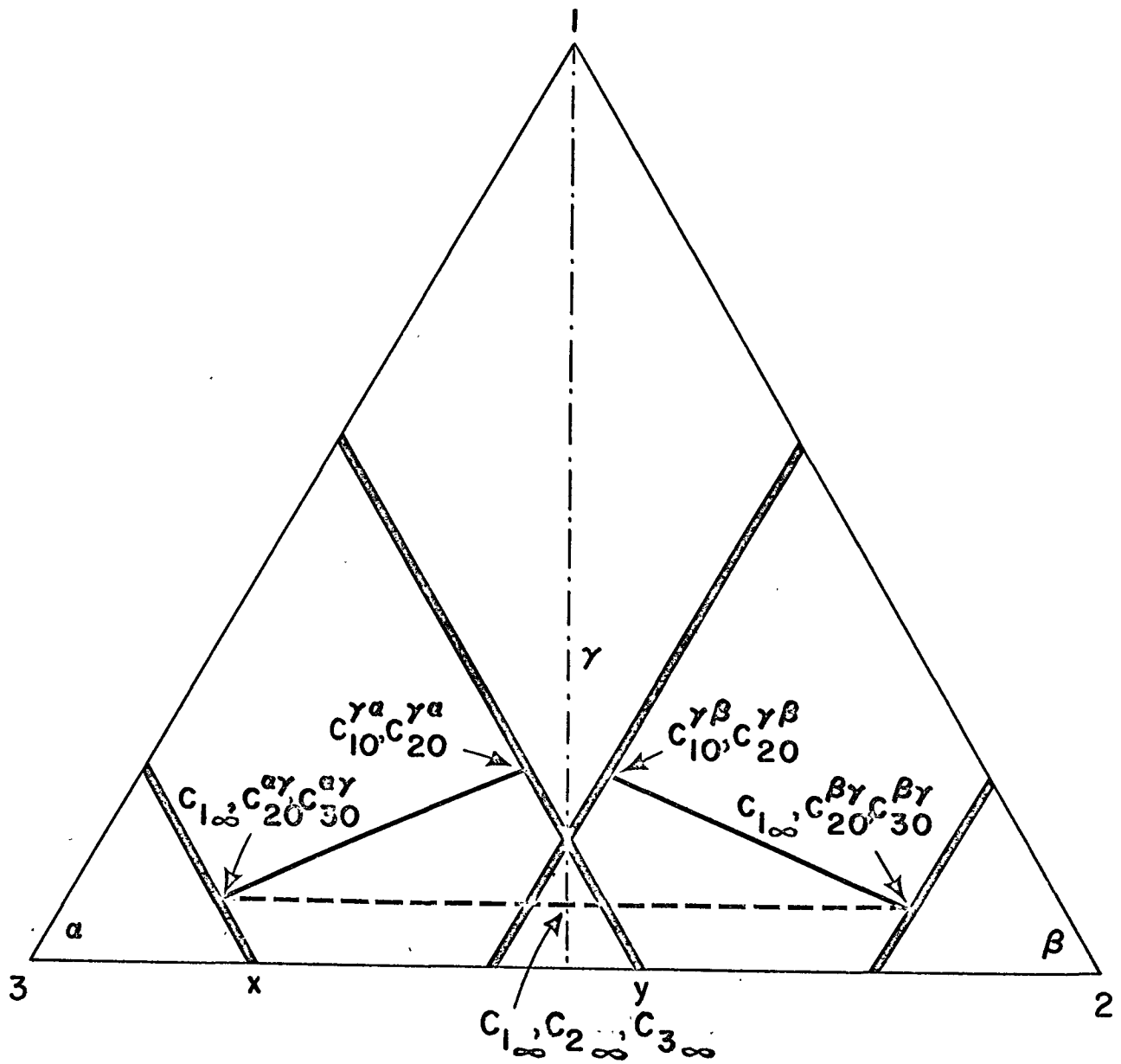


Fig. 10: Symmetric ternary phase diagram corresponding to the first thermodynamic version.



from eq. 3.57 we can immediately deduce that

$$C_{1\infty} = K_1 (C_{1\infty} + A_0) \quad (3.60)$$

and

$$-\frac{D_{11}}{v} \frac{b_n^2}{I} A_n = K_1 A_n \quad (3.61)$$

This system of equations leads to

$$A_0 = C_{1\infty} \left( \frac{1}{K_1} - 1 \right) \quad (3.62a)$$

$$A_n = 0 \quad \text{for} \quad n \neq 0 \quad (3.62b)$$

This important result implies that there is no segregation of element 1 in the precipitate phases, a result which is in accord with intuition.

In the parent phase we have for  $C_1$  the corresponding behaviour

$$C_1 = C_{1\infty} \left[ 1 + \left( \frac{1}{K_1} - 1 \right) e^{-\frac{v}{D_{11}} u} \right] \quad (3.63)$$

For element 2 the ratio of the concentrations follows a step function in  $y$  as developed in Appendix III. The calculations are very similar to the ones performed for the binary case, viz.,

$$\frac{C_{2p}}{C_2} = \frac{K_2^\alpha + K_2^\beta}{2} + \frac{2}{\pi} (K_2^\alpha - K_2^\beta) \sum_{n=1}^{\infty} \frac{1}{n} \sin \pi n \frac{S^\alpha}{S} \cos b_n y \quad (3.64)$$

where the concentrations are expressed by

$$C_2 = C_{2\infty} + \tau A_0 + B_0 + \sum_{n=1}^{\infty} B_n \cos b_n y \quad (3.65)$$

$$C_{2p} = C_{2\infty} + \frac{D_{22}}{v} \sum_{n=1}^{\infty} \frac{B_n b_n^2}{\lambda_n} \cos b_n y \quad (3.66)$$

To obtain these expressions we have used  $A_n = 0$  for  $n \neq 0$  in eqs. 3.55 and 3.50.

Eqs. 3.64, 3.65 and 3.66 are similar to eqs. 2.49, 2.51 and 2.52 for the binary case. We can immediately deduce expressions for the Fourier expansion coefficients

$$B_0 = C_{2\infty} \left[ \frac{(2a_0 + \frac{8\pi D}{Sv})(2a_0 + a_2 + \frac{4\pi D}{Sv}) - (a_1 + a_3)^2}{\mathcal{D}} - 1 \right] - C_{1\infty} \left( \frac{1}{K_1} - 1 \right) \quad (3.67a)$$

$$B_1 = 2 C_{2\infty} \frac{(a_1 + a_3)a_2 - (2 a_0 + \frac{8\pi D}{Sv})a_1}{\mathcal{D}} \quad (3.67b)$$

$$B_2 = 2 C_{2\infty} \frac{(a_1 + a_3)a_1 - (2 a_0 + a_2 + \frac{4\pi D}{Sv})a_2}{\mathcal{D}} \quad (3.67c)$$

with the same expression for  $\mathcal{D}$  as in eq. 2.55, viz.,

$$\mathcal{D} = a_0(2a_0 + \frac{8\pi D}{Sv})(2a_0 + a_2 + \frac{4\pi D}{Sv}) - a_0(a_1 + a_3)^2 + 2a_1a_2(a_1 + a_3) - a_1^2(2a_0 + \frac{8\pi D}{Sv}) - a_2^2(2a_0 + a_2 + \frac{4\pi D}{Sv}) \quad (3.68)$$

The  $a_n$  are the Fourier expansion coefficients of the step function in eq. 3.64. We can now substitute 3.67 into the expressions 3.65 and 3.66 for the concentrations.

To obtain the two relations between the parameters  $v$ ,  $S$  and  $S^\alpha/S$  we have to fulfill the second boundary condition at the junction of two lamellae. For the  $\alpha$  phase we obtain using eq. 3.65

$$-\cos \phi^\alpha = \int_0^{\frac{S^\alpha}{2}} \frac{p}{\sigma^\alpha} dy = \frac{h^\alpha RT}{\sigma^\alpha} \int_0^{\frac{S^\alpha}{2}} (C_{1p} + C_{2p} - C_{10}^{\alpha\gamma} - C_{20}^{\alpha\gamma}) dy \quad (3.69)$$

The reference state denoted by the subscript  $o$  is chosen to correspond to the state at zero pressure where the concentration of element 1 in both  $\alpha$  and  $\beta$  phases is equal to  $C_{1\infty}$ .

Eq. 3.69 yields

$$-\frac{\sigma^\alpha \cos \phi^\alpha}{h^\alpha RT} + (C_{1\infty} + C_{20}^\alpha) \frac{S^\alpha}{2} = \int_0^{\frac{S^\alpha}{2}} (C_{1p} + C_{2p}) dy \quad (3.70)$$

We now substitute in the integral the concentrations

$$C_{1p} = C_{1\infty} \quad (3.71a)$$

$$C_{2p} = C_{2\infty} - \frac{D_{22}}{v} \sum_{n=1}^{\infty} \frac{B_n b_n^2}{\lambda_n} \cos b_n y \quad (3.71b)$$

and obtain

$$\frac{\sigma^\alpha \cos \phi^\alpha}{h^\alpha RT} + (C_{2\infty} - C_{20}^\alpha) = \frac{D_{22}}{v} \sum_{n=1}^{\infty} \frac{B_n b_n^2}{\lambda_n} \sin \pi n \frac{S^\alpha}{S} \quad (3.72)$$

Similarly for the  $\beta$  lamella we have from 3.40b

$$-\cos \phi^\beta = \int_{\frac{S^\alpha}{2}}^{\frac{S}{2}} \frac{P}{\sigma^\beta} dy = \frac{h^\beta RT}{\sigma^\beta} \int_{\frac{S^\alpha}{2}}^{\frac{S}{2}} (C_{2p} - C_{20}^\beta) dy \quad (3.73)$$

and

$$\frac{\sigma^\beta \cos \phi^\beta}{h^\beta RT} + (C_{2\infty} - C_{20}^\beta) \frac{S^\beta}{2} = - \frac{D_{22}}{v} \sum_{n=1}^{\infty} \frac{B_n b_n}{\lambda_n \Gamma} \sin \pi n \frac{S^\alpha}{S} \quad (3.74)$$

Similarly to the binary case we can deduce a relation between  $S^\alpha$  and  $S^\beta$  by adding eqs. 3.72 and 3.74, viz.,

$$\frac{1}{RT} \left( \frac{\sigma^\alpha \cos \phi^\beta}{h^\alpha} + \frac{\sigma^\beta \cos \phi^\beta}{h^\beta} \right) + (C_{\infty} - C_{20}^\alpha) \frac{S^\alpha}{2} + (C_{2\infty} - C_{20}^\beta) \frac{S^\beta}{2} = 0 \quad (3.75)$$

This expression reduces to a simple proportionality relation (analogous to the binary lever rule) in the case where the two surface tensions  $\sigma^\alpha$  and  $\sigma^\beta$  are equal and the diagram is symmetric. Then the first term of eq. 3.75 vanishes. It is this particular case we consider in detail in the following.

A second relation can be obtained if we write

$$\frac{2}{RT} \frac{\sigma^\alpha \cos \phi^\alpha}{h^\alpha (C_{2\infty} - C_{20}^\alpha)} + S^\alpha = \frac{D_{22}}{v} \frac{2}{C_{2\infty} - C_{20}^\alpha} \sum_{n=1}^{\infty} \frac{B_n b_n}{\lambda_n \Gamma} \sin \pi n \frac{S^\alpha}{S} \quad (3.76a)$$

$$\frac{2}{RT} \frac{\sigma^\beta \cos \phi^\beta}{h^\beta (C_{2\infty} - C_{20}^\beta)} + S^\beta = - \frac{D_{22}}{v} \frac{2}{C_{2\infty} - C_{20}^\beta} \sum_{n=1}^{\infty} \frac{B_n b_n}{\lambda_n \Gamma} \sin \pi n \frac{S^\alpha}{S} \quad (3.76b)$$

and add to obtain

$$\frac{2}{RT} \left( \frac{\sigma^\alpha \cos \phi^\alpha}{h^\alpha (C_{2\infty}^\alpha - C_{20}^\alpha)} + \frac{\sigma^\beta \cos \phi^\beta}{h^\beta (C_{2\infty}^\beta - C_{20}^\beta)} \right) + S = \quad (3.77)$$

$$\frac{2 D_{22}}{v} \left( \frac{1}{C_{2\infty}^\alpha - C_{20}^\alpha} - \frac{1}{C_{2\infty}^\beta - C_{20}^\beta} \right) \sum_{n=1}^{\infty} \frac{B_n b_n}{\lambda_n} \sin \pi n \frac{S^\alpha}{S}$$

In the symmetrical configuration which we are considering this reduces to

$$\phi + S = \frac{C}{C_{2\infty}} \frac{4\pi D_{22}}{v} \sum_{n=1}^{\infty} \frac{B_n b_n}{\lambda_n} \sin \pi n \frac{S^\alpha}{S} \quad (3.78)$$

where we have adopted the notation

$$\phi = \frac{4}{RT} \frac{\sigma^\alpha \cos \phi^\alpha}{h^\alpha (C_{2\infty}^\alpha - C_{20}^\alpha)} \quad (3.79a)$$

$$C = - \frac{C_{2\infty}}{\pi} \frac{1}{C_{2\infty}^\alpha - C_{20}^\alpha} \quad (3.79b)$$

We can see from the symmetric phase diagram of Fig. 10 that

$$C_{2\infty} - C_{20}^{\alpha\gamma} = - (C_{2\infty} - C_{20}^{\beta\gamma}) \quad (3.80)$$

Therefore eq. 3.75 yields

$$S^\alpha = S^\beta \quad (3.81)$$

Substituting this equality in eq. 3.78 we finally obtain a relation between  $v$  and  $S$ .

Now we shall perform the calculations for the Fourier coefficients up to the second order in  $n$ . Taking account of the equality of lamellae thickness we obtain from eq. 3.64

$$a_0 = \lambda = \frac{K_2^\alpha + K_2^\beta}{2} \quad a_1 = \mu = \frac{2}{\pi} (K_2^\alpha - K_2^\beta) \quad (3.82a;b)$$

$$a_2 = 0 \quad a_3 = -\frac{\mu}{3} \quad (3.82c;d)$$

and for the coefficients  $B_0$ ,  $B_1$  and  $B_2$

$$B_0 = C_{2\infty} \left[ \frac{(2\lambda + \frac{8\pi D_{22}}{Sv})(2\lambda + \frac{4\pi D_{22}}{Sv}) - \frac{4}{9}\mu^2}{\lambda(2\lambda + \frac{8\pi D_{22}}{Sv})(2\lambda + \frac{4\pi D_{22}}{Sv}) - \frac{4}{9}\lambda\mu^2 - \mu^2(2\lambda + \frac{8\pi D_{22}}{Sv})} - 1 \right] - C_{1\infty} \left( \frac{1}{K_1} - 1 \right) \quad (3.83a)$$

$$B_1 = -C_{2\infty} \frac{2(2\lambda + \frac{8\pi D_{22}}{Sv})\mu}{\lambda(2\lambda + \frac{8\pi D_{22}}{Sv})(2\lambda + \frac{4\pi D_{22}}{Sv}) - \frac{4}{9}\lambda\mu^2 - \mu^2(2\lambda + \frac{8\pi D_{22}}{Sv})} \quad (3.83b)$$

$$B_2 = C_{2\infty} \frac{\frac{4}{3}\mu^2}{\lambda(2\lambda + \frac{8\pi D_{22}}{Sv})(2\lambda + \frac{4\pi D_{22}}{Sv}) - \frac{4}{9}\lambda\mu^2 - \mu^2(2\lambda + \frac{8\pi D_{22}}{Sv})} \quad (3.83c)$$

We can substitute these coefficients into eq. 3.78 after division by  $S$  to yield

$$\frac{\phi}{S} + 1 = C \frac{\frac{8\pi D_{22}}{Sv} \frac{2\lambda + \frac{8\pi D_{22}}{Sv}}{\lambda(2\lambda + \frac{8\pi D_{22}}{Sv})(2\lambda + \frac{4\pi D_{22}}{Sv}) - \mu^2(2\lambda + \frac{8\pi D_{22}}{Sv}) - \frac{4}{9}\lambda\mu^2}}{\lambda(2\lambda + \frac{8\pi D_{22}}{Sv})(2\lambda + \frac{4\pi D_{22}}{Sv}) - \mu^2(2\lambda + \frac{8\pi D_{22}}{Sv}) - \frac{4}{9}\lambda\mu^2} \quad (3.84)$$

We introduce the dimensionless parameter

$$X = \frac{8\pi D_{22}}{Sv} \quad (3.85)$$

and write eq. 3.84 analogously to eq. V.9 as

$$\frac{\phi}{S} + 1 = C \frac{\mu X (2\lambda + X)}{\frac{\lambda}{2}(X + 2\lambda)(X + 4\lambda) - \mu^2(X + 2\lambda) - \frac{4}{9}\lambda\mu^2} \quad (3.86)$$



and finally as in eq. V.10 we get

$$\frac{\lambda}{2} \left( \frac{\phi}{S} + 1 \right) (X^2 + 2 \frac{3\lambda^2 - \mu^2}{\lambda} X + 8 \lambda^2 - \frac{44}{9} \mu^2) = C \mu X (2\lambda + X) \quad (3.87)$$

In order to have positive values of  $X$  which satisfy eq. 3.87 we need to fulfill the same thermodynamic condition as demonstrated in Appendix V. This condition imposes a restriction on  $\lambda/\mu$  given by

$$2 C < \frac{\lambda}{\mu} < -\frac{\pi}{4} \quad (3.88)$$

The lower limit depends on the concentration of the addition element. We now examine the variation of  $C$  with the concentration  $C_\infty$ . From eq. 3.79b we have

$$2 C = -\frac{2 C_{2\infty}}{\pi} \frac{1}{C_{2\infty} - C_{20}^{\alpha\gamma}} \quad (3.89)$$

The concentration  $C_{20}^{\alpha\gamma}$  which corresponds to the reference state, is given by eq. 3.40a for the phase boundary at zero pressure, viz.,

$$C_1^{\alpha\gamma} - C_{1\infty} + C_2^{\alpha\gamma} - C_{20}^{\alpha\gamma} = 0 \quad (3.90)$$

If we let  $x$  be the value of the concentration of element 2 in the binary limit where  $x_{1\infty}$  vanishes then

$$x_{20}^{\alpha\gamma} = x - x_{1\infty} \quad (3.91)$$

Furthermore the value of  $x_{2\infty}$  must be such as to satisfy the symmetry of the original composition in the parent phase, viz.,

$$x_{2\infty} = \frac{1 - x_{1\infty}}{2} \quad (3.92)$$

From eqs. 3.91 and 3.92 we deduce the variation of  $2C$  with  $x_{1\infty}$ , i.e.,

$$2C = - \frac{2(1 - x_{1\infty})}{\pi(1 - 2x + x_{1\infty})} \quad (3.93)$$

Inequality 3.88 then gives for the left hand side

$$\frac{8}{\pi} \frac{1 - x_{1\infty}}{1 + x_{1\infty} - 2x} > \frac{x + y - 2xy}{y - x} \quad (3.94)$$

Or equivalently

$$\frac{8}{\pi} (1 - x_{1\infty})(y - x) > (1 + x_{1\infty} - 2x)(x + y - 2xy) \quad (3.95)$$

$$\frac{8}{\pi} (1 - x_{1\infty}) - (1 - 2x)(1 + x_{1\infty} - 2x) > \left[ \frac{8}{\pi} (1 - x_{1\infty}) + (1 + x_{1\infty} - 2x) \right] K^\alpha \quad (3.96)$$

and finally

$$(1 + x_{1\infty} - 2x)(1 + K^\alpha - 2x) < \frac{8}{\pi} (1 - x_{1\infty})(1 - K^\alpha) \quad (3.97)$$

This gives the condition for  $x_{1\infty}$

$$x_{1\infty} < \frac{\frac{8}{\pi} (1 - K^\alpha) - (1 - 2x)(1 + K^\alpha - 2x)}{\frac{8}{\pi} (1 - K^\alpha) + (1 + K^\alpha - 2x)} \quad (3.98)$$

As we have seen in the binary case (eq. 2.69) inequality 3.88 is unnecessarily restrictive and as before this is due to the limitation of the first order expansion. The condition imposed by eq. 3.98 should not therefore be taken as definitive as we shall see from a more rigorous calculation that the limit for  $x_{1\infty}$  lies in the  $\alpha - \beta$  two phase region very close to the three phase equilibrium triangle.

We can examine the variations of the critical lamellar spacing with  $x_{1\infty}$ . From eq. 3.79a we have

$$\phi = \frac{8 \sigma^\alpha \cos \phi^\alpha}{RT} \frac{1}{h^\alpha (1 + x_{1\infty} - 2x)} \quad (3.99)$$

and the critical lamellar spacing is given by eq. V.43 as

$$S_c = \frac{\phi}{2C \frac{\mu}{\lambda} - 1} \quad (3.100)$$

We see that an increase in  $x_{1\infty}$  decreases  $\phi$  but at the same time the denominator of  $S_c$  goes rapidly to zero and  $S_c$  tends towards infinity as  $x_{1\infty}$  approaches  $(x_{1\infty})_{lim}$ . This behaviour with variations in composition of the addition element is analogous to the effect of raising the temperature in the binary case. In both cases the velocity vanishes and the lamellar spacing becomes very large as a particular composition or temperature is attained.

### III.C THEORY OF TERNARY SYSTEMS WITH THE SECOND THERMODYNAMIC VERSION

We shall here introduce the equations pertaining to the second boundary condition because they will be needed later for the calculation of the Fourier expansion coefficients. Substituting the pressure relation of eq. 3.45a into eq. 3.56a we get

$$-\cos\phi^a = \int_0^{S^\alpha} \frac{P}{\sigma^\alpha} dy = \frac{RT}{\sigma^\alpha} \int_0^{S^\alpha} (k_1^\alpha C_1^{\alpha\gamma} + k_2^\alpha C_2^{\alpha\gamma} - k_1^\alpha C_{10}^{\alpha\gamma} - k_2^\alpha C_{20}^{\alpha\gamma}) dy \quad (3.101)$$

Here we have chosen the reference state such that  $C_{10}^{\alpha\gamma} = C_{10}^{\beta\gamma} = C_{1\infty}$ . This uniquely determines the other reference compositions if we know the ternary diagram. The reference concentrations are designated by the subscript o. We can substitute into eq. 3.101 the expressions for the concentrations  $C_1^{\alpha\gamma}$  and  $C_2^{\alpha\gamma}$  given by eqs. 3.51 to yield

$$-\frac{\sigma^\alpha \cos \phi^\alpha}{RT} - \frac{S^\alpha}{2} k_2^\alpha (C_{2\infty} - C_{20}^{\alpha\gamma}) = \quad (3.102)$$

$$-\frac{1}{v} \int_0^{\frac{S^\alpha}{2}} \left\{ \sum_{n=1}^{\infty} \left[ k_1^\alpha D_{11} \frac{A_n b_n^2}{\lambda_n} + k_2^\alpha (D_{11} \tau \frac{A_n}{\lambda_n} + D_{22} \frac{B_n}{\lambda_n}) b_n^2 \right] \cos b_n y \right\} dy$$

and after integration we obtain

$$\frac{\sigma^\alpha \cos \phi^\alpha}{RT} + \frac{S^\alpha}{2} k_2^\alpha (C_{2\infty} - C_{20}^{\alpha\gamma}) = \quad (3.103)$$

$$\frac{1}{v} \sum_{n=1}^{\infty} \left[ D_{11} (k_1^\alpha + k_2^\alpha \tau) \frac{A_n b_n}{\lambda_n} + D_{22} k_2^\alpha \frac{B_n b_n}{\lambda_n} \right] \sin n\pi \frac{S^\alpha}{S}$$

Alternatively if we divide both members by  $k_2^\alpha$  we get

$$\frac{\sigma^\alpha \cos \phi^\alpha}{RT} + \frac{S^\alpha}{2} (C_{2\infty} - C_{20}^{\alpha\gamma}) = \quad (3.104)$$

$$\frac{1}{v} \sum_{n=1}^{\infty} \left[ D_{11} \left( \frac{k_1^\alpha}{k_2^\alpha} + \tau \right) \frac{A_n b_n}{\lambda_n} + D_{22} \frac{B_n b_n}{\lambda_n} \right] \sin \pi n \frac{S^\alpha}{S}$$

Similarly from eqs. 3.45b and 3.56b we obtain for the  $\beta$  phase

$$-\cos \phi^\beta = \frac{RT}{\sigma^\beta} \int_{\frac{S^\alpha}{2}}^{\frac{S}{2}} [(k_1^\beta - k_3^\beta)(C_1^{\beta\gamma} - C_{1\infty}) - k_3^\beta (C_2^{\beta\gamma} - C_{20}^{\beta\gamma})] dy \quad (3.105)$$

Substituting in this equation the concentrations  $C_1^{\beta\gamma}$  and  $C_2^{\beta\gamma}$  via their expressions 3.51 we have

$$-\frac{\sigma^\beta \cos \phi^\beta}{RT} + k_3^\beta (C_{2\infty} - C_{20}^{\beta\gamma}) \frac{S^\beta}{2} = \quad (3.106)$$

$$-\frac{1}{v} \int_{\frac{S^\alpha}{2}}^{\frac{S}{2}} \sum_{n=1}^{\infty} \left[ (k_1^\beta - k_3^\beta) D_{11} \frac{A_n b_n^2}{\lambda_n} - k_3^\beta \tau \frac{A_n b_n^2}{\lambda_n} - k_3^\beta D_{22} \frac{B_n b_n^2}{\lambda_n} \right] \cos b_n y \quad dy$$

and after integration we get

$$\frac{\sigma^\beta \cos \phi^\beta}{RT} - k_3^\beta (C_{2\infty} - C_{20}^{\beta\gamma}) \frac{S^\beta}{2} = \quad (3.107)$$

$$- \frac{1}{v} \sum_{n=1}^{\infty} \left[ D_{11} (k_1^\beta - k_3^\beta - \tau k_3^\beta) \frac{A_n b_n}{\lambda_n} - D_{22} k_3^\beta \frac{B_n b_n}{\lambda_n} \right] \sin \pi n \frac{S^\alpha}{S}$$

We can also divide by  $-k_3^\beta$  to obtain

$$\frac{\sigma^\beta \cos \phi^\beta}{RT} + (C_{2\infty} - C_{20}^{\beta\gamma}) \frac{S^\beta}{2} = \quad (3.108)$$

$$- \frac{1}{v} \sum_{n=1}^{\infty} \left[ D_{11} \left( 1 + \tau - \frac{k_1^\beta}{k_3^\beta} \right) \frac{A_n b_n}{\lambda_n} + D_{22} \frac{B_n b_n}{\lambda_n} \right] \sin \pi n \frac{S^\alpha}{S}$$

One relation between  $S^\alpha$ ,  $S^\beta$  and  $v$  is obtained by addition of eqs. 3.104 and 3.108.

$$\frac{1}{RT} \left( \frac{\sigma^\alpha \cos \phi^\alpha}{k_2^\alpha} - \frac{\sigma^\beta \cos \phi^\beta}{k_3^\beta} \right) + \frac{S^\alpha}{S} (C_{2\infty} - C_{20}^{\alpha\gamma}) + \frac{S^\beta}{2} (C_{2\infty} - C_{20}^{\beta\gamma}) \quad (3.109)$$

$$= - \frac{D_{11}}{v} \left( \frac{k_1^\alpha}{k_2^\alpha} + \frac{k_1^\beta}{k_3^\beta} - 1 \right) \sum_{n=1}^{\infty} \frac{A_n b_n}{\lambda_n} \sin \pi n \frac{S^\alpha}{S}$$

In contradistinction to the binary case (eq. 2.88) the right hand side of this equation is not equal to zero. The expression for the  $B_n$  coefficients has disappeared but we still have a summation involving the coefficients  $A_n$ .

A second equation between  $S$ ,  $v$  and  $\frac{S^\alpha}{S}$  is obtained if we write eqs. 3.104 and 3.108 in the form

$$\frac{2\sigma^\alpha \cos\phi^\alpha}{RTk_2^\alpha (C_{2\infty} - C_{20}^{\alpha\gamma})} + S^\alpha = \quad (3.110a)$$

$$\frac{2}{v} \left( \frac{1}{C_{2\infty} - C_{20}^{\alpha\gamma}} \right) \sum_{n=1}^{\infty} \left[ D_{11} \left( \frac{k_1^\alpha}{k_2^\alpha} + \tau \right) \frac{A_n b_n}{\lambda_n} + D_{22} \frac{B_n b_n}{\lambda_n} \right] \sin \pi n \frac{S^\alpha}{S}$$

$$\frac{2\sigma^\beta \cos\phi^\beta}{RT k_3^\beta (C_{2\infty} - C_{20}^{\beta\gamma})} + S^\beta = \quad (3.110b)$$

$$\frac{-2}{v} \left( \frac{1}{C_{2\infty} - C_{20}^{\beta\gamma}} \right) \sum_{n=1}^{\infty} \left[ D_{11} \left( 1 + \tau - \frac{k_1^\beta}{k_3^\beta} \right) \frac{A_n b_n}{\lambda_n} + D_{22} \frac{B_n b_n}{\lambda_n} \right] \sin \pi n \frac{S^\alpha}{S}$$



and add them together to give

$$\frac{2}{RT} \left[ \frac{\sigma^\alpha \cos \phi^\alpha}{k_2^\alpha (C_{2\infty} - C_{20}^{\alpha\gamma})} - \frac{\sigma^\beta \cos \phi^\beta}{k_3^\beta (C_{2\infty} - C_{20}^{\beta\gamma})} \right] + S = \quad (3.111)$$

$$\frac{2 D_{11}}{v} \left( \frac{\frac{k_1^\alpha}{k_2^\alpha} + \tau}{C_{2\infty} - C_{20}^{\alpha\gamma}} - \frac{1 + \tau - \frac{k_1^\beta}{k_3^\beta}}{C_{2\infty} - C_{20}^{\beta\gamma}} \right) \sum_{n=1}^{\infty} \frac{A_n b_n}{\lambda_n} \sin \pi n \frac{S^\alpha}{S}$$

$$+ \frac{2 D_{22}}{v} \left( \frac{1}{C_{2\infty} - C_{20}^{\alpha\gamma}} - \frac{1}{C_{2\infty} - C_{20}^{\beta\gamma}} \right) \sum_{n=1}^{\infty} \frac{B_n b_n}{\lambda_n} \sin \pi n \frac{S^\alpha}{S}$$

We must now evaluate the Fourier series coefficients using the complex ratios 3.44. As it is demonstrated in Appendix XI they can be written in the form XI.9

$$\frac{C_1^{\alpha\gamma}}{C_{10}^{\alpha\gamma}} - \frac{C_2^{\alpha\gamma}}{C_{20}^{\alpha\gamma}} = \frac{C_1^{\gamma\alpha}}{C_{10}^{\gamma\alpha}} - \frac{C_2^{\gamma\alpha}}{C_{20}^{\gamma\alpha}} \quad \frac{C_1^{\alpha\gamma}}{C_{10}^{\alpha\gamma}} - \frac{C_3^{\alpha\gamma}}{C_{30}^{\alpha\gamma}} = \frac{C_1^{\gamma\alpha}}{C_{10}^{\gamma\alpha}} - \frac{C_3^{\gamma\alpha}}{C_{30}^{\gamma\alpha}} \quad (3.112a;b)$$

$$\frac{C_1^{\beta\gamma}}{C_{10}^{\beta\gamma}} - \frac{C_2^{\beta\gamma}}{C_{20}^{\beta\gamma}} = \frac{C_1^{\gamma\beta}}{C_{10}^{\gamma\beta}} - \frac{C_2^{\gamma\beta}}{C_{20}^{\gamma\beta}} \quad \frac{C_1^{\beta\gamma}}{C_{10}^{\beta\gamma}} - \frac{C_3^{\beta\gamma}}{C_{30}^{\beta\gamma}} = \frac{C_1^{\gamma\beta}}{C_{10}^{\gamma\beta}} - \frac{C_3^{\gamma\beta}}{C_{30}^{\gamma\beta}} \quad (3.112c;d)$$

or

$$x_1 C_{20}^{\gamma\alpha} \Delta C_1^{\alpha\gamma} - x_2 C_{10}^{\gamma\alpha} \Delta C_2^{\alpha\gamma} = x_2 C_{20}^{\alpha\gamma} \Delta C_1^{\gamma\alpha} - x_1 C_{10}^{\alpha\gamma} \Delta C_2^{\gamma\alpha} \quad (3.113a)$$

$$x_1 C_{20}^{\gamma\beta} \Delta C_1^{\beta\gamma} - C_{10}^{\gamma\beta} \Delta C_2^{\beta\gamma} = C_{20}^{\beta\gamma} \Delta C_1^{\gamma\beta} - x_1 C_{10}^{\beta\gamma} \Delta C_2^{\gamma\beta} \quad (3.113b)$$

$$C_{20}^{\gamma\alpha} \Delta C_1^{\alpha\gamma} + (C_{20}^{\gamma\alpha} + x_2 C_{30}^{\gamma\alpha}) \Delta C_2^{\alpha\gamma} = x_2 C_{20}^{\alpha\gamma} \Delta C_1^{\gamma\alpha} + (C_3^{\alpha\gamma} + x_2 C_{20}^{\alpha\gamma}) \Delta C_2^{\gamma\alpha} \quad (3.113c)$$

$$x_2 C_{20}^{\gamma\beta} \Delta C_1^{\beta\gamma} + (C_{30}^{\gamma\beta} + x_2 C_{20}^{\gamma\beta}) \Delta C_2^{\beta\gamma} = C_{20}^{\beta\gamma} \Delta C_1^{\gamma\beta} + (C_{20}^{\beta\gamma} + x_2 C_{30}^{\beta\gamma}) \Delta C_2^{\gamma\beta} \quad (3.113d)$$

In the last set of equations we have inserted

$$x_1^\alpha = x_1^\beta = x_1 \quad \text{and} \quad x_2^\alpha = x_2^\beta = x_2 \quad (3.114)$$

into eqs. 3.44 to take account of the symmetry of the diagram (Fig. 11).

In these approximations where higher powers of  $\Delta C$  have been ignored it is essential that the reference states  $C_{10}^{\alpha\gamma}$  and  $C_{10}^{\beta\gamma}$  be chosen in the vicinity of the solution for the concentrations in the precipitate phases. The best way of assuring this is to choose both of them equal to their actual average value  $C_{1\infty}$ .

Either system of equations written above allows us in principle to evaluate all the coefficients  $A_n$  and  $B_n$  for the Fourier series. Unfortunately we have found such a development to be either intractable or

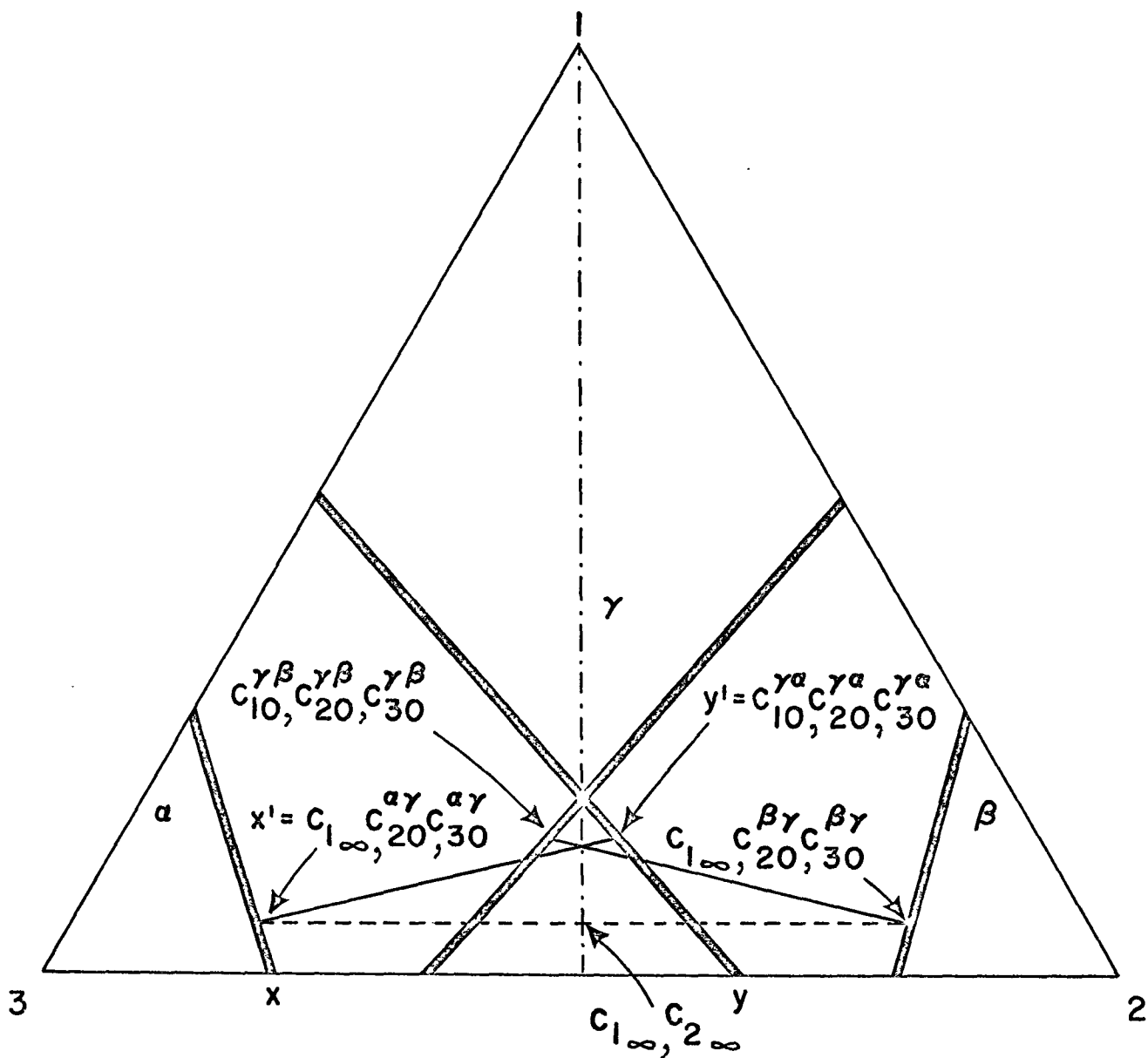


Fig. 11: Symmetric ternary phase diagram corresponding to the second thermodynamic version.

uninformative. We therefore proceed to restrict this rather general thermodynamic calculation to special cases. In all the subsequent discussion we assume that  $k_2^\alpha = -k_3^\beta$  and  $\sigma^\alpha = \sigma^\beta$  so that the first left hand term of eq. 3.109 vanishes. We can see first of all that as  $D_{11}$  tends to zero  $S^\alpha$  tends to  $S^\beta$  (but never rigorously equal to) so that the spacing becomes uniform. This does not, however, imply that the solute distributions in the various phases achieve symmetric configurations, and indeed if  $D_{21}$  is different from zero they will in general be unsymmetric.

If on the other hand  $D_{11}$  goes to  $D_{22}$  so that we can approximate  $D_{21}$  to zero then a perfect symmetry (thermodynamic and kinetic) is achievable with  $S^\alpha$  exactly equal to  $S^\beta$ . In Appendix XI we have used the set of equations 3.112 to evaluate  $A_0$  and  $A_1$  and the latter is found to be non-zero. This implies in relation to eq. 3.109 that since  $D_{11}$  is different from zero and  $k_1^\alpha/k_2^\alpha + k_1^\beta/k_3^\beta$  is generally not equal to unity, the summation on the right hand side must converge to zero. This is the limit of our achievement in treating the ternary problem on the basis of a reasonably general kind of thermodynamics. In the following we further restrict the calculation to a simpler form of thermodynamics which approaches that of a pseudo-binary.

If we replace eqs. 3.113a;b by

$$C_{20}^{\gamma\alpha} \Delta C_1^{\alpha\gamma} = x_2 C_{20}^{\alpha\gamma} \Delta C_1^{\gamma\alpha} \quad (3.115a)$$

$$x_2 C_{20}^{\gamma\beta} \Delta C_1^{\beta\gamma} = C_{20}^{\beta\gamma} \Delta C_1^{\gamma\beta} \quad (3.115b)$$

we thereby effectively insist that composition variations due to pressure lie parallel to the 2-3 side of the triangle. We must emphasize at this point that although our restrictions are increasingly severe, they are still less restrictive with respect to composition changes in the product phases than those used by Hillert in his binary treatment since we still allow segregation of component 2. However, with respect to component 1, as the solution will demonstrate, our restriction is similar to Hillert's. We emphasize that such a restriction has hopes of being valid only if the tie-lines are closely parallel to the 2-3 side of the composition triangle.

We can now deduce the ratios of increments

$$\frac{\Delta C_1^{\alpha Y}}{\Delta C_1^{Y\alpha}} = \frac{x_2 C_{20}^{\alpha Y}}{C_{20}^{Y\alpha}} \quad (3.116a)$$

and

$$\frac{\Delta C_1^{BY}}{\Delta C_1^{YB}} = \frac{C_{20}^{BY}}{x_2 C_{20}^{YB}} \quad (3.116b)$$

From eqs. 3.113c;d we also have the ratios of increments

$$\frac{\Delta C_2^{\alpha\gamma}}{\Delta C_2^{\gamma\alpha}} = \frac{C_{30}^{\alpha\gamma} + x_2 C_{20}^{\alpha\gamma}}{C_{20}^{\gamma\alpha} + x_2 C_{30}^{\gamma\alpha}} \quad (3.116c)$$

and

$$\frac{\Delta C_2^{\beta\gamma}}{\Delta C_2^{\gamma\beta}} = \frac{C_{20}^{\beta\gamma} + x_2 C_{30}^{\beta\gamma}}{C_{30}^{\gamma\beta} + x_2 C_{20}^{\gamma\beta}} \quad (3.116d)$$

From Fig. 11 we can see that the two last ratios are equal for a symmetrical thermodynamic configuration. These expressions are identical in form to those (eqs. 2.78 and 2.79) for the binary system. As demonstrated in Appendix XI we can evaluate the Fourier coefficients

$$A_0 = C_{10}^{\gamma\alpha} - C_{1\infty} \quad (3.117a)$$

$$A_n = 0 \quad \text{for } n \neq 0 \quad (3.117b)$$

$$B_{2i-1} = \frac{2}{\pi} [K(C_{20}^{\gamma\alpha} - C_{20}^{\gamma\beta}) - (C_{20}^{\alpha\gamma} - C_{20}^{\beta\gamma})] \frac{\frac{1}{2i-1} \sin(2i-1) \frac{\pi}{2}}{K + \frac{2\pi D_{22}}{Sv} (2i-1)} \quad (3.117c)$$

$$B_{2i} = 0 \quad (3.117d)$$

where

$$K = \frac{C_{30}^{\alpha\gamma} + x_2 C_{20}^{\alpha\gamma}}{C_{20}^{\gamma\alpha} + x_2 C_{30}^{\gamma\alpha}} = \frac{C_{20}^{\beta\gamma} + x_2 C_{30}^{\beta\gamma}}{C_{30}^{\gamma\beta} + x_2 C_{20}^{\gamma\beta}} \quad (3.118)$$

These are very similar in form to those for the corresponding binary problem.

Now substituting these values for the coefficients in eqs. 3.109 and 3.111 we obtain

$$S^\alpha = S^\beta \quad (3.119)$$

and

$$\frac{\phi}{S} + 1 = C' \times \sum_{i=1}^{\infty} \frac{1}{(2i-1) [K + X(2i-1)]} \quad (3.120)$$

where

$$\phi = \frac{4 \sigma^\alpha \cos \phi^\alpha}{k_2^\alpha RT (C_{2\infty}^\alpha - C_{20}^{\alpha\gamma})} \quad (3.121a)$$

$$C' = -\frac{4}{\pi^2} \frac{K (C_{20}^{\gamma\alpha} - C_{20}^{\gamma\beta}) - (C_{20}^{\alpha\gamma} - C_{20}^{\beta\gamma})}{C_{2\infty} - C_{20}^{\alpha\gamma}} \quad (3.121b)$$

$$X = \frac{2\pi D_{22}}{Sv} \quad (3.121c)$$

Eq. 3.120 is identical to eq. 2.93 but the necessary condition for the existence of a physical solution in the steady state is expressed now in terms of  $x_{1\infty}$ . As shown in Appendix XII we now have the condition XII.29 or

$$0 < x_{1\infty} < \frac{(2y - 1)(y - x)}{2(x_1 - 1)y(1 - y)} \quad (3.122)$$

We have shown in the Appendix XII that this bound lies symmetrically within the two-phase  $\alpha$ - $\beta$  region just below the three-phase field. Indeed, if we had not introduced the restriction on the thermodynamics implied by eqs. 3.116 the bound would exactly correspond to the lower edge of the three-phase field (point M on Fig. 12).

The quantity  $C'$  which we defined in eq. 3.121b can be written in terms of  $x'$  and  $y'$  with the convention of XI.13, viz.,

$$C' = \frac{8}{\pi^2} \left[ 1 - \frac{x'(1 - x')(1 - 2y')}{y'(1 - y')(1 - 2x')} \right] \quad (3.123)$$



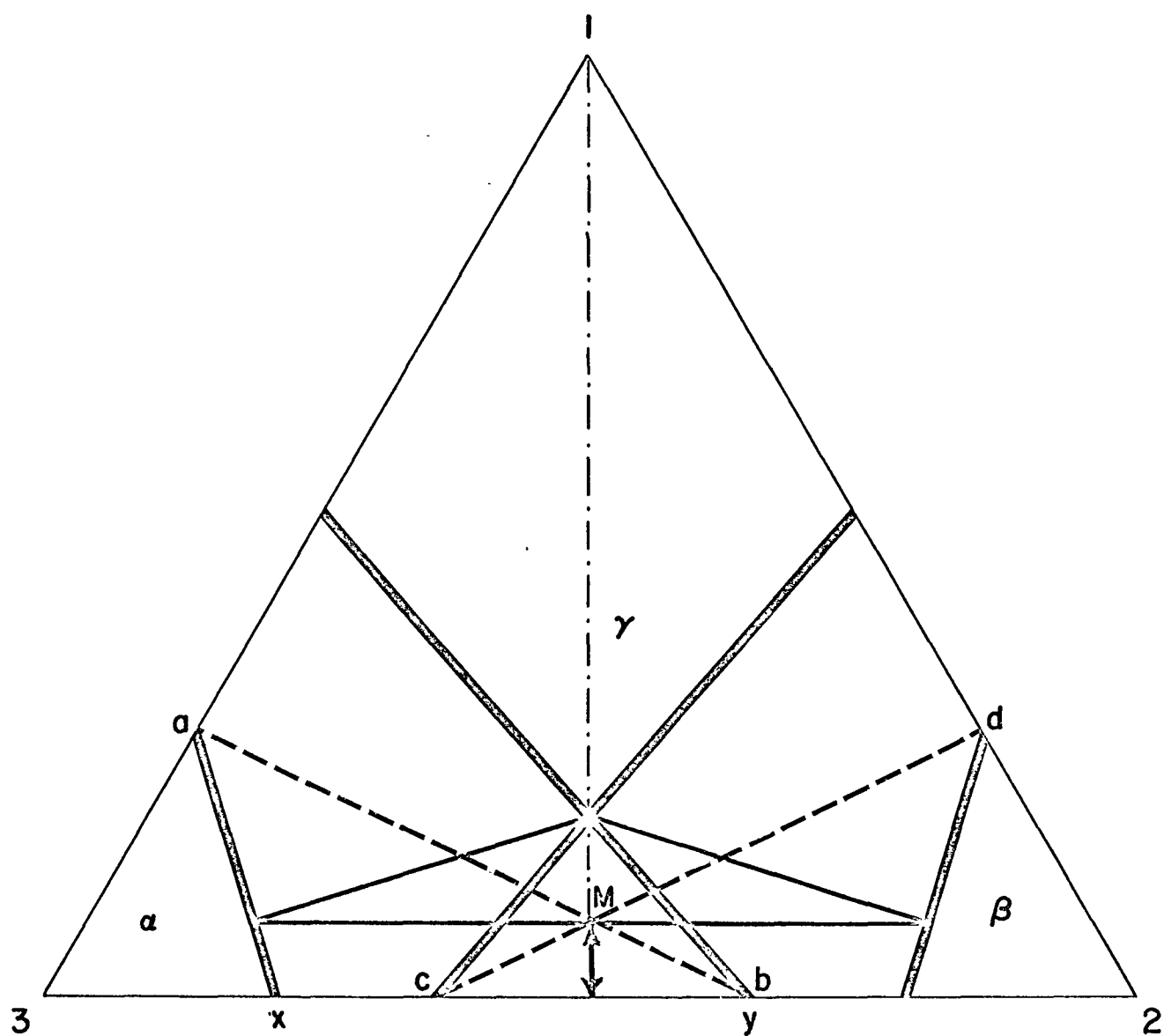


Fig. 12: Domain of variation of  $C_{1\infty}$  deduced for the second thermodynamic version ( $\leftrightarrow$ ).

As we approach the upper limit for  $x_{1\infty}$  the factor  $1 - 2y'$  vanishes and  $C'$  goes to the value  $8/\pi^2$ .

We can also examine the variation with  $x_{1\infty}$  of  $\phi$  as defined in eq. 3.121a. This is

$$\phi = \frac{4 \sigma^\alpha \cos \phi^\alpha}{RT} \frac{2x(1-y)}{(x-y) \left\{ 1 - 2x + x_{1\infty} \left[ (x_1 - 1) \frac{1-y}{y-x} - 1 \right] \right\}} \quad (3.124)$$

The curly bracket in the denominator of  $\phi$  goes to zero for negative values of  $x_{1\infty}$  so there is no situation where  $\phi$  goes to infinity. In fact we see that when  $x_{1\infty}$  increases  $\phi$  decreases, a conclusion which is in agreement with eq. 3.99, the result for our first thermodynamic version.

The critical lamellar spacing  $S_c$  can be expressed as in eq. 2.99b by

$$S_c = \frac{\phi}{C' \frac{\pi}{8} - 1} \quad (3.125)$$

and we can see from previous considerations that it increases with  $x_{1\infty}$  and becomes infinite as we approach the upper limit for  $x_{1\infty}$ .

To gain an idea of the influence of the addition element on the precipitation velocity we refer to the analogue of eq. 2.98 which yields a velocity

$$v = \frac{2\pi D_{22}}{K} \frac{C' \frac{\pi^2}{8} - 1}{1 - 0.1819 C'} \frac{1}{S} \frac{1 - \frac{S_c}{S}}{1 + \frac{\phi'}{S}} \quad (3.126)$$

As  $x_{1\infty}$  increases,  $C'$  decreases and goes to the limit  $8/\pi^2$ , but  $K$  expressed by

$$K = \frac{x' (1 - x')}{y' (1 - y')} \quad (3.127)$$

does not vary significantly. If we suppose as is usual that the optimum lamellar spacing is given by some constant multiple of  $S_c$  then the last fraction in eq. 3.126 remains approximately constant and  $v$  will therefore decrease with the addition of element 1 to vanish at the upper limit for  $x_{1\infty}$ . This is of course to be expected since for this type of phase diagram the supersaturation decreases with  $x_{1\infty}$  and the velocity vanishes at the limit given by 3.122. Note that in this approximation, the cross term indexed by  $D_{21}$  has no effect on the velocity.

It is disappointing that the only tractable case for ternary systems which we have thus far been able to identify (this section) is so restrictive in character that certain important ternary effects already known and identified become trivial. For example, although the diffusion cross terms as measured by  $D_{21}$  modify the concentration profiles in the  $\gamma$  phase unsymmetrically, the interface compositions are automatically adjusted in such a way that the transport of component 2 is unaffected so there is no overall effect on the velocity of growth (the parameter  $\tau$

which appears in eqs. 3.107 and 3.108 disappears in deriving the key equation 3.109) and it disappears from the right hand side of eq. 3.111 because the  $A_n$  vanish for  $n > 0$ . The effect of the addition element is therefore exhibited through a reduction in the driving force for the reaction. It is our surmise on the basis of experience with this and other ternary diffusion problems that the cross effects in eutectoid reactions can be ignored for all but the most precise calculations.

It is worth enquiring whether the segregation factor  $\phi$  has the same significance as in the binary case. Reference to eq. 3.111 shows that its general form is the same as in the binary case and we have no reason to believe that the thermodynamic parameters which appear are of significantly different magnitudes than in the binary case. We conclude therefore that the contribution of  $\phi$  will usually be negligible but in special cases where both  $x'$  and  $y'$  are large the term represents a significant contribution to the stored free energy.

#### IV. COMPARISON OF THEORY WITH EXPERIMENTS

In performing our literature survey we sought experimental investigations on pearlite transformations for which accurate information is given on the phase diagram, the diffusion coefficient, the surface tensions and wherein accurate velocity vs. spacing measurements are given. We concentrated our search on isothermal precipitation reactions, particularly eutectoid reactions. Since in the theory we have performed exploitable calculations only for the symmetrical configuration it was advisable to seek systems which conform as nearly as possible to ideal symmetry. Unfortunately we were not able to find any system which met all the requirements. We have, therefore, adopted the study of Asundi and West<sup>34,35</sup> on the Cu-Al system which comes nearest to meeting our theoretical requirements. In this case where the phase diagram is not strictly symmetric it was necessary to idealize slightly by distorting the diagram. Although it would certainly have been more reliable to utilize the general treatment to check the theory it is felt that no major error is introduced in attaining a tractable symmetric solution to the problem.

We also found it to be useful to apply our symmetrical configuration theory to the much studied Fe-C system even though the distortion required to bring the phase diagram to symmetry is excessive. Although the quantitative comparisons will be in question, the qualitative results are interesting.

A/ DETAILS OF THE CALCULATION OF THE  $v(S)$  RELATIONSHIP

In section II-D 2 we obtained a complete relation between the growth rate  $v$  and the lamellar spacing  $S$  (eq. 2.93). We have undertaken to plot the  $v(S)$  curves for the two aforementioned binary systems at various temperatures. In both of these alloys we will assume that the optimum velocities and spacings are those given by a point on the  $v(S)$  curves corresponding to 1.5 times the spacing at the maximum of the  $v(S)$  curves (see section I). The binary  $v(S)$  relation for the completely symmetric case, eq. 2.96, is

$$\frac{1}{C'} \left( \frac{\phi}{S} + 1 \right) = f(Z) \quad (4.1)$$

where

$$\phi = - \frac{4}{RT} \frac{\sigma^\alpha \cos \phi^\alpha}{k^\alpha (C_\infty - C_{10}^{\alpha Y})} \quad (4.2a)$$

$$C' = - \frac{4}{\pi^2} \frac{K(C_{10}^{\alpha Y} - C_{10}^{\beta Y}) - (C_{10}^{\alpha Y} - C_{10}^{\beta Y})}{C_\infty - C_{10}^{\beta Y}} \quad (4.2b)$$

and

$$Z = \frac{2\pi D}{KSv} \quad (4.2c)$$

All physical values of the spacing  $S$  will be larger than the critical lamellar spacing  $S_c$  as expressed by eq. 2.99b.

$$S_c = \frac{\phi}{C' \frac{\pi}{8} - 1} \quad (4.3)$$

To plot the curves  $v$  vs.  $S$  we choose successive values of the spacing  $S$  and calculate numerically the value of the left hand side of eq. 4.1. We then look in the Table 1 to find the corresponding value of  $Z$ . With eq. 4.2c we can calculate  $v$ . These operations were performed on a desk computer.

#### B/ ALUMINUM BRONZE BINARY SYSTEM

This system has a eutectoid transformation at  $565^{\circ}\text{C}$  and 11.8 wt% aluminum which reasonably closely conforms to a symmetric configuration. Asundi and West<sup>34</sup> have performed experiments to define the thermokinetic properties of these alloys and have gathered data on the pearlite transformation. Using diffusion couples they determined the diffusion coefficient in the parent phase between  $646$  and  $750^{\circ}\text{C}$ . However, they did not perform measurements in the vicinity of the eutectoid transformation so their extrapolation of the curve  $D$  vs.  $1/T$  (Fig. 13) is subject to a large uncertainty.

In another set of experiments, Asundi and West<sup>35</sup> evaluated the growth rate of the precipitates as a function of the lamellar spacing and the temperature. The starting alloys contained 11.8 and 12.4 wt% aluminum, respectively. With the first eutectoid alloy the growth rate

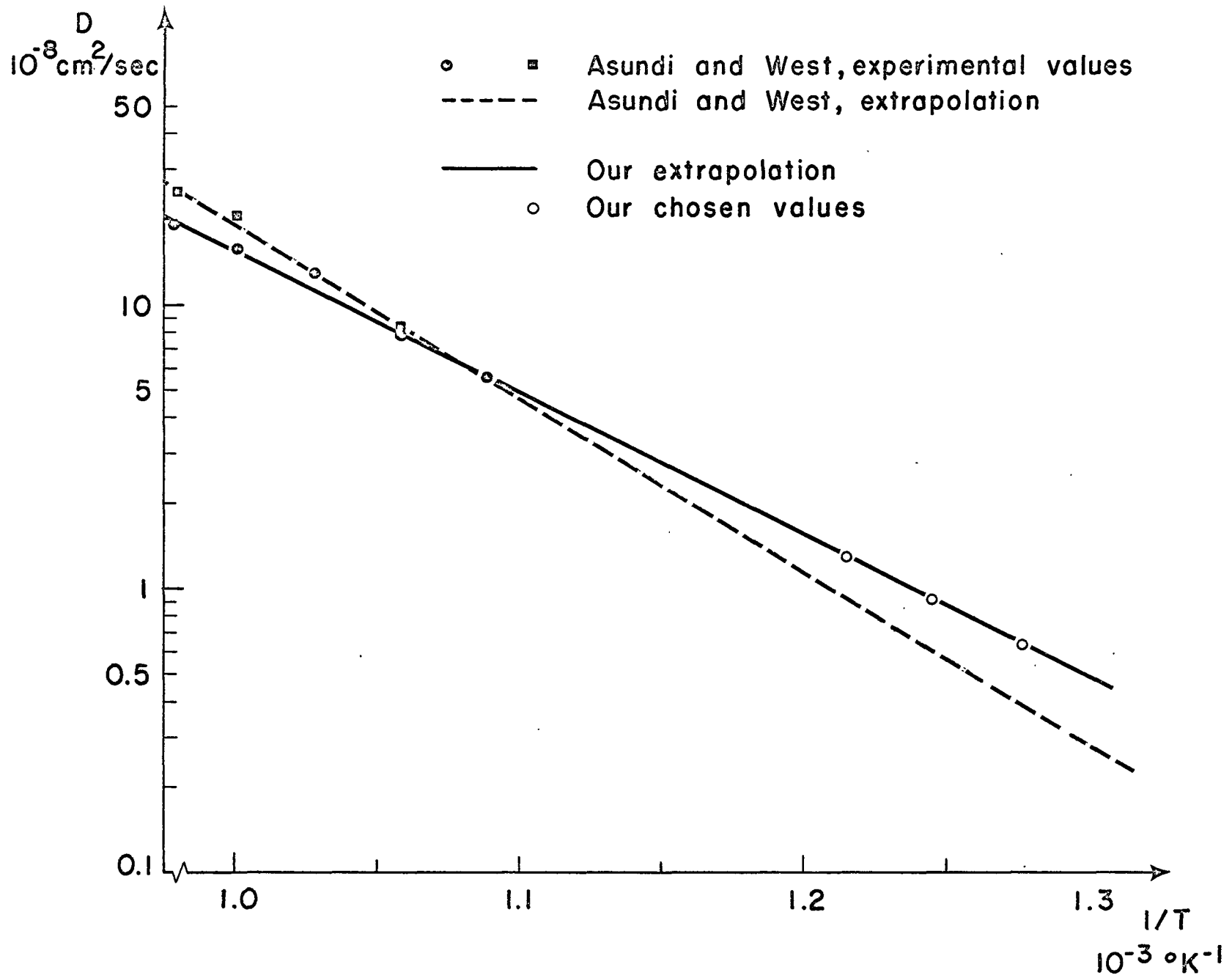


Fig. 13: Diffusion coefficient as a function of temperature for the Cu-Al system.



increased with increasing undercooling down to 525°C, then sharply decreased with further undercooling. At 525°C it is known that a metastable austenitic phase begins to precipitate thus explaining the rapid inhibition of the pearlite reaction.

Asundi and West confirm this interpretation since with the second alloy, which is strongly hypereutectoid, the pearlite precipitation starts only at low temperatures (400 to 500°C) and evolves entirely from the metastable  $\gamma$  phase, its velocity always decreasing with increasing undercooling. We may expect that our predicted values of the velocity will not correspond to the experimental ones whenever the secondary reaction manifests itself.

We have based our calculations on the binary diagram given by Hansen<sup>36</sup>. We have symmetrized this to Fig. 14, the pure component being chosen as  $\text{AlCu}_n$  where  $n = 5$  (corresponding to 23.6 wt% aluminum). All mole fractions must be expressed in terms of this compound if the thermodynamic relations are to be valid. The solubility limits have been appropriately arranged to completely symmetrize the diagram.

We designate in Table II in standard notation the values extracted from Hansen and the adjusted values which we used to

Table II

Adjustment of composition values in symmetrization of the Cu-Al phase diagram

Temperature °C	$\Delta T$ °C	nonsymmetric diagram				symmetric diagram	
		$x_{10}^{\alpha\gamma}$ wt% Al	$x_{10}^{\gamma\alpha}$ wt% Al	$x_{10}^{\beta\gamma}$ wt% Al	$x_{10}^{\gamma\beta}$ wt% Al	x wt% $\text{AlCu}_n$	y wt% $\text{AlCu}_n$
550	15	8.05	11.9	15.5	11.7	34.1	50.4
530	35	8.12	12.0	15.5	11.6	34.4	50.8
510	55	8.20	12.1	15.4	11.5	34.7	51.3

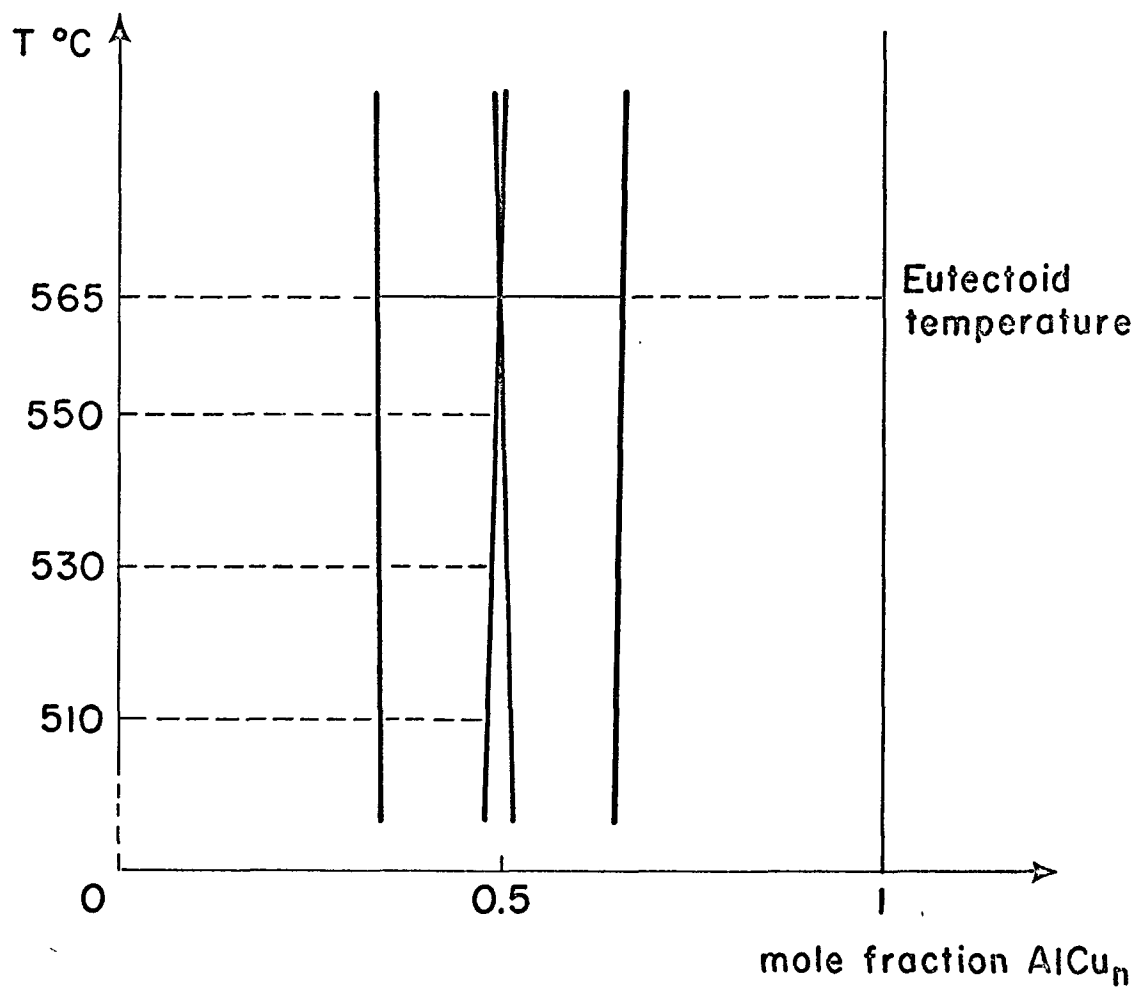


Fig. 14: Symmetricized phase diagram for the Cu-Al system.

construct the symmetric diagram of Fig. 14.

We can now deduce from eq. VII.43

$$x = \frac{y(1-x)}{x(1-y)} \quad (4.4)$$

and therefore, from eq. II.8

$$k^\alpha = \frac{y(1-x)}{x(1-y)} - 1 \quad (4.5)$$

From eq. VII.44 we obtain

$$K = \frac{x(1-x)}{y(1-y)} \quad (4.6)$$

and from eq. VII.47 we have

$$\frac{\pi^2}{8} C' - 1 = - \frac{x(1-x)(1-2y)}{y(1-y)(1-2x)} \quad (4.7)$$

and substituting in eq. VII.40 we obtain

$$\frac{\phi}{S_c} = - \frac{x(1-x)(1-2y)}{y(1-y)(1-2x)} \quad (4.8)$$

and

$$C' = \frac{8}{\pi^2} \left(1 + \frac{\phi}{S_c}\right) \quad (4.9)$$

Eq. VII.53 gives us the expression

$$\phi = \frac{4 \sigma^\alpha M}{RT k^\alpha (1 - 2x)} \quad (4.10)$$

where  $\rho$  is the density of the eutectoid alloy and  $M$  is its molecular weight.

We can now deduce Table III. Since for this system the segregation term  $\phi/S_c$  is rather small we cannot expect our result to be significantly different than that obtained with a Hillert type calculation.

Table III

Temperature °C	$k^\alpha$	$K$	$\phi/S_c$	$\phi$ $10^{-6}$ cm.	$S_c$ $10^{-5}$ cm.	$C'$
550	0.96	0.90	0.024	0.54	2.26	0.83
530	0.97	0.90	0.049	0.56	1.15	0.85
510	0.98	0.91	0.076	0.59	0.78	0.87

Parameters for calculating the  $v(S)$  relationship for the Cu-Al system.

In all the calculations we have chosen a surface tension  $\sigma = 400$  ergs/cm<sup>2</sup> which is typical of a solid-solid interface of some coherency and for the

diffusion coefficients the values are reported in Table IV and shown on Fig. 13.

Table IV

Temperature °C	550	530	510
D 10 <sup>-9</sup> cm <sup>2</sup> /sec	13.0	9.2	6.4

Variation of the diffusion coefficient with temperature for the Cu-Al system.

With all parameters defined we have numerically calculated and plotted the curves  $v$  vs.  $S$  for three undercoolings as shown in Figs. 15, 16 and 17. Since it was found that  $K/X = 10^{-2}$  in the first calculation, the curves of these figures were evaluated using the approximate theory (cf. section II-C 2 and eq. 2.98). For comparison we have also given the curves calculated with a Hillert type model. The optimum values of  $v$  and  $S$  for each temperature are reported in Table V.

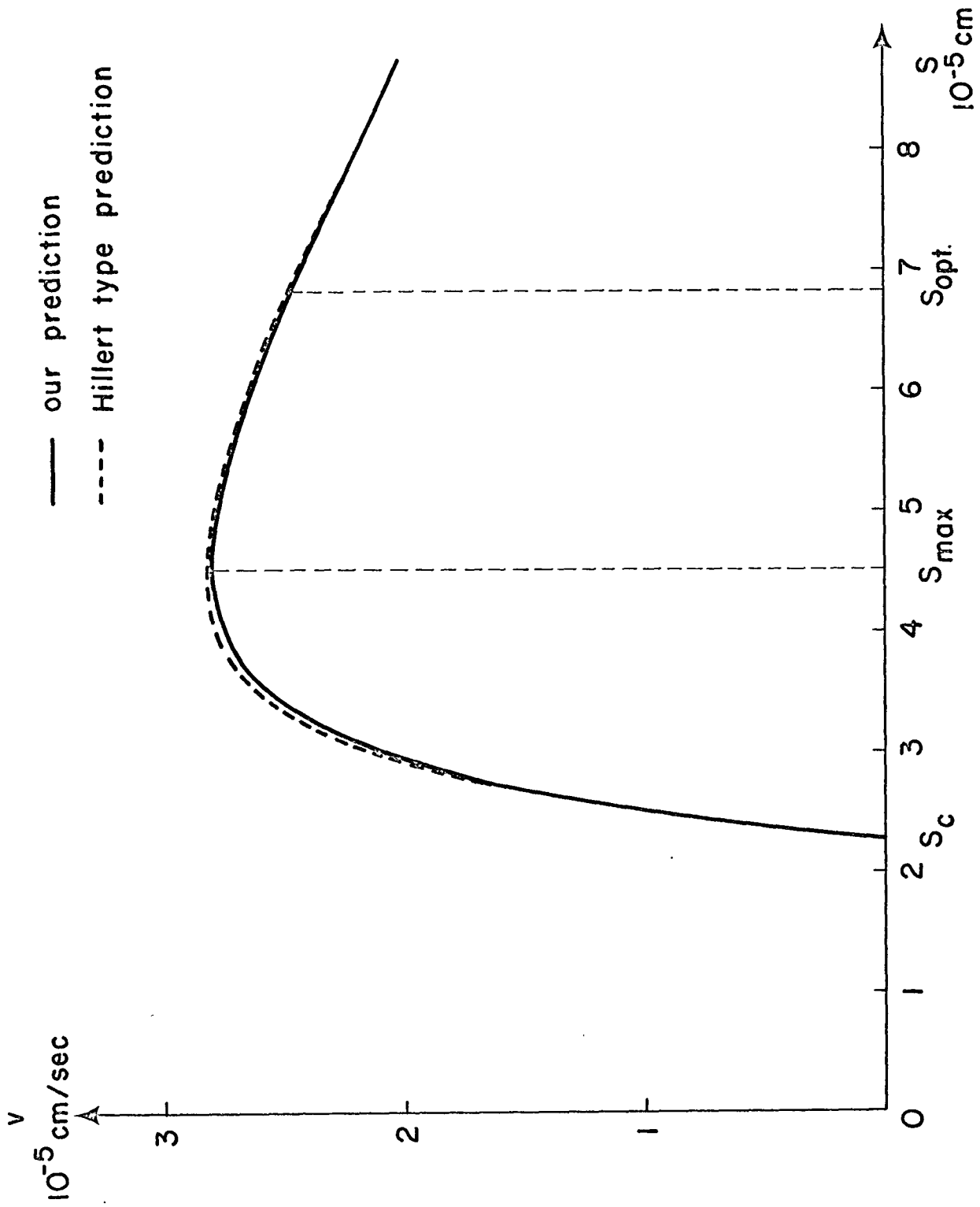


Fig. 15: Theoretical curve  $v(S)$  at  $550^{\circ}\text{C}$  for the Cu-Al system

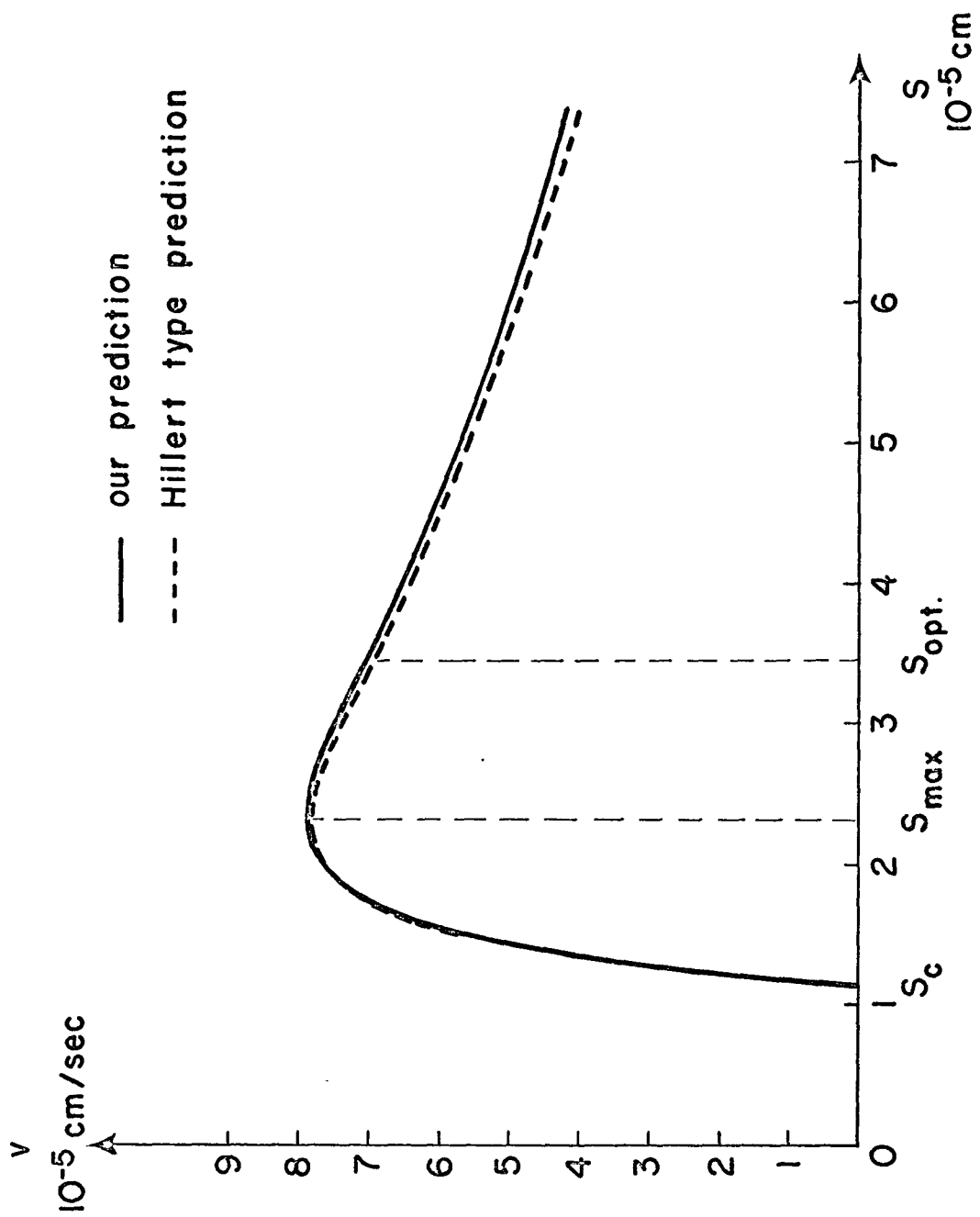


Fig. 16: Theoretical curve  $v(S)$  at  $530^{\circ}\text{C}$  for the Cu-Al system

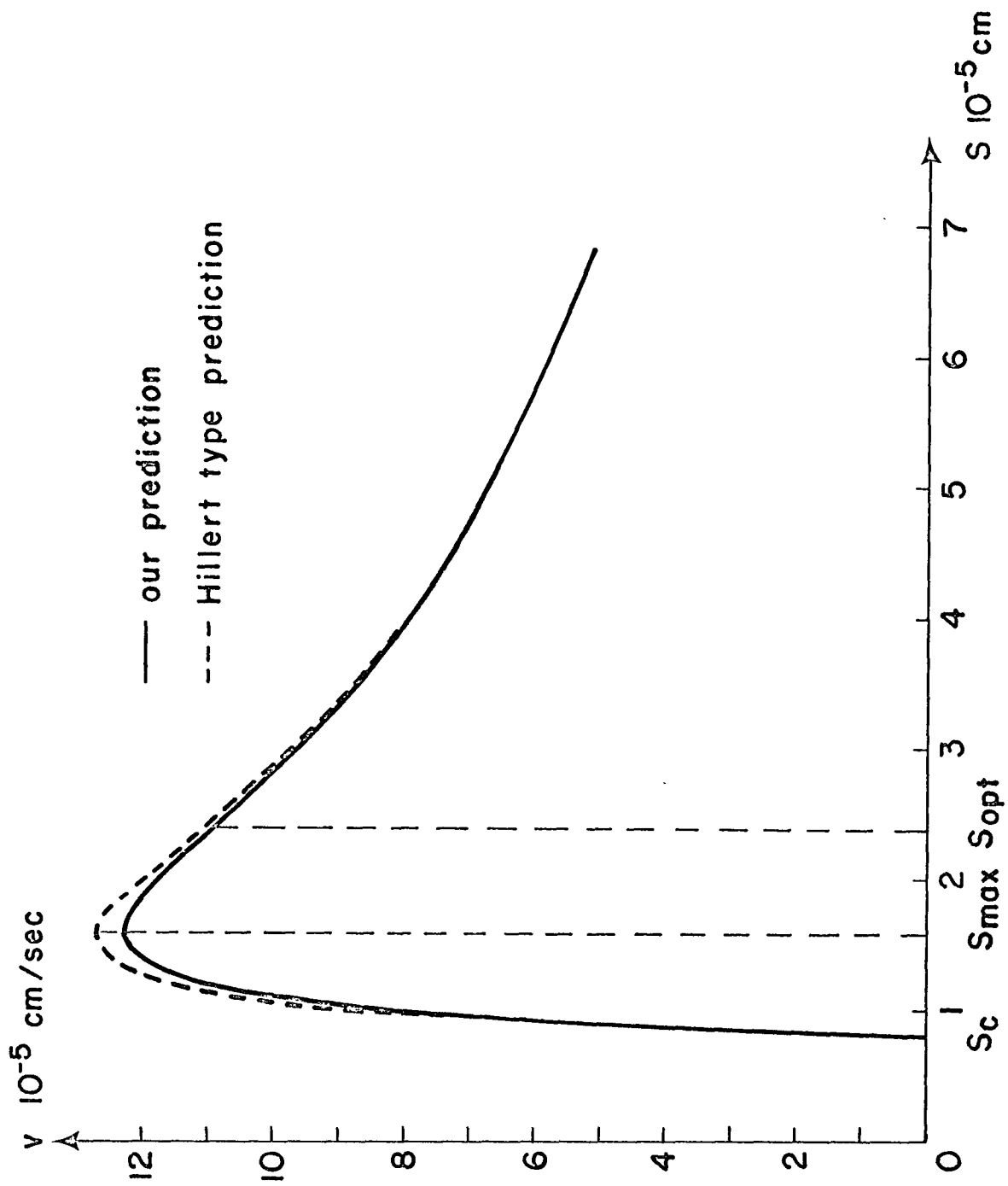


Fig. 17: Theoretical curve  $v(S)$  at  $510^{\circ}\text{C}$  for the Cu-Al system



Table V

Temperature °C	$v_{opt.}$ $10^{-5}$ cm/sec	$S_{opt.}$ $10^{-5}$ cm
550	2.48	6.84
530	7.01	3.50
510	10.94	2.39

Predicted optimum velocity and lamellar spacing for the Cu-Al system.

To compare our predictions with the experiments we have plotted the temperature versus the optimum velocity in Fig. 18 and the inverse of the spacing vs. the temperature in Fig. 19. We find that for appreciable undercooling the predicted velocities are significantly smaller than the experimental values and in contradiction to the experiments. However, they agree to the extent that they both vary as a monotonically increasing function of decreasing temperature in the range of temperatures between 525 and 565°C. The experimental inversion at lower temperatures may be explained by the secondary reaction (see earlier discussion) rather than by a decrease in the diffusion coefficient with temperature. Our predicted values of the lamellar spacing are in good accord with the experimental values.

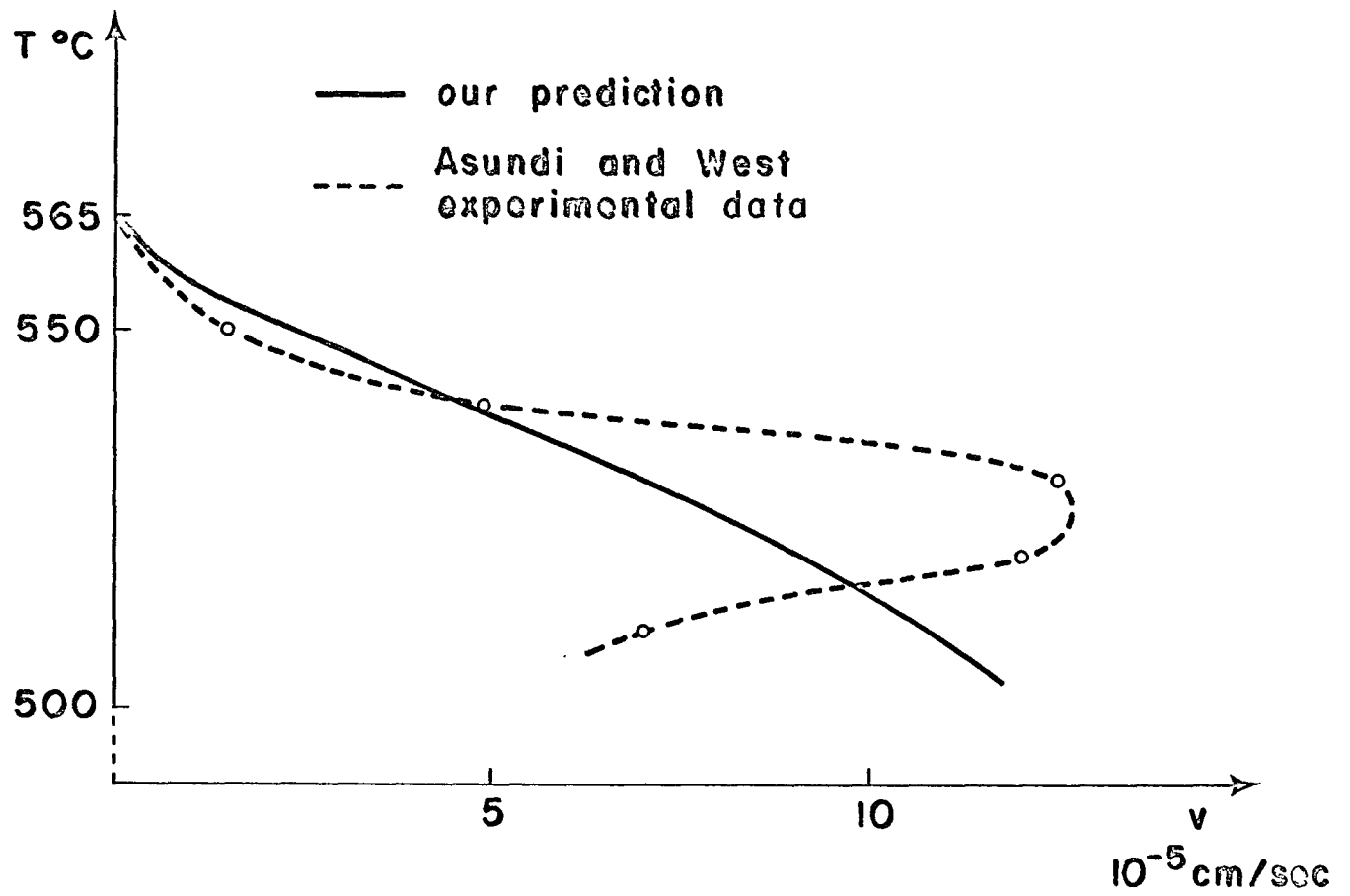


Fig. 18: Plot of  $v$  versus temperature for the Cu-Al system.

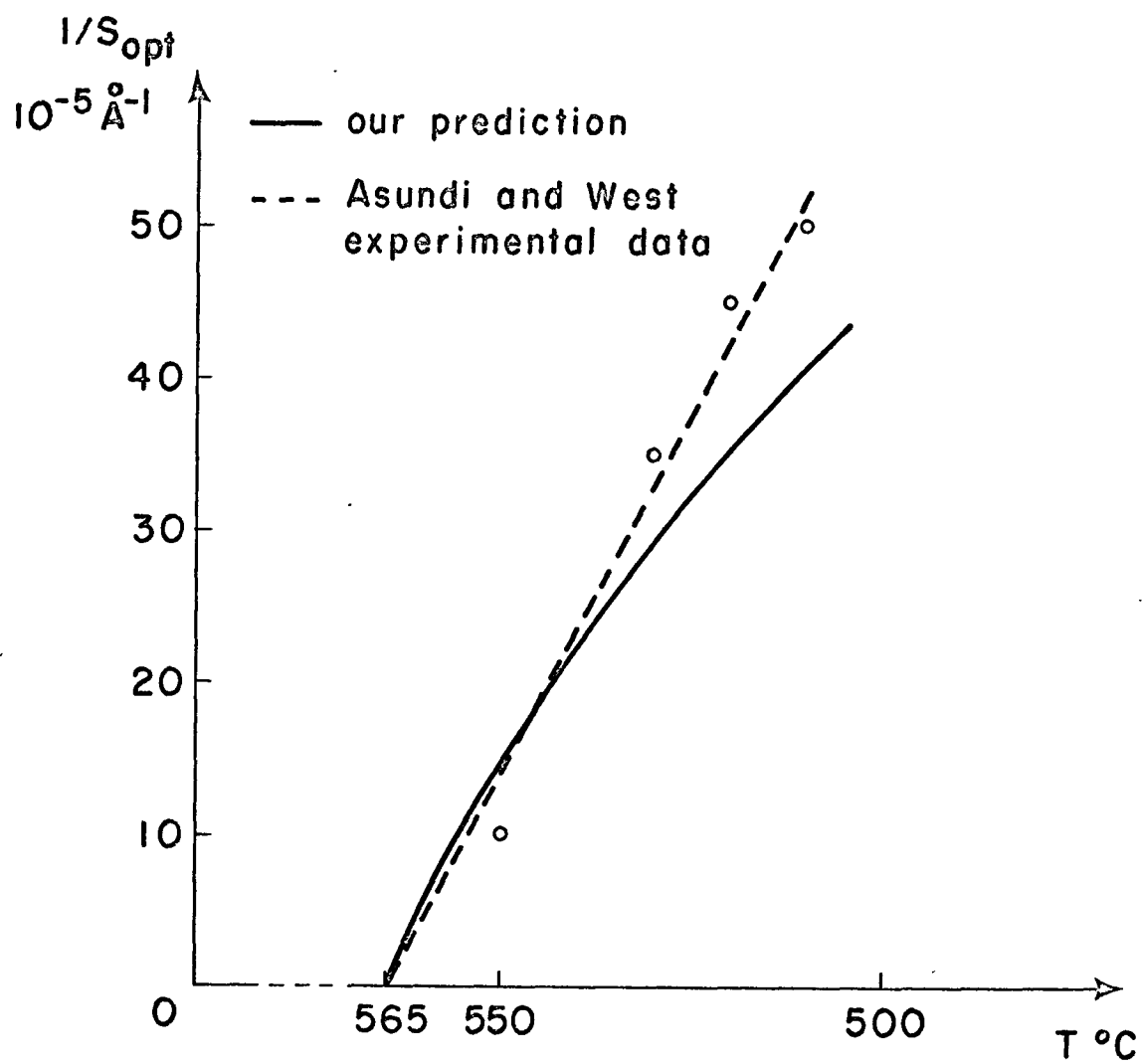


Fig. 19: Plot of  $1/S$  versus temperature for the Cu-Al system

## C/ IRON CARBON BINARY SYSTEM

We consider now the eutectoid transformation in the Fe-C system which occurs at  $728^{\circ}\text{C}$  and 0.765 wt% carbon. The austenite parent  $\gamma$  phase transforms into the precipitate ferrite  $\alpha$  phase and cementite  $\beta$  phase. While the pearlite transformation has been often investigated<sup>14-20,37</sup> we shall only consider here the most recent data due to Brown and Ridley<sup>37</sup>. They have worked on very pure base metal binary and ternary alloys and have presented a very comprehensive survey of the experimental relation between velocity, spacing and temperature. Although from their analysis of the data they conclude with Cahn<sup>12</sup> that the transformation occurs by a surface diffusion mechanism, we will nonetheless proceed with our analysis on the basis of volume diffusion.

This system is very far from a symmetrical configuration so our idealization of it will be rather drastic. The ferrite austenite phase boundaries have been carefully determined by Smith<sup>38</sup> and Mehl and Wells<sup>39</sup> and the austenite cementite phase boundaries have been determined by Smith<sup>40</sup>. Fig. 20 shows the extrapolation of the binary diagram which we used as the basis for the idealization and Table VI gives the corresponding values for the concentrations at three different undercoolings.

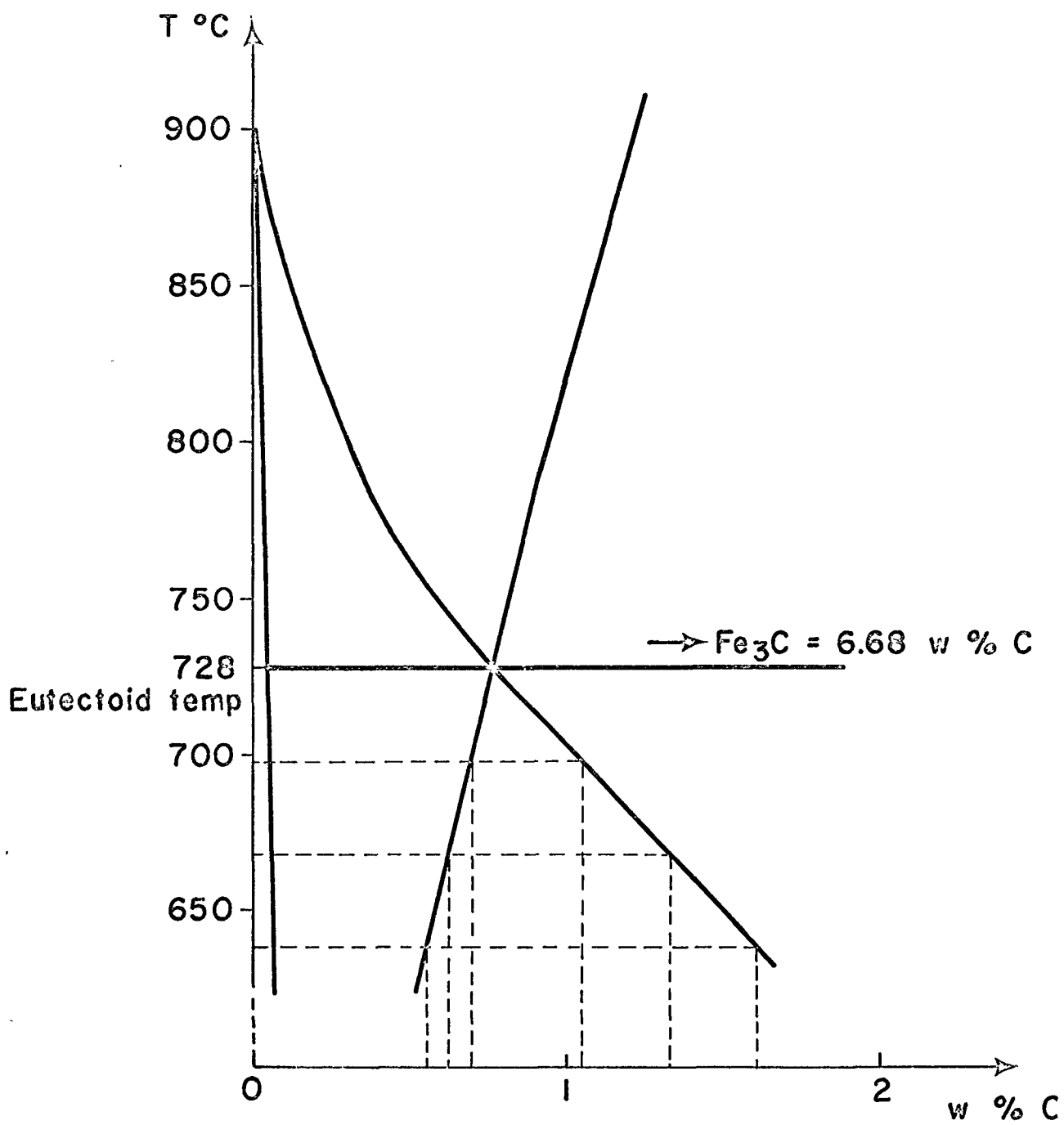


Fig. 20: Phase diagram for the Fe-C system

Table VI

Temperature °C	$\Delta T$ °C	$x_{10}^{\alpha\gamma}$ wt% C	$x_{10}^{\gamma\alpha}$ wt% C	$x_{10}^{\beta\gamma}$ wt% C	$x_{10}^{\gamma\beta}$ wt% C
698	30	0.025	1.05	6.69	0.69
668	60	0.029	1.33	6.69	0.62
638	90	0.032	1.61	6.69	0.55

Tabulated phase diagram for the Fe-C system.

Since the precipitation reaction yields ferrite and cementite we must choose these two phases as extremities of a binary diagram and all concentrations must be referred to  $Fe_3C$  as the pure component. We constitute an ideal diagram by locating the eutectoid transformation at the center of the diagram keeping invariant the total angle between the phase boundaries for the austenite in equilibrium with the ferrite and cementite phases, respectively. We also assign one half of the solubility of carbon in the ferrite to the  $Fe_3C$  phase thus obtaining a completely symmetric diagram as shown in Fig. 21. The values of  $x$  and  $y$  for this diagram are given in Table VII.

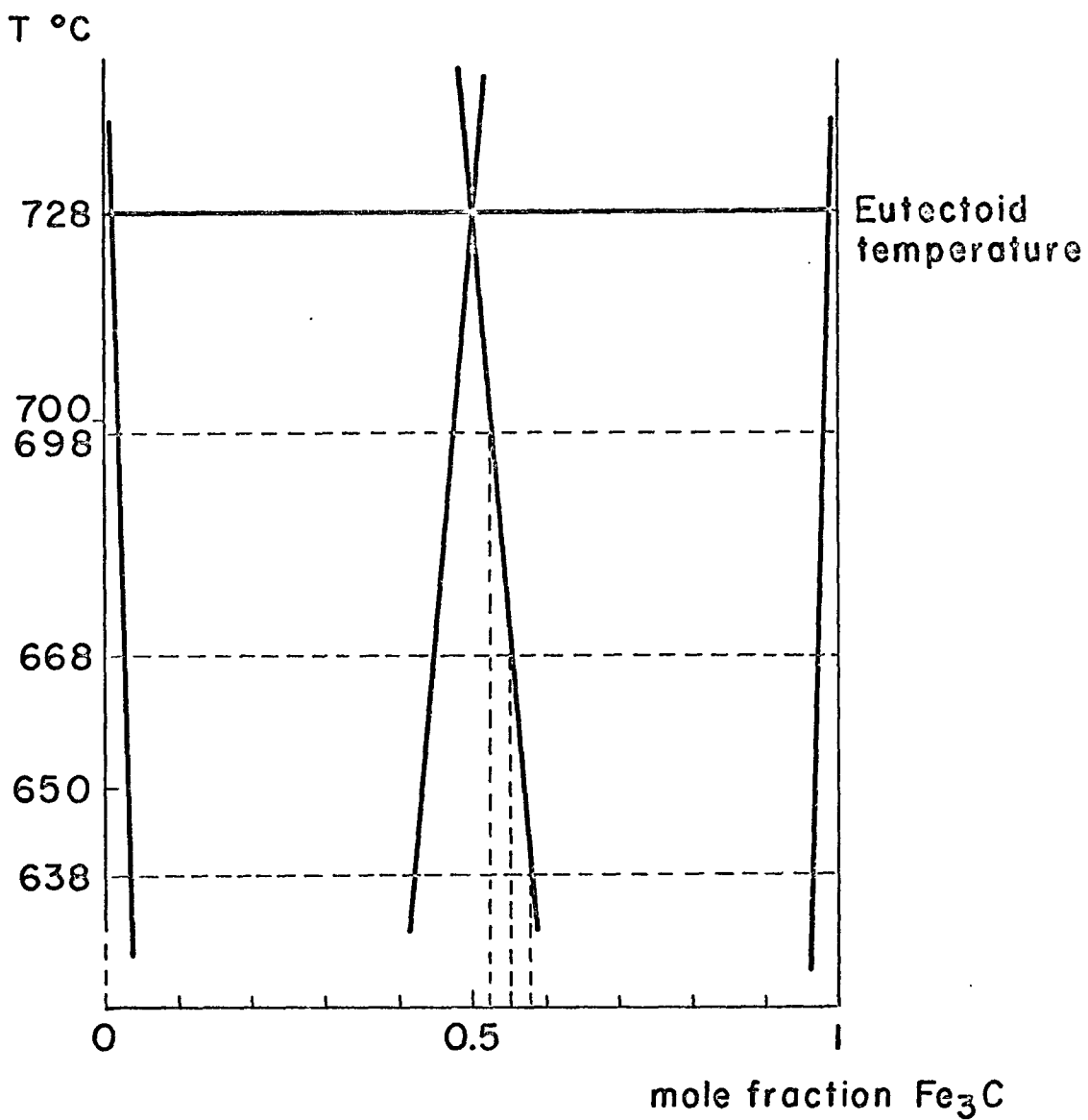


Fig. 21: Symmetricized phase diagram for the Fe-C system

Table VII

Temperature °C	x wt% Fe <sub>3</sub> C	y wt% Fe <sub>3</sub> C
698	0.19	52.65
668	0.21	55.27
638	0.24	57.88

Adjusted and tabulated phase diagram for the Fe-C system.

Now with the application of eqs. 4.5, 4.6, 4.8, 4.10 and 4.9 we deduce Table VIII.

Table VIII

Temperature °C	$k^\alpha$	K $10^{-3}$	$\phi/S_c$ $10^{-4}$	$\phi$ $10^{-9}$ cm	$S_c$ $10^{-6}$ cm	$C'$
698	588.2	7.54	4.02	1.98	4.92	0.81
668	576.7	8.63	9.13	2.08	2.28	0.81
638	569.6	9.85	1.56	2.18	1.39	0.81

Parameters used for calculation of the  $v(S)$  relation for the Fe-C system.



Again we see that the  $\phi/S_C$  factor is negligible so we expect that our numerical results will be identical to those given by a Hillert type calculation. In all the calculations we have taken  $\sigma = 1000 \text{ ergs/cm}^2$  for the surface tension which lies within the range of probable values given by Kramer et al.<sup>41</sup>. The diffusion coefficients are given by the Wells-Mehl formula<sup>42</sup>, the carbon concentration being that for the eutectoid composition. We present in Table IX the values of the diffusion coefficients used as a function of temperature.

Table IX

Temperature °C	698	668	638
D $10^{-9} \text{ cm}^2/\text{sec.}$	9.75	5.73	3.25

Variation of the diffusion coefficient with temperature for the Fe-C system.

We now plot the curves  $v$  vs.  $S$  for the three different temperatures as shown in Fig. 22, 23 and 24. We find  $K/X = 10^{-2}$  so again the approximation is valid and the simplified formula is identical to Hillert's relation. We observe as expected that the maximum of the curves occurs for  $S = 2 S_C$ . We present in Table X the optimum values for  $v$  and  $S$ .

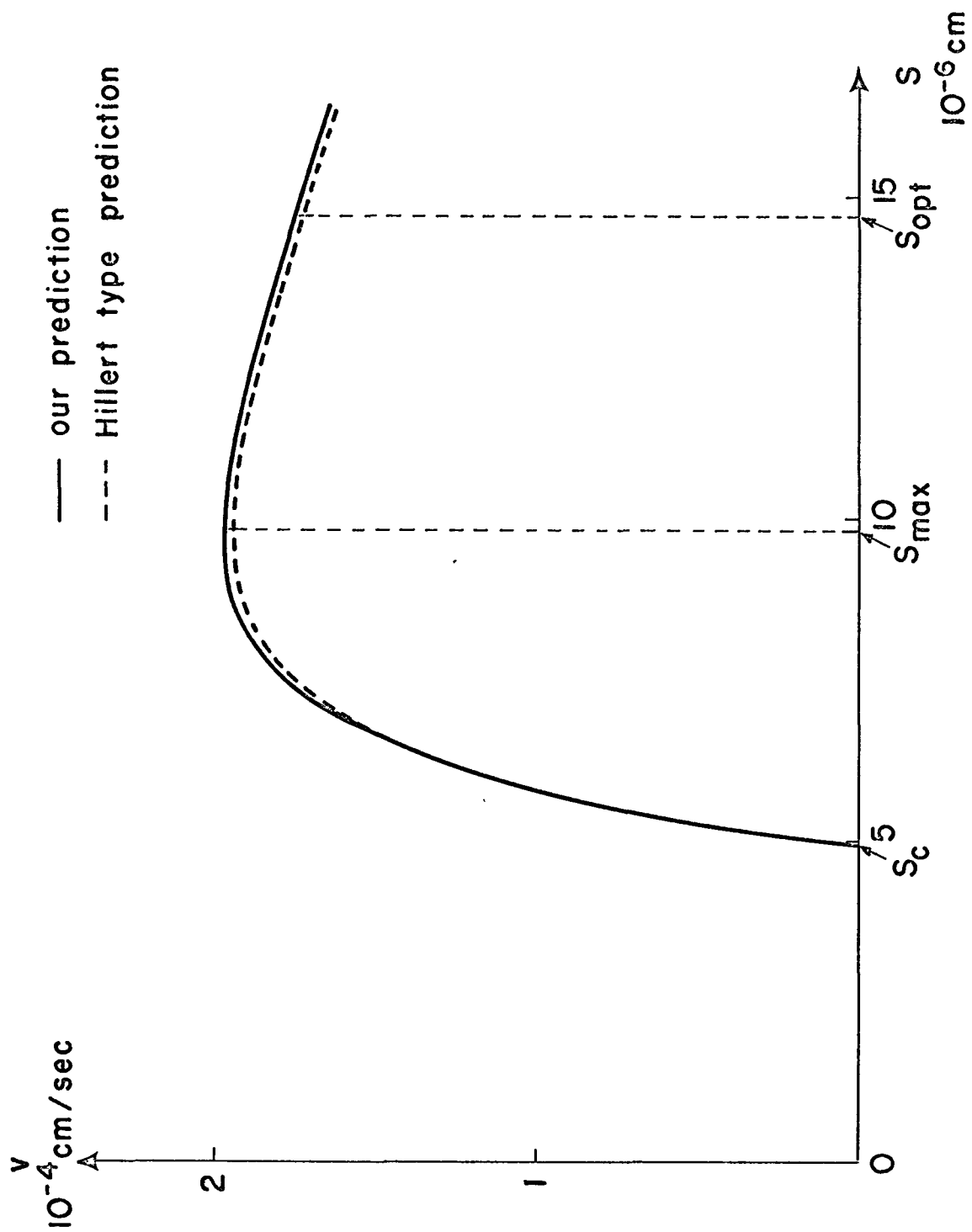


Fig. 22: Theoretical curve  $v(S)$  at  $698^{\circ}\text{C}$  for the Fe-C system

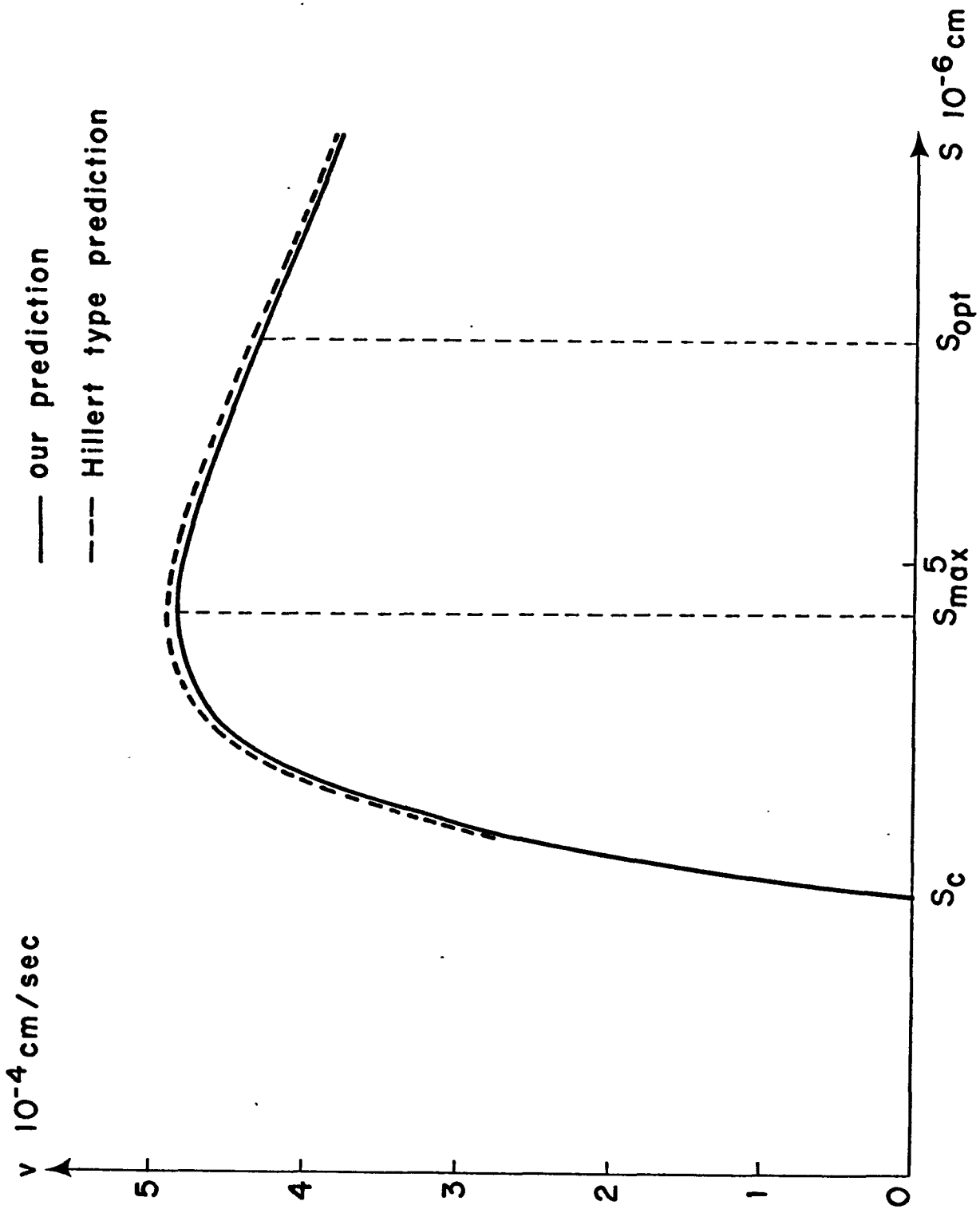


Fig. 23: Theoretical curve  $v(S)$  at  $668^{\circ}\text{C}$  for the Fe-C system

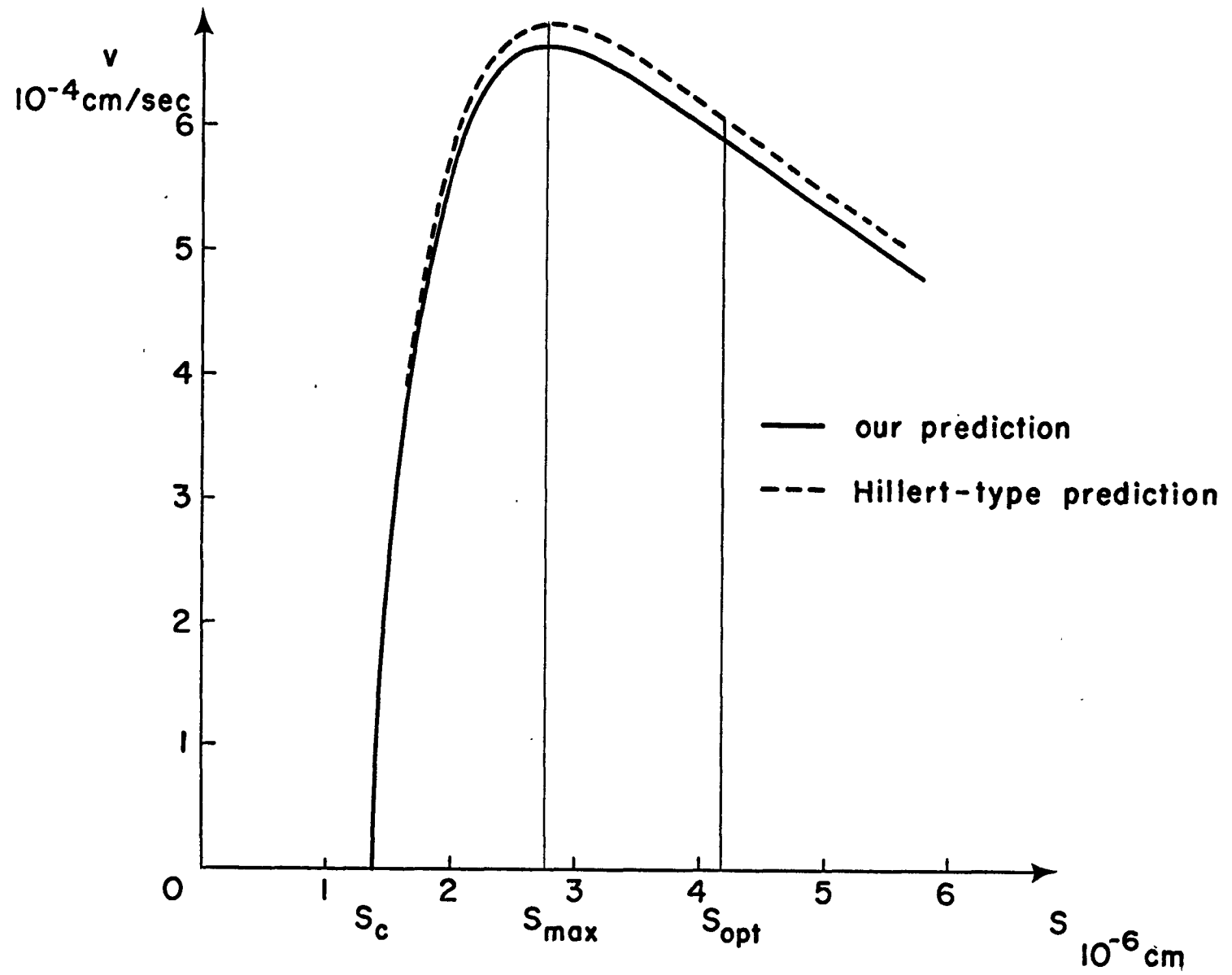


Fig. 24: Theoretical curve  $v(S)$  at  $638^\circ\text{C}$  for the Fe-C system.

Table X

Temperature °C	$v_{opt.}$ $10^{-4}$ cm/sec	$S_{opt.}$ $10^{-6}$ cm
698	1.75	14.77
668	4.30	6.84
638	5.88	4.19

Predicted optimum values for the velocity and lamellar spacing for the Fe-C system.

To compare our predictions with the data of Brown and Ridley<sup>37</sup> we plot the velocity vs. temperature on Fig. 25 and the inverse of the spacing vs. temperature in Fig. 26. We can see that the predicted spacings are too small by about 30% and the predicted velocities are about 1/4 of the experimental values. This discrepancy can be attributed either to the crudity of our approximation to the phase diagram or to a contribution to the carbon transfer via phase boundary diffusion as Cahn and others have maintained<sup>11,37</sup> (or to both reasons).

#### D/ EFFECT OF THE STORED FREE ENERGY

It has been observed for certain binary alloy systems that pearlite samples held at a uniform temperature for a prolonged time undergo a secondary transformation leading to a much coarser lamellar structure<sup>46</sup>.

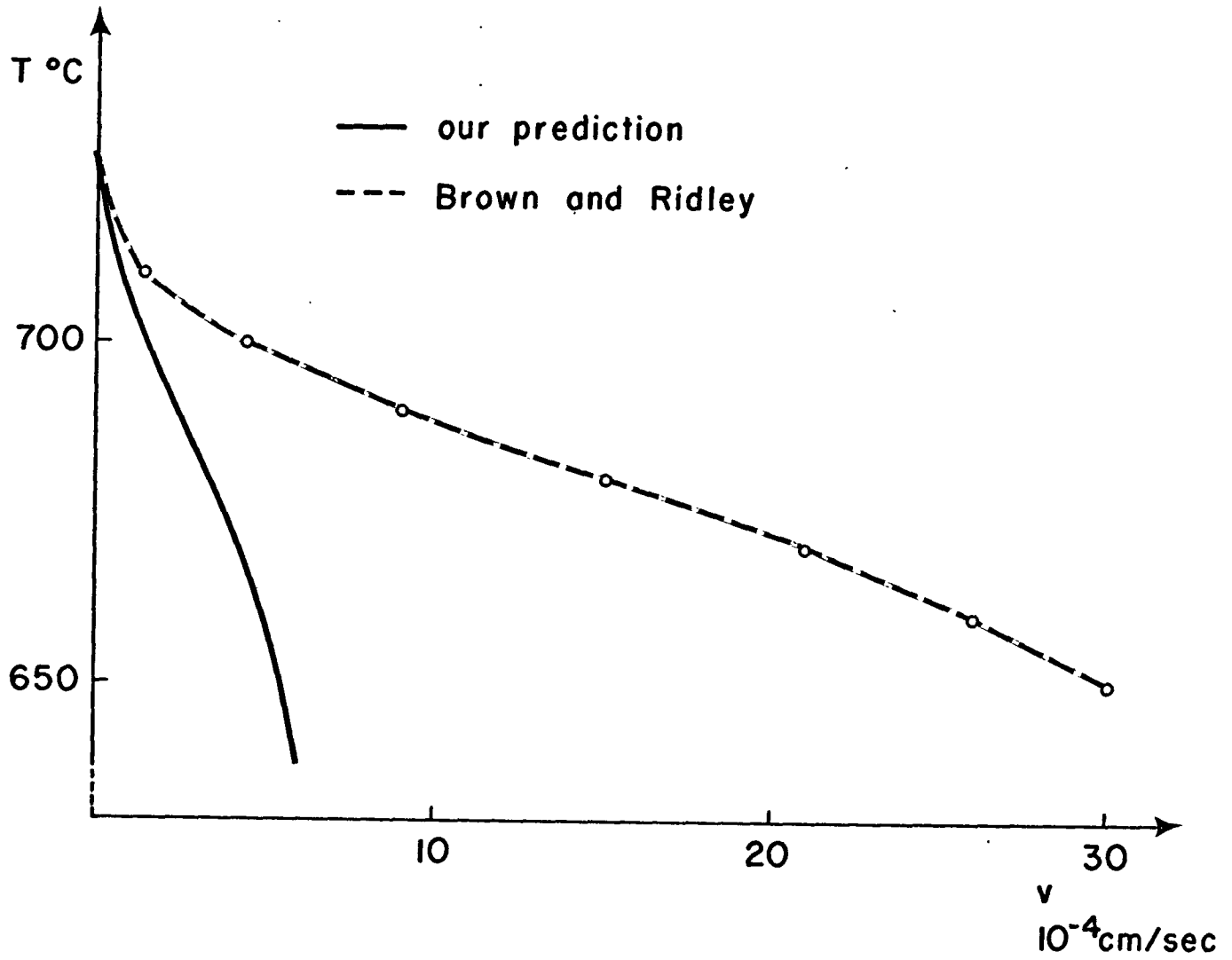


Fig. 25: Plot of velocity versus temperature for the Fe-C system.

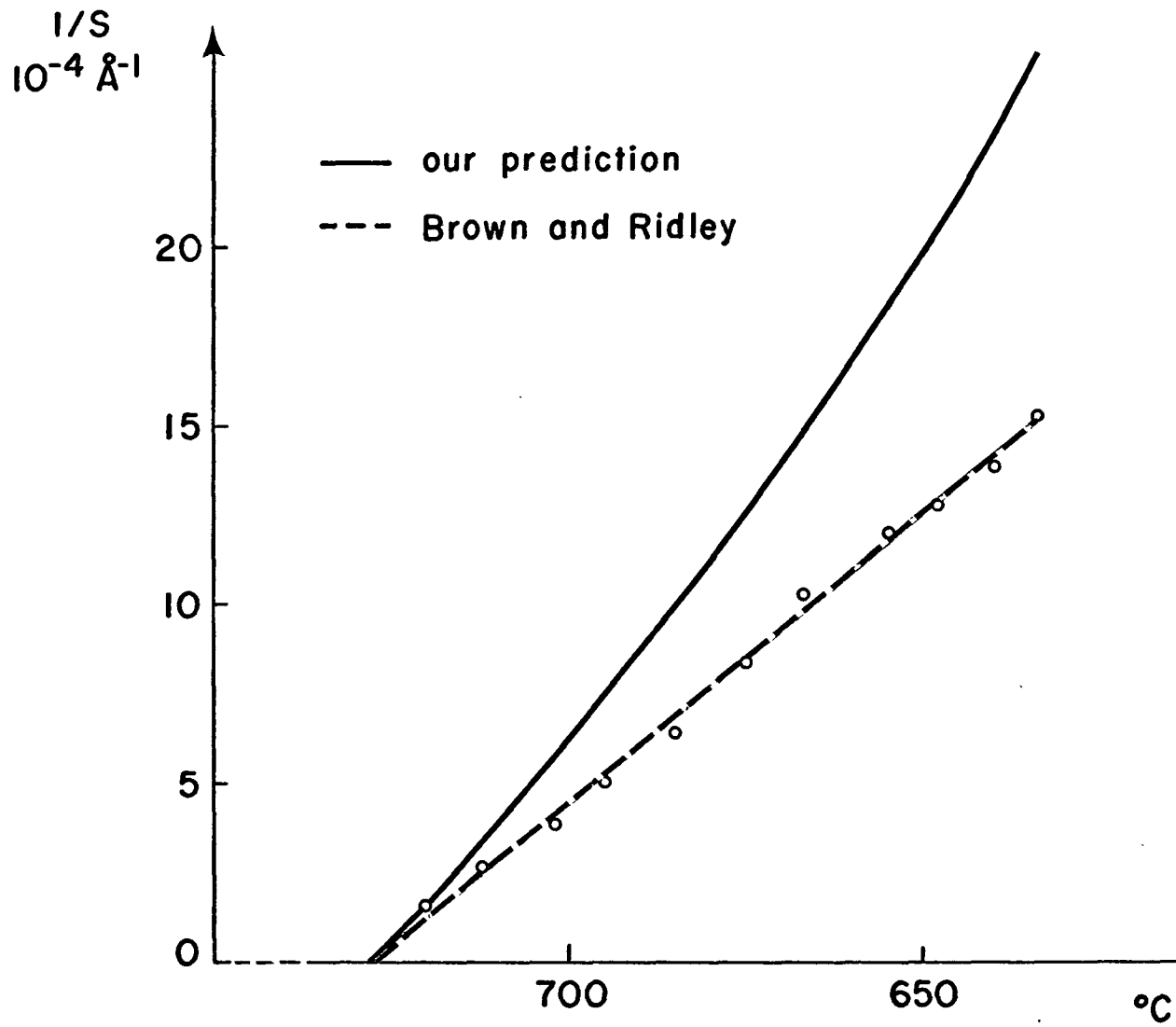


Fig. 26: Plot of the inverse of lamellar spacing versus temperature for the Fe-C system.

This is strongly suggestive that in these systems a large amount of stored free energy remains in the system following the primary precipitation and that this may be accounted for in part by the free energy of solute segregation represented by the factor  $\phi$  as discussed in section III. Although most of the stored free energy is associated with  $\alpha$ - $\beta$  surface, it is hard to see how this could serve as the sole driving force for a second cooperative (lamellar) reaction since surfaces are much more likely to participate in non-cooperative agglomeration and ripening processes. One can then understand, if our premise is correct, why the secondary cooperative reaction is rare and only occurs for cases where  $\phi$  is unusually large.

This secondary reaction has been studied by Fillnow and Mack<sup>43</sup> in the beryllium-copper binary system, by Spencer and Mack<sup>44</sup> in the copper-indium binary system and by Speich and Mack<sup>45</sup> in the silver-cadmium binary system. From the micrographs presented by Spencer and Mack<sup>66</sup> the secondary pearlitic appear to have lamellar spacings about five times those in the primary pearlitic. This means that a large part of the driving force for the secondary reaction must come from the surfaces remaining. We presume that if this energy is sufficiently augmented by the  $\phi$  factor and by the stored energy associated with the zero curvature metastable free energies of  $\alpha$  and  $\beta$  (increment corresponding to 4-7 on Fig. 8) then the cooperative secondary reaction can proceed.

To test the significance of  $\phi$  in this respect we have estimated the value of this parameter as a function of temperature by suitably symmetrizing the phase diagrams of the four likely eutectoid systems:



Cu-Be, Cu-In, Ag-Cd and Cu-Al as recorded in Table XI.

Table XI

System	Eutectoid temperature $^{\circ}\text{C}$	Temperature $^{\circ}\text{C}$	$\phi/S_c$
Cu-Be	608	592	0.02
		550	0.07
Cu-In	574	570	0.01
		547	0.07
Ag-Cd	440	420	0.20
		400	0.66
Cu-Al	565	550	0.02
		510	0.08

Predicted values of the parameter  $\phi/S_c$  for the Cu-Be Cu-In and Cd-Ag systems as a function of temperature.

In all cases  $\phi$  is substantial for undercoolings of 30 to 50 $^{\circ}\text{C}$ , and in the case of Ag-Cd it is very large indeed. As noted above, the secondary pearlite reactions do in fact occur in the systems Ag-Cd, Cu-In and Cu-Be, but not in Cu-Al. Our result is perhaps indicative if not unequivocal.

## SUMMARY AND CONCLUSIONS

1. The theory of the binary lamellar eutectoid reaction for volume diffusion has been extended to account for solute segregation within the product phases.
2. A new invariant of the system,  $\phi$ , with the units of a spacing or length has been identified and evaluated. This is shown to represent the free energy stored as solute segregation in the product phases, just as the critical spacing,  $S_c$ , represents the free energy stored as surfaces.
3. It has been demonstrated for symmetric binary systems that the effect of this segregation on the stable spacing will usually be small, but in a few easily identifiable cases can account for 10% or more of the free energy stored in the product phases and thus lead to predicted lamellar spacings appreciably greater than those obtained when segregation is neglected.
4. Solute segregation in the product phases is relatively high in the systems Cu-In, Cu-Be and Ag-Cd. We have proposed that the occurrence of a secondary coarse grained eutectoid reaction may be associated with the exceptionally rich storage of volume free energy in the product phases of these reactions.
5. Available data for Cu-Al and Fe-C systems has been compared with the predictions of our theory for symmetric eutectoids and in the case of Cu-Al the results are salutary. In the case of Fe-C the velocities

predicted are too low by a factor of about six suggesting either that the symmetric model is inadequate, or that phase boundary diffusion is speeding up the reaction.

6. The binary theory has been extended to solutions with a dilute ternary addition using ternary diffusion theory and a multicomponent formulation of the Gibbs-Thomson relation.
7. The segregation factor  $\phi$  appears in the ternary relations in a form which is entirely analogous to its form in the binary relations and there is no suggestion that its magnitude will be greater for ternaries than for boundaries. It is therefore likely that its effects may in most cases be neglected.
8. The theory for ternary systems, while complete in principle, proves to be intractable in all but the simplest version of the solution thermodynamics. It is concluded that the effect of the third element on the binary eutectoid reaction is mainly through its effect on the phase diagram. Any addition element which lowers the eutectoid temperature will retard the reaction for a given temperature of reaction.
9. In our simplest version, the ternary diffusion cross effects cancel out, a result which may be common, if not general.
10. Future theoretical work must be aimed at simplifying and approximating the complex equations for non-symmetric configurations in both binary and ternary systems.
11. Consideration should be given to extending the theory to mixed volume and interface diffusion control.
12. Experiments should be designed and systems chosen so as to make best use of the theory at its current state of development.

## APPENDIX 1

### INTEGRATION OF THE GIBBS-DUHEM EQUATIONS FOR A BINARY DILUTE SOLUTION: FIRST THERMODYNAMIC VERSION

The composition  $(x_1^{Y\alpha}, x_2^{Y\alpha})$ ,  $(x_1^{\alpha Y}, x_2^{\alpha Y})$  and the activities  $a_1$  and  $a_2$  of two binary phases  $\gamma$  and  $\alpha$ , respectively, must for equilibrium comply with the Gibbs-Duhem relations:

$$x_1^{Y\alpha} d\ln a_1 + x_2^{Y\alpha} d\ln a_2 = \frac{V^Y}{RT} dP^Y \quad (I.1)$$
$$x_1^{\alpha Y} d\ln a_1 + x_2^{\alpha Y} d\ln a_2 = \frac{V^\alpha}{RT} dP^\alpha$$

The  $\gamma$  phase will always be considered as the parent phase from which either the  $\alpha$  or the  $\beta$  phase precipitates. We shall assume that the molar volumes  $V^\alpha$ ,  $V^\beta$  and  $V^\gamma$  are not affected by pressure changes and are constant.

Further, the pressure changes will be taken into account only in the precipitate phases, the parent phase remaining always at a constant pressure ( $dP^\gamma = 0$ ). This assumption has been already invoked by Hillert<sup>6,7</sup>.

We can therefore write

$$x_1^{\gamma\alpha} d\ln a_1 + x_2^{\gamma\alpha} d\ln a_2 = 0 \quad (I.2)$$

$$x_1^{\alpha\gamma} d\ln a_1 + x_2^{\alpha\gamma} d\ln a_2 = \frac{V^\alpha}{RT} dP$$

We then eliminate  $d\ln a_2$  between the two equations to obtain

$$\left(x_1^{\alpha\gamma} - x_1^{\gamma\alpha} \frac{x_2^{\alpha\gamma}}{x_2^{\gamma\alpha}}\right) d\ln a_1 = \frac{V^\alpha}{RT} dP \quad (I.3)$$

We assume here that component 1 is the solute and, in the precipitate phase,  $x_1^{\alpha\gamma}$  is small. We, therefore, take the Henrian solution approximation with

$$d\ln a_1 = d\ln x_1^{\alpha\gamma} \quad (I.4)$$

which yields

$$\left(1 - \frac{x_1^{\gamma\alpha}}{x_1^{\alpha\gamma}} \frac{x_2^{\alpha\gamma}}{x_2^{\gamma\alpha}}\right) d x_1^{\alpha\gamma} = \frac{V^\alpha}{RT} dP \quad (I.5)$$

In order to integrate such a differential equation, we need to know the composition of the phase  $\gamma$  which has the same activity as the phase  $\alpha$  for a given  $x_1^{\alpha\gamma}$ . Such information will be given by a relation between  $x_1^{\alpha\gamma}$  and  $x_1^{\gamma\alpha}$ . As a working relation, we propose here that

$$\frac{x_1^{\alpha\gamma}}{x_1^{\gamma\alpha}} = K^\alpha \quad (I.6)$$

where  $K^\alpha$  is independent of pressure.

Such an expression implies particular shapes for the free-energy composition diagrams of the  $\alpha$  and  $\gamma$  phases which are not unrealistic.

Now, we can write

$$\left(1 - \frac{1}{K^\alpha} \frac{1 - x_1^{\alpha\gamma}}{1 - \frac{x_1^{\alpha\gamma}}{K^\alpha}}\right) dx_1^{\alpha\gamma} = \frac{V^\alpha}{RT} dP \quad (1.7)$$

or

$$\begin{aligned} \frac{V^\alpha}{RT} dP &= \left(1 - \frac{1 - x_1^{\alpha\gamma}}{K^\alpha - x_1^{\alpha\gamma}}\right) dx_1^{\alpha\gamma} = \frac{K^\alpha - 1}{K^\alpha - x_1^{\alpha\gamma}} dx_1^{\alpha\gamma} \\ &= (1 - K^\alpha) d \ln (K^\alpha - x_1^{\alpha\gamma}) \end{aligned} \quad (1.8)$$

We can integrate this expression to obtain

$$\frac{V^\alpha}{RT} P = (1 - K^\alpha) \ln \frac{K^\alpha - x_1^{\alpha\gamma}}{K^\alpha - x_{10}^{\alpha\gamma}} = (1 - K^\alpha) \ln \left[ 1 + \left( \frac{K^\alpha - x_1^{\alpha\gamma}}{K^\alpha - x_{10}^{\alpha\gamma}} - 1 \right) \right] \quad (1.9)$$

The quantity

$$\frac{K^\alpha - x_1^{\alpha\gamma}}{K^\alpha - x_{10}^{\alpha\gamma}} - 1 = \frac{x_{10}^{\alpha\gamma} - x_1^{\alpha\gamma}}{K^\alpha - x_{10}^{\alpha\gamma}} \quad (1.10)$$

is very small compared with unity and the right hand side can be approximated

by

$$\frac{V^\alpha}{RT} P = \frac{K^\alpha - 1}{K^\alpha - x_{10}^{\alpha\gamma}} (x_1^{\alpha\gamma} - x_{10}^{\alpha\gamma}) \quad (\text{I.11})$$

so finally

$$P = RT h^\alpha (C_{10}^{\alpha\gamma} - C_1^{\alpha\gamma}) \quad (\text{I.12})$$

with

$$h^\alpha = \frac{1 - K^\alpha}{K^\alpha - x_{10}^{\alpha\gamma}} \quad (\text{I.13})$$

The same calculations can be carried out for the  $\beta$  phase where now the mole fraction  $x_2^{\beta\gamma}$  is small. We obtain, with similar approximations, the following expressions. Firstly

$$\frac{V^\beta}{RT} dP = (x_2^{\beta\gamma} - x_1^{\beta\gamma} \frac{x_2^{\gamma\beta}}{x_1^{\gamma\beta}}) d \ln a_2 \quad (\text{I.14})$$

Next we assume

$$\ln a_2 = \ln x_2^{\beta\gamma} \quad \text{and} \quad K^\beta = \frac{x_1^{\beta\gamma}}{x_1^{\gamma\beta}} \quad (\text{I.15})$$

where  $K^\beta$  is independent of pressure.

The latter expression is less realistic than eq. I.6 since it implies

a very unsymmetric free energy composition diagram for the  $\gamma$  phase as will be discussed below. We then have

$$\begin{aligned} \frac{V^\beta}{RT} dP &= \left(1 - \frac{x_1^{\beta\gamma}}{x_1^{\gamma\beta}} \frac{x_2^{\gamma\beta}}{x_2^{\beta\gamma}}\right) dx_2^{\beta\gamma} = - \left(1 - K^\beta \frac{1 - x_1^{\beta\gamma}}{1 - x_1^{\beta\gamma}}\right) dx_1^{\beta\gamma} \\ &= - \left(1 - \frac{K^\beta - x_1^{\beta\gamma}}{1 - x_1^{\beta\gamma}}\right) dx_1^{\beta\gamma} = - \frac{1 - K^\beta}{1 - x_1^{\beta\gamma}} dx_1^{\beta\gamma} \\ &= (1 - K^\beta) d \ln (1 - x_1^{\beta\gamma}) \end{aligned} \quad (I.16)$$

By integration we obtain

$$\begin{aligned} \frac{V^\beta}{RT} P &= (1 - K^\beta) \ln \frac{1 - x_1^{\beta\gamma}}{1 - x_{10}^{\beta\gamma}} = (1 - K^\beta) \ln \left[1 + \left(\frac{1 - x_1^{\beta\gamma}}{1 - x_{10}^{\beta\gamma}} - 1\right)\right] \\ &= (1 - K^\beta) \ln \left(1 - \frac{x_{10}^{\beta\gamma} - x_1^{\beta\gamma}}{1 - x_{10}^{\beta\gamma}}\right) = \frac{K^\beta - 1}{1 - x_{10}^{\beta\gamma}} (x_1^{\beta\gamma} - x_{10}^{\beta\gamma}) \end{aligned} \quad (I.17)$$

and in terms of concentrations we have therefrom

$$P = RT h^\beta (C_1^{\beta\gamma} - C_{10}^{\beta\gamma}) \quad (I.18)$$

with

$$h^\beta = \frac{K^\beta - 1}{1 - x_{10}^{\beta\gamma}} \quad (I.19)$$



We can demonstrate that  $h^\alpha = -h^\beta$  in a symmetrical configuration.

Since as shown in Fig. 5

$$x_0^{\beta\gamma} = 1 - x_0^{\alpha\gamma} \quad (\text{I.20a})$$

$$x_0^{\gamma\beta} = 1 - x_0^{\gamma\alpha} \quad (\text{I.20b})$$

then

$$K^\beta = \frac{x_{10}^{\beta\gamma}}{x_{10}^{\gamma\beta}} = \frac{1 - x_{10}^{\alpha\gamma}}{1 - \frac{x_{10}^{\alpha\gamma}}{K^\alpha}} = K^\alpha \frac{1 - x_{10}^{\alpha\gamma}}{K^\alpha - x_{10}^{\alpha\gamma}} \quad (\text{I.21})$$

and if we substitute the expression for  $K^\beta$  into  $h^\beta$  we obtain

$$h^\beta = \frac{K^\beta - 1}{x_{10}^{\alpha\gamma}} = \frac{1}{x_{10}^{\alpha\gamma}} \left( K^\alpha \frac{1 - x_{10}^{\alpha\gamma}}{K^\alpha - x_{10}^{\alpha\gamma}} - \frac{K^\alpha - x_{10}^{\alpha\gamma}}{K^\alpha - x_{10}^{\alpha\gamma}} \right) = \frac{1 - K^\alpha}{K^\alpha - x_{10}^{\alpha\gamma}} = -h^\alpha \quad (\text{I.22})$$

We represent in Fig. 27 the variation of the composition with pressure according to this particular assumption. We note that starting with a symmetrical temperature-composition diagram (symmetry for  $x_{10}^{\alpha\gamma}$ ,  $x_{10}^{\gamma\alpha}$ ,  $x_{10}^{\beta\gamma}$ ,  $x_{10}^{\gamma\beta}$ ) the pressure deforms the diagram unsymmetrically for  $x_{10}^{\gamma\alpha}$  and  $x_{10}^{\gamma\beta}$ . Such an unsymmetric influence of the pressure is not an unusual one. However, it has been taken for the sake of mathematical simplicity and we acknowledge its limitations.

We can interpret this assumption with the help of a free energy composition diagram. In Fig. 28 we schematically represent the free energy

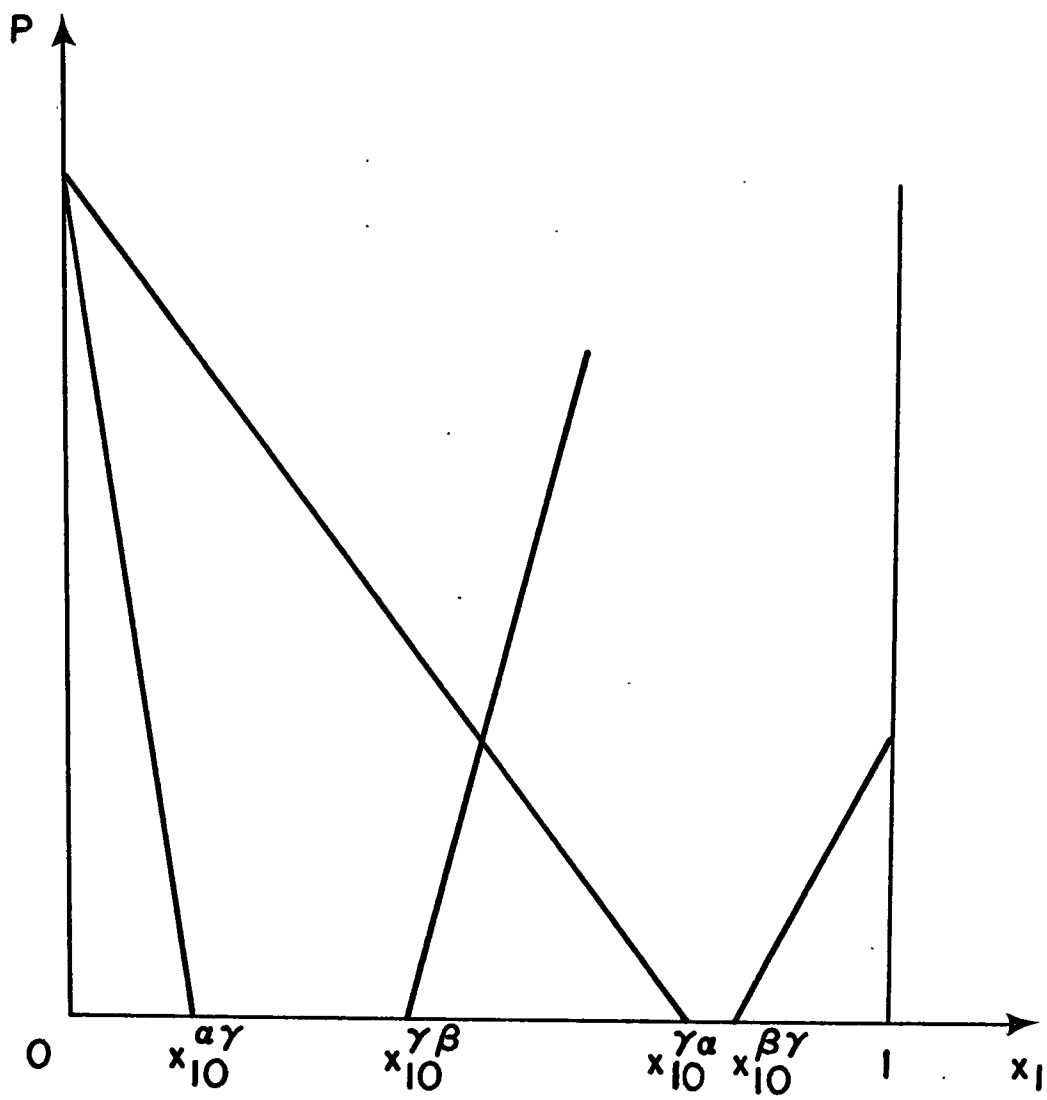


Fig. 27: Effect of pressure on the concentrations corresponding to first thermodynamic version of the Gibbs-Thomson equations.

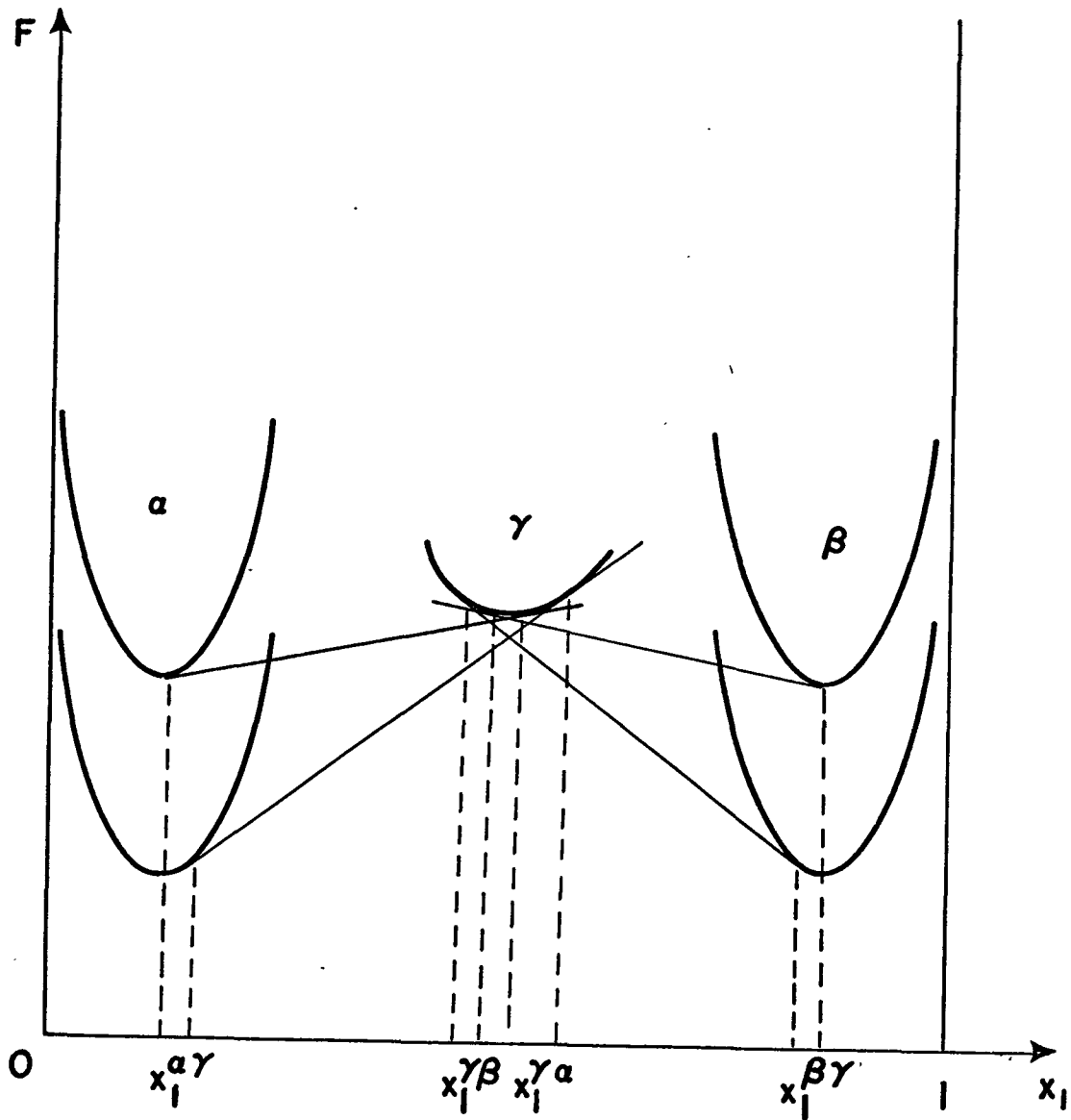


Fig. 28: Free energy-composition diagram corresponding to the first thermodynamic version.

curves for the equilibria between the  $\alpha - \gamma$  and  $\beta - \gamma$  phases. We suppose as is usual that the effect of pressure is to move the free energy curves of the  $\alpha$  and  $\beta$  phases straight upwards. We have chosen here a representation where we are in a symmetrical equilibrium configuration and where the two free energy curves of the  $\alpha$  and  $\beta$  phases are approximately parabolic. We see that it is necessary to draw the free energy curve of the  $\gamma$  phase unsymmetric so as to represent the conditions imposed by the ratios  $K^\alpha = x_1^{\alpha\gamma}/x_1^{\gamma\alpha}$  and  $K^\beta = x_1^{\beta\gamma}/x_1^{\gamma\beta}$ . This situation may be physically acceptable for small ranges of pressure but clearly lacks generality.

## APPENDIX II

### INTEGRATION OF THE GIBBS-DUHEM EQUATION FOR A BINARY DILUTE SOLUTION: SECOND THERMODYNAMIC VERSION

Similarly to the calculations carried out in Appendix I, we can again obtain eq. I.4

$$\left(1 - \frac{x_1^{\gamma\alpha} x_2^{\alpha\gamma}}{x_1^{\alpha\gamma} x_2^{\gamma\alpha}}\right) d x_1^{\alpha\gamma} = \frac{V^\alpha}{RT} d P \quad (\text{II.1})$$

The relation between the composition of the phases  $\gamma$  and  $\alpha$  in equilibrium will now be assumed to be given by

$$\frac{x_1^{\gamma\alpha}}{x_1^{\alpha\gamma}} \frac{x_2^{\alpha\gamma}}{x_2^{\gamma\alpha}} = x^\alpha \quad (\text{II.2})$$

where  $x^\alpha$  is independent of pressure. From this expression we can deduce  $x_1^{\alpha\gamma}$  as a function of  $x_1^{\gamma\alpha}$

$$x_1^{\gamma\alpha} (1 - x_1^{\alpha\gamma}) = x^\alpha x_1^{\alpha\gamma} (1 - x_1^{\gamma\alpha}) \quad (\text{II.3})$$

$$x_1^{\gamma\alpha} = x_1^{\alpha\gamma} [x_1^{\gamma\alpha} + x^\alpha (1 - x_1^{\gamma\alpha})] \quad (\text{II.4})$$

and, finally

$$x_1^{\alpha\gamma} = \frac{x_1^{\gamma\alpha}}{(1 - x^\alpha) x_1^{\gamma\alpha} + x^\alpha} \quad (\text{II.5})$$

The integration of equation (II.1) gives directly

$$(1 - x^\alpha) (x_1^{\alpha\gamma} - x_{10}^{\alpha\gamma}) = \frac{V^\alpha}{RT} P \quad (\text{II.6})$$

and

$$P = RT K^\alpha (C_{10}^{\alpha\gamma} - C_1^{\alpha\gamma}) \quad (\text{II.7})$$

with

$$K^\alpha = x^\alpha - 1 \quad (\text{II.8})$$

We can obtain the relation between P and the concentration in the  $\gamma$  phase by substituting eq. II.5 into eq. II.7 to obtain

$$P = RT K^\alpha \left[ \frac{C_{10}^{\gamma\alpha}}{(1 - x^\alpha) C_{10}^{\gamma\alpha} + x^\alpha} - \frac{C_1^{\gamma\alpha}}{(1 - x^\alpha) C_1^{\gamma\alpha} + x^\alpha} \right] \quad (\text{II.9})$$

Taking account of eq. II.8, we have similarly

$$P = RT \left( \frac{C_{10}^{\gamma\alpha}}{\frac{x^\alpha}{x^\alpha - 1} - C_{10}^{\gamma\alpha}} - \frac{C_1^{\gamma\alpha}}{\frac{x^\alpha}{x^\alpha - 1} - C_1^{\gamma\alpha}} \right) \quad (\text{II.10})$$

The same procedure can be carried out for the equilibrium between the phase  $\gamma$  and  $\beta$ , noting that component 2 is this time the dilute solute in phase  $\beta$ . The equivalent to eq. II.1 is

$$\left(1 - \frac{x_2^{\gamma\beta}}{x_2^{\beta\gamma}} \frac{x_1^{\beta\gamma}}{x_1^{\gamma\beta}}\right) d x_2^{\beta\gamma} = \frac{V^\beta}{RT} d P \quad (\text{II.11})$$

The relation between the compositions of the two phases in equilibrium will be given by

$$\frac{x_2^{\gamma\beta}}{x_2^{\beta\gamma}} \frac{x_1^{\beta\gamma}}{x_1^{\gamma\beta}} = x^\beta \quad (\text{II.12})$$

where  $x^\beta$  is independent of pressure.

In the symmetrical case, we note that  $x^\alpha = x^\beta$ . We can integrate equation II.11 or the equivalent

$$-(1 - x^\beta) d x_1^{\beta\gamma} = \frac{V^\beta}{RT} d P \quad (\text{II.13})$$

giving

$$(1 - x^\beta) (x_{10}^{\beta\gamma} - x_1^{\beta\gamma}) = \frac{V^\beta}{RT} P \quad (\text{II.14})$$

and, finally

$$P = RT K^\beta (c_{10}^{\beta\gamma} - c_1^{\beta\gamma}) \quad (\text{II.15})$$

with

$$K^\beta = 1 - x^\beta \quad (\text{II.16})$$

Here again, we note that in the symmetrical case,  $K^\beta = -K^\alpha$ . We can also deduce the relation between  $P$  and the concentration in the phase  $\gamma$  from a combination of eqs. II.12 and II.15, giving

$$P = RT x^\beta \left( \frac{C_{10}^{\gamma\beta}}{\frac{1}{1-x^\beta} - C_{10}^{\gamma\beta}} - \frac{C_1^{\gamma\beta}}{\frac{1}{1-x^\beta} - C_1^{\gamma\beta}} \right) \quad (\text{II.17})$$

The influence of the pressure for a symmetrical diagram is the same for the  $\gamma$  phase in equilibrium with the phases  $\alpha$  and  $\beta$ . This is not apparent from a comparison of eqs. II.10 and II.17 but it can be easily shown by exchanging the indices 1 to 2 and the superscript  $\alpha$  to  $\beta$  so as to obtain

$$P = RT \left( \frac{C_{20}^{\gamma\beta}}{\frac{x^\beta}{x^\beta - 1} - C_{20}^{\gamma\beta}} - \frac{C_2^{\gamma\beta}}{\frac{x^\beta}{x^\beta - 1} - C_2^{\gamma\beta}} \right) \quad (\text{II.18})$$

Since, in the symmetrical case  $x^\beta = x^\alpha$  and  $C_{20}^{\gamma\beta} = C_{10}^{\gamma\alpha}$  we can readily see that the influence of pressure on  $C_1^{\gamma\alpha}$  is the same as on  $C_2^{\gamma\beta}$  which preserves the symmetry.

We represent in Fig. 29 the variations of all compositions with pressure. We note, as required by thermodynamics, that the curves for



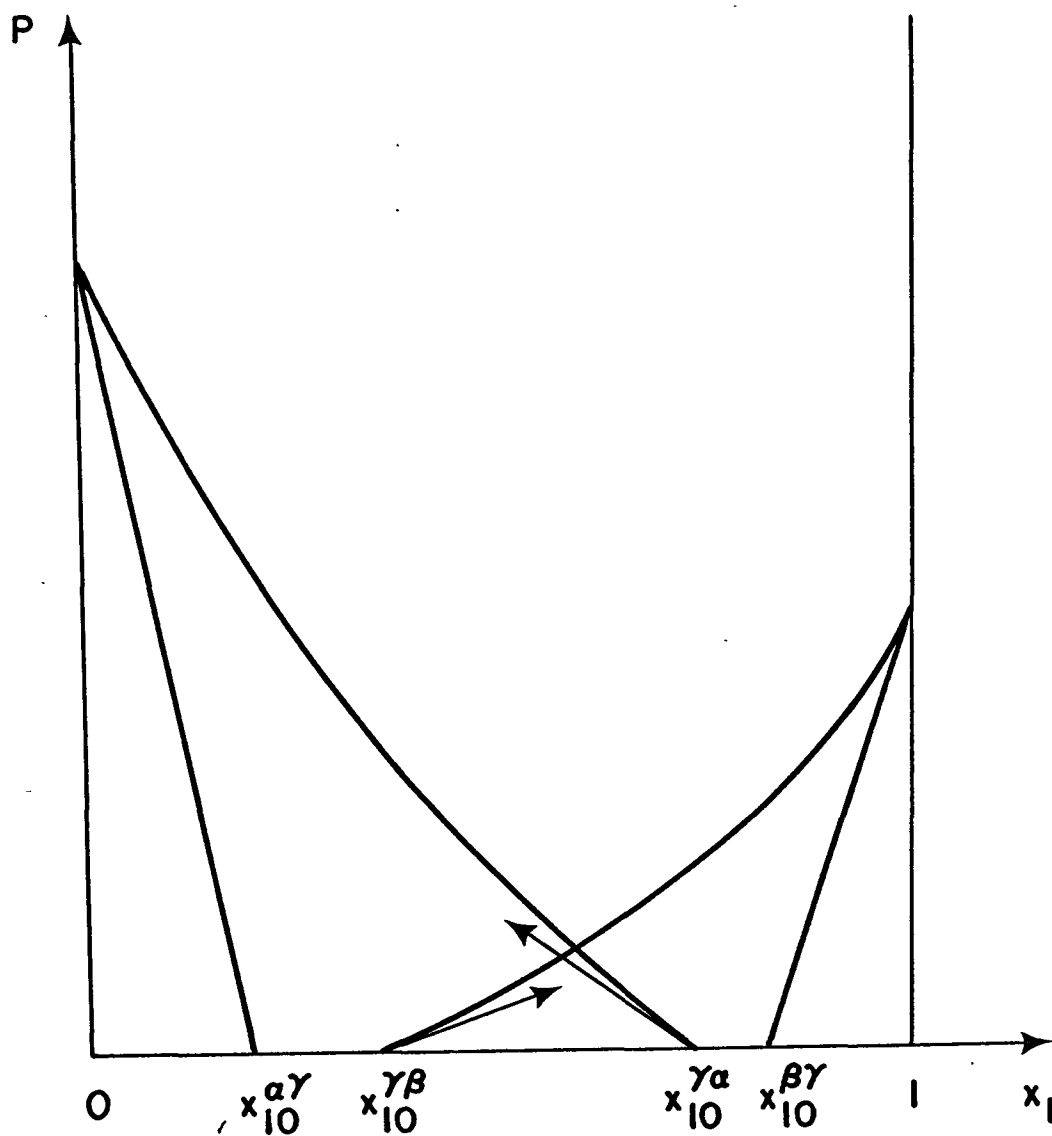


Fig. 29: Effect of pressure on the concentrations corresponding to second thermodynamic version of the Gibbs-Thomson equations.

$C_1^{\alpha\gamma}$ ,  $C_1^{\gamma\alpha}$  and  $C_1^{\beta\gamma}$ ,  $C_1^{\gamma\beta}$  intersect, respectively, for  $C_1$  equal to 0 and unity.

We suppose, as in Appendix I, that the effect of the pressure is to displace the free energy curves of the  $\alpha$  and  $\beta$  phases upwards as shown in Fig. 30. We can clearly see that the ratios  $\chi^\alpha$  and  $\chi^\beta$  can accommodate a wide range of free energy composition diagrams and phase diagrams which are derived therefrom.

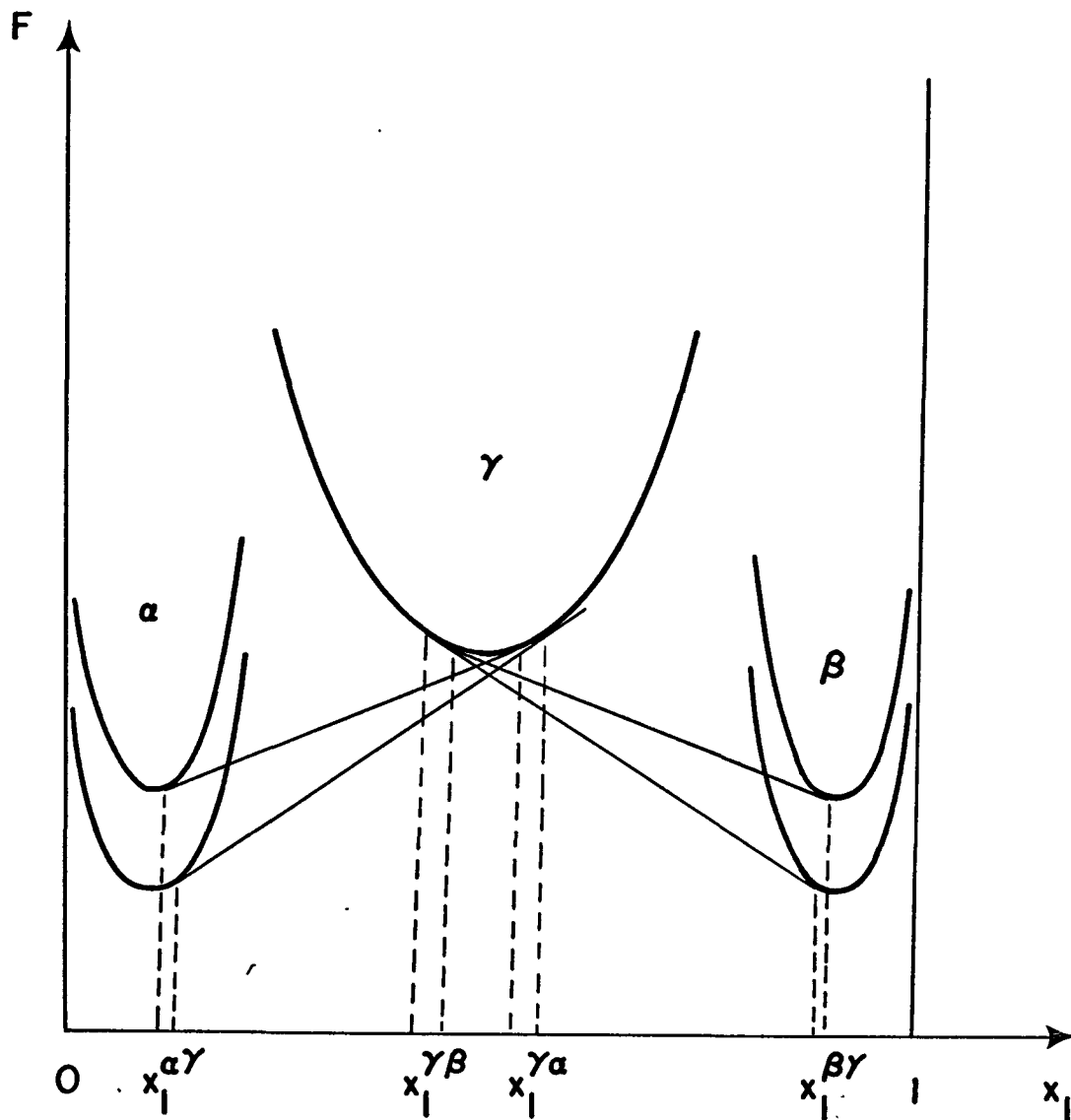


Fig. 30: Free energy-composition diagram corresponding to the second thermodynamic version.

### APPENDIX III

#### CALCULATION OF THE FOURIER SERIES COEFFICIENTS FOR A STEP FUNCTION

We want here to represent by a Fourier series the variation of the function shown in Fig. 31, and having the values

$$K(y) = \begin{cases} K_1 & \text{when } -\frac{S^\alpha}{2} < y < \frac{S^\alpha}{2} \\ K_2 & \text{when } \frac{S^\alpha}{2} < y < \frac{S^\alpha}{2} + S^\beta \end{cases} \quad (\text{III.1})$$

We therefore want to express  $K(y)$  in the form

$$K(y) = \sum_{n=0}^{\infty} a_n \cos b_{ny} \quad (\text{III.2})$$

where

$$a_0 = \frac{K_1 + K_2}{2} \quad (\text{III.3})$$

and

$$a_n = \frac{2}{S} \left( \int_{-\frac{S^\alpha}{2}}^{\frac{S^\alpha}{2}} K_1 \cos b_n y \, dy + \int_{\frac{S^\alpha}{2}}^{\frac{S^\alpha}{2} + S^\beta} K_2 \cos b_n y \, dy \right) \quad (\text{III.4})$$

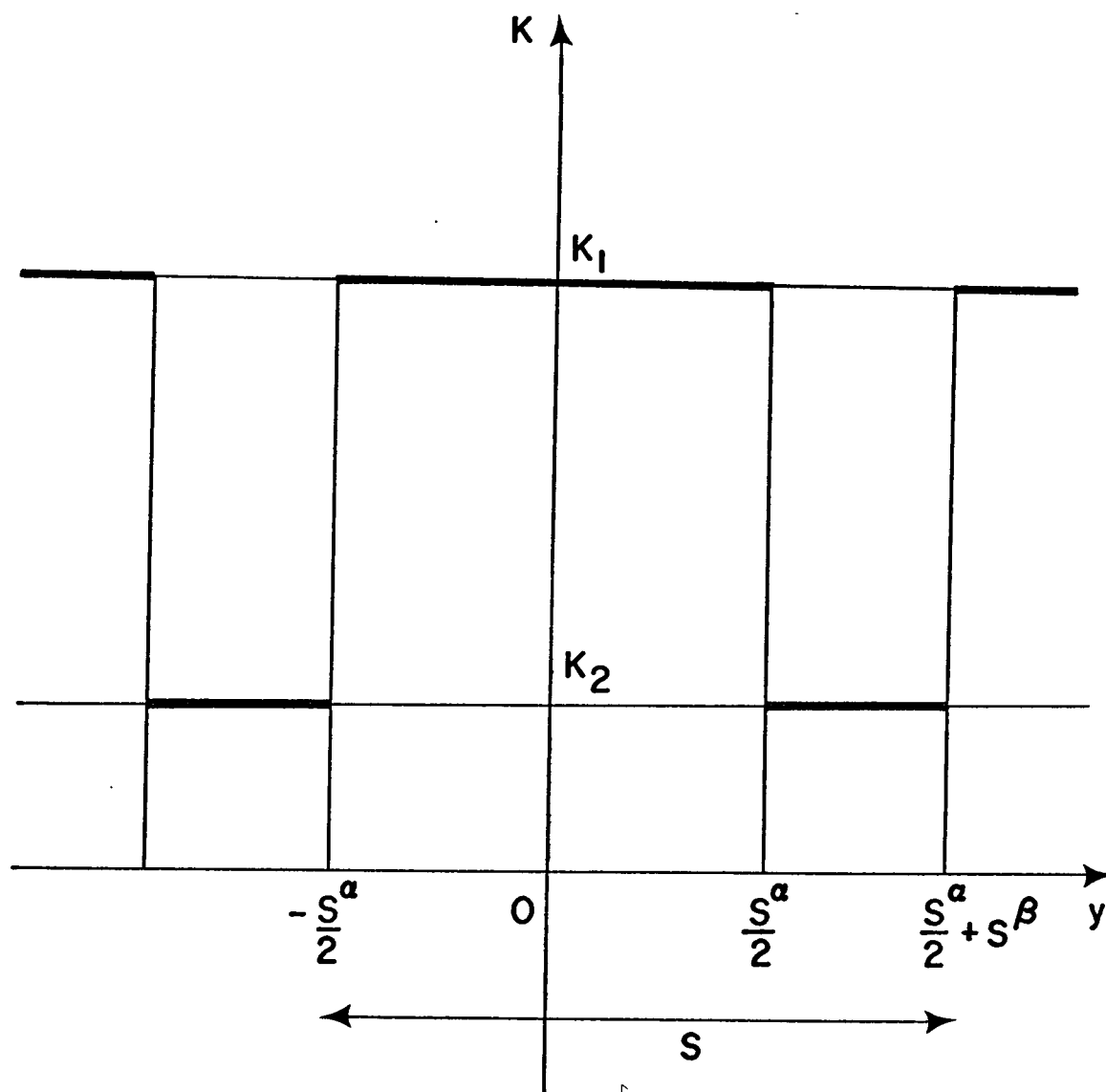


Fig. 31: Representation of a step function.

$$\begin{aligned}
&= \frac{2}{S} b_n \left( K_1 \left[ \sin b_n y \right] \frac{S^\alpha}{2} + K_2 \left[ \sin b_n y \right] \frac{S^\alpha}{2} + S^\beta \right) \\
&= \frac{2}{\pi n} \left[ K_1 \sin \pi n \frac{S^\alpha}{S} + \frac{K_2}{2} \sin b_n \left( \frac{S^\alpha}{2} + S^\beta \right) - \sin b_n \frac{S^\alpha}{2} \right] \\
&= \frac{2}{\pi n} \left( K_1 \sin \pi n \frac{S^\alpha}{S} + K_2 \cos \pi n \sin b_n \frac{S^\beta}{2} \right)
\end{aligned}$$

However,

$$\sin b_n \frac{S^\beta}{2} = \sin b_n \left( \frac{S}{2} - \frac{S^\alpha}{2} \right) = -\cos \pi n \sin \pi n \frac{S^\alpha}{S} \quad (\text{III.5})$$

so that:

$$a_n = \frac{2}{\pi n} \left[ K_1 \sin \pi n \frac{S^\alpha}{S} - K_2 (\cos \pi n)^2 \sin \pi n \frac{S^\alpha}{S} \right] \quad (\text{III.6})$$

or finally

$$a_n = \frac{2 (K_1 - K_2)}{\pi} \frac{1}{n} \sin \pi n \frac{S^\alpha}{S} \quad (\text{III.7})$$

## APPENDIX IV

### CALCULATION OF THE FOURIER SERIES COEFFICIENTS BY APPLICATION OF THE FIRST THERMODYNAMIC VERSION OF THE GIBBS-THOMSON RELATION FOR BINARY SYSTEMS

In the application of the Gibbs-Duhem equation we have seen for our first thermodynamic version that the coefficients of the Fourier series are determined by eq. 2.50

$$\sum_{n=0}^{\infty} a_n \cos b_n y = \frac{C_{\infty} + \frac{D}{v} \sum_{n=1}^{\infty} \frac{A_n b_n^2}{\lambda_n} \cos b_n y}{C_{\infty} + \sum_{n=0}^{\infty} A_n \cos b_n y} \quad (\text{IV.1})$$

From Hillert's evaluation of the  $A_n$  coefficients, eq. 2.34, we know that the series in both the numerator and denominator of eq. IV.1 are slowly convergent. Further, we shall see that it is sufficient to adopt one order of expansion more for the step function than for the concentration expansions. To prove this we carry out preliminary calculations to the third order in all series:

$$a_0 + a_1 \cos b_1 y + a_2 \cos b_2 y + a_3 \cos b_3 y + \dots$$

(IV.2)

$$\frac{C_\infty + \frac{D}{v} \left( \frac{A_1 b_1^2}{\lambda_1} \cos b_1 y + \frac{A_2 b_2^2}{\lambda_2} \cos b_2 y + \frac{A_3 b_3^2}{\lambda_3} \cos b_3 y + \dots \right)}{C_\infty + A_0 + A_1 \cos b_1 y + A_2 \cos b_2 y + A_3 \cos b_3 y + \dots}$$

We define

$$2 (C_\infty + A_0) = A'_0 \quad (IV.3)$$

and we multiply the denominator by  $K(y)$ , making use of the identity

$$\cos b_i y \cos b_j y = \frac{1}{2} \cos b_{i+j} y + \frac{1}{2} \cos b_{i-j} y \quad (IV.4)$$

we thus obtain

$$(a_0 + a_1 \cos b_1 y + a_2 \cos b_2 y + a_3 \cos b_3 y + \dots)$$

$$\left( \frac{A'_0}{2} + A_1 \cos b_1 y + A_2 \cos b_2 y + A_3 \cos b_3 y + \dots \right)$$

(IV.5)

$$= \frac{1}{2} (a_0 A'_0 + a_1 A_1 + a_2 A_2 + a_3 A_3 + \dots)$$

(over)



$$+ \frac{1}{2} (2a_0 A_1 + a_1 A'_0 + a_1 A_2 + a_2 A_1 + a_2 A_3 + a_3 A_2 + \dots) \cos b_1 y$$

$$+ \frac{1}{2} (2a_0 A_2 + a_1 A_1 + a_1 A_3 + a_2 A'_0 + a_3 A_1 + \dots) \cos b_2 y$$

$$+ \frac{1}{2} (2a_0 A_3 + a_1 A_2 + a_2 A_1 + a_3 A'_0 + \dots) \cos b_3 y$$

We can now identify these coefficients with those of  $C_p$ , to obtain

$$a_0 A'_0 + a_1 A_1 + a_2 A_2 + a_3 A_3 = 2 C_\infty \quad (\text{IV.6a})$$

$$a_1 A'_0 + (2a_0 + a_2) A_1 + (a_1 + a_3) A_2 + a_2 A_3 = \frac{2 D}{v} \frac{A_1 b_1^2}{\lambda_1} \quad (\text{IV.6b})$$

$$a_2 A'_0 + (a_1 + a_3) A_1 + 2a_0 A_2 + a_1 A_3 = \frac{2 D}{v} \frac{A_2 b_2^2}{\lambda_2} \quad (\text{IV.6c})$$

$$a_3 A'_0 + a_2 A_1 + a_1 A_2 + 2a_0 A_3 = \frac{2 D}{v} \frac{A_3 b_3^2}{\lambda_3} \quad (\text{IV.6d})$$

This system of equations can be written after ordering as

$$a_0 A'_0 + a_1 A_1 + a_2 A_2 + a_3 A_3 = 2 C_\infty \quad (\text{IV.7a})$$

$$a_1 A'_0 + (2a_0 + a_2 - \frac{2 D}{v} \frac{b_1^2}{\lambda_1}) A_1 + (a_1 + a_3) A_2 + a_2 A_3 = 0 \quad (\text{IV.7b})$$

$$a_2 A'_0 + (a_1 + a_3) A_1 + \left(2a_0 - \frac{2D}{v} \frac{b_2^2}{\lambda_2}\right) A_2 + a_1 A_3 = 0 \quad (\text{IV.7c})$$

$$a_3 A'_0 + a_2 A_1 + a_1 A_2 + \left(2a_0 - \frac{2D}{v} \frac{b_3^2}{\lambda_3}\right) A_3 = 0 \quad (\text{IV.7d})$$

From this point on we shall simplify by replacing  $\lambda_n$  by  $-b_n$  which is a good approximation (see discussion of eq. 2.5).

It is worth observing that the coefficient matrix of the A's is symmetric and that calculations to a higher order can be easily extrapolated from this matrix:

$$\begin{pmatrix} a_0 & & & & \\ & a_1 & & & \\ & & a_2 & & \\ & & & a_3 & \\ & a_1 & 2a_0 + a_2 + \frac{4\pi D}{5v} & & \\ & & a_1 + a_3 & & a_2 \\ & a_2 & & 2a_0 + \frac{8\pi D}{5v} & \\ & & & & a_1 \\ & a_3 & & & & 2a_0 + \frac{12\pi D}{5v} \end{pmatrix} \quad (\text{IV.8})$$

We can also see that, if we limit ourselves to the second order in  $A_n$ , our result will be significantly more accurate if we retain the term  $a_3$ . We have then the system of equations

$$a_0 A'_0 + a_1 A_1 + a_2 A_2 = 2 C_\infty \quad (\text{IV.9a})$$

$$a_1 A'_0 + (2a_0 + a_2 + \frac{4\pi D}{Sv}) A_1 + (a_1 + a_3) A_2 = 0 \quad (\text{IV.9b})$$

$$a_2 A'_0 + (a_1 + a_3) A_1 + (2a_0 + \frac{8\pi D}{Sv}) A_2 = 0 \quad (\text{IV.9c})$$

which are easily solved by combination of the two last equations. We get

$$\begin{aligned} & [ (2a_0 + \frac{8\pi D}{Sv})(2a_0 + a_2 + \frac{4\pi D}{Sv}) - (a_1 + a_3)^2 ] A_1 = \\ & - [ (2a_0 + \frac{8\pi D}{Sv}) a_1 - (a_1 + a_3) a_2 ] A'_0 \end{aligned} \quad (\text{IV.10a})$$

$$\begin{aligned} & [ (2a_0 + \frac{8\pi D}{Sv})(2a_0 + a_2 + \frac{4\pi D}{Sv}) - (a_1 + a_3)^2 ] A_2 = \\ & - [ (2a_0 + a_2 + \frac{4\pi D}{Sv}) a_2 - (a_1 + a_3) a_1 ] A'_0 \end{aligned} \quad (\text{IV.10b})$$

and equivalently

$$A_1 = \frac{(a_1 + a_3) a_2 - (2a_0 + \frac{8\pi D}{Sv}) a_1}{(2a_0 + \frac{8\pi D}{Sv})(2a_0 + a_2 + \frac{4\pi D}{Sv}) - (a_1 + a_3)^2} \quad (\text{IV.11a})$$

$$A_2 = \frac{(a_1 + a_3) a_1 - (2a_0 + \frac{8\pi D}{Sv}) a_2}{(2a_0 + \frac{8\pi D}{Sv})(2a_0 + a_2 + \frac{4\pi D}{Sv}) - (a_1 + a_3)^2} \quad (\text{IV.11b})$$

We can substitute these expressions for  $A_1$  and  $A_2$  into eq. IV.9 to yield

$$\begin{aligned} & \left[ a_0 \left( 2a_0 + \frac{8\pi D}{Sv} \right) \left( 2a_0 + a_2 + \frac{4\pi D}{Sv} \right) - a_0 (a_1 + a_3)^2 + 2a_1 a_2 (a_1 + a_3) - a_1^2 \left( 2a_0 + \frac{8\pi D}{Sv} \right) \right. \\ & \left. - a_2^2 \left( 2a_0 + a_2 + \frac{4\pi D}{Sv} \right) \right] A'_0 = 2C_\infty \left[ \left( 2a_0 + \frac{8\pi D}{Sv} \right) \left( 2a_0 + a_2 + \frac{4\pi D}{Sv} \right) - (a_1 + a_3)^2 \right] \end{aligned} \quad (\text{IV.12})$$

Solving for  $A'_0$  we finally obtain

$$A'_0 = C_\infty \left[ \frac{\left( 2a_0 + \frac{8\pi D}{Sv} \right) \left( 2a_0 + a_2 + \frac{4\pi D}{Sv} \right) - (a_1 + a_3)^2}{\mathcal{D}} - 1 \right] \quad (\text{IV.13a})$$

$$A_1 = 2C_\infty \frac{(a_1 + a_3) a_2 - \left( 2a_0 + \frac{8\pi D}{Sv} \right) a_1}{\mathcal{D}} \quad (\text{IV.13b})$$

$$A_2 = 2C_\infty \frac{(a_1 + a_3) a_1 - \left( 2a_0 + a_2 + \frac{4\pi D}{Sv} \right) a_2}{\mathcal{D}} \quad (\text{IV.13c})$$

with

$$\begin{aligned} \mathcal{D} = & a_0 \left( 2a_0 + \frac{8\pi D}{Sv} \right) \left( 2a_0 + a_2 + \frac{4\pi D}{Sv} \right) - a_0 (a_1 + a_3)^2 + 2a_1 a_2 (a_1 + a_3) - a_1^2 \left( 2a_0 + \frac{8\pi D}{Sv} \right) \\ & - a_2^2 \left( 2a_0 + a_2 + \frac{4\pi D}{Sv} \right) \end{aligned} \quad (\text{IV.14})$$

## APPENDIX V

### COMPLETE SOLUTION OF THE PROBLEM IN THE SYMMETRICAL CONFIGURATION FOR THE FIRST THERMODYNAMIC VERSION

We shall assume in this calculation a symmetrical binary diagram, surface tensions all equal and  $x_{\infty} = 0.5$  mole fraction. The three triple point angles are therefore equal to  $2\pi/3$  and as we have already pointed out from eq. 2.61,  $S^{\alpha} = S^{\beta}$ . This greatly simplifies our calculations since we are left only with eq. 2.62, in which we have

$$a_0 = \frac{K^{\alpha} + K^{\beta}}{2}; a_1 = \mu = \frac{2}{\pi} (K^{\alpha} - K^{\beta}); a_2 = 0; a_3 = -\frac{\mu}{3} \quad (V.1)$$

From eq. 2.54 we deduce the expression for the coefficients

$$A_0 = C_{\infty} \left[ \frac{(2\lambda + \frac{8\pi D}{Sv}) (2\lambda + \frac{4\pi D}{Sv}) - \frac{4}{9} \mu^2}{\lambda(2\lambda + \frac{8\pi D}{Sv})(2\lambda + \frac{4\pi D}{Sv}) - \frac{4}{9} \lambda \mu^2 - \mu^2 (2\lambda + \frac{8\pi D}{Sv})} - 1 \right] \quad (V.2a)$$

$$A_1 = -C_{\infty} \frac{2\mu(2\lambda + \frac{8\pi D}{Sv})}{(2\lambda + \frac{8\pi D}{Sv})(2\lambda + \frac{4\pi D}{Sv}) - \frac{4}{9} \lambda \mu^2 - \mu^2 (2\lambda + \frac{8\pi D}{Sv})} \quad (V.2b)$$

$$A_2 = -C_{\infty} \frac{2 \frac{2}{3} \mu^2}{\lambda(2\lambda + \frac{8\pi D}{Sv})(2\lambda + \frac{4\pi D}{Sv}) - \frac{4}{9} \lambda \mu^2 - \mu^2 (2\lambda + \frac{8\pi D}{Sv})} \quad (V.2c)$$

We substitute the expressions for these coefficients into eq. 2.62 to obtain

$$\phi + S = 4 C_{\infty} \frac{D}{V} \mu \left( \frac{1}{C_{\infty} - C_{10}^{\beta\gamma}} - \frac{1}{C_{\infty} - C_{10}^{\alpha\gamma}} \right) \frac{(2\lambda + \frac{8\pi D}{Sv})}{\lambda (2\lambda + \frac{8\pi D}{Sv}) (2\lambda + \frac{4\pi D}{Sv}) - \frac{4}{g} \lambda \mu^2 - \mu^2 (2\lambda + \frac{8\pi D}{Sv})} \quad (V.3)$$

where in general

$$\phi = - \frac{2}{RT} \left[ \frac{\sigma^{\alpha} \cos \phi^{\alpha}}{h^{\alpha} (C_{\infty} - C_{10}^{\alpha\gamma})} + \frac{\sigma^{\beta} \cos \phi^{\beta}}{h^{\beta} (C_{\infty} - C_{10}^{\beta\gamma})} \right] \quad (V.4)$$

or for our symmetrical case

$$\phi = - \frac{4}{RT} \frac{\sigma^{\alpha} \cos \phi^{\alpha}}{h^{\alpha} (C_{\infty} - C_{10}^{\alpha\gamma})} \quad (V.5)$$

We divide both members of eq. V.3 by S and collect within the equation the group  $8\pi D/Sv$  to give

$$\frac{\phi}{S} + 1 = - \frac{C_{\infty}}{2\pi} \frac{8\pi D}{Sv} \mu \left( \frac{1}{C_{\infty} - C_{10}^{\beta\gamma}} - \frac{1}{C_{\infty} - C_{10}^{\alpha\gamma}} \right) \frac{(2\lambda + \frac{8\pi D}{Sv})}{\frac{\lambda}{2} (2 + \frac{8\pi D}{Sv}) (4\lambda + \frac{8\pi D}{Sv}) - \frac{4}{g} \lambda \mu^2 - \mu^2 (2\lambda + \frac{8\pi D}{Sv})} \quad (V.6)$$

With the further notation

$$\chi = \frac{8\pi D}{Sv} \quad (V.7)$$

and

$$C = \frac{C_{\infty}}{2\pi} \left( \frac{1}{C_{\infty} - C_{10}^{\beta\gamma}} - \frac{1}{C_{\infty} - C_{10}^{\alpha\gamma}} \right) \quad (V.8)$$

we have the equivalent equation

$$\frac{\phi}{S} + 1 = C \frac{\mu X (2\lambda + X)}{\frac{\lambda}{2} (2\lambda + X) (4\lambda + X) - \mu^2 (2\lambda + X) - \frac{4}{9} \lambda \mu^2} \quad (V.9)$$

and finally

$$\frac{\lambda}{2} \left( \frac{\phi}{S} + 1 \right) (X^2 + 2 \frac{3\lambda^2 - \mu^2}{\lambda} X + 8\lambda^2 - \frac{44}{9} \mu^2) = C_{\mu} X (2\lambda + X) \quad (V.10)$$

As eq. V.10 stands we can in principle derive an expression for  $v$  in terms of  $S$  and look for the maximum of  $v(S)$ . However, it is not possible to derive a formal expression for  $v$  as a function of  $S$  which is as transparent as the one given by Hillert in eq. 2.44. Rather than attempt a numerical solution we shall approach this problem using geometrical considerations.

For a given  $S$ ,  $X$  is function of  $v$  only and, the roots of eq. V.10 will give the corresponding values of  $v$ . We regard both members of eq. V.10 as the equations of two parabolas,  $y_1$  and  $y_2$ , respectively, for the left and right hand side as shown on Fig. 32. The roots of eq. V.10 are the abscissas of the intersections of these two parabolas. We note that  $y_1$  is explicitly dependent upon  $S$  and that  $y_2$  is independent of  $S$ , viz.,

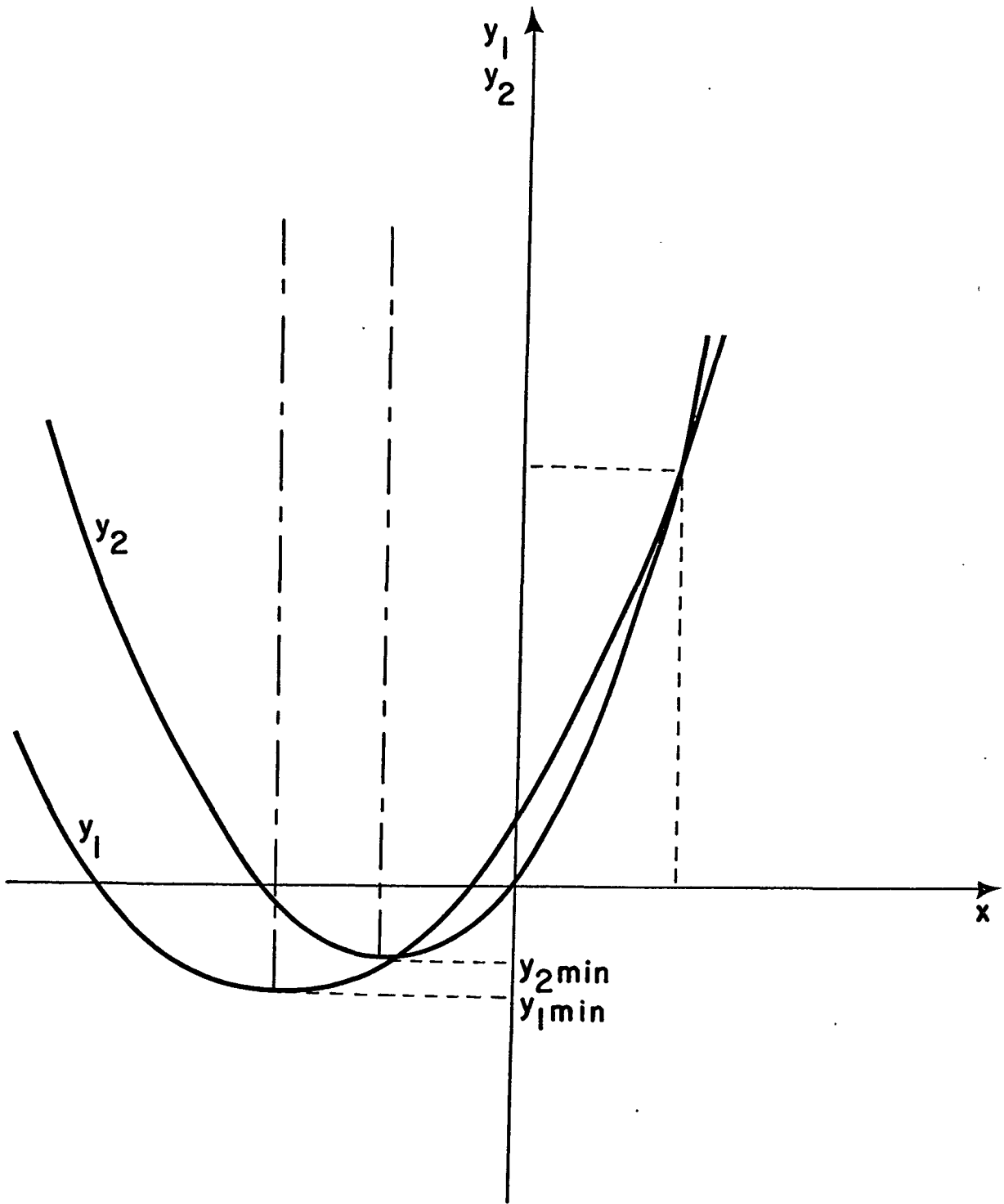


Fig. 32: Representation of the two parabolas  $y_1$  and  $y_2$  as a function of  $x$ .



$$y_1 = \frac{\lambda}{2} \left( \frac{\phi}{2} + 1 \right) \left( X^2 + 2 \frac{3\lambda^2 - \mu^2}{\lambda} X + 8\lambda^2 - \frac{44}{9} \mu^2 \right) \quad (\text{V.11a})$$

$$y_2 = C\mu X (2\lambda + X) \quad (\text{V.11b})$$

Furthermore, the parabola  $y_1$  intersects the  $X$  axis at two points which remain the same for all values of  $S$ . Their abscissas are the roots of the polynomial

$$X^2 + 2 \frac{3\lambda^2 - \mu^2}{\lambda} X + 8\lambda^2 - \frac{44}{9} \mu^2 = 0 \quad (\text{V.12})$$

or

$$X = - \frac{3\lambda^2 - \mu^2}{\lambda} \pm \Delta \quad (\text{V.13a})$$

with

$$\Delta^2 = \left( \frac{3\lambda^2 - \mu^2}{\lambda} \right)^2 - 8\lambda^2 + \frac{44}{9} \mu^2 \quad (\text{V.13b})$$

We shall see below that these roots are always negative. The minimum of the parabola  $y_1$  is given by:

$$y_{1 \min} = - \frac{\lambda}{2} \left( \frac{\phi}{2} + 1 \right) \left[ \left( \frac{3\lambda^2 - \mu^2}{\lambda} \right)^2 + \frac{44}{9} \mu^2 - 8\lambda^2 \right] \quad (\text{V.14a})$$

at

$$X_{\min} = - \frac{3\lambda^2 - \mu^2}{\lambda} \quad (\text{V.14b})$$

This minimum is large in absolute value when  $S$  is small and when  $S$  goes to infinity

$$\lim_{S \rightarrow \infty} (y_1 \min) = -\frac{\lambda}{2} \left[ \left( \frac{3\lambda^2 - \mu^2}{\lambda} \right)^2 + \frac{44}{9} \mu^2 - 8\lambda^2 \right] \quad (\text{V.15})$$

The parabola defined by  $y_2$ , eq. V.11b, goes through the origin and the abscissa  $X = -2\lambda$ . Its minimum is given by

$$y_{2\min} = -C\mu\lambda^2 \quad (\text{V.16a})$$

at

$$X_{\min} = -\lambda \quad (\text{V.16b})$$

Since physically  $S$  and  $v$  can have only positive values we are only interested in the results for positive values of  $X$ . This imposes certain conditions upon the relative positions of the parabolas, i.e., upon the values of  $\lambda$  and  $\mu$ , which in turn are taken directly from the phase diagram.

We first examine the allowed values for  $\lambda/\mu$ . From eq. V.1 we deduce

$$\frac{\lambda}{\mu} = \frac{\pi}{4} \frac{K^\alpha + K^\beta}{K^\alpha - K^\beta} \quad (\text{V.17})$$

It is a well-known fact, that keeping the  $K$ 's positive, the minimum in absolute value of this ratio is  $\frac{\pi}{4}$ . In fact  $\frac{\lambda}{\mu}$  is always

negative and we have the bounds

$$\frac{\lambda}{\mu} < -\frac{\pi}{4} \quad (\text{V.18})$$

We can see now why the parabola  $y_1$  intersects the X axis for negative values of X since the sum of the roots of eq. V.12 is negative, i.e., from eq. V.18

$$-\frac{3\lambda^2 - \mu^2}{\lambda} < 0 \quad (\text{V.19})$$

and the product of the roots is always positive

$$8\lambda^2 - \frac{44}{9} \mu^2 > 0 \quad (\text{V.20})$$

with the bounds imposed in eq. V.18.

From Fig. 32 it can be easily seen that in order to have intersections of the two parabolas for positive values of X, the minimum of  $y_1$  should be close to the X axis. In other words S must be large and there must exist a critical value of S (called  $S_c$ ) below which we do not have physical solutions.

We now look for that condition which assures a positive intersection when  $S = \infty$ . Consider

$$\frac{\lambda}{2} (X^2 + 2 \frac{3\lambda^2 - \mu^2}{\lambda} X + 8\lambda^2 - \frac{44}{9} \mu^2) = C_\mu X (2\lambda + X) \quad (\text{V.21})$$

which, when ordered in X, is

$$(1 - 2C \frac{\mu}{\lambda}) x^2 + 2 \left( \frac{3\lambda^2 - \mu^2}{\lambda} - 2C\mu \right) x + 8\lambda^2 - \frac{44}{9} \mu^2 = 0 \quad (V.22)$$

From Fig. 32 we can see that we will always have a negative root so that we must require that the product of the two roots of eq. V.22 is negative. This condition is expressed by

$$\frac{8\lambda^2 - \frac{44}{9} \mu^2}{1 - 2C \frac{\mu}{\lambda}} < 0 \quad (V.23)$$

Since we know that the numerator is always positive the equivalent condition is expressed by

$$\frac{\lambda}{\mu} > 2C \quad (V.24)$$

In order therefore to obtain a physical answer to our problem the phase diagram should give us a  $\frac{\lambda}{\mu}$  fulfilling the condition

$$2C < \frac{\lambda}{\mu} < -\frac{\pi}{4} \quad (V.25)$$

Note that these conditions have been obtained from eq. V.3 and are therefore dependent upon the order of expansion to which we have taken the Fourier series. We do not know if such conditions will strictly hold when we take a higher order of expansion or when we go to  $n = \infty$ .

We try now to express these conditions as functions of  $x = x_{10}^{\alpha\gamma}$  and  $y = x_{10}^{\gamma\alpha}$ . We have

$$K^\alpha = \frac{x}{y} \quad (V.26)$$

and

$$K^\beta = \frac{1-x}{1-y} \quad (V.27)$$

If we now replace  $K^\alpha$  and  $K^\beta$  by these expressions in eq. V.17 we obtain

$$\frac{\lambda}{\mu} = \frac{\pi}{4} \frac{\frac{x}{y} + \frac{1-x}{1-y}}{\frac{x}{y} - \frac{1-x}{1-y}} \quad (V.28)$$

$$= \frac{\pi}{4} \frac{x+y-2xy}{x-y} \quad (V.29)$$

In the same way we can find from eq. V.8 an expression for  $2C$  as a function of  $x$  and  $y$ , viz.,

$$2C = \frac{2}{\pi} \frac{1}{2x-1} \quad (V.30)$$

and the conditions of eq. V.25 can now be written as

$$\frac{2}{\pi} \frac{1}{2x-1} < \frac{\pi}{4} \frac{x+y-2xy}{x-y} < -\frac{\pi}{4} \quad (V.31)$$

or equivalently

$$\frac{8}{\pi^2} \frac{1}{1-2x} > \frac{x+y-2xy}{y-x} > 1 \quad (\text{V.32})$$

Since  $y - x$  is a positive quantity, the inequality on the right means that

$$x + y - 2xy > y - x \quad (\text{V.33})$$

or

$$2x(1-y) > 0 \quad (\text{V.34})$$

which is always satisfied. If we now consider the left hand side inequality of V.32, we have

$$\frac{8}{\pi^2} (y-x) > (1-2x)(x+y-2xy) \quad (\text{V.35})$$

and equivalently

$$\frac{8}{\pi^2} - (1-2x)^2 > \left[ \frac{8}{\pi^2} + (1-2x) \right] \frac{x}{y} \quad (\text{V.36})$$

Since  $x/y$  is equal to  $K^\alpha$  we have finally

$$(1-2x+K^\alpha)(1-2x) < (1-K^\alpha) \frac{8}{\pi^2} \quad (\text{V.37})$$

This inequality impose the condition upon  $x$

$$x_{lim} < x < \frac{1}{2} \quad (V.38)$$

where  $x_{lim}$  is the smallest root of the quadratic form in V.37 and is given by

$$x_{lim} = \frac{1}{4} \left\{ (2 + K^\alpha) - \sqrt{(2 + K^\alpha)^2 - 4 \left[ 1 + K^\alpha - (1 - K^\alpha) \frac{8}{\pi^2} \right]} \right\} \quad (V.39)$$

Condition V.38 states that the solubility  $x$  in the  $\alpha$  phase must be between a minimum value ( $\sim 0.1$ ) and  $\frac{1}{2}$ . This condition could be in contradiction to our thermodynamic requirement that the solubility be small. We have not been able to decide if this latter condition is general because it was derived from calculations performed to a limited harmonic. As we shall see in the following Appendices for more general thermodynamic assumptions the restriction for a symmetric diagram does not appear. If now we order eq. V.10 in  $x$  we obtain

$$\left[ \frac{\lambda}{2} \left( \frac{\phi}{S} + 1 \right) - C\mu \right] x^2 + \left[ (3\lambda^2 - \mu^2) \left( \frac{\phi}{S} + 1 \right) - 2C\lambda\mu \right] x - \frac{44}{9} \mu^2 \frac{\lambda(\phi + 1)}{2S} = 0 \quad (V.40)$$

One root of this equation goes to infinity when the coefficient of  $x^2$  vanishes. This gives us for  $S = S_c$ ,

$$\frac{\phi}{S_c} + 1 = 2 C \frac{\mu}{\lambda} \quad (V.41)$$

or

$$S_c = \frac{\phi}{2 C \frac{\mu}{\lambda} - 1} \quad (\text{V.42})$$

Since  $X$  goes to infinity for this finite value of  $S$  we further deduce from eq. V.6 that the velocity must vanish at  $S = S_c$ . We have therefore just calculated the critical lamellar spacing. Now as  $S$  increases and goes to infinity the minimum of the parabola  $y_1$  goes up as shown in Fig. 32. We can therefore see that  $X$  reaches a minimum for very large values of  $S$  and from eq. V.6 we deduce that the velocity vanishes again. Accordingly there must be a value of  $S$  which gives a maximum for  $v$ . From this argument we conclude that a complete calculation should give a curve  $v(S)$  similar to the one drawn in Fig. 4.



## APPENDIX VI

GENERAL CALCULATION OF THE FOURIER SERIES COEFFICIENTS BY APPLICATION OF THE  
SECOND THERMODYNAMIC VERSION OF THE GIBBS-THOMSON RELATION FOR BINARY SYSTEMS

From eqs. 2.80 and 2.81 we can write

$$\frac{C_{\infty} - \alpha'_0 + \sum_{n=1}^{\infty} \left( \frac{D}{v} \frac{A_n b_n^2}{\lambda_n} - \alpha'_n \right) \cos b_n y}{C_{\infty} + A_0 - \alpha_0 + \sum_{n=1}^{\infty} (A_n - \alpha_n) \cos b_n y} = \sum_{n=0}^{\infty} a_n \cos b_n y \quad (\text{VI.1})$$

with the notation

$$B_0 = 2 (C_{\infty} + A_0 - \alpha_0) \quad \text{and} \quad B_n = A_n - \alpha_n \quad (\text{VI.2})$$

We can see that the product of the denominator by the K series is exactly the same as for the case treated in Appendix V. By identification with the series in the numerator we have to the second harmonic

$$a_0 B_0 + a_1 B_1 + a_2 B_2 = 2 (C_{\infty} - \alpha'_0) \quad (\text{VI.3a})$$

$$a_1 B_0 + (2a_0 + a_2) B_1 + (a_1 + a_3) B_2 = 2 \left( \frac{D}{v} \frac{A_1 b_1^2}{\lambda_1} - \alpha' \right) \quad (\text{VI.3b})$$

$$a_2 B_0 + (a_1 + a_3) B_1 + 2a_0 B_2 = 2 \left( \frac{D}{v} \frac{A_2 b_2^2}{\lambda_2} - \alpha' \right) \quad (\text{VI.3c})$$

From now on we will adopt the approximation  $\lambda_n = -b_n$ . We therefore order this system in  $B_n$  obtaining

$$a_0 B_0 + a_1 B_1 + a_2 B_2 = 2 (C_\infty - \alpha'_0) \quad (\text{VI.4a})$$

$$a_1 B_0 + \left( 2a_0 + a_2 + \frac{4\pi D}{Sv} \right) B_1 + (a_1 + a_3) B_2 = -2 \left( \frac{2\pi D}{Sv} \alpha_1 + \alpha'_1 \right) \quad (\text{VI.4b})$$

$$a_2 B_0 + (a_1 + a_3) B_1 + \left( 2a_0 + \frac{8\pi D}{Sv} \right) B_2 = -2 \left( \frac{4\pi D}{Sv} \alpha_2 + \alpha'_2 \right) \quad (\text{VI.4c})$$

Note here that the two last equations contain a right hand side in contradistinction to the problem treated in Appendix V. To solve this system we will have recourse to matrix notation. The system can be written in the symbolic form

$$d_{11} Y_1 + d_{12} Y_2 + d_{13} Y_3 = X_1 \quad (\text{VI.5a})$$

$$d_{12} Y_1 + d_{22} Y_2 + d_{23} Y_3 = X_2 \quad (\text{VI.5b})$$

$$d_{13} Y_1 + d_{23} Y_2 + d_{33} Y_3 = X_3 \quad (\text{VI.5c})$$

subject to the matrix equality

$$\begin{pmatrix} d_{11} & d_{12} & d_{13} \\ d_{12} & d_{22} & d_{23} \\ d_{13} & d_{23} & d_{33} \end{pmatrix} = \begin{pmatrix} a_0 & a_1 & a_2 \\ a_1 & 2a_0 + a_2 + \frac{4\pi D}{Sv} & a_1 + a_3 \\ a_2 & a_1 + a_3 & 2a_0 + \frac{8\pi D}{Sv} \end{pmatrix} \quad (\text{VI.6})$$

The determinant of this matrix is

$$\mathcal{D} = d_{11}(d_{22}d_{33} - d_{23}^2) - d_{12}(d_{12}d_{33} - d_{23}d_{13}) + d_{13}(d_{12}d_{23} - d_{22}d_{13}) \quad (\text{VI.7a})$$

$$\begin{aligned} &= a_0(2a_0 + \frac{8\pi D}{Sv})(2a_0 + a_2 + \frac{4\pi D}{Sv}) - a_0(a_1 + a_3)^2 + 2a_1a_2(a_1 + a_3) - a_1^2(2a_0 + \frac{8\pi D}{Sv}) \\ &\quad - a_2^2(2a_0 + a_2 + \frac{4\pi D}{Sv}) \end{aligned} \quad (\text{VI.7b})$$

The Y's can now be expressed in terms of the X's by the relation

$$Y_1 = \frac{1}{\mathcal{D}} [(d_{22}d_{33} - d_{23}^2)X_1 - (d_{12}d_{33} - d_{23}d_{13})X_2 + (d_{12}d_{23} - d_{22}d_{13})X_3] \quad (\text{VI.8a})$$

$$Y_2 = \frac{1}{\mathcal{D}} [-(d_{12}d_{33} - d_{13}d_{23})X_1 + (d_{11}d_{33} - d_{13}^2)X_2 - (d_{11}d_{23} - d_{13}d_{12})X_3] \quad (\text{VI.8b})$$

$$Y_3 = \frac{1}{\mathcal{D}} [(d_{12}d_{23} - d_{13}d_{22})X_1 - (d_{11}d_{23} - d_{13}d_{12})X_2 + (d_{11}d_{22} - d_{12}^2)X_3] \quad (\text{VI.8c})$$

Taking account of equality (V.6) we obtain by substitution

$$\begin{aligned} \mathcal{D} Y_1 = & \left[ (2a_0 + a_2 + \frac{4\pi D}{Sv})(2a_0 + \frac{8\pi D}{Sv}) - (a_1 + a_3)^2 \right] X_1 - \left[ a_1 (2a_0 + \frac{8\pi D}{Sv}) - (a_1 + a_3) a_2 \right] X_2 \\ & + \left[ a_1 (a_1 + a_3) - (2a_0 + a_2 + \frac{4\pi D}{Sv}) a_2 \right] X_3 \end{aligned} \quad (\text{VI.9a})$$

$$\mathcal{D} Y_2 = \left[ a_2 (a_1 + a_3) - a_1 (2a_0 + \frac{8\pi D}{Sv}) \right] X_1 + \left[ a_0 (2a_0 + \frac{8\pi D}{Sv}) - a_2^2 \right] X_2 - \left[ a_0 (a_1 + a_3) - a_1 a_2 \right] X_3 \quad (\text{VI.9b})$$

$$\begin{aligned} \mathcal{D} Y_3 = & \left[ a_1 (a_1 + a_3) - a_2 (2a_0 + a_2 + \frac{4\pi D}{Sv}) \right] X_1 - \left[ a_0 (a_1 + a_3) - a_2 a_1 \right] X_2 \\ & + \left[ a_0 (2a_0 (2a_0 + a_2 + \frac{4\pi D}{Sv}) - a_1^2) \right] X_3 \end{aligned} \quad (\text{IV.9c})$$

The coefficients  $A_n$  are obtained from the system (VI.9) as

$$\begin{aligned} A_0 = \alpha_0 - C_\infty + \frac{1}{2\mathcal{D}} \left\{ \left[ (2a_0 + a_2 + \frac{4\pi D}{Sv})(2a_0 + \frac{8\pi D}{Sv}) - (a_1 + a_3)^2 \right] X_1 \right. \\ \left. - \left[ a_1 (2a_0 + \frac{8\pi D}{Sv}) - (a_1 + a_3) a_2 \right] X_2 + \left[ a_1 (a_1 + a_3) - a_2 (2a_0 + a_2 + \frac{4\pi D}{Sv}) \right] X_3 \right\} \end{aligned} \quad (\text{VI.10a})$$

$$\begin{aligned} A_1 = \alpha_1 + \frac{1}{\mathcal{D}} \left\{ \left[ (a_2 (a_1 + a_3) - a_1 (2a_0 + \frac{8\pi D}{Sv})) \right] X_1 + \left[ a_0 (2a_0 + \frac{8\pi D}{Sv}) - a_2^2 \right] X_2 \right. \\ \left. - \left[ a_0 (a_1 + a_3) - a_1 a_2 \right] X_3 \right\} \end{aligned} \quad (\text{VI.10b})$$

$$\begin{aligned} A_2 = \alpha_2 + \frac{1}{\mathcal{D}} \left\{ \left[ (a_1 (a_1 + a_3) - a_2 (2a_0 + a_2 + \frac{4\pi D}{Sv})) \right] X_1 - \left[ a_0 (a_1 + a_3) - a_2 a_1 \right] X_2 \right. \\ \left. + \left[ a_0 (2a_0 + a_2 + \frac{4\pi D}{Sv}) - a_1^2 \right] X_3 \right\} \end{aligned} \quad (\text{VI.10c})$$

where the  $X$ 's are given by

$$X_1 = 2 (C_\infty - \alpha'_0) \quad (\text{VI.11a})$$

$$X_2 = -2 \left( \frac{2\pi D}{Sv} \alpha_1 + \alpha'_1 \right) \quad (\text{VI.11b})$$

$$X_3 = -2 \left( \frac{4\pi D}{Sv} \alpha_2 + \alpha'_2 \right) \quad (\text{VI.11c})$$

## APPENDIX VII

### COMPLETE SOLUTION OF THE PROBLEM IN THE SYMMETRICAL CONFIGURATION WITH THE SECOND THERMODYNAMIC VERSION

As in Appendix V we consider a symmetrical binary diagram, equal surface tensions and  $x_{\infty} = 0.5$  mole fraction. In this case, as we have seen in section II-C,  $K_{\alpha} = K_{\beta}$  and eq. 2.80 reduces to the proportionality relation

$$\frac{C_p - C_{p0}}{C - C_0} = K \quad (\text{VII.1})$$

where  $K$  is now a constant equal to  $K_{\alpha}$ . Furthermore, we have, from eqs. 2.83 and 2.84

$$\alpha_0 = C_{\infty} \quad \alpha_n = \frac{2 (C_{10}^{\gamma\alpha} - C_{10}^{\gamma\beta})}{\pi} \sin n \frac{\pi}{2} \quad (\text{VII.2})$$

$$\alpha'_0 = C_{\infty} \quad \alpha'_n = \frac{2 (C_{10}^{\alpha\gamma} - C_{10}^{\beta\gamma})}{\pi} \sin n \frac{\pi}{2} \quad (\text{VII.3})$$

Substituting these expressions in eq. VII.1, we obtain

$$\sum_{n=1}^{\infty} \left( \frac{D}{v} \frac{A_n b_n^2}{\lambda_n} - \alpha'_n \right) \cos b_n y = K \left[ A_0 + \sum_{n=1}^{\infty} (A_n - \alpha_n) \cos b_n y \right] \quad (\text{VII.4})$$

Since all the  $\alpha$ 's vanish for  $n$  even, we deduce that

$$A_{2i} = 0 \text{ including } i = 0 \quad (\text{VII.5})$$

Then, subject to  $\lambda_n = -b_n$ , we have the system

$$-A_{2i-1} \frac{2\pi(2i-1)D}{Sv} - \alpha'_{2i-1} = K(A_{2i-1} - \alpha_{2i-1}) \quad (\text{VII.6})$$

which leads to

$$A_{2i-1} = \frac{K \alpha_{2i-1} - \alpha'_{2i-1}}{K + \frac{2\pi(2i-1)D}{Sv}} \quad (\text{VII.7})$$

and, finally

$$A_{2i-1} = \frac{2}{\pi} \left[ K(C_{10}^{\gamma\alpha} - C_{10}^{\gamma\beta}) - (C_{10}^{\alpha\gamma} - C_{10}^{\beta\gamma}) \right] \frac{\frac{1}{2i-1} \sin(2i-1)\frac{\pi}{2}}{K + \frac{2\pi D}{Sv} (2i-1)} \quad (\text{VII.8})$$

If we substitute the expression for these coefficients into eq. 2.89 we obtain

$$\phi + S = -\frac{2\pi D}{Sv} \frac{4}{\pi^2} \frac{K(C_{10}^{\gamma\beta} - C_{10}^{\gamma\alpha}) - (C_{10}^{\alpha\gamma} - C_{10}^{\beta\gamma})}{C_{\infty} - C_{10}^{\beta\gamma}} \sum_{i=1}^{\infty} \frac{1}{(2i-1) \left[ K + \frac{2\pi D}{Sv} (2i-1) \right]} \quad (\text{VII.9})$$

where

$$\phi = -\frac{4}{RT} \frac{\sigma^{\alpha} \cos \phi^{\alpha}}{K^{\alpha} (C_{\infty} - C_{10}^{\alpha\gamma})} \quad (\text{VII.10})$$

We now adopt the notation

$$C' = -\frac{4}{\pi^2} \frac{K(C_{10}^{\gamma\alpha} - C_{10}^{\gamma\beta}) - (C_{10}^{\alpha\gamma} - C_{10}^{\beta\gamma})}{C_{\infty} - C_{10}^{\beta\gamma}} \quad (\text{VII.11a})$$

and

$$\chi = \frac{2\pi D}{Sv} \quad (\text{VII.11b})$$

We can then write eq. VII.9, after division by  $S$ , as

$$\frac{\phi}{S} + 1 = C' \chi \sum_{i=1}^{\infty} \frac{1}{(2i-1)[K + \chi(2i-1)]} \quad (\text{VII.12})$$

Unfortunately, the series on the right hand side cannot be rigorously expressed as a simple analytic function. However, to a good approximation we can extract from eq. VII.12 a simple  $v(S)$  relation. In most physical systems of interest  $K$  is a small quantity (confirmation is given in the numerical applications) and we have already assumed that  $\chi$  is large in comparison to unity. After division by  $\chi$  eq. VII.12 can be written in the form

$$\frac{\phi}{S} + 1 = C' \sum_{i=1}^{\infty} \frac{1}{(2i-1)^2 \left[1 + \frac{K}{(2i-1)\chi}\right]} \quad (\text{VII.13})$$

We multiply both members of this equation by  $1 + K/\chi$  and obtain

$$\left(\frac{\phi}{S} + 1\right)\left(1 + \frac{K}{\chi}\right) = C' \sum_{i=1}^{\infty} \frac{1 + \frac{K}{\chi}}{(2i-1)^2 \left[1 + \frac{K}{(2i-1)\chi}\right]} \quad (\text{VII.14})$$



The recurrent term under the summation can be expanded to the first order as follows:

$$\frac{1 + \frac{K}{X}}{(2i-1)^2 \left[ 1 + \frac{K}{(2i-1)X} \right]} = \frac{1}{(2i-1)^2} \left( 1 + \frac{K}{X} \right) \left[ 1 - \frac{K}{(2i-1)X} + \dots \right] \quad (\text{VII.15})$$

and after multiplication

$$\frac{1 + \frac{K}{X}}{(2i-1)^2 \left[ 1 + \frac{K}{(2i-1)X} \right]} = \frac{1}{(2i-1)^2} + \left[ \frac{1}{(2i-1)^2} - \frac{1}{(2i-1)^3} \right] \frac{K}{X} + \dots \quad (\text{VII.16})$$

Thus we can write eq. VII.14 as

$$\begin{aligned} \left( \frac{\phi}{S} + 1 \right) \left( 1 + \frac{K}{X} \right) = C' \left\{ \sum_{i=1}^{\infty} \frac{1}{(2i-1)^2} + \right. \\ \left. \left[ \sum_{i=1}^{\infty} \frac{1}{(2i-1)^2} - \sum_{i=1}^{\infty} \frac{1}{(2i-1)^3} \right] \frac{K}{X} + \dots \right\} \end{aligned} \quad (\text{VII.17})$$

The evaluation of the two series gives

$$\sum_{i=1}^{\infty} \frac{1}{(2i-1)^2} = \frac{\pi^2}{8} = 1.2337 \quad (\text{VII.18})$$

and

$$\sum_{i=1}^{\infty} \frac{1}{(2i-1)^3} = 1.0518 \quad (\text{VII.19})$$

After multiplication of both members by  $X$ , eq. VII.17 can be written numerically as

$$\left(\frac{\phi}{S} + 1\right)(K + X) = C' \left(\frac{\pi^2}{8} X + 0.1819 K\right) \quad (\text{VII.20})$$

We can now solve for  $X$  to obtain

$$\left(\frac{\pi^2}{8} C' - 1 - \frac{\phi}{S}\right) X = \left(1 - 0.1819 C' + \frac{\phi}{S}\right) K \quad (\text{VII.21})$$

and with eq. VII.11 we deduce the  $v(S)$  relation

$$v = \frac{2\pi D}{K} \frac{1}{S} \frac{\frac{\pi^2}{8} C' - 1 - \frac{\phi}{S}}{1 - 0.1819 C' + \frac{\phi}{S}} \quad (\text{VII.22})$$

which we write under the definitive form

$$v = \Omega' \frac{1}{S} \frac{1 - \frac{S_c}{S}}{1 + \frac{\phi'}{S}} \quad (\text{VII.23})$$

where

$$S_c = \frac{\phi}{C' \frac{\pi^2}{8} - 1} \quad (\text{VII.24a})$$

$$\phi' = \frac{\phi}{1 - 0.1819 C'} \quad (\text{VII.24b})$$

and

$$\Omega' = \frac{2\pi D}{K} \frac{C' \frac{\pi^2}{8} - 1}{1 - 0.1819 C'} \quad (\text{VII.24c})$$

It is important to note that eq. VII.23 has been derived for the symmetric configuration and under the assumption that  $K/X$  is very small in comparison to unity.

We consider next a rigorous treatment of eq. VII.12. Let us imagine that the expansion is limited to some high order in  $i$ . We obtain

$$\frac{\Phi}{S} + 1 = C' X \left[ \frac{1}{K + X} + \frac{1}{3(K + 3X)} + \dots + \frac{1}{(2i-1) [K + (2i-1)X]} \right] \quad (\text{VII.25})$$

We can place all the terms in the bracket on the right hand side over a common denominator  $\delta$ , where

$$\delta = 1 \times 3X \dots \times (2i-1) (K + X)(K + 3X) \dots [K + (2i-1)X] \quad (\text{VII.26})$$

In all the following we shall define  $\binom{2i-1}{\pi}$  as the number which is the product of all the odd integers up to  $2i-1$ . We have in this notation

$$\delta = \binom{2i-1}{\pi} (K + X)(K + 3X) \dots K + (2i-1)X \quad (\text{VII.27})$$

This is a polynomial of degree  $i$ . Its roots are all negative and of the form  $-K/(2j-1)$ . The coefficient of the highest power in  $X$  can

be written as

$$\left(\frac{2i-1}{\pi}\right)^2 \quad \text{(VII.28)}$$

The coefficient of the term of zeroth power in  $X$  is always positive and is  $\left(\frac{2i-1}{\pi}\right)^2 K^i$ .

Now the numerator, designated as  $v$ , is a sum of  $i$  terms which can be written in the form

$$v = \left(\frac{2i-1}{\pi}\right)^2 \sum_{j=1}^i \frac{1}{2j-1} (K+X) \dots [K+(2j-3)X][K+(2j+1)X] \dots K+(2i-1)X \quad \text{(VII.29)}$$

each term of this sum contains a factor identical to  $\delta$  except that the  $K+(2j-1)X$  sub-factor is missing. Thus  $v$  is a polynomial of degree  $i-1$  and the coefficient of highest power in  $X$  is

$$\left(\frac{2i-1}{\pi}\right)^2 \sum_{j=1}^i \frac{1}{(2j-1)^2} \quad \text{(VII.30)}$$

These considerations are necessary for the deduction of the general conditions imposed on the phase diagram by the existence of physical solutions and for exact evaluation of the critical lamellar spacing.

We can now write eq. VII.25 as

$$\left(\frac{\phi}{S} + 1\right) \delta = C' X v \quad \text{(VII.31)}$$

and follow a line of reasoning analogous to the one used in Appendix V. We call the left hand function  $y_1$  and the right hand function  $y_2$ . The function  $y_1$  depends upon  $S$  but its roots are all negative as we have

already seen. By a recurrence argument one can demonstrate that the function  $y_2$  also has all negative roots and passes through the origin. Both functions are of the same degree and can only have zero or one intersection for positive  $X$ . As in Appendix V, to make sure that we have a positive intersection, we set  $S$  equal to infinity in eq. VII.31 to give

$$\delta = C' X \nu \quad (\text{VII.32})$$

This equation can be written in the form of a polynomial of degree  $i$ , the roots of which give the intersections of  $y_1(S=\infty)$  and  $y_2$ . Since as we have seen above the coefficient of the zeroth power in  $X$  is always positive, the sign of the product of the roots is given by the sign of the coefficient of the highest power in  $X$ . From eqs. VII.28, VII.30 and VII.32 this coefficient is given explicitly by

$$\left(\frac{2i-1}{\pi}\right)^2 \left[1 - C' \sum_{j=1}^i \frac{1}{(2j-1)^2}\right] \quad (\text{VII.33})$$

To assure a positive intersection we need to have

$$(-1)^i \left[1 - C' \sum_{j=1}^i \frac{1}{(2j-1)^2}\right] \begin{cases} < 0 \text{ when } i \text{ is even} \\ < 0 \text{ when } i \text{ is odd} \end{cases} \quad (\text{VII.34})$$

or, more generally

$$1 - C' \sum_{j=1}^i \frac{1}{(2j-1)^2} < 0 \quad (\text{VII.35})$$

and, finally

$$C' > \frac{1}{\sum_{j=1}^i \frac{1}{(2j-1)^2}} \quad (\text{VII.36})$$

If we now let  $i$  go to infinity we have

$$C' > \frac{1}{\sum_{j=1}^{\infty} \frac{1}{(2j-1)^2}} = \frac{8}{\pi^2} \quad (\text{VII.37})$$

When this condition is satisfied a positive critical lamellar spacing exists and we can determine it. Indeed it is that spacing for which eq. VII.31 has a root at infinity. We therefore equate to zero the coefficient of the highest power of  $X$  in eq. VII.31. This gives

$$\frac{\phi}{S_c} + 1 - C' \sum_{j=1}^i \frac{1}{(2j-1)^2} = 0 \quad (\text{VII.38})$$

and finally

$$S_c = \frac{\phi}{C' \sum_{j=1}^i \frac{1}{(2j-1)^2} - 1} \quad (\text{VII.39})$$

Now when we again let  $i$  go to infinity, we obtain

$$S_c = \frac{\phi}{C' \frac{\pi^2}{8} - 1} \quad (\text{VII.40})$$

It is gratifying to note that the value of  $S_c$  obtained rigorously here is identical to the one obtained in eq. VII.24a, a fact which verifies the precision of eq. VII.23.

Inequality VII.37 represents a condition on the phase diagram and the experimental conditions to assure a physical solution. To understand its meaning with respect to the phase diagram we again simplify our notation and call

$$x = \frac{x_{10}^{\alpha\gamma}}{x_{10}^{\alpha\gamma}} \quad \text{and} \quad y = \frac{x_{10}^{\gamma\alpha}}{x_{10}^{\gamma\alpha}} \quad (\text{VII.41})$$

(not to be confused with the geometrical coordinates)

From eq. II.2 we then have

$$x = \frac{\frac{x_{10}^{\gamma\alpha}}{x_{10}^{\alpha\gamma}} \frac{x_{20}^{\alpha\gamma}}{x_{20}^{\gamma\alpha}}}{\frac{x_{10}^{\alpha\gamma}}{x_{10}^{\alpha\gamma}} \frac{x_{20}^{\gamma\alpha}}{x_{20}^{\gamma\alpha}}} = \frac{y(1-x)}{x(1-y)} \quad (\text{VII.42})$$

and from eq. 2.92 we have

$$K = \frac{\frac{x_{20}^{\alpha\gamma}}{x_{10}^{\alpha\gamma}} + x \frac{x_{10}^{\alpha\gamma}}{x_{10}^{\alpha\gamma}}}{\frac{x_{10}^{\gamma\alpha}}{x_{10}^{\gamma\alpha}} + x \frac{x_{20}^{\gamma\alpha}}{x_{20}^{\gamma\alpha}}} = \frac{1 - x + \frac{y(1-x)}{x(1-y)}x}{y + \frac{y(1-x)}{x(1-y)}(1-y)} \quad (\text{VII.43})$$

$$K = \frac{x(1-x)}{y(1-y)} \quad (\text{VII.44})$$

and from eq. VII.10 we have for  $C'$

$$C' = \frac{4}{\pi^2} \frac{K (C_{10}^{\gamma\alpha} - C_{10}^{\gamma\beta}) + (C_{10}^{\beta\gamma} - C_{10}^{\alpha\gamma})}{C_{10}^{\beta\gamma} - C_{\infty}} \quad (\text{VII.45})$$

or

$$C' = \frac{4}{\pi^2} \frac{\frac{x(1-x)}{y(1-y)} (y-1+y) + (1-x-x)}{1-x-0.5} \quad (\text{VII.46})$$

and, finally

$$C' = \frac{8}{\pi^2} \left[ 1 - \frac{x(1-x)(1-2y)}{y(1-y)(1-2x)} \right] \quad (\text{VII.47})$$

The condition expressed by eq. VII.37 is then written in this notation as

$$\frac{8}{\pi^2} \left[ 1 - \frac{x(1-x)(1-2y)}{y(1-y)(1-2x)} \right] > \frac{8}{\pi^2} \quad (\text{VII.48})$$

or

$$\frac{x(1-x)(1-2y)}{y(1-y)(1-2x)} < 0 \quad (\text{VII.49})$$

Since in all our physical cases  $x$ ,  $y$ ,  $1-x$  and  $1-y$  are positive quantities, this reduces to

$$(1-2x)(1-2y) < 0 \quad (\text{VII.50})$$

Since for the symmetric case in the zone of low undercooling  $y > 0.5$  and  $x < 0.5$ , this condition is always satisfied.



We will now express the critical lamellar spacing as a function of  $x$  and  $y$ . We need first to know the expression for  $\phi$ . From eq. 2.16 and VII.10 we have

$$k^\alpha = x^\alpha - 1 = \frac{y(1-x)}{x(1-y)} - 1 \quad (\text{VII.51})$$

$$k^\alpha = \frac{y-x}{x(1-y)} \quad (\text{VII.52})$$

and

$$\phi = -\frac{8}{RT} \sigma^\alpha \cos \phi^\alpha \frac{y(1-y)^2}{(y-x)(1-2x)} \quad (\text{VII.53})$$

Then from eq. VII.40 we obtain

$$S_c = \frac{8}{RT} \sigma^\alpha \cos \phi^\alpha \frac{x(1-y)y(1-y)(1-2x)}{(y-x)(1-2x)x(1-x)(1-2y)} \quad (\text{VII.54})$$

or

$$S_c = -\frac{8}{RT} \sigma^\alpha \cos \phi^\alpha \frac{y(1-y)^2}{(1-x)(y-x)(2y-1)} \quad (\text{VII.55})$$

We finally calculate the coefficient  $\Omega'$  as a function of  $x$  and  $y$ . From eq. VII.24c we have

$$\Omega' = 2\pi D \frac{\frac{x(1-x)}{y(1-y)} \frac{2y-1}{1-2x}}{\frac{x(1-x)}{y(1-y)} \left\{ 1 - 0.1819 \frac{8}{\pi^2} \left[ 1 - \frac{x(1-x)(2y-1)}{y(1-y)(1-2x)} \right] \right\}} \quad (\text{VII.56})$$

or

$$\Omega' = \frac{2\pi D}{0.8526} \frac{2y - 1}{1 - 2x} \frac{1}{1 - 0.2133 \frac{x(1 - x)(2y - 1)}{y(1 - y)(1 - 2x)}} \quad (\text{VII.57})$$

## APPENDIX VIII

### COMPARISON BETWEEN OUR $v(S)$ RELATION AND HILLERT'S RELATION FOR A SYMMETRIC CONFIGURATION

We will compare the critical lamellar spacing  $S_c^H$  given by a Hillert type calculation to  $S_c$  given by our second thermodynamic version for binary systems. The Gibbs-Thomson equation used by Hillert is expressed in terms of concentrations in the austenite  $\gamma$  phase and its coefficient is given specifically for the Fe-C binary system. To make a fair comparison with our result it is necessary to use in his theory the same Gibbs-Thomson equation written for the concentration in the parent phase as is implied by our thermodynamic analysis. In this case the Gibbs-Thomson equation referred to the  $\gamma$  phase is given by eq. II.10 and yields

$$P = RT \left( \frac{C_{10}^{\gamma\alpha}}{\frac{x^\alpha}{x^\alpha - 1} - C_{10}^{\gamma\alpha}} - \frac{C_1^{\gamma\alpha}}{\frac{x^\alpha}{x^\alpha - 1} - C_1^{\gamma\alpha}} \right) \quad (\text{VIII.1})$$

which is non-linear. We can however obtain a linear expression by taking a Taylor expansion to the first order. The first derivative of  $P$  with respect to  $C_1^{\gamma\alpha}$  is given by

$$\frac{dP}{dC_1^{\gamma\alpha}} = - RT \frac{\frac{x^\alpha}{x^\alpha - 1}}{\left(\frac{x^\alpha}{x^\alpha - 1} - C_1^{\gamma\alpha}\right)^2} \quad (\text{VIII.2})$$

and the coefficient  $H_\alpha$  of eq. 2.35 is equal to this derivative when  $C_1^{\gamma\alpha}$  is equal to  $C_{10}^{\gamma\alpha}$ . Thus we obtain

$$P = H_\alpha (C_1^{\gamma\alpha} - C_{10}^{\gamma\alpha}) \quad (\text{VIII.3})$$

where

$$H_\alpha = \left[ \frac{dP}{dC_1^{\gamma\alpha}} \right]_{C_{10}^{\gamma\alpha}} \quad (\text{VIII.4})$$

or

$$H_\alpha = \frac{\frac{x^\alpha}{x^\alpha - 1}}{\left(\frac{x^\alpha}{x^\alpha - 1} - C_{10}^{\gamma\alpha}\right)^2} \quad (\text{VIII.5})$$

The variations of the pressure with the concentrations according to the Gibbs-Thomson equation VIII.3 are illustrated in Fig. 29. It is represented by the tangent to the hyperbola at the point  $C_{10}^{\gamma\alpha}$  where the pressure is equal to zero. We have shown in Appendix II that for the symmetrical configuration, the effect of pressure on the composition in

the parent phase is the same with respect to both the  $\alpha$  and  $\beta$  phases. Therefore, the two hyperbolae of Fig. 29 are symmetrical and the slopes at the point  $x_{10}^{\gamma\alpha}$  and  $x_{10}^{\gamma\beta}$  are equal and opposite. In other words

$$H_{\alpha} = - H_{\beta} \quad (\text{VIII.6})$$

Since we have maintained that Hillert's calculations are strictly valid only in the symmetrical configuration (p. 28) we make the comparison in this particular case. We again adopt the convention expressed by eq. 2.67 and obtain

$$x^{\alpha} = \frac{y(1-x)}{x(1-y)} \quad (\text{VIII.7})$$

and

$$\frac{x^{\alpha}}{1-x^{\alpha}} = \frac{y(1-x)}{y-x} \quad (\text{VIII.8})$$

We substitute these in the expression VIII.5 for  $H_{\alpha}$  and get

$$H_{\alpha} = \frac{(1-x)(y-x)}{y(1-y)^2} \quad (\text{VIII.9})$$

From eq. 2.43 we therefore obtain in the symmetrical configuration

$$S_c^H = - \frac{\sigma^\alpha \cos \phi^\alpha}{RT} \frac{8}{C_o^{\gamma\alpha} - C_o^{\alpha}} \frac{1}{H_\alpha} \quad (\text{VIII.10})$$

or

$$S_c^H = - \frac{8 \sigma^\alpha \cos \phi^\alpha}{RT} \frac{y (1 - y)^2}{(2y - 1) (1 - x) (y - x)} \quad (\text{VIII.11})$$

This expression is to be compared with our expression 2.102. We note the identity of the two critical lamellar spacings in the very particular case of the symmetrical configuration. It can thus be concluded that the inclusion of the effect of solute segregation in the product phases ( $\phi \neq 0$ ) does not change the value of the critical lamellar spacing.

In eq. 2.44 we have the relation between  $v$  and  $S$  as deduced via Hillert's calculation. For comparison we shall calculate the expression for the coefficient  $\Omega$  as a function of  $x$  and  $y$ . From eq. 2.42 we get

$$\Omega = \frac{\pi^3 D}{4} \frac{1}{\sum_{i=1}^{\infty} \frac{1}{(2i-1)^3}} \frac{2y-1}{1-2x} \quad (\text{VIII.12})$$

or, with eq. VII.19

$$\Omega = \frac{\pi^3 D}{4.2072} \frac{2y-1}{1-2x} \quad (\text{VIII.13})$$

Taking the ratio of the two coefficients  $\Omega$  and  $\Omega'$ , with eq. VII.57 we obtain

$$\frac{\Omega'}{\Omega} = \frac{1}{1 - 0.2133 \frac{x(1-x)(2y-1)}{y(1-y)(1-2x)}} \quad (\text{VIII.14})$$

Note that when the solubility  $x$  is very small ( $\phi$  is also very small) the two coefficients are equal.

## APPENDIX IX

### INTEGRATION OF THE GIBBS-DUHEM EQUATION FOR A TERNARY DILUTE SOLUTION WITH THE FIRST THERMODYNAMIC VERSION

With the same assumptions made in Appendices I and II concerning the effect of pressure on the precipitate phases, we can write the ternary Gibbs-Duhem equation:

$$x_1^{Y\alpha} d \ln a_1 + x_2^{Y\alpha} d \ln a_2 + x_3^{Y\alpha} d \ln a_3 = 0 \quad (\text{IX.1a})$$

$$x_1^{\alpha Y} d \ln a_1 + x_2^{\alpha Y} d \ln a_2 + x_3^{\alpha Y} d \ln a_3 = \frac{V^\alpha}{RT} d P \quad (\text{IX.1b})$$

In the present notation component 3 is the solvent so that elements 1 and 2 are dilute in the precipitate phase  $\alpha$ . We can eliminate  $d \ln a_3$  between the two equations of system IX.1 to give

$$\left(x_1^{\alpha Y} - x_1^{Y\alpha} \frac{x_3^{\alpha Y}}{x_3^{Y\alpha}}\right) d \ln a_1 + \left(x_2^{\alpha Y} - x_2^{Y\alpha} \frac{x_3^{\alpha Y}}{x_3^{Y\alpha}}\right) d \ln a_2 = \frac{V^\alpha}{RT} d P \quad (\text{IX.2})$$

If we take the Henrian solution approximation for components 1 and 2

$$d \ln a_1 = d \ln x_1^{\alpha Y} \quad d \ln a_2 = d \ln x_2^{\alpha Y} \quad (\text{IX.3})$$



we obtain

$$\left(1 - \frac{x_1^{\gamma\alpha}}{x_1^{\alpha\gamma}} \frac{x_3^{\alpha\gamma}}{x_3^{\gamma\alpha}}\right) d x_1^{\alpha\gamma} + \left(1 - \frac{x_2^{\gamma\alpha}}{x_2^{\alpha\gamma}} \frac{x_3^{\alpha\gamma}}{x_3^{\gamma\alpha}}\right) d x_2^{\alpha\gamma} = \frac{V^\alpha}{RT} d P \quad (\text{IX.4})$$

The same can be carried out for the phases  $\gamma$  and  $\beta$  where element 2 is the solvent and element 1 and 3 are dilute in the precipitate  $\beta$  phase. Thus

$$\left(1 - \frac{x_1^{\gamma\beta}}{x_1^{\beta\gamma}} \frac{x_3^{\beta\gamma}}{x_3^{\gamma\beta}}\right) d x_1^{\beta\gamma} + \left(1 - \frac{x_2^{\gamma\beta}}{x_2^{\beta\gamma}} \frac{x_3^{\beta\gamma}}{x_3^{\gamma\beta}}\right) d x_2^{\beta\gamma} = \frac{V^\beta}{RT} d P \quad (\text{IX.5})$$

Eq. IX.5 can be written entirely in terms of differentials of elements 1 and 2 by the substitution

$$d x_3^{\beta\gamma} = - d x_1^{\beta\gamma} - d x_2^{\beta\gamma} \quad (\text{IX.6})$$

and we obtain

$$\frac{x_2^{\beta\gamma}}{x_2^{\gamma\beta}} \left(\frac{x_3^{\gamma\beta}}{x_3^{\beta\gamma}} - \frac{x_1^{\gamma\beta}}{x_1^{\beta\gamma}}\right) d x_1^{\beta\gamma} - \left(1 - \frac{x_3^{\gamma\beta}}{x_3^{\beta\gamma}} \frac{x_2^{\beta\gamma}}{x_2^{\gamma\beta}}\right) d x_2^{\beta\gamma} = \frac{V^\beta}{RT} d P \quad (\text{IX.7})$$

Eqs. IX.4 and IX.7 could be integrated if we had thermodynamic information about the compositions of the two phases in equilibrium. In analogy with the binary case, and as an introduction to the methodology, we first suggest that the extremities of the tie lines be related by the ratios

$$\frac{x_1^{\alpha\gamma}}{x_1^{\gamma\alpha}} = K_1^\alpha \quad \frac{x_2^{\alpha\gamma}}{x_2^{\gamma\alpha}} = K_2^\alpha \quad \frac{x_3^{\alpha\gamma}}{x_3^{\gamma\alpha}} = K_3^\alpha \quad (\text{IX.8a,b,c})$$

$$\frac{x_1^{\beta\gamma}}{x_1^{\gamma\beta}} = K_1^\beta \quad \frac{x_2^{\beta\gamma}}{x_2^{\gamma\beta}} = K_2^\beta \quad \frac{x_3^{\beta\gamma}}{x_3^{\gamma\beta}} = K_3^\beta \quad (\text{IX.8d,e,f})$$

All members of this system of equations cannot be satisfied in the general case. Indeed, if we consider that the equilibrium between the phases  $\alpha$  and  $\gamma$  and the expressions containing the ratios  $K_1^\alpha$  and  $K_2^\alpha$  are satisfied then the expressions containing  $K_3^\alpha$  cannot be true. However, the ratio  $K_3^\alpha$  is superfluous when  $x_3^{\alpha\gamma}$  and  $x_3^{\gamma\alpha}$  are both constant, i.e., when the phase boundaries for both the  $\alpha\gamma$  and  $\beta\gamma$  equilibria are parallel to the opposite side of the ternary triangle as shown on Fig. 8. This restriction can be somewhat relaxed because we always consider dilute solutions for the  $\alpha$  phase which has  $x_3^{\alpha\gamma} = 1$  and in many cases the boundary for the  $\gamma$  phase is not very different from parallel to one side of the phase diagram triangle.

Under these restrictions we can integrate eq. IX.4 to give

$$\left(1 - \frac{K_3^\alpha}{K_1^\alpha}\right) (x_1^{\alpha\gamma} - x_{10}^{\alpha\gamma}) + \left(1 - \frac{K_3^\alpha}{K_2^\alpha}\right) (x_2^{\alpha\gamma} - x_{20}^{\alpha\gamma}) = \frac{V^\alpha}{RT} P \quad (\text{IX.9})$$

and the condition of parallelism is expressed by

$$1 - \frac{K_3^\alpha}{K_1^\alpha} = 1 - \frac{K_3^\alpha}{K_2^\alpha} \quad \text{or} \quad K_1^\alpha = K_2^\alpha \quad (\text{IX.10})$$

Similarly, for eq. IX.7, the condition of parallelism is expressed by

$$K_1^\beta = K_3^\beta \quad (\text{IX.11})$$

and we obtain finally

$$h^\alpha (x_1^{\alpha\gamma} + x_2^{\alpha\gamma} - x_{10}^{\alpha\gamma} - x_{20}^{\alpha\gamma}) = \frac{V^\alpha}{RT} P \quad (\text{IX.12a})$$

and

$$h^\beta (x_2^{\beta\gamma} - x_{20}^{\beta\gamma}) = \frac{V^\beta}{RT} P \quad (\text{IX.12b})$$

with

$$h^\alpha = 1 - \frac{K_3^\alpha}{K_1^\alpha} = 1 - \frac{K_3^\alpha}{K_2^\alpha} \quad (\text{IX.13a})$$

and

$$h^\beta = - \left( 1 - \frac{K_2^\beta}{K_3^\beta} \right) \quad (\text{IX.13b})$$

Note that in the symmetric case where we require that  $K_1^\alpha = K_1^\beta$ , we have the further equalities (Fig. 10)

$$K_2^\alpha = K_3^\beta = K_1^\alpha = K_1^\beta \quad (\text{IX.14a})$$

and

$$K_2^\beta = K_3^\alpha \quad (\text{IX.14b})$$

We then obtain

$$h^{\alpha} = - h^{\beta} \quad (\text{IX.15})$$

The pressure has the same effect on the phase boundaries for the phase  $\alpha$  and  $\beta$  with respect to the phase  $\gamma$ . In terms of concentrations we can write eq. IX.12 alternatively as

$$P = RT h^{\alpha} (C_1^{\alpha\gamma} + C_2^{\alpha\gamma} - C_{10}^{\alpha\gamma} - C_{20}^{\alpha\gamma}) \quad (\text{IX.16a})$$

$$P = RT h^{\beta} (C_2^{\beta\gamma} - C_{20}^{\beta\gamma}) \quad (\text{IX.16b})$$

In the symmetrical case the system IX.16 can be written in terms of the concentrations in the parent phase  $\gamma$  as

$$P = RT H^{\alpha} (C_1^{\gamma\alpha} + C_2^{\gamma\alpha} - C_{10}^{\gamma\alpha} - C_{20}^{\gamma\alpha}) \quad (\text{IX.17a})$$

$$P = RT H^{\beta} (C_2^{\gamma\beta} - C_{20}^{\gamma\beta}) \quad (\text{IX.17b})$$

with

$$H^{\alpha} = h^{\alpha} K_1^{\alpha} \quad (\text{IX.18a})$$

$$H^{\beta} = h^{\beta} K_2^{\beta} \quad (\text{IX.18b})$$

Here, as in the binary case, the pressure does not have the same influence on the  $\gamma$  phase boundary in relation to the  $\alpha$  and  $\beta$  phases. This corresponds to a rather skew  $\gamma$  phase free energy surface (cf. Fig. 27).

## APPENDIX X

### INTEGRATION OF THE GIBBS-DUHEM EQUATIONS FOR A TERNARY DILUTE SOLUTION WITH THE SECOND THERMODYNAMIC VERSION

With the same assumptions as in the Appendix IX we have the  
eqs. IX.4 and IX.5

$$\left(1 - \frac{x_1^{\gamma\alpha} x_3^{\alpha\gamma}}{x_1^{\alpha\gamma} x_3^{\gamma\alpha}}\right) dx_1^{\alpha\gamma} + \left(1 + \frac{x_2^{\gamma\alpha} x_3^{\alpha\gamma}}{x_2^{\alpha\gamma} x_3^{\gamma\alpha}}\right) dx_2^{\alpha\gamma} = \frac{V^\alpha}{RT} dP \quad (X.1)$$

$$\left(1 - \frac{x_1^{\gamma\beta} x_2^{\beta\gamma}}{x_1^{\beta\gamma} x_2^{\gamma\beta}}\right) dx_1^{\beta\gamma} + \left(1 + \frac{x_3^{\gamma\beta} x_2^{\beta\gamma}}{x_3^{\beta\gamma} x_2^{\gamma\beta}}\right) dx_2^{\beta\gamma} = \frac{V^\beta}{RT} dP \quad (X.2)$$

This time the relations which we take between the compositions of  
the parent  $\gamma$  phase and the precipitate  $\alpha$  and  $\beta$  phases are

$$\frac{x_1^{\gamma\alpha} x_3^{\alpha\gamma}}{x_1^{\alpha\gamma} x_3^{\gamma\alpha}} = x_1^\alpha \qquad \frac{x_2^{\gamma\alpha} x_3^{\alpha\gamma}}{x_2^{\alpha\gamma} x_3^{\gamma\alpha}} = x_2^\alpha$$

(over)

(X.3)

$$\frac{x_1^{\gamma\beta}}{x_1^{\beta\gamma}} \frac{x_2^{\beta\gamma}}{x_2^{\gamma\beta}} = x_1^\beta \qquad \frac{x_2^{\beta\gamma}}{x_2^{\gamma\beta}} \frac{x_3^{\gamma\beta}}{x_3^{\beta\gamma}} = x_2^\beta$$

where the  $x$ 's are assumed to be independent of the pressure. Under such conditions the integration of eqs. X.1 and X.2 are trivial, viz.,

$$k_1^\alpha (x_1^{\alpha\gamma} - x_{10}^{\alpha\gamma}) + k_2^\alpha (x_2^{\alpha\gamma} - x_{20}^{\alpha\gamma}) = \frac{V^\alpha}{RT} P \quad (X.4)$$

$$k_1^\beta (x_1^{\beta\gamma} - x_{10}^{\beta\gamma}) + k_3^\beta (x_3^{\beta\gamma} - x_{30}^{\beta\gamma}) = \frac{V^\beta}{RT} P \quad (X.5)$$

or, in terms of concentrations,

$$P = RT [k_1^\alpha (C_1^{\alpha\gamma} - C_{10}^{\alpha\gamma}) + k_2^\alpha (C_2^{\alpha\gamma} - C_{20}^{\alpha\gamma})] \quad (X.6)$$

$$P = RT [(k_1^\beta - k_3^\beta)(C_1^{\beta\gamma} - C_{10}^{\beta\gamma}) - k_3^\beta (C_2^{\beta\gamma} - C_{20}^{\beta\gamma})] \quad (X.7)$$

where

$$\begin{aligned} k_1^\alpha &= 1 - x_1^\alpha & k_2^\alpha &= 1 - x_2^\alpha \\ k_1^\beta &= 1 - x_1^\beta & k_3^\beta &= 1 - x_3^\beta \end{aligned} \quad (X.8)$$

From eqs. X.4 and X.5 we can readily see the possibility of a

symmetrical influence of the pressure since in the symmetrical situation (Fig. 11)

$$x_1^\alpha = x_1^\beta \quad \text{and} \quad x_2^\alpha = x_3^\beta \quad (\text{X.9})$$

In the same way as in the binary case it can be shown that the  $\gamma$  phase boundaries are symmetrically influenced by the pressure. To obtain the relation for  $x_1^{\alpha\gamma}$  as a function of  $x_1^{\gamma\alpha}$  and  $x_2^{\gamma\alpha}$ , and similarly for  $x_2^{\alpha\gamma}$ , it is necessary to solve the system X.3 to give

$$\frac{x_1^{\gamma\alpha}}{x_1^{\alpha\gamma}} = x_1^\alpha \frac{x_3^{\gamma\alpha}}{x_3^{\alpha\gamma}} \quad (\text{X.10})$$

$$\frac{x_1^{\gamma\alpha}}{x_1^{\alpha\gamma}} = \frac{x_1^\alpha x_2^{\gamma\alpha}}{x_2^\alpha x_2^{\alpha\gamma}}$$

which gives in turn

$$x_1^{\alpha\gamma} = \frac{x_1^{\gamma\alpha}}{x_1^{\gamma\alpha} + \frac{x_1^\alpha}{x_2^\alpha} x_2^{\gamma\alpha} + x_1^\alpha x_3^{\gamma\alpha}} \quad (\text{X.11})$$

$$x_2^{\alpha\gamma} = \frac{x_2^{\gamma\alpha}}{x_1^{\gamma\alpha} + \frac{x_1^\alpha}{x_2^\alpha} x_2^{\gamma\alpha} + x_1^\alpha x_3^{\gamma\alpha}} \frac{x_1^\alpha}{x_2^\alpha}$$

We can now substitute these in eq. X.4 to give

$$\frac{k_1^\alpha x_1^{\gamma\alpha} + k_2^\alpha \frac{x_1^\alpha}{x_2^\alpha} x_2^{\gamma\alpha}}{x_1^{\gamma\alpha} + \frac{x_1^\alpha}{x_2^\alpha} x_2^{\gamma\alpha} + x_1^\alpha x_3^{\gamma\alpha}} - \frac{k_1^\alpha x_{10}^{\gamma\alpha} + k_2^\alpha \frac{x_1^\alpha}{x_2^\alpha} x_{20}^{\gamma\alpha}}{x_{10}^{\gamma\alpha} + \frac{x_1^\alpha}{x_2^\alpha} x_{20}^{\gamma\alpha} + x_1^\alpha x_{30}^{\gamma\alpha}} = \frac{V^\alpha}{RT} P \quad (X.12)$$

The same calculation can be carried out with eqs. X.3 and X.5 to yield

$$\frac{k_1^\beta x_1^{\gamma\beta} + k_3^\beta \frac{x_1^\beta}{x_3^\beta} x_3^{\gamma\beta}}{x_1^{\gamma\beta} + \frac{x_1^\beta}{x_3^\beta} x_3^{\gamma\beta} + x_1^\beta x_2^{\gamma\beta}} - \frac{k_1^\beta x_{10}^{\gamma\beta} + k_3^\beta \frac{x_1^\beta}{x_3^\beta} x_{30}^{\gamma\beta}}{x_{10}^{\gamma\beta} + \frac{x_1^\beta}{x_3^\beta} x_{30}^{\gamma\beta} + x_1^\beta x_{20}^{\gamma\beta}} = \frac{V^\beta}{RT} P \quad (X.13)$$

Now it can be seen from eqs. X.12 and X.13 that keeping  $x_1^{\gamma\alpha}$  and  $x_1^{\gamma\beta}$  identical for the symmetric case, the pressure will influence  $x_2^{\gamma\alpha}$  and  $x_3^{\gamma\beta}$  in the same way. Therefore the boundaries for the  $\gamma$  phase in equilibrium with the  $\alpha$  or  $\beta$  phases will be displaced the same amount when the pressure changes.

In Fig. 9 we show a non-symmetric ternary isotherm which is included within the present approximation. We have included the tie lines for completeness. This demonstrates the rather considerable generality of the approximation.



## APPENDIX XI

### CALCULATION OF THE FOURIER SERIES COEFFICIENTS FOR TERNARY SOLUTIONS UNDER THE SECOND THERMODYNAMIC VERSION

The Fourier expansion coefficients for the concentrations are calculated according to the thermodynamic requirement of equilibrium between all phases. We assume that this requirement is properly expressed by the complex ratios introduced in Appendix X and by the ratios X.3. Typically, such ratios can be written in the form

$$\frac{C_1^{Y\alpha}}{C_1^{\alpha Y}} \frac{C_2^{\alpha Y}}{C_2^{Y\alpha}} = x \quad (\text{XI.1})$$

In the process of linearization of these equations we will express all variations as

$$\frac{(C_{10}^{Y\alpha} + \Delta C_1^{Y\alpha})(C_{20}^{\alpha Y} + \Delta C_2^{\alpha Y})}{(C_{10}^{\alpha Y} + \Delta C_1^{\alpha Y})(C_{20}^{Y\alpha} + \Delta C_2^{Y\alpha})} = x \quad (\text{XI.2})$$

Developing the product and neglecting all  $(\Delta C)^2$  we obtain

$$\frac{C_{10}^{Y\alpha} C_{20}^{\alpha Y} + C_{20}^{\alpha Y} \Delta C_1^{Y\alpha} + C_{10}^{Y\alpha} \Delta C_2^{\alpha Y}}{C_{10}^{\alpha Y} C_{20}^{Y\alpha} + C_{20}^{Y\alpha} \Delta C_1^{\alpha Y} + C_{10}^{\alpha Y} \Delta C_2^{Y\alpha}} = x = \frac{C_{10}^{Y\alpha} C_{20}^{\alpha Y}}{C_{10}^{\alpha Y} C_{20}^{Y\alpha}} \quad (\text{XI.3})$$

As indicated in the right hand side, the reference state designated by the index 0 must itself satisfy the condition imposed by the ratio.

Thus we can rearrange eq. XI.3 to obtain

$$\frac{C_{20}^{\alpha\gamma} \Delta C_1^{\gamma\alpha} + C_{10}^{\gamma\alpha} \Delta C_2^{\alpha\gamma}}{C_{20}^{\gamma\alpha} \Delta C_1^{\alpha\gamma} + C_{10}^{\alpha\gamma} \Delta C_2^{\gamma\alpha}} = \chi = \frac{C_{10}^{\gamma\alpha} C_{20}^{\alpha\gamma}}{C_{10}^{\alpha\gamma} C_{20}^{\gamma\alpha}} \quad (\text{XI.4})$$

If now we divide the first fraction by the last one, we have

$$\frac{\frac{C_1^{\gamma\alpha}}{C_{10}^{\gamma\alpha}} + \frac{\Delta C_2^{\alpha\gamma}}{C_{20}^{\alpha\gamma}}}{\frac{\Delta C_1^{\alpha\gamma}}{C_{10}^{\alpha\gamma}} + \frac{\Delta C_2^{\gamma\alpha}}{C_{20}^{\gamma\alpha}}} = 1 \quad (\text{XI.5})$$

which leads to

$$\frac{\Delta C_1^{\gamma\alpha}}{C_{10}^{\gamma\alpha}} + \frac{\Delta C_2^{\alpha\gamma}}{C_{20}^{\alpha\gamma}} = \frac{\Delta C_1^{\alpha\gamma}}{C_{10}^{\alpha\gamma}} + \frac{\Delta C_2^{\gamma\alpha}}{C_{20}^{\gamma\alpha}} \quad (\text{XI.6})$$

or grouping the concentrations of the same phase:

$$\frac{\Delta C_1^{\alpha\gamma}}{C_{10}^{\alpha\gamma}} - \frac{\Delta C_2^{\alpha\gamma}}{C_{20}^{\alpha\gamma}} = \frac{\Delta C_1^{\gamma\alpha}}{C_{10}^{\gamma\alpha}} - \frac{\Delta C_2^{\gamma\alpha}}{C_{20}^{\gamma\alpha}} \quad (\text{XI.7})$$

This expression is quite general, whatever is the ratio  $\chi$ . The information given by the number  $\chi$  is also contained in the values of the concentrations at the reference state. Therefore, from the four equations of X.3 written as

$$\begin{aligned}
 \frac{C_1^{\gamma\alpha}}{C_1^{\alpha\gamma}} - \frac{C_3^{\alpha\gamma}}{C_3^{\gamma\alpha}} &= x_1^\alpha & \frac{C_2^{\gamma\alpha}}{C_2^{\alpha\gamma}} - \frac{C_3^{\alpha\gamma}}{C_3^{\gamma\alpha}} &= x_2^\alpha \\
 \frac{C_1^{\gamma\beta}}{C_1^{\beta\gamma}} - \frac{C_2^{\beta\gamma}}{C_2^{\gamma\beta}} &= x_1^\beta & \frac{C_2^{\beta\gamma}}{C_2^{\gamma\beta}} - \frac{C_3^{\gamma\beta}}{C_3^{\beta\gamma}} &= x_2^\beta
 \end{aligned}
 \tag{XI.8}$$

we can deduce the four linearized equations

$$\begin{aligned}
 \frac{C_1^{\alpha\gamma}}{C_{10}^{\alpha\gamma}} - \frac{C_2^{\alpha\gamma}}{C_{20}^{\alpha\gamma}} &= \frac{C_1^{\gamma\alpha}}{C_{10}^{\gamma\alpha}} - \frac{C_2^{\gamma\alpha}}{C_{20}^{\gamma\alpha}} & \frac{C_1^{\alpha\gamma}}{C_{10}^{\alpha\gamma}} - \frac{C_3^{\alpha\gamma}}{C_{30}^{\alpha\gamma}} &= \frac{C_1^{\gamma\alpha}}{C_{10}^{\gamma\alpha}} - \frac{C_3^{\gamma\alpha}}{C_{30}^{\gamma\alpha}} \\
 \frac{C_1^{\beta\gamma}}{C_{10}^{\beta\gamma}} - \frac{C_2^{\beta\gamma}}{C_{20}^{\beta\gamma}} &= \frac{C_1^{\gamma\beta}}{C_{10}^{\gamma\beta}} - \frac{C_2^{\gamma\beta}}{C_{20}^{\gamma\beta}} & \frac{C_1^{\beta\gamma}}{C_{10}^{\beta\gamma}} - \frac{C_3^{\beta\gamma}}{C_{30}^{\beta\gamma}} &= \frac{C_1^{\gamma\beta}}{C_{10}^{\gamma\beta}} - \frac{C_3^{\gamma\beta}}{C_{30}^{\gamma\beta}}
 \end{aligned}
 \tag{XI.9}$$

The Fourier coefficients can be calculated as usual by the analysis of step functions. If we write these four equations in the general form

$$\begin{aligned}
 \frac{C_{1p}}{C_{1po}} - \frac{C_{2p}}{C_{2po}} &= \frac{C_1}{C_{10}} - \frac{C_2}{C_{20}} \\
 \frac{C_{1p}}{C_{1po}} - \frac{1 - C_{1p} - C_{2p}}{C_{3po}} &= \frac{C_1}{C_{10}} - \frac{1 - C_1 - C_2}{C_{30}}
 \end{aligned}
 \tag{XI.10}$$

This is a convenient form since the factors  $1/C$  which multiply every term can be expressed simply as step functions with their coefficients taken from Appendix III.

As our only application of this approach we treat the case of a symmetrical configuration. In this situation the series for  $1/C_{10}$  and  $1/C_{1p0}$  reduce to constants.

We need first of all to define our reference state. In eq. 2.67 we assumed the convention for the binary case

$$(x_{20}^{\alpha\gamma})_{\text{binary}} = x \qquad (x_{20}^{\gamma\alpha})_{\text{binary}} = y \qquad (\text{XI.11})$$

(Note that since we have designated element 1 as the addition element we must modify our indices so that 1 is replaced by 2) Our knowledge of the ternary diagram (Fig. 11) in the symmetrical configuration is completed if we are given the value of  $x_1$ . Indeed in this case from eq. XI.8 and at the binary limit we have for  $x_2$

$$x_2 = \frac{y(1-x)}{x(1-y)} \qquad (\text{XI.12})$$

Since we know where the phase boundaries have to intersect the 2 - 3 binary diagram, to completely specify the reference state it is necessary only to know the value of  $C_{1\infty}$ . For the ternary reference state we adopt the notation

$$\begin{aligned} x_{10}^{\alpha\gamma} &= x_{1\infty} \\ x_{20}^{\alpha\gamma} &= x' \\ x_{30}^{\alpha\gamma} &= 1 - x_{1\infty} - x' \end{aligned} \qquad (\text{XI.13})$$

From these we can deduce the values for the reference concentrations in the  $\gamma$  phase if we call  $x_{20} = y'$ ,

$$x_2 = \frac{y(1-x)}{x(1-y)} = \frac{x_{20}^{\gamma\alpha} x_{20}^{\alpha\gamma}}{x_{20}^{\alpha\gamma} x_{30}^{\gamma\alpha}} = \frac{y'(1-x_{1\infty}-x')}{x' x_{30}^{\gamma\alpha}} \quad (\text{XI.14})$$

and hence

$$x_{30}^{\gamma\alpha} = \frac{x(1-y)}{y(1-x)} \frac{y'}{x'} (1-x_{1\infty}-x') \quad (\text{XI.15})$$

Similarly we have

$$\frac{x_{10}(1-x_{1\infty}-x')}{x_{1\infty} \frac{x}{y} \frac{(1-y)}{(1-x)} \frac{y'}{x'} (1-x_{1\infty}-x')} = x_1 \quad (\text{XI.16})$$

$$x_{10}^{\gamma\alpha} = x_1 x_{1\infty} \frac{x}{y} \frac{(1-y)}{(1-x)} \frac{y'}{x'} \quad (\text{XI.17})$$

The  $\alpha$  phase boundary for zero pressure has the equation X.6, viz.,

$$(x_1 - 1)(x_1^{\alpha\gamma} - x_{1\infty}) + \frac{y-x}{x(1-y)} (x_2^{\alpha\gamma} - x') = 0 \quad (\text{XI.18})$$

If we note that this line intersects the binary diagram at the point  $(x_{10}^{\alpha\gamma})_{\text{binary}} = x$  we obtain the value for  $x'$ , for a given  $x_{1\infty}$ , as

$$x' = x [1 - x_{1\infty}(x_1 - 1) \frac{(1-y)}{y-x}] \quad (\text{XI.19})$$

The value of  $y'$  as a function of  $x_{1\infty}$ ,  $x$  and  $y$  is obtained from

$$x_{10}^{\gamma\alpha} + x_{20}^{\gamma\alpha} + x_{30}^{\gamma\alpha} = 1 = x_1 x_{1\infty} \frac{x}{y} \frac{(1-y)}{(1-x)} \frac{y'}{x'} + y' + \frac{x}{y} \frac{(1-y)}{(1-x)} \frac{y'}{x'} (1 - x_{1\infty} - x') \quad (\text{XI.20})$$

and is given by

$$y' = y \left[ 1 - x_{1\infty} (x_1 - 1) \frac{1-y}{y-x} \right] \quad (\text{XI.21})$$

In summary, substituting eq. XI.19 into XI.13, the reference state is completely defined with the knowledge of the diagram ( $x_1$ ,  $x$  and  $y$ ) and the given value of  $x_{1\infty}$ .

In the following we shall only perform the calculations up to the first order in  $A_n$  and  $B_n$ . Furthermore from this point on we assume that in the symmetrical case the right hand side of eq. 3.109 is sufficiently close to zero that we are able to set  $S^\alpha$  equal to  $S^\beta$ . We have then

$$\frac{1}{c_{2p0}} = \begin{cases} \frac{1}{c_{20}^{\alpha\gamma}} \\ \frac{1}{c_{20}^{\beta\gamma}} \end{cases} = \lambda_1 + \mu_1 \cos b_1 y + \dots$$

$$\frac{1}{c_{20}} = \begin{cases} \frac{1}{c_{20}^{\gamma\alpha}} \\ \frac{1}{c_{20}^{\gamma\beta}} \end{cases} = \lambda_2 + \mu_2 \cos b_1 y \dots$$

(over)

$$\frac{1}{C_{30p}} = \begin{cases} \frac{1}{C_{30}^{\alpha\gamma}} \\ \frac{1}{C_{30}^{\beta\gamma}} \end{cases} = \lambda_1 - \mu_1 \cos b_1 y + \dots$$

(XI.22)

$$\frac{1}{C_{30}} = \begin{cases} \frac{1}{C_{30}^{\gamma\alpha}} \\ \frac{1}{C_{30}^{\gamma\beta}} \end{cases} = \lambda_2 - \mu_2 \cos b_1 y + \dots$$

The expansions for  $C_1$ ,  $C_2$ ,  $C_{1p}$  and  $C_{2p}$  are those given in eqs. 3.34 and 3.51. The first equation of XI.10 can be written as

$$\frac{C_{1p}}{C_{1\infty}} - \frac{C_1}{C_{10}^{\gamma\alpha}} = \frac{C_{2p}}{C_{2p0}} - \frac{C_2}{C_{20}} \quad (\text{XI.23})$$

and we have immediately the expression for the left hand side

$$\frac{C_{1p}}{C_{1\infty}} - \frac{C_1}{C_{10}^{\gamma\alpha}} = \left(1 - \frac{C_{1\infty}}{C_{10}^{\gamma\alpha}} - \frac{A_0}{C_{10}^{\gamma\alpha}}\right) - \left(\frac{1}{C_{1\infty}} \frac{D_{11}}{\nu} \frac{b_1^2}{\lambda_1^2} + \frac{1}{C_{10}^{\gamma\alpha}}\right) \cos b_1 y + \dots \quad (\text{XI.24})$$

By multiplication of the series we obtain

$$\frac{C_{2p}}{C_{2p0}} = \left[ \lambda_1 C_{2\infty} - \frac{1}{2\nu} (\tau D_{11} \frac{A_1 b_1^2}{\lambda_1^2} + D_{22} \frac{B_1 b_1^2}{\lambda_1^2}) \right] + \left[ \mu_1 C_{2\infty} - \frac{\lambda_1}{\nu} (\tau D_{11} \frac{A_1 b_1^2}{\lambda_1^2} + D_{22} \frac{B_1 b_1^2}{\lambda_1^2}) \right] \cos b_1 y + \dots \quad (\text{XI.25})$$

and

$$\frac{C_2}{C_2} = [\lambda_2(C_{2\infty} + A_0 + B_0) + \frac{\mu_2}{2}(\tau A_1 + B_1)] + [\mu_2(C_{2\infty} + A_0 + B_0) + \lambda_2(\tau A_1 + B_1)] \cos b_1 y + \dots \quad (\text{XI.26})$$

Subtraction of eq. XI.26 from XI.25 yields

$$\frac{C_{2p}}{C_{2po}} - \frac{C_2}{C_{2o}} = [C_{2\infty}(\lambda_1 - \lambda_2) - \lambda_2 \tau A_0 - \lambda_2 B_0 - \frac{1}{2}(\frac{\mu_1}{v} D_{11} \frac{b_1^2}{\lambda_1^I} + \lambda_2) \tau A_1 - \frac{1}{2}(\frac{\mu_1}{v} D_{22} \frac{b_1^2}{\lambda_1^{II}} + \mu_2) B_1] \quad (\text{XI.27})$$

$$+ [C_{2\infty}(\mu_1 - \mu_2) - \mu_2 \tau A_0 - \mu_2 B_0 - (\frac{\lambda_1}{v} D_{11} \frac{b_1^2}{\lambda_1^I} + \lambda_2) \tau A_1 - (\frac{\lambda_1}{v} D_{22} \frac{b_1^2}{\lambda_1^{II}} + \lambda_2) B_1] \cos b_1 y + \dots$$

In the same way we can write the second equation of XI.10 as

$$\frac{C_{1p}}{C_{1\infty}} - \frac{C_1}{C_{1o}^{\gamma\alpha}} = \frac{1 - C_{1p} - C_{2p}}{C_{3po}} - \frac{1 - C_1 - C_2}{C_{3o}} \quad (\text{XI.28})$$

and we obtain

$$\frac{1 - C_{1p} - C_{2p}}{C_{3po}} = \{ \lambda_1 C_{2\infty} - \frac{\mu_1}{2v} [ (\tau+1) D_{11} \frac{A_1 b_1^2}{\lambda_1^I} + D_{22} \frac{B_1 b_1^2}{\lambda_1^{II}} ] \} \quad (\text{XI.29})$$

$$+ \{ \mu_1 C_{2\infty} + \frac{\lambda_1}{v} [ (\tau+1) D_{11} \frac{A_1 b_1^2}{\lambda_1^I} + D_{22} \frac{B_1 b_1^2}{\lambda_1^{II}} ] \} \cos b_1 y + \dots$$



$$\frac{1 - C_1 - C_2}{C_{30}} = \lambda_2 [C_{2\infty} - (\tau+1)A_0 - B_0] + \frac{\mu_2}{2} [(\tau+1)A_1 + B_1] \quad (XI.30)$$

$$+ \{ -\mu_2 [C_{2\infty} - (\tau+1)A_0 - B_0] - \lambda_2 [(\tau+1)A_1 + B_1] \} \cos b_1 y + \dots$$

Subtraction of eq. XI.29 from eq. XI.30 yields

$$\frac{1 - C_{1p} - C_{2p}}{C_{3p0}} - \frac{1 - C_1 - C_2}{C_{30}} = \quad (XI.31)$$

$$\{ C_{2\infty}(\lambda_1 - \lambda_2) + \lambda_2(\tau+1)A_0 + \lambda_2 B_0 - \frac{1}{2} \left[ \frac{\mu_1}{v} D_{11} \frac{b_1^2}{\lambda_1^2} + \mu_2 \right] (\tau+1)A_1 - \frac{1}{2} \left[ \frac{\mu_1}{v} D_{22} \frac{b_1^2}{\lambda_1^2} + \mu_2 \right] B_1 \}$$

$$+ \{ -C_{2\infty}(\mu_1 - \mu_2) - \mu_2(\tau+1)A_0 - \mu_2 B_0 + \left[ \frac{\lambda_1}{v} D_{11} \frac{b_1^2}{\lambda_1^2} + \lambda_2 \right] (\tau+1)A_1$$

$$+ \left[ \frac{1}{v} D_{22} \frac{b_1^2}{\lambda_1^2} + \lambda_2 \right] B_1 \} \cos b_1 y + \dots$$

We have to identify eq. XI.24 with the two eqs. XI.27 and XI.31 to obtain the system of four equations for the coefficients  $A_0$ ,  $A_1$ ,  $B_0$ , and  $B_1$ . This identification yields

$$1 - \frac{C_{1\infty}}{C_{10}^{\gamma\alpha}} - \frac{A_0}{C_{10}^{\gamma\alpha}} = C_{2\infty}(\lambda_1 - \lambda_2) + \lambda_2(\tau+1)A_0 + \lambda_2 B_0 - \frac{1}{2} \left( \frac{\mu_1}{v} D_{11} \frac{b_1^2}{\lambda_1^2} + \mu_2 \right) (\tau+1)A_1$$

$$- \frac{1}{2} \left( \frac{\mu_1}{v} D_{22} \frac{b_1^2}{\lambda_1^2} + \mu_2 \right) B_1 \quad (XI.32a)$$

$$1 - \frac{C_{1\infty}}{C_{10}^{\gamma\alpha}} - \frac{A_0}{C_{10}^{\gamma\alpha}} = C_{2\infty}(\lambda_1 - \lambda_2) - \lambda_2 \tau A_0 - \lambda_2 B_0 - \frac{1}{2} \left( \frac{\mu_1}{v} D_{11} \frac{b_1^2}{\lambda_1} + \mu_2 \right) \tau A_1$$

$$- \frac{1}{2} \left( \frac{\mu_1}{v} D_{22} \frac{b_1^2}{\lambda_1} + \mu_2 \right) B_1 \quad (\text{XI.32b})$$

$$\frac{1}{C_{1\infty}} \frac{D_{11}}{v} \frac{b_1^2}{\lambda_1} + \frac{1}{C_{10}^{\gamma\alpha}} = -C_{2\infty}(\mu_1 - \mu_2) - \mu_2(\tau + 1)A_0 - \mu_2 B_0 + \left( \frac{\lambda_1}{v} D_{11} \frac{b_1^2}{\lambda_1} + \lambda_2 \right) (\tau + 1)A_1$$

$$- \left( \frac{\lambda_1}{v} D_{22} \frac{b_1^2}{\lambda_1} + \lambda_2 \right) B_1 \quad (\text{XI.32c})$$

and

$$\frac{1}{C_{1\infty}} \frac{D_{11}}{v} \frac{b_1^2}{\lambda_1} + \frac{1}{C_{10}^{\gamma\alpha}} = C_{2\infty}(\mu_1 - \mu_2) - \mu_2 \tau A_0 - \mu_2 B_0 - \left( \frac{\lambda_1}{v} D_{11} \frac{b_1^2}{\lambda_1} + \lambda_2 \right) \tau A_1$$

$$- \left( \frac{\lambda_1}{v} D_{22} \frac{b_1^2}{\lambda_1} + \lambda_2 \right) B_1 \quad (\text{XI.32d})$$

If we subtract the first two eqs. XI.32a and b and add the last two eqs. XI.32c and d we obtain two equations in  $A_0$ ,  $B_0$  and  $A_1$

$$0 = (2\tau + 1)\lambda_2 A_0 + 2\lambda_2 B_0 - \frac{\mu_1}{2} \left( \frac{1}{v} D_{11} \frac{b_1^2}{\lambda_1} + \mu_2 \right) A_1 \quad (\text{XI.33a})$$

and

$$\frac{2}{C_{1\infty}} \frac{D_{11}}{v} \frac{b_1^2}{\lambda_1} + \frac{2}{C_{10}^{\gamma\alpha}} = - (2\tau + 1)\mu_2 A_0 - 2\mu_2 B_0 + \left( \frac{\lambda_1}{v} D_{11} \frac{b_1^2}{\lambda_1} + \lambda_2 \right) A_1 \quad (\text{XI.33b})$$

If we add the first two eqs. XI.32a and b and subtract the last two eqs. XI.32c and d we obtain two equations in  $A_0$ ,  $A_1$  and  $B_1$ .

$$2 - \frac{2C_{1\infty}}{C_{10}^{\gamma\alpha}} - \frac{2A_0}{C_{10}^{\gamma\alpha}} = 2 C_{2\infty} (\lambda_1 + \lambda_2) + \lambda_2 A_0 - \frac{1}{2} \left( \frac{\mu_1}{v} D_{11} \frac{b_1^2}{\lambda_1} + \mu_2 \right) (2\tau + 1) A_1$$

$$- \left( \frac{\mu_1}{v} D_{22} \frac{b_1^2}{\lambda_1} + \mu_2 \right) B_1 \quad (\text{XI.34a})$$

and

$$2 C_{2\infty} (\mu_1 - \mu_2) = - \mu_2 A_0 + \left( \frac{\mu_1}{v} D_{11} \frac{b_1^2}{\lambda_1} + \lambda_2 \right) A_1 + 2 \left( \frac{\lambda_1}{v} D_{22} \frac{b_1^2}{\lambda_1} + \lambda_2 \right) B_1 \quad (\text{XI.34b})$$

These four equations constitute a system equivalent to XI.32.

From the two first equations we can immediately deduce  $A_1$  as

$$A_1 = \lambda_2 \frac{\frac{2}{C_{1\infty}} \frac{D_{11}}{v} \frac{b_1^2}{\lambda_1} + \frac{2}{C_{10}^{\gamma\alpha}}}{\lambda_2 \left( \frac{\lambda_1}{v} D_{11} \frac{b_1^2}{\lambda_1} + \lambda_2 \right) - \frac{\mu_2}{2} \left( \frac{\mu_1}{v} D_{11} \frac{b_1^2}{\lambda_1} + \mu_2 \right)} \quad (\text{XI.35})$$

Combining the last two equations of XI.34 to eliminate  $B_1$  we obtain the expression for  $A_0$  as a function of  $A_1$ , viz.,

$$2 \left[ 1 - \frac{C_{1\infty}}{C_{10}^{\gamma\alpha}} - C_{2\infty} (\lambda_1 - \lambda_2) \right] \left( \frac{\lambda_1}{v} D_{22} \frac{b_1^2}{\lambda_1} + \lambda_2 \right) + C_{2\infty} (\mu_1 - \mu_2) \left( \frac{\mu_1}{v} D_{22} \frac{b_1^2}{\lambda_1} + \mu_2 \right)$$

$$= \left[ \left( \lambda_2 + \frac{2}{C_{10}^{\gamma\alpha}} \right) \left( \frac{\lambda_1}{v} D_{22} \frac{b_1^2}{\lambda_1} + \lambda_2 \right) - \frac{1}{2} \mu_2 \left( \frac{\mu_1}{v} D_{22} \frac{b_1^2}{\lambda_1} + \mu_2 \right) \right] A_0 \quad (\text{XI.36})$$

(over)

$$+ \frac{1}{2} \left[ \left( \frac{\lambda_1}{v} D_{11} \frac{b_1^2}{\lambda_1} + \lambda_2 \right) \left( \frac{\mu_1}{v} D_{22} \frac{b_1^2}{\lambda_1} + \mu_2 \right) - \left( \frac{\mu_1}{v} D_{11} \frac{b_1^2}{\lambda_1} + \mu_2 \right) \left( \frac{\lambda_1}{v} D_{22} \frac{b_1^2}{\lambda_1} + \lambda_2 \right) \right] A_1$$

Finally, if we substitute the expression for  $A_1$  in eq. XI.36 we obtain  $A_0$ . With the expressions for  $A_0$  and  $A_1$  we can deduce those for  $B_0$  and  $B_1$  with the help of the first equation of XI.33 and the last equation of XI.34. Note that the coefficients  $A_0$ ,  $A_1$  and  $B_1$  do not depend on  $\tau$ . The effect of the off-diagonal diffusion coefficient appears in  $B_0$  only.

## APPENDIX XII

### APPROXIMATE CALCULATION OF THE FOURIER SERIES COEFFICIENTS FOR A TERNARY SOLUTION WITH THE SECOND THERMODYNAMIC VERSION IN THE SYMMETRICAL CONFIGURATION

The calculations performed in Appendix XI were rigorous and general and included a discussion of the symmetrical configuration. They led to complicated expressions which do not allow easy discussion. In this Appendix we adopt some simplifications which limit further the generality of the results but which allow us to perform more transparent calculations. In the presentation we will particularly note the parallelism with the binary treatment since the results reduce to the binary ones when  $C_{1\infty}$  goes to zero.

To calculate the Fourier series coefficients we must again satisfy the complex ratio requirement X.3 and in all the calculations we consider a symmetrical configuration only.

From the complex ratios we have

$$\frac{C_1^{\gamma\alpha}}{C_1^{\alpha\gamma}} \frac{C_2^{\alpha\gamma}}{C_2^{\gamma\alpha}} = \frac{x_1}{x_2} \quad (\text{XII.1})$$

and provided we can neglect terms of order  $(\Delta C)^2$ , we deduce

$$\frac{C_{20}^{\alpha\gamma} \Delta C_1^{\gamma\alpha} + C_{10}^{\gamma\alpha} \Delta C_2^{\alpha\gamma}}{C_{20}^{\gamma\alpha} \Delta C_1^{\alpha\gamma} + C_{10}^{\alpha\gamma} \Delta C_2^{\gamma\alpha}} = \frac{x_1}{x_2} \quad (\text{XII.2})$$

or

$$x_2 C_{20}^{\alpha\gamma} \Delta C_1^{\gamma\alpha} + x_2 C_{10}^{\gamma\alpha} \Delta C_2^{\alpha\gamma} = x_1 C_{20}^{\gamma\alpha} \Delta C_1^{\alpha\gamma} + x_1 C_{10}^{\alpha\gamma} \Delta C_2^{\gamma\alpha} \quad (\text{XII.3})$$

Now we group in eq. XII.3 the increments of concentration in the same phase to yield

$$x_1 C_{20}^{\gamma\alpha} \Delta C_1^{\alpha\gamma} - x_2 C_{10}^{\gamma\alpha} \Delta C_2^{\alpha\gamma} = x_2 C_{20}^{\alpha\gamma} \Delta C_1^{\gamma\alpha} - x_1 C_{10}^{\alpha\gamma} \Delta C_2^{\gamma\alpha} \quad (\text{XII.4})$$

also from the complex ratio we have

$$\frac{C_2^{\gamma\alpha}}{C_2^{\alpha\gamma}} \frac{C_3^{\alpha\gamma}}{C_3^{\gamma\alpha}} = x_2 \quad (\text{XII.5})$$

and we deduce that

$$\frac{C_{30}^{\alpha\gamma} \Delta C_2^{\gamma\alpha} - C_{20}^{\gamma\alpha} (\Delta C_1^{\alpha\gamma} + \Delta C_2^{\alpha\gamma})}{C_{30}^{\gamma\alpha} \Delta C_2^{\alpha\gamma} - C_{20}^{\alpha\gamma} (\Delta C_1^{\gamma\alpha} + \Delta C_2^{\gamma\alpha})} = x_2 \quad (\text{XII.6})$$

or

$$C_{20}^{\gamma\alpha} \Delta C_1^{\alpha\gamma} + (C_{20}^{\gamma\alpha} + x_2 C_{30}^{\gamma\alpha}) \Delta C_2^{\alpha\gamma} = x_2 C_{20}^{\alpha\gamma} \Delta C_1^{\gamma\alpha} + (C_{30}^{\alpha\gamma} + x_2 C_{20}^{\alpha\gamma}) \Delta C_2^{\gamma\alpha} \quad (\text{XII.7})$$

Similar expressions for the  $\beta$  phase can be obtained from the complex ratios

$$\frac{C_1^{\gamma\beta} C_2^{\beta\gamma}}{C_1^{\beta\gamma} C_2^{\gamma\beta}} = x_1 \quad (\text{XII.8})$$

and

$$\frac{C_2^{\beta\gamma} C_3^{\gamma\beta}}{C_2^{\gamma\beta} C_3^{\beta\gamma}} = x_2 \quad (\text{XII.9})$$

In summary we get four thermodynamic equations expressed in terms of the increments  $\Delta C$

$$x_1 C_{20}^{\gamma\alpha} \Delta C_1^{\alpha\gamma} - x_2 C_{10}^{\gamma\alpha} \Delta C_2^{\alpha\gamma} = x_2 C_{20}^{\alpha\gamma} \Delta C_1^{\gamma\alpha} - x_1 C_{10}^{\alpha\gamma} \Delta C_2^{\gamma\alpha} \quad (\text{XII.10a})$$

$$x_1 C_{20}^{\gamma\beta} \Delta C_1^{\beta\gamma} - C_{10}^{\gamma\beta} \Delta C_2^{\beta\gamma} = C_{20}^{\beta\gamma} \Delta C_1^{\gamma\beta} - x_1 C_{10}^{\beta\gamma} \Delta C_2^{\gamma\beta} \quad (\text{XII.10b})$$

$$C_{20}^{\gamma\alpha} \Delta C_1^{\alpha\gamma} + (C_{20}^{\gamma\alpha} + x_2 C_{30}^{\gamma\alpha}) \Delta C_2^{\alpha\gamma} = x_2 C_{20}^{\alpha\gamma} \Delta C_1^{\gamma\alpha} + (C_{30}^{\alpha\gamma} + x_2 C_{20}^{\alpha\gamma}) \Delta C_2^{\gamma\alpha} \quad (\text{XII.10c})$$

$$x_2 C_{20}^{\gamma\beta} \Delta C_1^{\beta\gamma} + (C_{30}^{\gamma\beta} + x_2 C_{20}^{\gamma\beta}) \Delta C_2^{\beta\gamma} = C_{20}^{\beta\gamma} \Delta C_1^{\gamma\beta} + (C_{20}^{\beta\gamma} + x_2 C_{30}^{\beta\gamma}) \Delta C_2^{\gamma\beta}$$

(XII.10d)

These are exactly equivalent to the set XI.9 and a complete solution based upon XII.10 will be just as intractable as before.

The two last equations of XII.10 are very similar to the equations which we found in the binary treatment, viz., eqs. 2.78 and 2.79. This suggests the possibility of invoking another slightly less general thermodynamic version which leads to much greater tractability. This is achieved by combining the requirements

$$C_{20}^{\gamma\alpha} \Delta C_1^{\alpha\gamma} = x_2 C_{20}^{\alpha\gamma} \Delta C_1^{\gamma\alpha} \quad (\text{XII.11a})$$

$$x_2 C_{20}^{\gamma\beta} \Delta C_1^{\beta\gamma} = C_{20}^{\beta\gamma} \Delta C_1^{\gamma\beta} \quad (\text{XII.11b})$$

with eqs. XII.10c and XII.10d to give

$$(C_{20}^{\gamma\alpha} + x_2 C_{20}^{\gamma\alpha}) \Delta C_2^{\alpha\gamma} = (C_{30}^{\alpha\gamma} + x_2 C_{20}^{\alpha\gamma}) \Delta C_2^{\gamma\alpha} \quad (\text{XII.11c})$$

$$(C_{30}^{\gamma\beta} + x_2 C_{20}^{\gamma\beta}) \Delta C_2^{\beta\gamma} = (C_{20}^{\beta\gamma} + x_2 C_{30}^{\beta\gamma}) \Delta C_2^{\gamma\beta} \quad (\text{XII.11d})$$

at the same time discarding (XII.10a and 10b).

As we shall see the new thermodynamics outlined above requires that for the symmetrical case as developed below there can be no segregation of component 1 either between or within precipitate phases. In other words,



this is analogous, for component 1 only, to Hillert's restriction on the precipitate concentrations in the binary case.

Now for the symmetric phase diagram we can take the ratios of increments of concentrations expressed in terms of Fourier expansions

$$\frac{\Delta C_{1p}}{\Delta C_1} = \begin{cases} x_2 \frac{C_{20}^{\alpha\gamma}}{C_{20}^{\gamma\alpha}} & \text{when } -\frac{S^\alpha}{2} < y < \frac{S^\alpha}{2} \\ \frac{1}{x_2} \frac{C_{30}^{\alpha\gamma}}{C_{30}^{\gamma\alpha}} = \frac{C_{20}^{\alpha\gamma}}{C_{20}^{\gamma\alpha}} & \text{when } \frac{S^\alpha}{2} < y < \frac{S^\alpha}{2} + S^\beta \end{cases} \quad (\text{XII.12})$$

and

$$\frac{\Delta C_{2p}}{\Delta C_2} = \frac{C_{30}^{\alpha\gamma} + x_2 C_{20}^{\alpha\gamma}}{C_{20}^{\gamma\alpha} + x_2 C_{30}^{\gamma\alpha}} \quad \text{for any } y \quad (\text{XII.13})$$

Eq. XII.12 can then be written in the form

$$\frac{-\frac{D_{11}}{v} \sum_{n=1}^{\infty} \frac{A_n b_n^2}{\lambda_n} \cos b_n y}{C_{1\infty} - C_{20}^{\gamma\alpha} + A_0 + \sum_{n=1}^{\infty} A_n \cos b_n y} \quad (\text{XII.14})$$

$$= \frac{C_{20}^{\alpha\gamma}}{C_{20}^{\gamma\alpha}} \frac{x_2+1}{2} + \frac{2(x_2-1)}{\pi} \sum_{n=1}^{\infty} \frac{1}{n} \sin \pi n \frac{S^\alpha}{S} \cos b_n y$$

The identification of the right and left hand side terms of the series after multiplication gives a homogenous system of equations in  $A_n$  for  $n \neq 0$  for which particularly

$$A_0 = C_{10}^{Y\alpha} - C_{1\infty} \quad (\text{XII.15a})$$

and

$$A_n = 0 \quad n \neq 0 \quad (\text{XII.15b})$$

This implies that for component 1 there is neither segregation within the phases nor partition between the precipitate phases. If we refer to eq. 3.109 where the right hand side is equal to zero because all the coefficients vanish we also see that it is justified to infer  $S^\alpha = S^\beta$ .

We can now write eq. XII.13 in the form

$$\frac{C_{2p} - C_{2p0}}{C_2 - C_{20}} = K = \frac{C_{30}^{\alpha\gamma} + x_2 C_{20}^{\alpha\gamma}}{C_{20}^{Y\alpha} + x_2 C_{30}^{Y\alpha}} \quad (\text{XII.16})$$

where  $C_{20}$  and  $C_{2p0}$  are step functions with the coefficients

$$\alpha_0 = \frac{C_{20}^{Y\alpha} + C_{20}^{Y\beta}}{2} = \frac{1 - C_{10}^{Y\alpha}}{2} \quad \alpha_n = \frac{2 (C_{20}^{Y\alpha} - C_{20}^{Y\beta})}{\pi} \sin n\frac{\pi}{2} \quad (\text{XII.17a;b})$$

$$\alpha'_0 = C_{2\infty} \quad \alpha'_n = \frac{2 (C_{20}^{\alpha\gamma} - C_{20}^{\alpha\beta})}{\pi} \sin n\frac{\pi}{2} \quad (\text{XII.18a;b})$$

The subsequent calculations are similar to those performed in Appendix VII and we obtain results analogous to equations VII.5 and VII.8, viz.,

$$B_0 = \tau (C_{1\infty} - C_{10}^{\gamma\alpha}) - \frac{1 - C_{10}^{\gamma\alpha}}{2} \quad (\text{XII.19})$$

And for the general term

$$B_{2i} = 0 \quad (\text{XII.20a})$$

and

$$B_{2i-1} = \frac{2}{\pi} [K(C_{20}^{\gamma\alpha} - C_{20}^{\gamma\beta}) - (C_{20}^{\alpha\gamma} - C_{20}^{\beta\gamma})] \frac{\frac{1}{2i-1} \sin (2i-1) \frac{\pi}{2}}{K + \frac{2\pi D_{22}}{Sv} (2i-1)} \quad (\text{XII.20b})$$

We can substitute this value of  $B_n$  in eq. 3.111 to yield

$$\frac{\phi}{S} + 1 = C' \frac{2\pi D_{22}}{Sv} \sum_{i=1}^{\infty} \frac{1}{(2i-1)[K + (2i-1) \frac{2\pi D_{22}}{Sv}]} \quad (\text{XII.21})$$

where

$$\phi = \frac{4 \sigma^{\alpha} \cos \phi^{\alpha}}{h_2^{\alpha} RT (C_{2\infty} - C_{20}^{\alpha\gamma})} \quad (\text{XII.22a})$$

and

$$C' = -\frac{4}{\pi^2} \frac{K (C_{20}^{\gamma\alpha} - C_{20}^{\gamma\beta}) - (C_{20}^{\alpha\gamma} - C_{20}^{\beta\gamma})}{C_{2\infty} - C_{20}^{\alpha\gamma}} \quad (\text{XII.22b})$$

We again adopt the notation

$$\chi = \frac{2\pi D_{22}}{Sv} \quad (\text{XII.23})$$

to obtain

$$\frac{\phi}{S} + 1 = C' \times \sum_{i=1}^{\infty} \frac{1}{(2i-1)[K + \chi(2i-1)]} \quad (\text{XII.24})$$

This equation is formally identical to the one which we found in Appendix VII as eq. VII.12 and we have an identical discussion. With the same notation as in XI.13, in order to have a solution to the physical problem we need to fulfill the condition expressed in VII.49, viz.,

$$\frac{x'(1-x')(1-2y')}{y'(1-y')(1-2x')} < 0 \quad (\text{XII.25})$$

or equivalently

$$(1-2x')(1-2y') < 0 \quad (\text{XII.26})$$

We have calculated in Appendix XI the expressions for  $x'$  and  $y'$  in terms of  $x$ ,  $y$  and  $x_{1\infty}$  (eqs. XI.19 and XI.21). Substituting these expressions into eq. XII.26 we obtain

$$(1-2x')(1-2y') = \left\{ 1-2x \left[ 1-x_{1\infty} (x_1-1) \frac{1-y}{y-x} \right] \right\} \left\{ 1-2y \left[ 1-x_{1\infty} (x_1-1) \frac{1-y}{y-x} \right] \right\} \quad (\text{XII.27})$$

$$= \left[ 1-2x + (x_1-1) \frac{2x(1-y)}{y-x} x_{1\infty} \right] \left[ 1-2y + (x_1-1) \frac{2y(1-y)}{y-x} x_{1\infty} \right] < 0 \quad (\text{XII.28})$$

Since  $x_1$  is larger than unity ( $= 10$ ) the condition XII.28 is equivalent to

$$0 < x_{1\infty} < \frac{(2y-1)(y-x)}{2(x_1-1)y(1-y)} \quad (\text{XII.29})$$

There is therefore a limit in the addition of element 1 for a given temperature in the ternary diagram above which no transformation can occur. We will now locate this limit in the ternary diagram.

Referring to Fig. 12 we see that the limit of pseudo-binary eutectoid reactions as a function of  $x_{1\infty}$  will be the first intersection of the symmetric composition line ( $x_1 + 2x_2 = 1$ ) with the three-phase region (point M). The value of  $x_{1\infty}$  corresponding to this is

$$x_{1\infty} = \frac{(y-x)(2y-1)}{2(x_1-1)y(1-y) - (y-x)} \quad (\text{XII.30})$$

We therefore see that since  $x_1 = 10$ , limit XII.29 lies just slightly below this value. Indeed, if we had not introduced the

restriction on the thermodynamics implied by eqs. XII.11 they would be exactly equal.

It is interesting to note that this limit coincides with the division between regions of high and low supersaturation as defined by Purdy et al<sup>29</sup> for pro-eutectoid reactions. These regions are defined by the lines ab and cd on Fig. 12 which intersect at the point M.

## LIST OF REFERENCES

1. J.A. Bell and W.C. Winegard, *J.Inst. of Metals*, 93 (1964-65) pp 318-9.
2. K.A. Jackson and J.D. Hunt, *Trans. AIME*, 236 (1966) pp 1129-42.
3. W.H. Brandt, *J. Appl. Phys.*, 16 (1945) pp 139-46.
4. E. Scheil, *Z. Metallkunde*, 37 (1946) pp 123-30.
5. C. Zener, *Trans AIME*, 167 (1946) pp 550-83.
6. M. Hillert, *Jernkont. Ann.*, 141 (1957) pp 757-89.
7. M. Hillert, *The Mechanism of Phase Transformations in Crystalline Solids*, Institute of Metals Monographs No 33 (1968) pp 231-47.
8. W.A. Tiller, *Liquid Metals and Solidification*, ASM (1958) pp 276-318.
9. B. Chalmers, *Principle of Solidification*, John Wiley and Sons (1964) pp 201.
10. J.S. Kirkaldy, *Energetics in Metallurgical Phenomena*, (1968) New York, Gordon and Breach.
11. J.W. Cahn and W.C. Hagel, *Decomposition of Austenite by Diffusional Processes*, Interscience (1962) pp 167-92.
12. J.W. Cahn, *Acta Met.*, 7 (1959) pp 18-28.
13. J.M. Shapiro and J.S. Kirkaldy, *Acta Met.*, 16 (1968) pp 579-85.
14. K.N. Tu and D. Turnbull, *Acta Met.*, 15 (1967) pp 369-76.
15. K.N. Tu and D. Turnbull, *Acta Met.*, 15 (1967) pp 1317-23.
16. K.N. Tu and D. Turnbull, *Acta Met.*, 17 (1969) pp 1263-79.
17. Y.C. Liu and H. I. Aaronson, *Acta Met.*, 16, pp 1343-58 (1968).

18. H. I. Aaronson and Y. C. Liu, *Scripta Met.*, 2, pp 1-13 (1968).
19. B.E. Sundqvist, *Acta Met.*, 16 (1968) pp 1413-27.
20. B.E. Sundqvist, *Acta Met.*, 17 (1969) pp 967-78.
21. J.S. Kirkaldy, *Scripta Met.*, 2 (1968) pp 565-68.
22. J.W. Cahn, reference 17 in article by K.A. Jackson and J.D. Hunt, *Trans. AIME*, 236 (1966) pp 1129-42.
23. J.S. Kirkaldy, Private communication.
24. D. Turnbull, Bristol Conference, (1954) pp 203-11.
25. D. Turnbull, *Acta Met.*, 3 (1955) pp 55-63.
26. H.W. Kerr, J.A. Bell and W.C. Winegard, *J. Australian Inst. Metals*, 10 (1965) pp 64-9.
27. H.W. Kerr, A. Plumtree and W.C. Winegard, *J. Inst. Metals*, 93 (1964-65) pp 63.
28. J.S. Kirkaldy, *Can. J. Phys.*, 36 (1958) pp 907-16.
29. G.R. Purdy, D.H. Weichert and J.S. Kirkaldy, *Trans. AIME*, 230 (1964) pp 1025-34.
30. M. Hillert, Private communication to J.S. Kirkaldy.
31. H. Eves, *Elementary Matrix Theory*, Allyn and Bacon Inc., Boston (1966).
32. J.S. Kirkaldy and G.R. Purdy, *Canadian J. Physics*, 47 (1969) pp 865-71.
33. J.S. Kirkaldy, Zia-Ul-Haq and L.C. Brown, *ASM Trans*, 56 (1963) pp 834-49.
34. M.K. Asundi and D.R. West, *J. Inst. Metals*, 92 (1963-4) pp 428-30.
35. M.K. Asundi and D.R. West, *J. Inst. Metals*, 94 (1966) pp 19-23.
36. M. Hansen, *Constitution of Binary Alloys*, McGraw Hill Co. (1958).
37. D. Brown and N. Ridley, *J. Iron and Steel Inst.*, (Sept. 1969) pp 1232-40.



38. R.P. Smith, Trans AIME, 224 (1962) pp 105-11.
39. R.F. Mehl and C. Wells, Trans AIME, 125 (1937) pp 429-69.
40. R.P. Smith, Trans AIME, 215 (1959) pp 954-57.
41. J.J. Kramer, G.M. Pound and R.F. Mehl, Acta Met., 6 (1958) pp 763-71.
42. C. Wells and R.F. Mehl, Trans AIME, 188 (1950) pp 553-60.
43. R.H. Fillnow and D.J. Mack, Trans AIME, 188 (1950) pp 1229-36.
44. C. W. Spencer and D.J. Mack, J. Inst. Metals, 82 (1953-54) pp 81-85.
45. G.R. Speich and D.J. Mack, Trans AIME, 197 (1953) pp 549-53.
46. C.W. Spencer and D. J. Mack, Decomposition of Austenite by Diffusional Processes, Interscience AIME (1962) pp 549-606.